University of Massachusetts Amherst

From the SelectedWorks of Min S. Yun

April, 1987

Molecular clouds and cloud cores in the inner Galaxy

N Z Scoville
Min S. Yun, *University of Massachusetts - Amherst*
D B Sanders
D P Clemens
W H Waller

Available at: https://works.bepress.com/min_yun/76/

bepress™

1987ApJS...63..821S

THE ASTROPHYSICAL JOURNAL SUPPLEMENT SERIES, 63:821–915, 1987 April
© 1987. The American Astronomical Society. All rights reserved. Printed in U.S.A.

MOLECULAR CLOUDS AND CLOUD CORES IN THE INNER GALAXY

N. Z. SCOVILLE AND MIN SU YUN
Division of Physics, Mathematics, and Astronomy, California Institute of Technology
D. P. CLEMENS
Steward Observatory, University of Arizona
D. B. SANDERS
Division of Physics, Mathematics, and Astronomy, California Institute of Technology
AND
W. H. WALLER
Department of Astronomy, University of Massachusetts
Received 1986 June 11; accepted 1986 September 24

ABSTRACT

CO data from the Massachusetts–Stony Brook Galactic Survey have been analyzed to generate a compilation of clouds and hot cloud cores in the first Galactic quadrant at $l = 8°$ to $l = 90°$ and $b = -1.°05$ to $b = +1°$. Three lists of CO emission regions are compiled: 1427 emission regions from the general cloud population measured at the 4 K boundary with CO peaks at $T_R^* \geq 5$ K; 255 hot cloud cores measured at the 8 K boundary with peak $T_R^* \geq 9$ K; and 95 clouds associated with 171 radio H II regions.

The clouds associated with H II regions exhibit systematically brighter CO peaks; they are a factor of 2—3 larger and have twice as large a mean velocity dispersion as the general cloud population. Both the H II region clouds and the hot core regions have a Galactic distribution characteristic of a spiral arm population, whereas the colder clouds are much less confined in Galactic azimuthal angle. For giant molecular clouds (GMCs) in the general population, there is no significant difference in the confinement of large or small clouds to the spiral arm locations.

Virial masses are obtained for the large sample of clouds with assigned kinematic distances. The mean H_2 density for a GMC of diameter 40 pc (at $T_R^* = 4$ K) is 180 cm^{-3}. For these clouds, a linear relationship is found between the H_2 column density (adopting $R_0 = 8.5$ kpc) and the integrated CO emission: $N_{H_2}(\text{cm}^{-2}) = 3.6 \times 10^{20} I_{CO}(\text{K km s}^{-1})$ for diameters in the range 10–100 pc. This relation holds equally well for clouds with and without H II regions. The variation in the Z-dispersion of clouds as a function of cloud mass suggests that more massive GMCs have smaller random velocities, as expected for equipartition. The distribution of H II region locations within GMCs can be approximated by a power law $\rho(r) \propto r^{-1}$, where r is measured from the CO emission centroid. The efficiency for massive star formation estimated from the number and luminosity of the H II regions within individual clouds is found to decrease with increasing cloud mass over the range 2×10^5 to 4×10^6 $M_\odot$.

Subject headings: galaxies: Milky Way — interstellar: molecules — nebulae: H II regions

I. INTRODUCTION

Virtually all star formation in the Galaxy occurs within molecular, not atomic, hydrogen clouds. Models for the structure and evolution of the Galaxy must then include a thorough understanding of the mechanisms of formation of both the molecular clouds and the young stars within them. In contrast to the H I emission, the CO emission which probes the H_2 is seen to arise from discrete clouds, each with a small line width ($\Delta V \sim 4$–10 km s^{-1}) compared with the total velocity width of the Galactic disk ($V_{LSR} = -5$ to 150 km s^{-1}). A typical line of sight through the inner Galactic disk will intersect three to eight of these giant molecular clouds (GMCs) of size 20–100 pc. (Limited studies of the distribution of cloud properties have been done in ^{13}CO by Stark 1979 and Liszt, Xiang, and Burton 1981 and in CO by Sanders, Scoville, and Solomon 1985.)

The recently completed Massachusetts–Stony Brook Galactic CO Survey (Sanders *et al.* 1986) provides an extensive data set for studies of the GMC properties. The 40,551 survey spectra were obtained on a well-sampled grid (mostly $3' \times 3'$ in l and b centered on the Galactic midplane) with a $45''$ beam. The characteristics of the survey were thus specifically designed to completely sample all GMCs in the first Galactic quadrant of size greater than 10 pc at distances less than 10 kpc. These high-resolution data are ideal for studies of cloud morphology, the cloud size distribution, the internal kinematics of clouds, and their thermal distributions. Preliminary publications of data from the survey have been presented in the form of (b, V) diagrams (Sanders *et al.*

© American Astronomical Society • Provided by the NASA Astrophysics Data System

1987ApJS...63..821S

1986), (l, V) diagrams (Clemens *et al.* 1986), and (l, b) diagrams (Clemens *et al.* 1986).

In this paper we present a complete list of CO emission regions and their measured parameters. Given the l and b coverage of this survey ($l = 8°$ to $90°$ and $b = -1.^{\circ}05$ to $+1°$), this compilation represents a nearly complete accounting of the molecular clouds in the first quadrant of the Galaxy with sizes greater than 20 pc. The largest list, containing 1427 objects, was generated by a computer search through the survey data for all CO peaks exceeding a 5 K (T_R^*) threshold. The cloud boundary is defined by all simply connected points in (l, b, V) 3-space above the 4 K (T_R^*) threshold. A second list of 255 objects was generated by automated search for all CO emission peaks exceeding 9 K. In several cases, more than one of the peaks in the 9 K list is included within a single cloud of the first list. The first list (referred to as 4 K clouds) was chosen with emission thresholds such that it would include virtually all GMCs with significant internal heating, presumably due to active star formation. On the other hand, the low threshold adopted for this list implies that in some areas several distinct clouds will be blended into a single entry. The second list (referred to as 8 K clouds) provides a fairly complete accounting of all hot cores within GMCs but does not provide an accurate assessment of the boundaries for the clouds in which these core regions are located.

A third list of objects is composed of CO emission regions associated with radio H II regions. For this group of clouds the threshold level for the cloud boundary was varied from cloud to cloud in order to obtain the largest possible extent for the cloud while at the same time maintaining isolation from neighboring emission regions. Maps of the CO emission and velocity fields are presented for this group of clouds. This list, including only those clouds with massive star formation, is particularly useful for studying the Galactic spiral structure. The H II–GMC list has the additional virtue that the majority of the objects have resolved kinematic distances as the result of their association with radio H II regions. The measured properties of this H II region–based sample are analyzed and cross-correlated.

II. CLOUD DEFINITION

The Massachusetts–Stony Brook Galactic CO Survey was obtained on the 14 m telescope of the Five College Radio Astronomy Observatory (FCRAO)[1] in New Salem, Massachusetts. A complete description of the survey coverage, data acquisition, and reduction is included in Sanders *et al.* (1986). The survey includes 40,551 spectra in longitude range $8°$–$90°$ at latitudes between $-1.^{\circ}05$ and $+1°$. Between $l = 18°$ and $l = 55°$ the spectra were obtained on a $3' \times 3'$ grid and at other longitudes on a $6' \times 6'$ grid. The velocity range of the survey included $V_{LSR} = -100$ to $+200$ km s^{-1} at a resolution of 1 km s^{-1}. All intensities were converted to Rayleigh-Jeans antenna temperatures, T_R^*, corrected for atmospheric extinction and the antenna spillover efficiency ($\eta_{FSS} = 0.7$). The noise level in the survey is $\Delta T_R^* = 0.4$ K (1 σ); thus all emission features and cloud boundaries above 1.2 K are significant. In this paper most of the cloud boundary and definition are performed at $T_R^* \geq 4$ K corresponding to 10 σ.

In generating a list of CO emission regions for the present study, an automated routine was developed to search through the 3-space of CO data (l, b, and V), locate local maxima in the CO temperatures, and find all 3-space points simply connected to these maxima above a specified threshold. This threshold serves to *define* the boundary for each emission region; however, it must be recognized that the full extent at 0 K intensity will often be more than a factor of 2 larger. Once a given (l, b, V) point has been included within the boundary of one cloud, the point is removed from the survey data set and does not enter within any other cloud.

Computerized schemes for cloud definition were employed, rather than manual measurement of the clouds (e.g., Myers *et al.* 1986) because of the very large number of emission regions and the need to experiment with the adopted peak and threshold parameters. Ideally, one would like measurements of the clouds with a 0 K threshold for each cloud boundary; however, low boundary thresholds are impractical in view of the noise in the data and the blending of adjacent clouds which occurs in crowded areas of the spatial-velocity plane. The degree of blending varies considerably across the area of the survey. Near the terminal velocity at $l = 30°$–$50°$, overlap of optically thick emission from separate clouds can occur at temperatures as high as 5 K, while at higher longitudes and lower velocities, clouds are seldom blended, even at the 2 K level. With too high a threshold the emission regions become severely truncated, and it is impossible to obtain a reliable estimate of the cloud size and emission integrals. On the other hand, if one wishes to compare the properties of clouds from one area of the Galactic plane to another, it is clearly necessary to have a uniform measurement criteria. For several of the clouds, we have varied the threshold temperature to investigate how the measured parameters depend on it (see below).

a) CO *Emission Regions*

Our primary list of emission regions is based upon a 4 K threshold for the cloud boundary. Within each region with points exceeding 4 K, it was required that there be at least three data points (l, b, and V) with temperature exceeding 4 K, and at least one point exceeding 5 K. The first condition was adopted because any emission region with less than three points will be unresolved in the survey; the second condition on the peak amplitude was adopted to avoid noise fluctuations from lower intensity emission regions registering as significant entries in the list. The primary list (hereafter referred to as the 4 K list) included in Table 1 contains 1427 entries; without the restrictive conditions the number was nearly twice as large. (In most of the analysis reported below, we restrict the samples further to include only objects with five or more points.) This list contains very diverse objects, many containing only the minimum of three (l, b, V) points, but one (No. 722) containing over 11,063 data points. The latter is clearly a blended feature at the terminal velocity.

[1]The Five College Radio Astronomy Observatory is operated with support of the National Science Foundation under grant AST 82-12252.

© American Astronomical Society • Provided by the NASA Astrophysics Data System

1987ApJS...63..821S

Clemens (1985*a*) developed algorithms for resolving these blended features, but they have not been applied to the full survey. Within many of the 4 K regions there are multiple hot cores, and a second search through the data was run with the two thresholds set at 8 and 9 K. This list of hot cores (referred to as the 8 K list) was then integrated into the 4 K list with the designations A, B, C,... for the successive core locations found in each of the 4 K emission regions.

For each emission region in Table 1 we have included a number of measured parameters. The position and intensity of peak CO emission are given, along with the centroid position and mean CO temperature for the entire emission region inside the 4 K boundary. The number of spatial-velocity data points within each cloud is given, and the maximum angular extent in l and b (from the minimum to the maximum l and b in degrees) and the velocity dispersion σ_V are listed. It must be cautioned that these spatial and velocity sizes are based only on points above 4 K. Since the survey data are sampled at 1 km s^{-1}, velocity dispersions $\lesssim$1 km s^{-1} (corresponding to $\Delta V_{\rm FWHM} = 2.3$ km s^{-1}) have a large uncertainty.

The Galactic position (galactocentric radius and near and far distances) were derived from the centroid l and V using the new rotation curve of Clemens (1985*b*) with the new solar constants ($R_0 = 8.5$ kpc and $\theta_0 = 220$ km s^{-1}). Clouds at $l < 20°$ and $-0.°66 < b < 0°$ were placed in the 3 kpc arm if their velocity was within 10 km s^{-1} of the expanding ring model given by Bania (1980), which was based on CO mapping of the 3 kpc arm. Assignment was made to the Cygnus arm if $74° < l < 86°$ and $V > -15$ km s^{-1}; the adopted distance and radius were assumed to be 1.5 and 7.7 kpc, respectively. We also attempted to resolve the near/far distance ambiguities using the derived Z centroid ($\langle Z \rangle$) and width (ΔZ) in Z. Any clouds for which the far distance assignment would imply a $\langle Z \rangle$ or ΔZ exceeding 120 pc (twice the Z half-width of 60 pc) are noted as being on the near side. Similarly, any clouds with differences between the near and far distances of $< 40\%$ are noted as being close to the tangential point.

The angular sizes in l and b ($\Delta l, \Delta b$) have in all cases been converted into a linear size ($\Delta L, \Delta B$) in parsecs assuming the clouds are at the near point distance. These sizes will be appropriate for all clouds flagged in the far right-hand column (3 KPC, CYG, NEAR, or TANG); for the remaining features the specified linear sizes must be increased by the ratio $d_{\rm FAR}/d_{\rm NEAR}$ if they are situated at the far point in the line of sight.

b) H II *Region Clouds*

A second list of clouds was generated starting from a sample of radio H II regions with measured recombination line velocities (Downes *et al.* 1980; Lockman 1987). All the H II regions of Downes *et al.* within the CO survey area were included (138 sources), and 33 additional sources were taken from the Lockman survey (selecting only strong sources which were well separated from the Downes *et al.* objects). In many cases a single cloud was found to contain multiple H II regions, so the final list includes only 95 distinct clouds. This cloud list based upon the sample of H II regions has several virtues:

1. The clouds with massive star formation will tend to have hot molecular gas and are therefore easier to delineate against the background of Galactic CO emission.
2. By virtue of their association with H II regions, most clouds can be assigned unambiguous kinematic distances, and thus the angular sizes measured for the clouds may be transformed into linear sizes. These clouds can also be unambiguously placed within the Galactic disk.

For the H II region–based sample of molecular clouds the search for an associated cloud was started at the (l, b, V) position of the H II region and extended out to 0.°2 radius and ± 10 km s^{-1} of the H II velocity. [The fact that all H II regions had CO emission within this search range suggests that a sufficiently wide (l, b, V)-space was searched.] Once a substantial CO peak was found, the (l, b, V)-space was searched for all simply connected points above a boundary. The level of the threshold for the boundary was varied depending on the complexity of the nearby emission field. In varying this boundary level, we aimed for optimum isolation of the cloud from the nearby background CO emission with the lowest possible cutoff temperature. [The resulting cloud maps were compared with the corresponding set of (b, V) diagrams for about a third of the total sample. Good agreement between the automated and manually mapped cloud boundaries was found in all but a few blended clouds (as can be verified by comparing Table 2 of this paper with Table 1 in Waller *et al.* 1987).]

The H II region clouds are shown in Figure 13 (at the end of this paper) via two different mappings. In the first, the total integrated intensity is mapped as a function of l and b for a velocity interval of 15–20 km s^{-1} centered on the central velocity of the CO peak identified with the H II region. In the second type, the integrated emission is shown only for those simply connected (l, b, V) points included within the cloud boundary at the specified threshold level. In both maps, symbols are shown at 3′ grid points to indicate the mean velocity for emission within the selected velocity range (shown in the legend at the top of the figure). In the second type of map, the horizontal bar at the lower right shows the linear scale assuming that the cloud is at the assigned distance to the H II region. The H II region distances given in Table 2 were reevaluated from the centroid l, b, and V of the associated CO cloud using the Clemens (1985*b*) rotation curve, and the twofold distance ambiguities were resolved following the assignments given by Downes *et al.* (1980).

Measured parameters of the clouds associated with the H II regions are given in Table 2. Aside from the measurements already described for Table 1, Table 2 also includes the H II region luminosity ($S_{6\ \rm cm} d^2$ in Jy kpc^2 based on the radio free-free emission) and the total CO luminosity integrated over the surface area of the cloud (K km s^{-1} pc^2; col. [20]). The cloud sizes are tabulated as the square root of the surface area, $A^{1/2}$, in parsecs.

In order to intercompare the sizes of the clouds associated with H II regions which were measured with *varying* cutoff temperatures (T_c; col. [22]), we derived an empirical "curve of

© American Astronomical Society • Provided by the NASA Astrophysics Data System

1987ApJS...63..821S

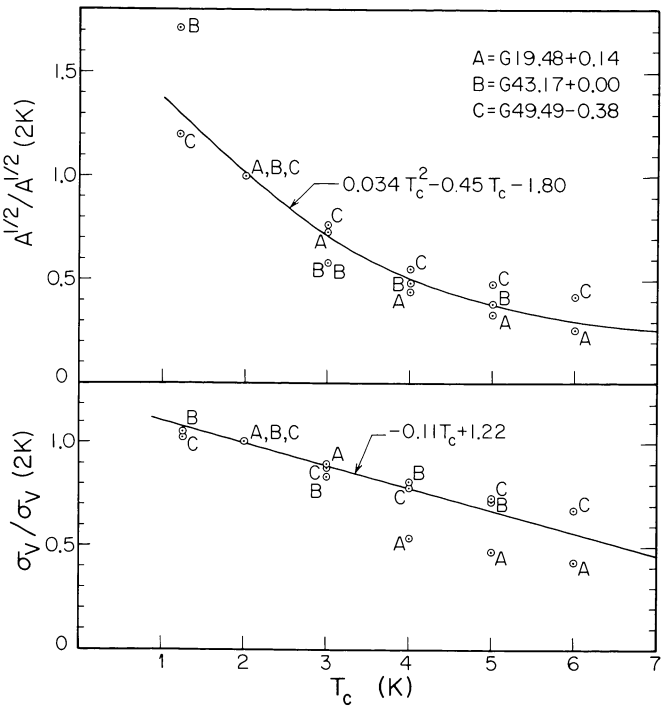

FIG. 1.—Growth curves for the sizes of clouds as determined by the square root of the projected area and the velocity dispersion are shown for four clouds from the H II region sample measured with variable cutoff temperature T_c. These clouds were selected for being in relatively unconfused areas of the (l, V)-plane, so that a range of T_c could be explored.

growth" based on the measured variation of the size and σ_V as a function of T_c. Three clouds (G19.48+0.14, G43.17+0.00, and G49.49−0.38) in unconfused areas of the (l, V)-plane were measured at cutoff temperatures varying from 1.2 to 6 K. (The requirement that the clouds be in an area of the Galactic plane with no background down to the 1 K level and that the clouds have bright peaks meant that there were very few clouds available for this growth-curve analysis.) In Figure 1 the sizes, $A^{1/2}$, and velocity dispersion, σ_V, normalized relative to their 2 K value are shown together with the best-fit growth curves:

$$A^{1/2}/A^{1/2}(2\text{ K}) = 0.034T_c^2 - 0.45T_c + 1.80 \qquad (1)$$

and

$$\sigma_V/\sigma_V(2\text{ K}) = -0.11T_c + 1.22. \qquad (2)$$

Although there are clear differences in the growth curves from cloud to cloud, these analytic relations provide the first-order correction needed to reduce the measured clouds to a common boundary value.

In the following sections we adopt as a measure of the mean cloud diameter a quantity which is the square root of the product of the maximum linear extents in the l and b directions. Thus

$$D \equiv (\Delta L \Delta B)^{1/2}, \qquad (3)$$

where ΔL and ΔB are the measurements given in columns (16) and (18) of Table 1. Equation (3) is strictly correct only for the case of elliptically shaped clouds with major axis aligned parallel or perpendicular to the Galactic plane, but the errors introduced for an arbitrary orientation are small. To convert the square root of the projected cloud area ($A^{1/2}$) which is tabulated for the H II region clouds in Table 2 (col. [19]) into an equivalent diameter, we have compared the two measures [$A^{1/2}$ and $(\Delta L \Delta B)^{1/2}$] for clouds measured in both lists at approximately the same cutoff temperature T_c. For clouds 35, 105, 164, 773, 918, and 1078, the mean value of $A^{1/2}/(\Delta L \Delta B)^{1/2} = 0.73 \pm 0.07$. For the H II region clouds, we therefore employ the conversion

$$D = (1.36 \pm 0.15)\, A^{1/2}. \qquad (4)$$

III. DISTRIBUTION OF CLOUD PROPERTIES

The two lists of CO emission regions (Tables 1 and 2) provide a comprehensive sample for investigation of the statistical properties of GMCs in the inner Galaxy and a basis for comparison of regions with and without massive star formation. In the following discussion we exclude cloud 772 from the 4 K list, since it is clearly a blend of many clouds near the tangential point.

In Figure 2 histograms of the CO peak temperatures, diameters, and velocity dispersions are shown for the 4 K and H II region samples. The mean value for each distribution is noted by the vertical arrow above the horizontal axis. Since all the parameters for the H II region sample were reduced to a 4 K boundary threshold as described in the previous section, the two sets of distribution functions should be directly comparable. From these figures it is immediately apparent that *the* H II *regions tend to be associated with systematically hotter, larger, and greater velocity dispersion* CO *emission regions*. That the H II region clouds have 50% higher peak temperatures is not at all surprising, since the presence of high-luminosity, massive stars within these regions will elevate the heat input to the dust and gas. The finding that the H II regions are associated with larger and more dispersive clouds is an important conclusion derived from these samples. Waller *et al.* (1987) compared the mean sizes of H II region clouds in their sample with the GMCs measured by Sanders, Scoville, and Solomon (1985) and also concluded that the H II region clouds were larger.

It is also clear from Figure 2 that the general cloud population (4 K) and the H II region clouds have very different forms for their distribution functions. For each parameter (T_p, D, and σ_V) the H II region sample exhibits a broad maximum in the number at an intermediate value of the parameter, whereas the general cloud population exhibits an increasing number of objects all the way down to the lower cutoff imposed by the survey resolution or the measurement techniques. Since the H II region clouds are presumably drawn from the general cloud population, it therefore must be the case that the formation of massive stars occurs preferentially in the large clouds and presumably causes these clouds to have higher peak CO temperatures.

The observed maximum in the distribution of velocity dispersions for the H II region clouds is more than a simple

© American Astronomical Society • Provided by the NASA Astrophysics Data System

1987ApJS...63..821S

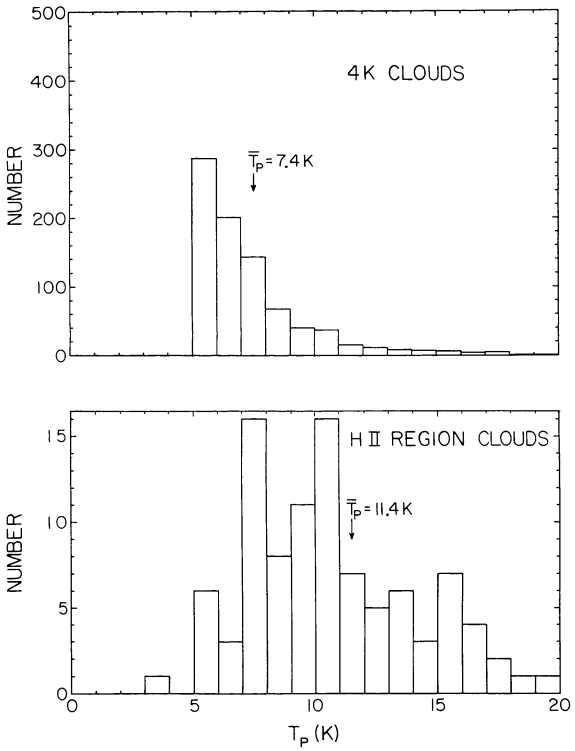

FIG. 2*a*

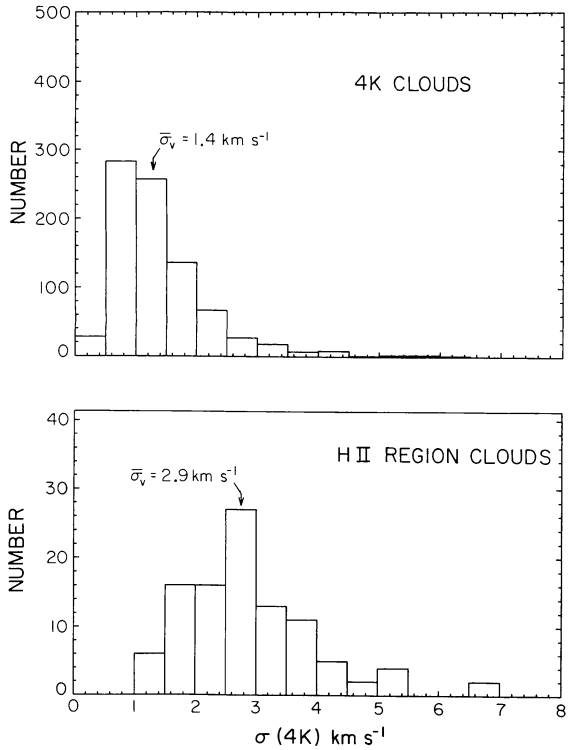

FIG. 2*b*

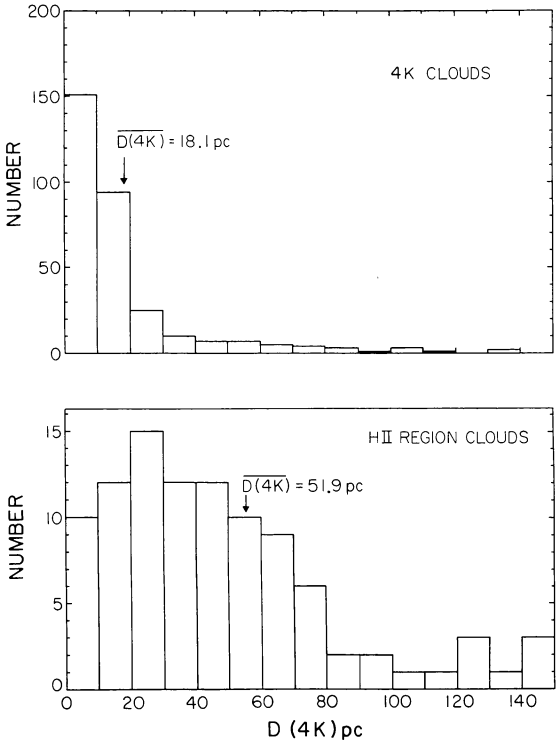

FIG. 2*c*

FIG. 2.—Distributions of (*a*) peak CO temperatures, (*b*) velocity dispersion, and (*c*) diameter are shown for the 4 K cloud list and the clouds associated with H II regions. Only clouds in Table 1 with more than five (l, b, V) sample points are included, and for the size distribution (Fig. 2*c*) only clouds with well determined distances are used.

corollary of the existence of a maximum in the distribution function of H II region cloud sizes combined with the fact that larger clouds are known to have greater values of σ_V. This follows from the fact that at the small-size end of the two cloud samples (D = 5–30 pc), the H II region clouds have systematically greater velocity dispersions than the general cloud population for the same size cloud (see § V).

IV. THE GALACTIC DISTRIBUTION OF CLOUDS

Important clues to understanding the formation and evolution of molecular clouds are provided by comparison of the large-scale distributions of clouds of differing size, temperature, and rates of star formation. With the large sample of clouds in the 4 K list we have analyzed the radial and azimuthal distributions of hot versus cold and large versus small clouds.

When comparing the distributions of clouds, special care must be taken to avoid the inherent biases resulting from variable confusion and blending in different areas of the (l, V)-plane. Thus, near the tangential velocity where the maximum velocity crowding occurs, our sample includes an increased number of large "clouds" due to blending of smaller clouds.

a) Distribution of Hot and Cold Clouds

Figures 3 and 4 show the (l, V) distributions and longitude histograms of objects in each of the samples: 4 K clouds, hot cores (8 K), and H II region clouds. The former sample exhibits a higher degree of uniformity within the region of (l, V)-space corresponding to the 4–7 kpc molecular cloud ring: a wedge from $l = 0°$ ($V = 0$ km s^{-1}) to $l = 20°$ ($V = 100$

© American Astronomical Society • Provided by the NASA Astrophysics Data System

1987ApJS...63..821S

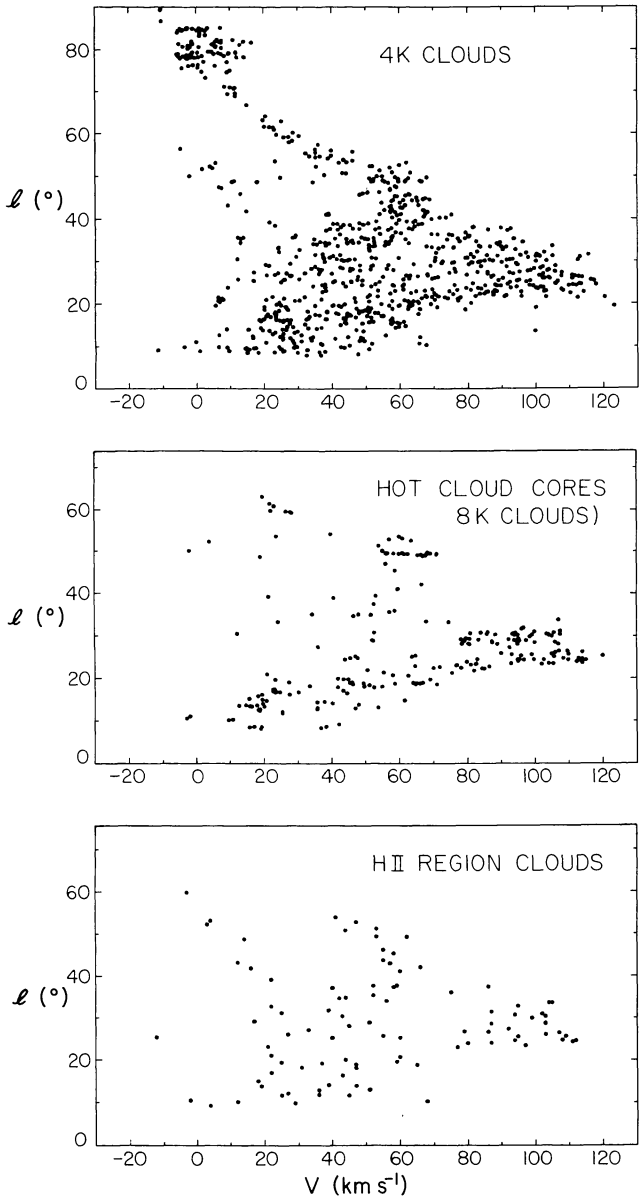

FIG. 3.—The (l, V) distribution of 4 K clouds, cloud cores, and H II region clouds is shown. The latter two samples exhibit tighter confinement in the (l, V)-plane, indicative of a spiral arm population.

km s^{-1}) and to $l = 50°$ ($V = 65$ km s^{-1}). On the other hand, both the hot cores and the H II region clouds are concentrated along two arcs corresponding to the Scutum and Sagittarius arms from $l = 0°$ ($V = 0$ km s^{-1}) to $l = 30°$ and $l = 50°$, respectively, at the velocity terminus.

It is expected that the Galactic distribution of clouds with massive star formation is somewhat better mapped using the centroid velocities and positions of the CO clouds rather than those of the recombination lines. The measurement uncertainties in the CO velocities are about 4 times smaller, and the CO values are unaffected by systematic gas flows which can occur within the H II regions. The (l, V) diagram shown for the H II region clouds thus yields a slightly more accurate definition of the sites of massive star formation than the equivalent recombination line map for the H II regions themselves (compare with Fig. 1 in Downes *et al.* 1980).

The statistical significance of the variations between the cloud samples is most easily judged by the $\pm n^{1/2}$ counting statistics for the bins in the histograms. The concentrations of hot cores and H II region clouds at $l \approx 30°$ and $l \approx 50°$ clearly exceed the fluctuations expected for a random sample.

The clustering for the hot cores cannot be ascribed to sample biases, since the cores were defined at a high enough intensity level that there should be no blending. On the basis of a similar analysis of the distribution of hot and cold cloud cores, Solomon, Sanders, and Rivolo (1985) concluded that the hot cores were significantly clumped in the Galactic plane, whereas the colder regions were distributed rather uniformly. Thus they suggested that the hot emission regions defined the Galactic (spiral) arms. This does not, however, answer the fundamental issue of the nature of the arms, since it is to be

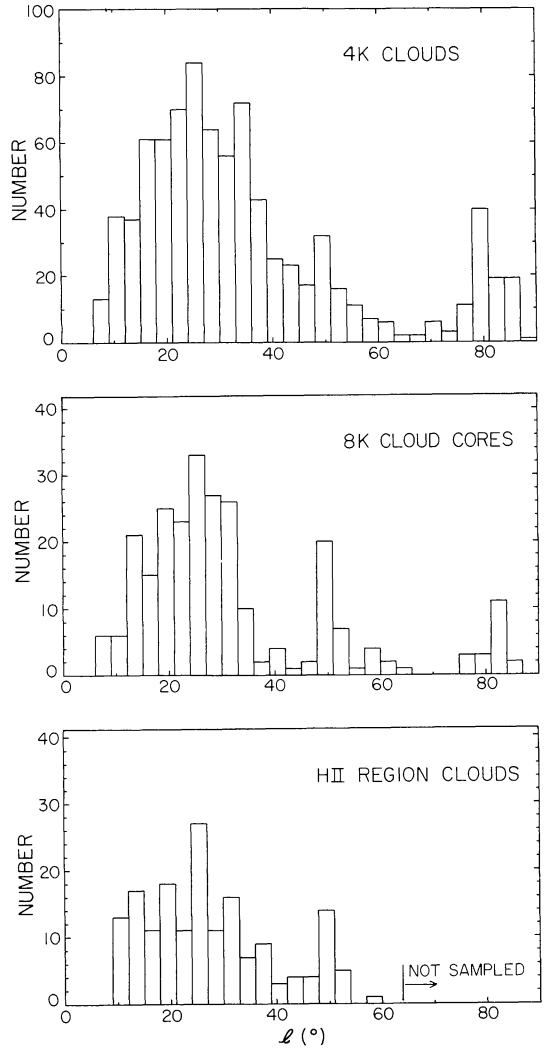

FIG. 4.—Histogram of the longitudes for the 4 K clouds, cloud cores, and H II region clouds. The latter two samples exhibit a marked deficiency in their number at $l = 35°$–$45°$ compared with the general cloud population.

© American Astronomical Society • Provided by the NASA Astrophysics Data System

1987ApJS...63..821S

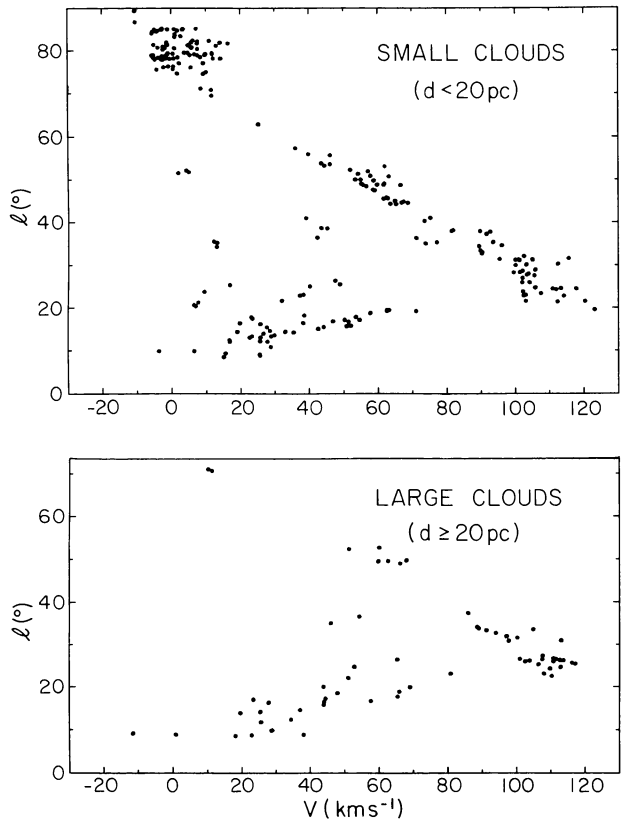

FIG. 5.—The (l, V) distribution of large ($D > 20$ pc) and small clouds is shown for objects in the 4 K sample. Only clouds with more than five (l, b, V) points are included.

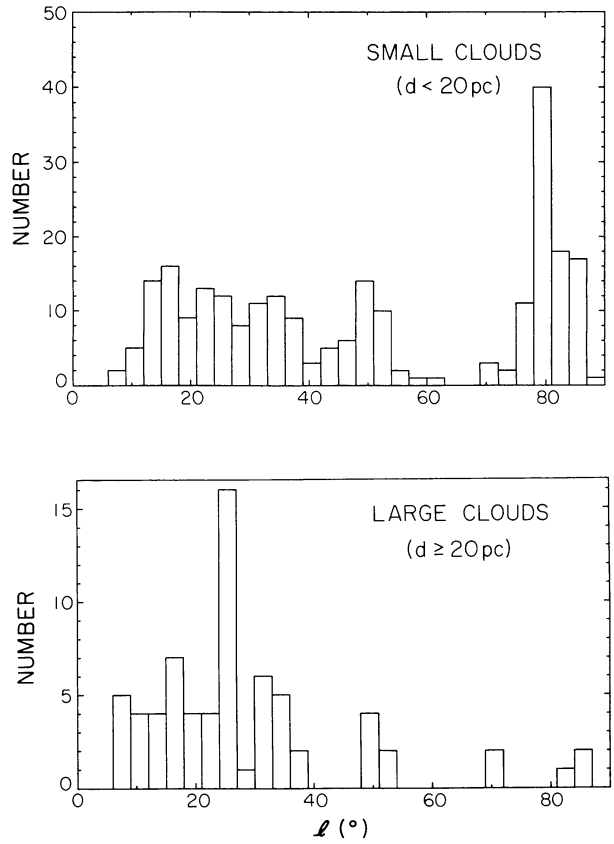

FIG. 6.—Longitude histogram for the large and small clouds from the 4 K sample (see Fig. 5).

expected that clouds with massive star formation will necessarily have higher peak CO temperatures (owing to the presence of luminous stars). These hotter H_2 regions will then necessarily exhibit the same confinement in the (l, V)-plane already known for the H II regions.

b) *Distribution of Large and Small Clouds*

The more interesting question is whether the arm population clouds are *intrinsically* different from the more widely distributed disk population clouds in a way that is not simply a *consequence* of the massive star formation. Figures 5 and 6 show the (l, V) distribution and longitude histogram of large and small clouds for the 4 K sample with the dividing line taken at 20 pc. (Here we include only the 314 clouds in Table 1 for which the distances are reasonably well determined as outlined in § II.) It is evident that the large and small clouds exhibit similar distributions, and neither is more clumped in Galactic azimuth (i.e., in spiral arms) than the other. This result, based on a very limited subsample of the clouds, suggests that the size spectrum for the GMCs is not greatly different between the arm and interarm regions. It must therefore be concluded that although high-mass star formation occurs preferentially in larger clouds, cloud size is not the *determining* factor for massive star formation.

The higher rate of massive star formation in the larger clouds cannot be simply a result of the greater mass of these clouds, since Solomon, Sanders, and Rivolo (1985) estimate that approximately 60% of the total Galactic CO emission (and therefore 60% of the total Galactic H_2—see § V) arises from the *cooler* disk population cloud cores, yet we have shown that the majority of the H II regions are associated with hotter, larger spiral arm clouds.

V. CLOUD MASSES, DENSITIES, AND CO LUMINOSITIES

To date, most estimates of the mass of molecular gas in the Galaxy have been based on measurements of the integrated CO emission using a simple constant of proportionality [generally $(2\text{–}4)\times 10^{20}$ H_2 cm^{-2} (K km s^{-1})$^{-1}$] to convert from the CO emission integral to H_2 column density (cf. Sanders, Solomon, and Scoville 1984; Bloemen *et al.* 1984). With the large sample of clouds defined in the present study, it becomes possible to test this assumption, estimating virial masses of individual clouds and correlating these masses with the observed CO luminosities. (A summary of these results and theoretical discussion is given by Scoville and Sanders 1987.)

For a cloud with a modestly peaked density distribution ($\rho = \rho_R R/r$, where $R = D/2$), the three-dimensional velocity dispersion averaged over the cloud in virial equilibrium (considering only gravity) is

$$\sigma_V(3-d) = \left(\frac{\pi}{4} G\rho_R\right)^{1/2} D. \quad (5)$$

© American Astronomical Society • Provided by the NASA Astrophysics Data System

1987ApJS...63..821S

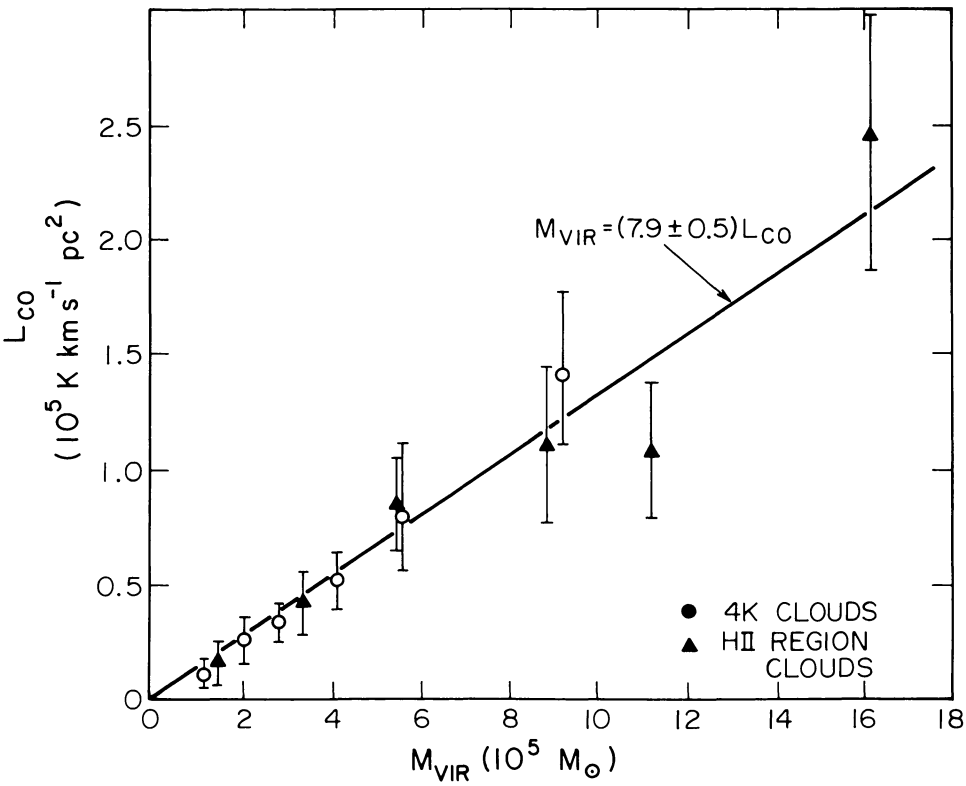

FIG. 7.—Variation of the CO luminosity L_{CO} (K km s^{-1} pc^2) integrated over the projected area of the clouds is shown as a function of the virial mass derived from the measured diameter and velocity dispersion. Only clouds for which the kinematic distance ambiguity is resolved are included in this sample. The straight line $M_{vir}=(7.9\pm0.5)L_{CO}$ is fitted to the binned data over the range $M_{vir}=10^5$ to 2×10^6 $M_\odot$. The CO luminosity, velocity dispersion, and cloud sizes were measured at the same cutoff temperature in each cloud (col. [22] of Table 2).

If σ_V is the *observed* one-dimensional velocity dispersion, then the mean density is

$$\langle\rho\rangle=\frac{3}{2}\rho_R=\frac{18}{\pi G}\left(\frac{\sigma_V}{D}\right)^2, \tag{6}$$

and the virial mass is

$$M_{vir}=\frac{3}{G}D\sigma_V^2. \tag{7}$$

For D and σ_V measured in pc and km s^{-1}, respectively, equation (7) becomes

$$M_{vir}=698D\sigma_V^2\ M_\odot. \tag{8}$$

(For a uniform-density cloud the derived virial mass is 25% less than that given by eq. [8].)[2]

[2]In our application of the virial theorem below, the adopted diameters and velocity dispersions were measured at intensity cutoffs from 1.1 to 5.5 K with a typical value of 4 K. From the growth-curve relations for D and σ_V (eqs. [1] and [2]), we estimate that the measured diameter and dispersion will need to be increased by factors of 1.83 and 1.28, respectively, to equal the true values at the 2 K boundary. Thus the virial masses would be 3 times as great at the 2 K boundaries as at the 4 K boundary.

In Figure 7 the derived virial masses are plotted as a function of the CO luminosities (K km s^{-1} pc^2), where both quantities are measured at the same cutoff T_c (which varies from cloud to cloud for the H II region clouds; see col. [22] in Table 2) and the clouds are binned in mass. (For the 4 K clouds the CO luminosity is calculated from $L_{CO}=2.35$ $\sigma_V\langle T\rangle A$, and A is given by eq. [4].) Although there is clearly a large scatter in the ratio L_{CO}/M_{vir} for each bin (as indicated by the dispersion bars), there is, on average, a linear increase in the CO luminosity with increasing mass over the range 10^5–10^6 $M_\odot$. This trend continues to hold for the few objects with $M_{vir}>2\times10^6$ $M_\odot$, but since there is a higher probability that the larger clouds are blends of several objects, we have not included them on the figure. The best-fit straight line gives

$$M_{vir}=(7.9\pm0.5)L_{CO}, \tag{9a}$$

where L_{CO} is in K km s^{-1} pc^2 and M_{vir} is in $M_\odot$. Dividing equation (9a) by a factor of 1.36 to remove the He contribution yields

$$M_{H_2}=(5.8\pm04)L_{CO}, \tag{9b}$$

which is equivalent to a conversion factor of 3.6×10^{20} H_2 cm^{-2} (K km s^{-1})$^{-1}$ for translating integrated CO line

© American Astronomical Society • Provided by the NASA Astrophysics Data System

1987ApJS...63..821S

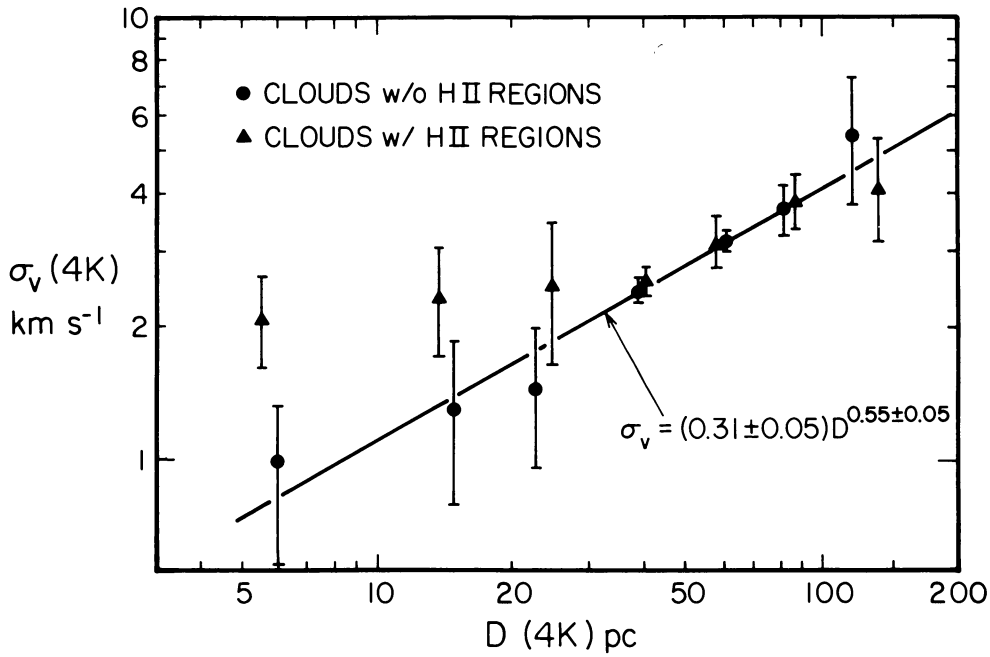

FIG. 8.—Diameter–velocity dispersion relation is shown for both the 4 K clouds and the clouds associated with H II regions. In each case the diameter and dispersion were reduced to the same cloud boundary temperature (4 K), using the growth curves shown in Fig. 1. The binned data for the 4 K sample are fitted by $\sigma_V(4\text{ K}) = (0.31+0.05)\,D(4\text{ K})^{0.55\pm0.05}$ km s^{-1} over the range $D(4\text{ K}) = 6$–120 pc. The H II regions obey this law at $D > 30$ pc but have almost constant $\sigma_V(4\text{ K}) = 2.5$ km s^{-1} below 30 pc.

intensities into H_2 column density. This conversion factor is 15% lower than the value adopted by Sanders, Solomon, and Scoville (1984) to estimate the total Galactic H_2 mass after compensation for the use of different values of R_0. ($M_{\rm vir}/L_{\rm CO} \propto R_0^{-1}$; here we used $R_0 = 8.5$ kpc as compared with $R_0 = 10$ kpc used by them.) Inclusion of the He content of the GMCs increases the total mass by a factor of 1.36, and the conversion factor for the *effective* H_2 mass becomes 4.9×10^{20} H_2 cm^{-2} (K km s^{-1})$^{-1}$.

It should be emphasized that the relationship derived above between CO luminosity and virial mass was based on GMCs with and without H II regions. No significant difference is seen in the ratio $M_{\rm vir}/L_{\rm CO}$ for the hotter H II region clouds ($\bar{T}_p = 11.4$ K, compared with $\bar{T}_p = 7.4$ K) despite the expectation that they might have a higher CO emissivity per unit mass of gas than colder clouds. There is some evidence in the sample of 4 K clouds that the H_2 conversion ratio depends on the cloud size. For $D = 20$ and 90 pc, the constants of proportionality could be 50% larger and smaller, respectively.

The clouds measured in our two samples also yield a well-defined relation between the velocity dispersion and the cloud diameter. In Figure 8 we show the binned data for the H II region and general cloud populations with both the dispersion and the diameter reduced to the 4 K threshold level. At $D > 30$ pc both samples are consistent with a single size/line-width relation

$$\sigma_V(4\text{ K}) = (0.31\pm0.05)\,D(4\text{ K})^{0.55\pm0.05}\text{ km s}^{-1}. \quad (10a)$$

For $D < 30$ pc, equation (10a) continues to hold for the general cloud population, but the H II region sample has a much shallower law—approximately constant $\sigma_V = 2$–3 km s^{-1}. If, as is customarily done, the velocity dispersion is estimated based on a 0 K threshold (rather than 4 K), then using equation (2a) to obtain the full velocity dispersion, we find

$$\sigma_V = (0.5\pm0.1)\,D^{0.55\pm0.05}\text{ km s}^{-1} \quad (10b)$$

for a cloud measured in spatial extent at the 4 K boundary. [Eq. (10) agrees well with the relation $\Delta V = (0.88\pm0.16)\,D^{0.62\pm0.05}$ found by Sanders, Scoville, and Solomon 1985, where their ΔV is the full line width at the 2 K level, which for a Gaussian line gives $\Delta V_{\rm FWHM} = 2.35\,\sigma_V$. (The majority of their cloud sample had $T_p = 3$–6 K.)]

Combining equations (6) and (10b), we find a mean density

$$\langle\rho\rangle = 8.0\times10^{-22}\left(\frac{D}{40\text{ pc}}\right)^{-0.9}\text{ g cm}^{-3} \quad (11a)$$

and

$$\langle n_{\rm H_2}\rangle = 180\left(\frac{D}{40\text{ pc}}\right)^{-0.9}\text{ cm}^{-3}. \quad (11b)$$

(To go from eq. [11a] to eq. [11b], the mass density was divided by a factor 1.36 to remove the He content.) Equation (11b) predicts that clouds of diameter 10–100 pc have mean H_2 number densities of from 625 to 80 cm^{-3}. The latter value is approximately a factor of 5 higher than the mean density required to be stable against the Galactic tidal force at $R \geq 3$ kpc, and thus it is unlikely that even the lowest density giant molecular clouds are significantly affected by tidal disruption.

© American Astronomical Society • Provided by the NASA Astrophysics Data System

1987ApJS...63..821S

As noted above, the smallest clouds in the H II region sample have approximately constant velocity dispersion. The mean value of $\sigma_V = 2.5$ km s^{-1} for this sample at $D(4\text{ K}) < 30$ pc implies a mean H_2 density of 3000 cm^{-3} for $D = 10$ pc (i.e., a factor of 5 higher than for the same size non–H II region cloud). Alternative interpretations for the larger velocity dispersion in the small H II region clouds are that the H II regions generate significant internal motions in excess of what the cloud would ordinarily have (and this energy input is most noticeable in the smaller clouds) or that the H II region clouds have recently undergone cloud collisions which may be causally linked to the formation of high-mass stars (cf. Scoville, Sanders, and Clemens 1986). On the basis of the present data, we cannot rule out one of these explanations in favor of the other.

Although there is no significant difference in the azimuthal distributions of large and small clouds in the H II region sample, we do find a larger dispersion in Z (perpendicular to the Galactic plane) for the lower mass GMCs.[3] In Figure 9 the Z dispersion is shown for the H II region clouds in the mass range 5×10^4–3×10^6 $M_\odot$. The variation as a function of mass is best fitted by the power law

$$\sigma_Z = 100\left(M_{\rm vir}/10^5\ M_\odot\right)^{-0.4\pm0.1}\ \text{pc}. \qquad (12)$$

A similar functional form has been found by Stark (1982) for a limited sample of "spiral arm" clouds. Assuming that the Z motion of the clouds is determined solely by the gravitational potential of the Galactic disk, equation (12) implies that the cloud-cloud velocity dispersion decreases as $M_{\rm vir}^{-1/2}$, as expected for equipartition of the GMC kinetic energy. In order for the random kinetic energy of clouds to be in equipartition, they must survive several cloud-cloud collision times or more than 5×10^7 years (Kwan 1986). (A more precise evaluation of this lower limit on the cloud lifetime requires a detailed modeling of the cloud collisions taking account of gravitational focusing and the actual space density of clouds in and outside of arms.)

[3] This analysis cannot be extended to the 4 K cloud sample because the clouds in that sample with resolved distance ambiguities were selected on the basis of their high Z distance.

VI. THE LOCATIONS OF H II REGIONS IN GIANT MOLECULAR CLOUDS

One model for the formation of massive stars, the progenitors of giant H II regions, proposes that the successive generations or episodes of OB star formation are triggered by the compression of neutral gas at the periphery of the high-pressure H II regions from preceding generations of OB stars (e.g., Elmegreen and Lada 1977). If the formation of the first-generation H II regions is caused by an exterior, Galactic-scale phenomenon such as the shock associated with a spiral density wave, one might expect a preponderance of H II regions appearing on the surface of clouds as "blisters" (cf. Israel 1978).

In a recent investigation Waller *et al.* (1987) have analyzed the positions of 54 H II regions relative to the cloud centers and find only weak evidence for peripheral H II regions; most appear centrally concentrated with a radial probability den-

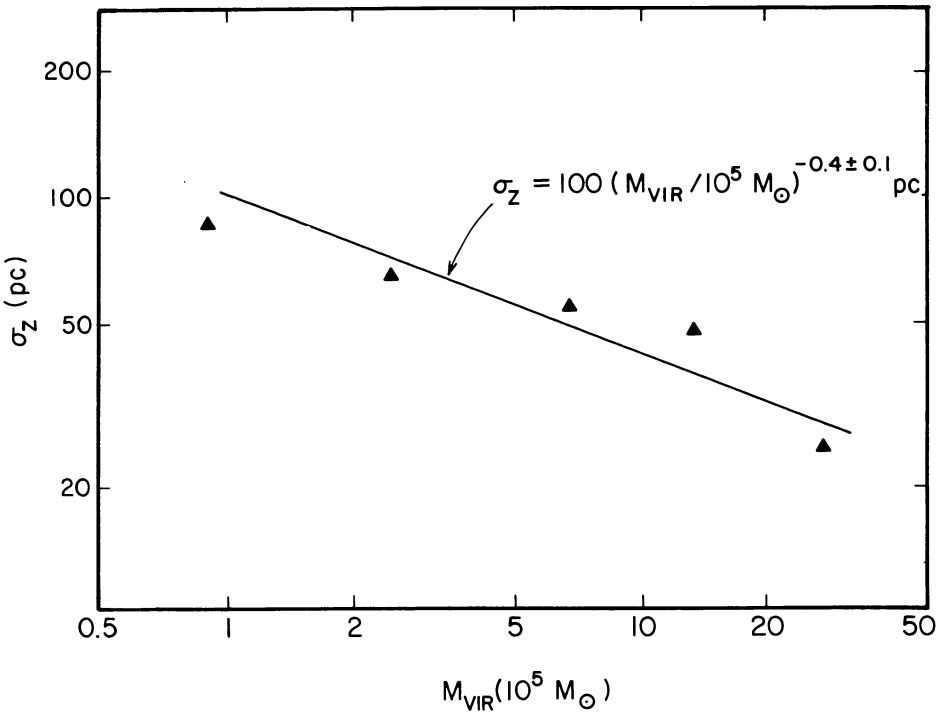

FIG. 9.—The dispersion in Z is shown as a function of virial mass (corrected to the 2 K boundary) for the H II region clouds. The mass bins were chosen to have between 15 and 25 clouds each. The systematic decrease in σ_Z for more massive GMCs is consistent with equipartition of the cloud random kinetic energies.

© American Astronomical Society • Provided by the NASA Astrophysics Data System

1987ApJS...63..821S

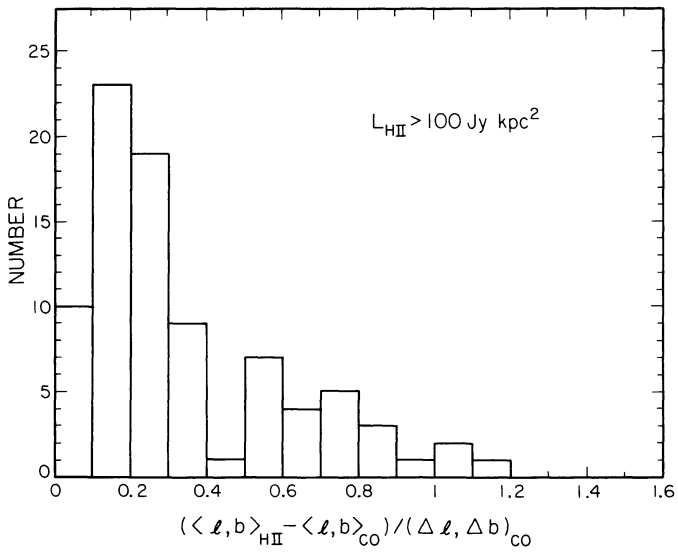

FIG. 10.—Distribution of offsets for the H II region locations relative to the centroids of their associated GMCs is shown, normalized by the cloud radii at the 2 K boundary. Only luminous H II regions for which $L_{H\ II} > 100$ Jy kpc^2 are used here.

sity proportional to r^{-1} (which is probably similar to the internal H_2 mass distribution). With the larger sample of H II region clouds contained in Table 2 for which we now have full two-dimensional maps [rather than the (b, V) maps used by Waller *et al.* 1987], we reexamine this issue.

Figure 10 shows the distribution of offsets in the positions for 86 H II regions with $L_{H\ II} > 100$ Jy kpc^2 from the cloud centroid position measured in CO. The offsets are in each case normalized by the cloud radius, corrected using equation (1) to the 2 K level. This distribution exhibits a peak near the cloud centroids (in the 0.1–0.2 bin) and falls off gradually at larger offsets. Fewer than a third of the luminous H II regions are found outside 50% of the 2 K radius. For power-law distributions of H II regions ($\rho \propto r^{\alpha}$), approximately 50% and 65% of the H II regions are projected outside $R/2$ for $\alpha = -1$ and $\alpha = 0$, respectively (see Waller *et al.* 1987). Thus the observed distribution shown in Figure 10 indicates a probability density slightly more concentrated toward the cloud CO centroids than r^{-1} but not as steep as r^{-2} (which peaks at zero offset). It should be noted that the position we adopt for the cloud center (the CO emission centroid) will be biased toward the location of the H II region because of the heating of the OB stars. Thus, the distribution of H II region locations derived here will exhibit a false bias toward the apparent cloud centers; this problem is not encountered in the analysis of Waller *et al.* (1987), who defined the cloud centers from the center of the outer emission contours.

Offsets in velocity between the H II regions and the CO centroids are shown in Figure 11. The offsets are symmetrically distributed about 0 km s^{-1}, and the mean offset is +0.4 km s^{-1}. The dispersion of the velocity offsets is ~ 2.9 km s^{-1}. The lack of a velocity bias for the radio H II regions relative to their progenitor clouds contrasts with the significant blueshift for optical H II regions found by Fich, Treffers, and Blitz (1982) and Israel (1978). In the latter case this bias was undoubtedly due to the selection effect that optical H II regions *must* be on the near side of the clouds (in order to avoid extinction), and they are then relatively free to expand toward rather than away from us.

In order to analyze the efficiency for massive star formation in clouds of different mass, we show in Figure 12 the H II region free-free luminosity normalized by the cloud mass for clouds in five mass bins between 2×10^5 and 4×10^6 $M_\odot$. Also shown is the normalized number of giant H II regions ($L_{H\ II} > 30$ Jy kpc^2) as a function of cloud mass. The figure demonstrates that both the efficiency (per unit mass of H_2) for UV emission and for formation of separate OB clusters decreases for high-mass clouds compared with lower mass clouds within this mass range. Thus the formation rate for massive stars is not simply proportional to the total mass of H_2 in a cloud but must depend on other factors (either the Galactic location or the internal properties of the clouds). The cloud mass spectrum for H II region clouds (for which the histogram is given in Fig. 12) is shallower [$N(M) \propto M^{-1.0 \pm 0.4}$] than that for the general cloud population [$N(M) \propto M^{-1.6}$; Liszt, Xiang, and Burton 1981 and Sanders, Scoville, and Solomon 1985). (See Scoville, Sanders, and Clemens 1986 for a discussion of these results.)

VII. CONCLUSIONS

Our analysis of the Massachusetts–Stony Brook Galactic CO Survey has yielded three samples of GMCs and cloud cores for study of the properties and Galactic distribution of molecular emission regions: (1) A complete list (Table 1) of all emission regions with at least one (l, b, V) point exceeding $T_R^* = 5$ K; the properties of these regions are measured out to the 4 K boundary. (2) A complete list (Table 1) of all hot cloud cores with $T_R^* \geq 9$ K measured at the 8 K boundary. (3) Maps (Fig. 13) and measured parameters (Table 2) for 95 clouds associated with 171 radio H II regions.

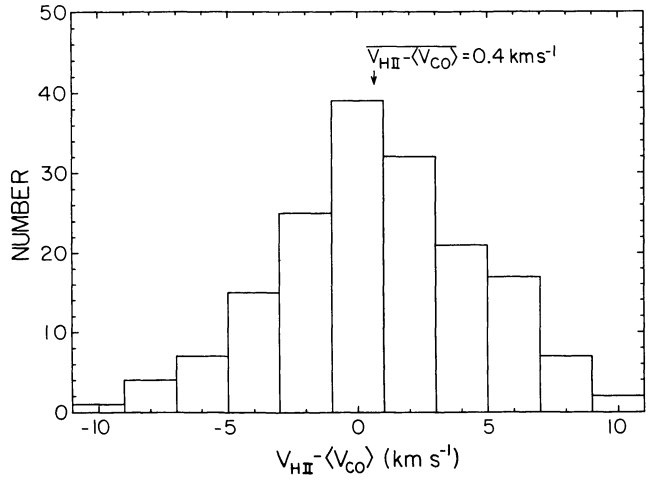

FIG. 11.—Distribution of velocity offsets between H II regions and their associated GMCs is shown. All 171 H II regions listed in Table 2 are used here. The dispersion of the Gaussian fitted to the distribution is $\sigma_V = 2.9$ km s^{-1}. Note that no systematic offset is found between the radio recombination line velocities and the CO centroid velocities.

© American Astronomical Society • Provided by the NASA Astrophysics Data System

1987ApJS...63..821S

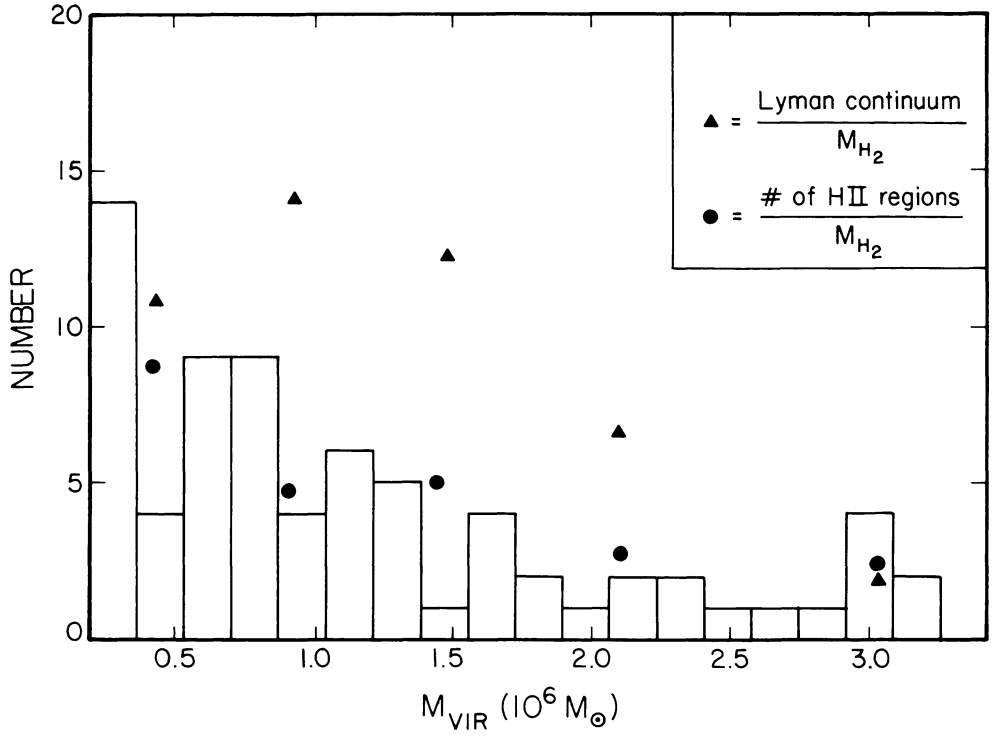

FIG. 12.—Relative efficiency (per unit mass of H_2) for Lyman continuum luminosity and for formation of discrete giant H II regions is shown as a function of virial mass for the H II region clouds.

The major results of our analysis of these three samples are the following:

1. The H II region clouds have systematically hotter cores; they are also larger, and have greater internal velocity dispersion than the general cloud population. However, the *efficiency* for O star formation per unit mass of gas decreases with increased cloud mass over the range 2×10^5–4×10^6 $M_\odot$.

2. Both the general cloud population and the H II region clouds exhibit a strong peak at the 4–7 kpc molecular cloud ring; the hotter GMCs exhibit a more segregated (l, V) distribution than the colder clouds of the general cloud population, suggesting that the former are more confined to the Galactic spiral arms. No significant difference is found in the azimuthal distribution of large and small GMCs.

3. For the clouds with and without H II regions, the virial masses are correlated with the CO luminosity [$M_{vir}(M_\odot) = 7.9L_{CO}$ (K km s^{-1} pc^2)], and the derived relation between integrated CO emission and H_2 column density is $N_{H_2}(cm^{-2}) = 3.6\times10^{20}$ I_{CO}(K km s^{-1}), assuming $R_0 = 8.5$ kpc. The mean H_2 density for a typical GMC of diameter 40 pc at $T_R^* = 4$ K is 180 cm^{-3}.

4. The distribution of H II region positions relative to the CO centroids of the GMCs suggests that their distribution is approximately a power law $\rho(r) \propto r^{-1}$.

This research was supported in part by National Science Foundation grants AST 84-12473 (N. Z. S.) and AST 82-12252 (W. H. W.), by the National Aeronautics and Space Administration *IRAS* Extended Mission Program at the Infrared Processing and Analysis Center grant (D. B. S.) and an *IRAS* General Investigator Grant (N. Z. S. and D. P. C.). M. Yun was supported by a Caltech Summer Undergraduate Research Fellowship and D. Clemens by a B. J. Bok Fellowship at Steward Observatory. We thank Jay Lockman for communicating the results of his H II region survey in advance of publication.

REFERENCES

Bania, T. M. 1980, *Ap. J.*, **242**, 95.
Bloemen, J. B. G. M., Carneo, P. A., Hermsen, W., Lebrun, F., Maddalena, R. J., Strong, A. W., and Thaddeus, P. 1984, *Astr. Ap.*, **139**, 37.
Clemens, D. P. 1985*a*, Ph.D. thesis, University of Massachusetts.
———. 1985*b*, *Ap. J.*, **295**, 422.
Clemens, D. P., Sanders, D. B., Scoville, N. Z., and Solomon, P. M. 1986, *Ap. J. Suppl.*, **60**, 297.
Downes, D., Wilson, T. L., Bieging, J., and Wink, J. 1980, *Astr. Ap. Suppl.*, **40**, 379.
Elmegreen, B. G., and Lada, C. J. 1977, *Ap. J.*, **214**, 725.
Fich, M., Treffers, R. R., and Blitz, L. 1982, in *Regions of Recent Star Formation*, ed. R. S. Roger and P. E. Dewdney (Dordrecht: Reidel), p. 201.
Israel, F. 1978, *Astr. Ap.*, **70**, 769.
Kwan, J. 1986, private communication.
Liszt, H. S., Xiang, D., and Burton, W. B. 1981, *Ap. J.*, **249**, 532.
Lockman, F. J. 1987, in preparation.

© American Astronomical Society • Provided by the NASA Astrophysics Data System

1987ApJS...63..821S

Myers, P. C., Dame, T. M., Thaddeus, P., Cohen, R. S., Silverberg, R. F., Dwek, E., and Hauser, M. G. 1986, *Ap. J.*, **301**, 398.
Sanders, D. B., Clemens, D. P., Scoville, N. Z., and Solomon, P. M. 1986, *Ap. J. Suppl.*, **60**, 1.
Sanders, D. B., Scoville, N. Z., and Solomon, P. M. 1985, *Ap. J.*, **289**, 373.
Sanders, D. B., Solomon, P. M., and Scoville, N. Z. 1984, *Ap. J.*, **276**, 182.
Scoville, N. Z., and Sanders, D. B. 1987, Interstellar Processes, ed. D. Hollenbach and H. Thronson (Dordrecht: Reidel), in press.
Scoville, N. Z., Sanders, D. B., and Clemens, D. P. 1986, *Ap. J.* (*Letters*), **310**, L77.
Solomon, P. M., Sanders, D. B., and Rivolo, R. 1985, *Ap. J.* (*Letters*), **292**, L19.
Stark, A. A. 1979, Ph.D. thesis, Princeton University.
Stark, A. A. 1982, *Kinematics, Dynamics and Structure of the Milky Way*, ed. W. L. H. Shuter (Dordrecht: Reidel), p. 127.
Waller, W. H., Clemens, D. P., Sanders, D. B., and Scoville, N. Z. 1987, *Ap. J.*, **314**, 397.

D. P. Clemens: Steward Observatory, University of Arizona, Tucson, AZ 85721

D. B. Sanders: Physics Department, Caltech 320-47, Pasadena, CA 91125

N. Z. Scoville and M. S. Yun: Astronomy Department, Caltech 105-24, Pasadena, CA 91125

W. H. Waller: Five College Radio Astronomy Observatory, University of Massachusetts, Amherst, MA 01003

© American Astronomical Society • Provided by the NASA Astrophysics Data System

1987ApJS...63..821S

(This Page Intentionally Left Blank)

© American Astronomical Society • Provided by the NASA Astrophysics Data System

1987ApJS...63..821S

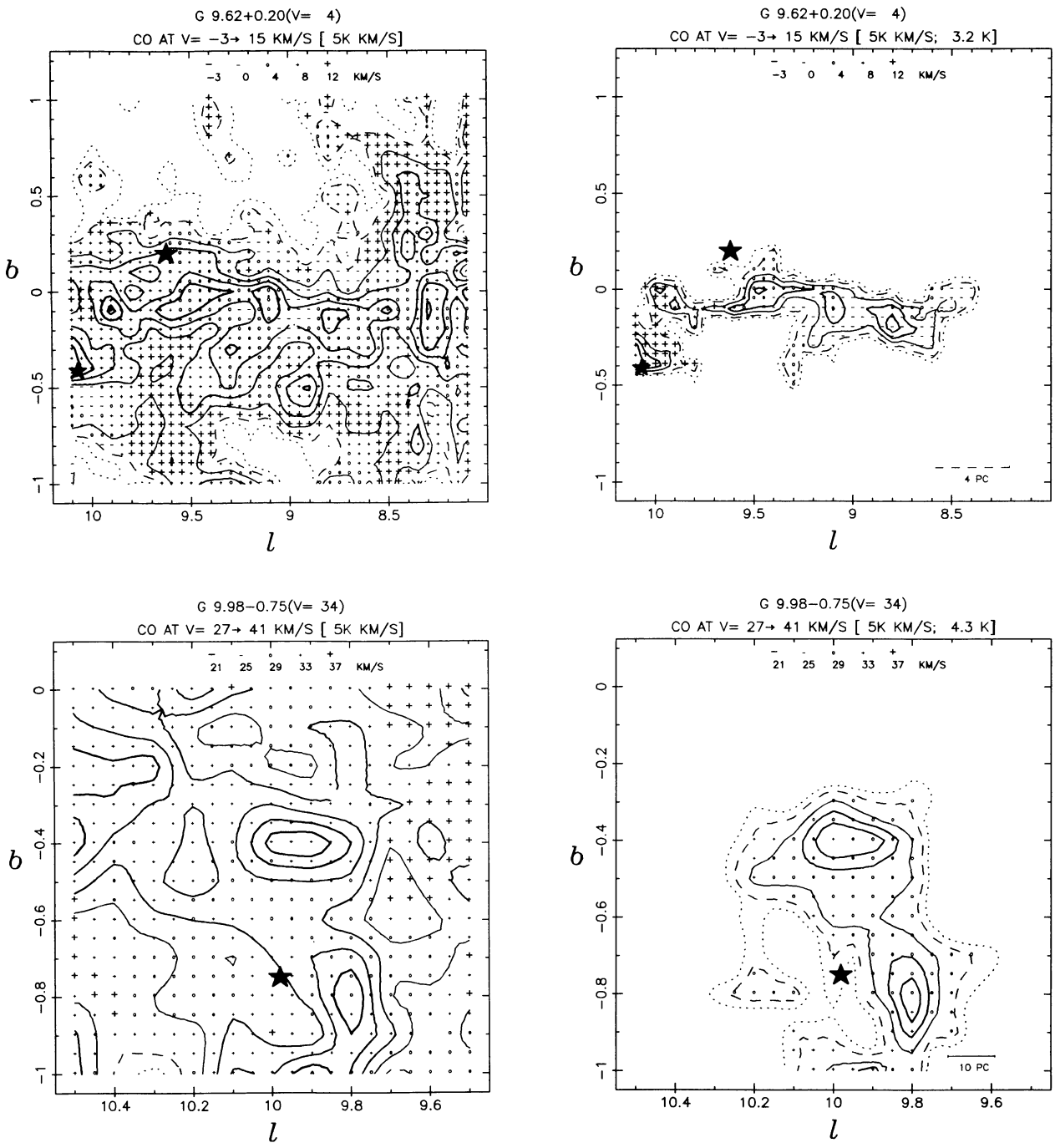

FIG. 13.—Maps of the integrated CO emission in the vicinity of 171 radio H II regions. For each group of associated H II regions two maps are shown: first, the integrated CO emission over a 15–20 km s^{-1} range centered close to the H II region position; second, the integrated CO emission including all (l, b, V) points above the boundary cutoff temperature T_c which are simply connected to the CO emission peak. The second map in each case serves to isolate the CO emission associated with the H II region from the background CO emission. The contours of integrated intensity are in units of 1,2,4,6,... times the number given in the caption at the top of each map. The cutoff temperature T_c is specified at the right of the caption at the top of the second map in each case. The plus, minus, and open circle symbols superposed on the contour maps on a 3′ grid (the sampling interval for most of the CO survey) indicate the CO centroid velocity for emission within the range of integration specified in the caption. The stars indicate the locations of H II regions within 10 km s^{-1} of the CO centroid velocity, and the largest star is the position of the H II region specified in the caption. The H II regions outside the cloud boundary in a given map will generally be found in association with another cloud or within the mapped cloud if the cutoff temperature is lowered. The bar at the lower right in the second map in each case shows the linear scale for the assumed distance of the H II region. When this bar is dashed, the near-far distance ambiguity for the H II region has not been resolved and the near distance is assumed.

© American Astronomical Society • Provided by the NASA Astrophysics Data System

1987ApJS...63..821S

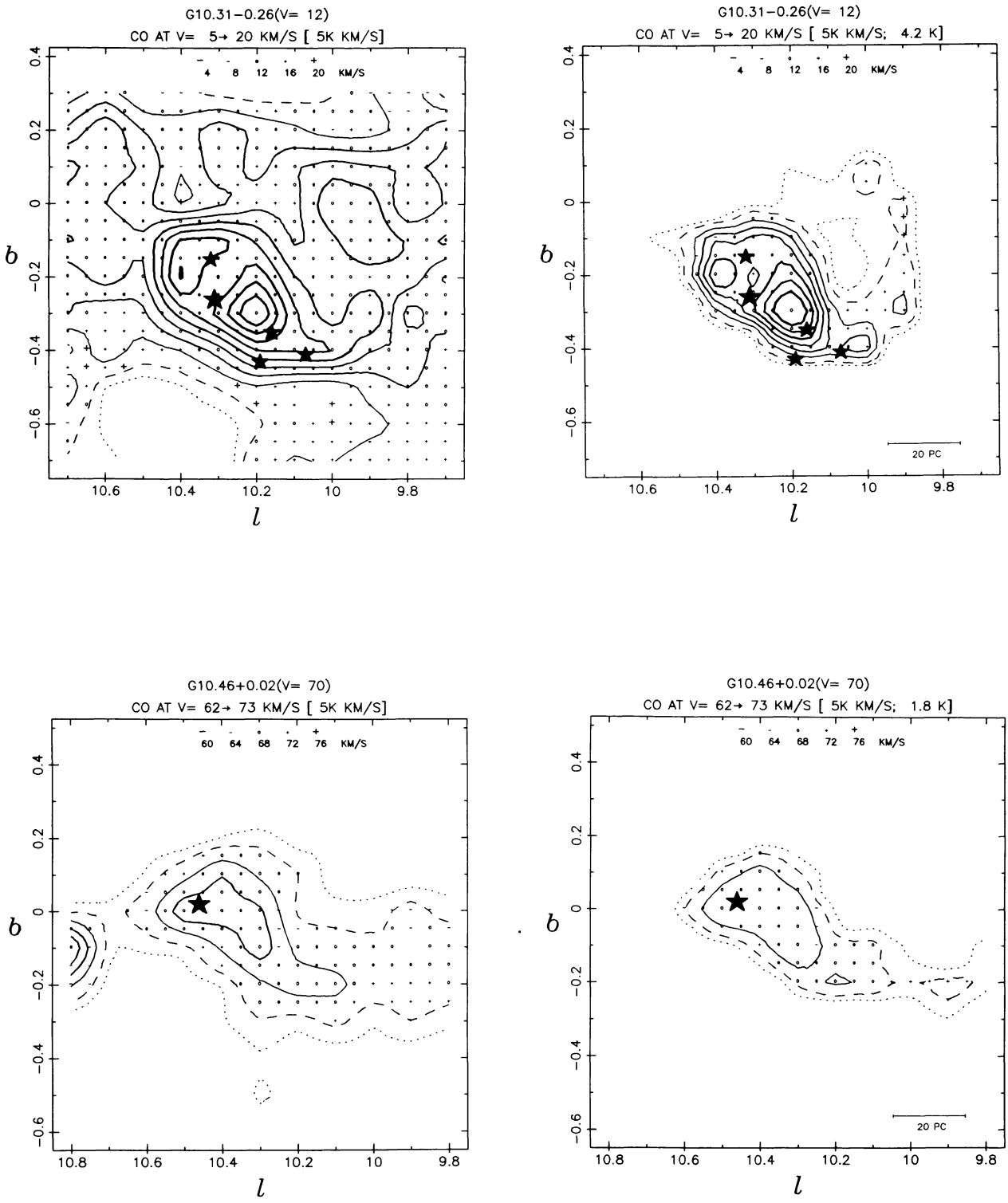

FIG. 13—*Continued*

© American Astronomical Society • Provided by the NASA Astrophysics Data System

1987ApJS...63..821S

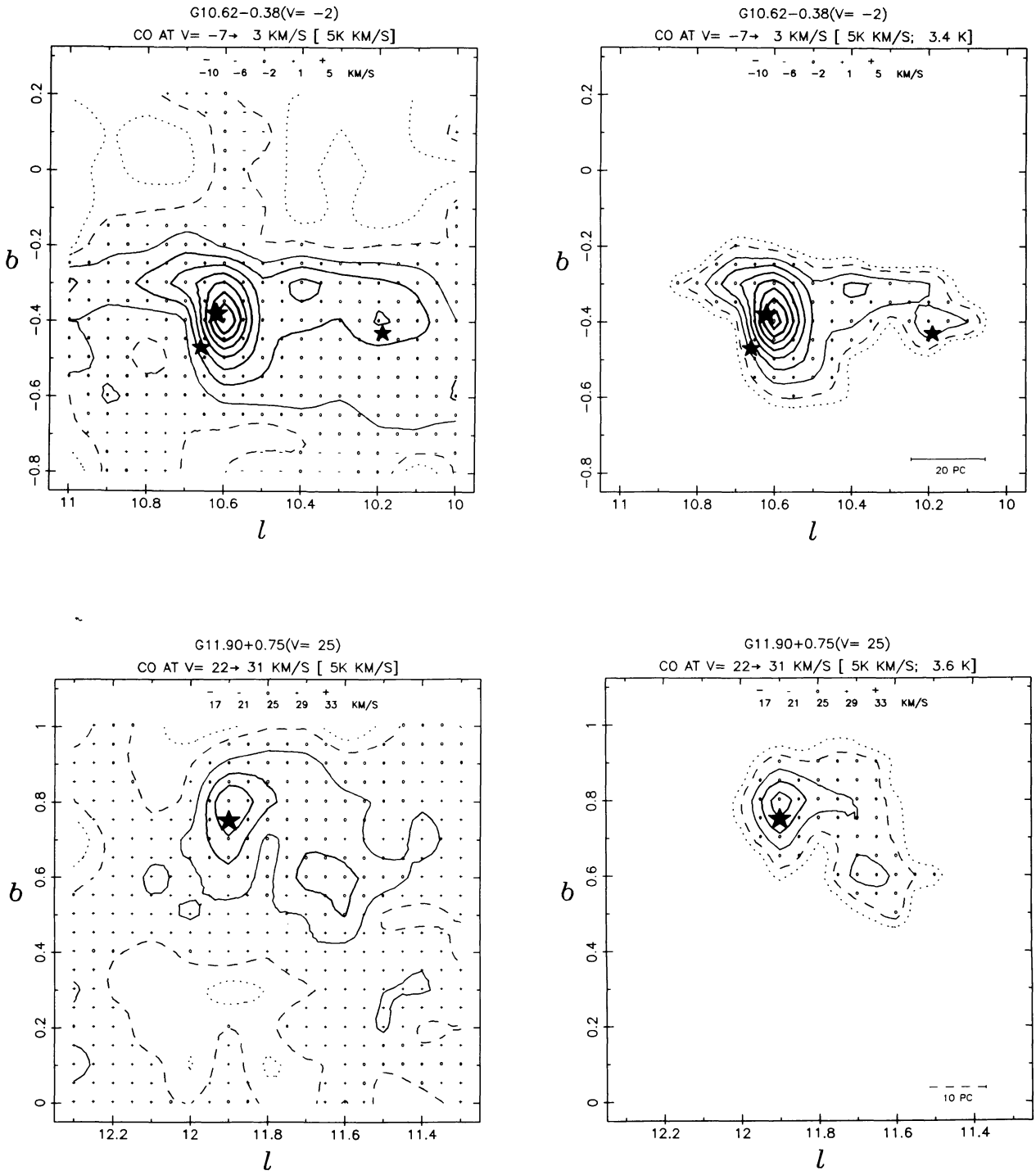

FIG. 13—*Continued*

© American Astronomical Society • Provided by the NASA Astrophysics Data System

1987ApJS...63..821S

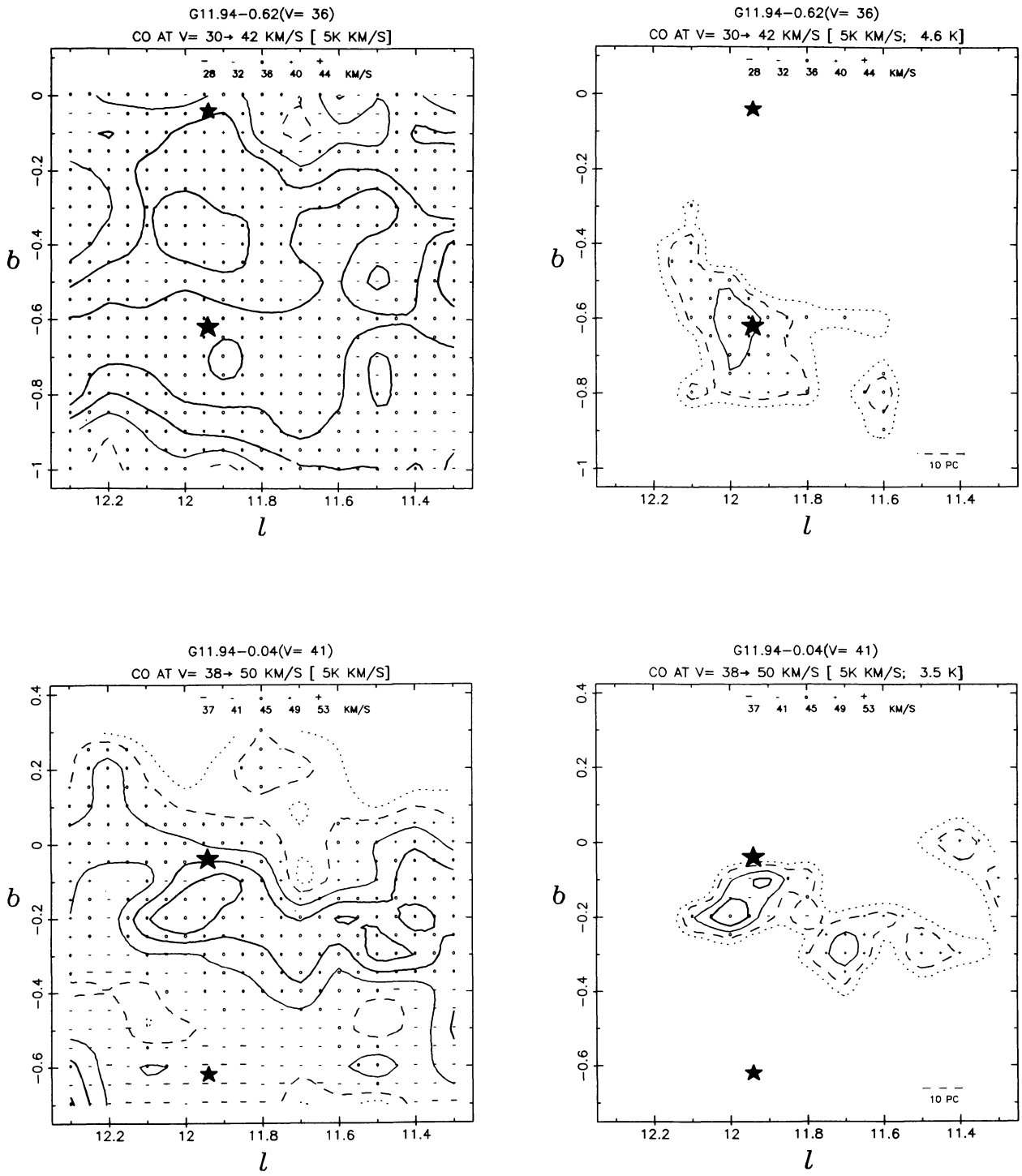

FIG. 13—*Continued*

© American Astronomical Society • Provided by the NASA Astrophysics Data System

1987ApJS...63..821S

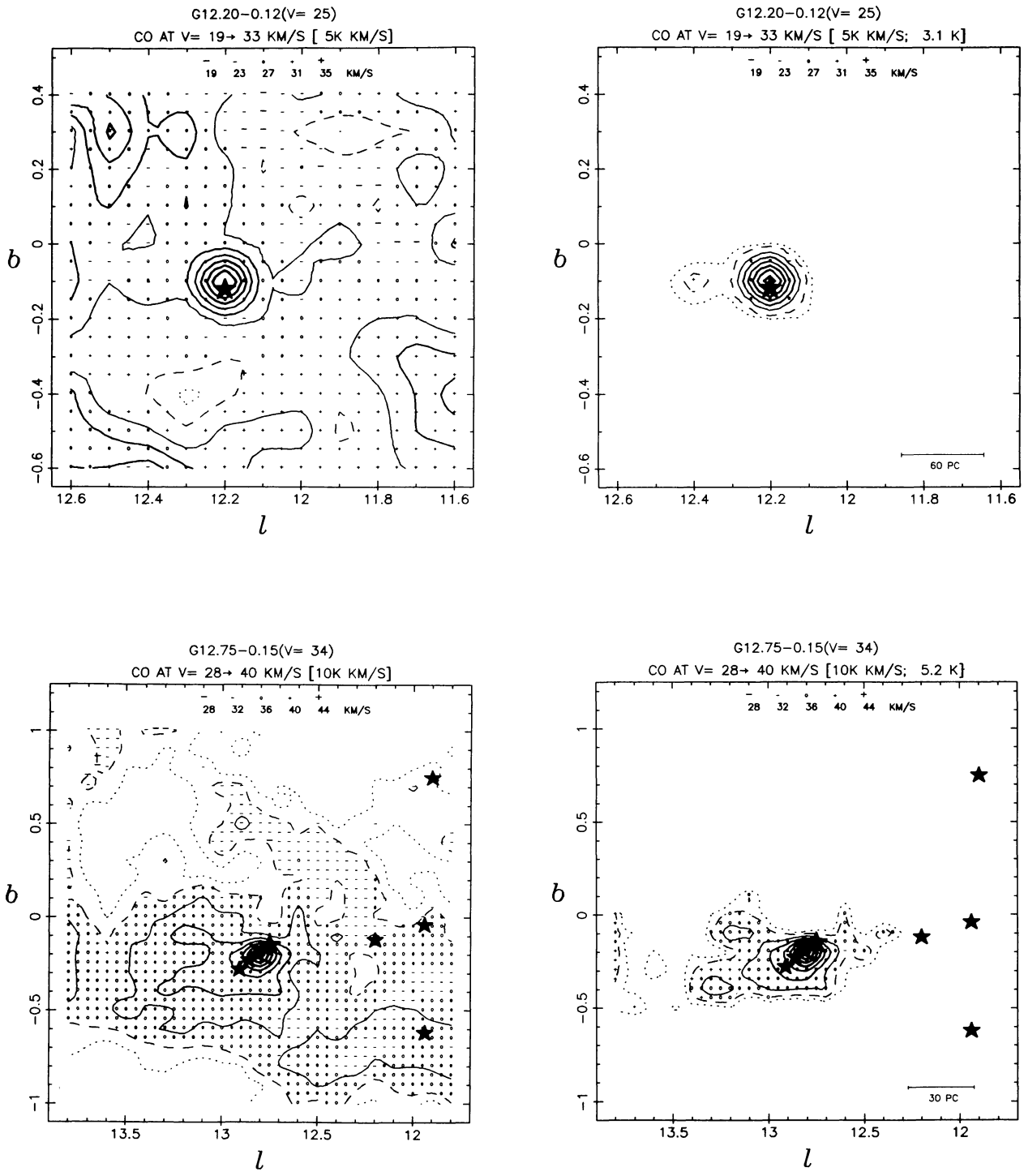

FIG. 13—*Continued*

© American Astronomical Society • Provided by the NASA Astrophysics Data System

1987ApJS...63..821S

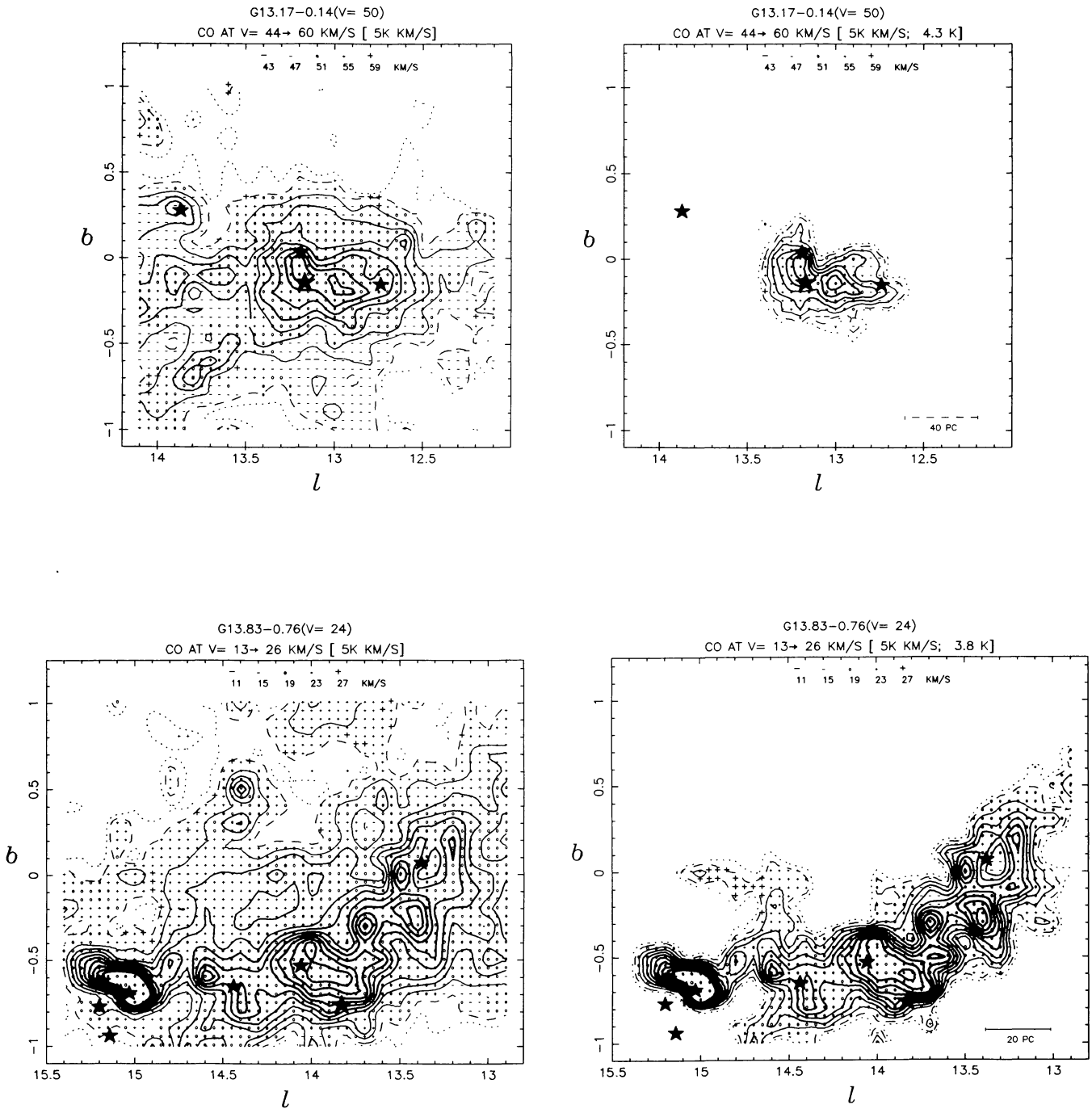

FIG. 13—*Continued*

© American Astronomical Society • Provided by the NASA Astrophysics Data System

1987ApJS...63..821S

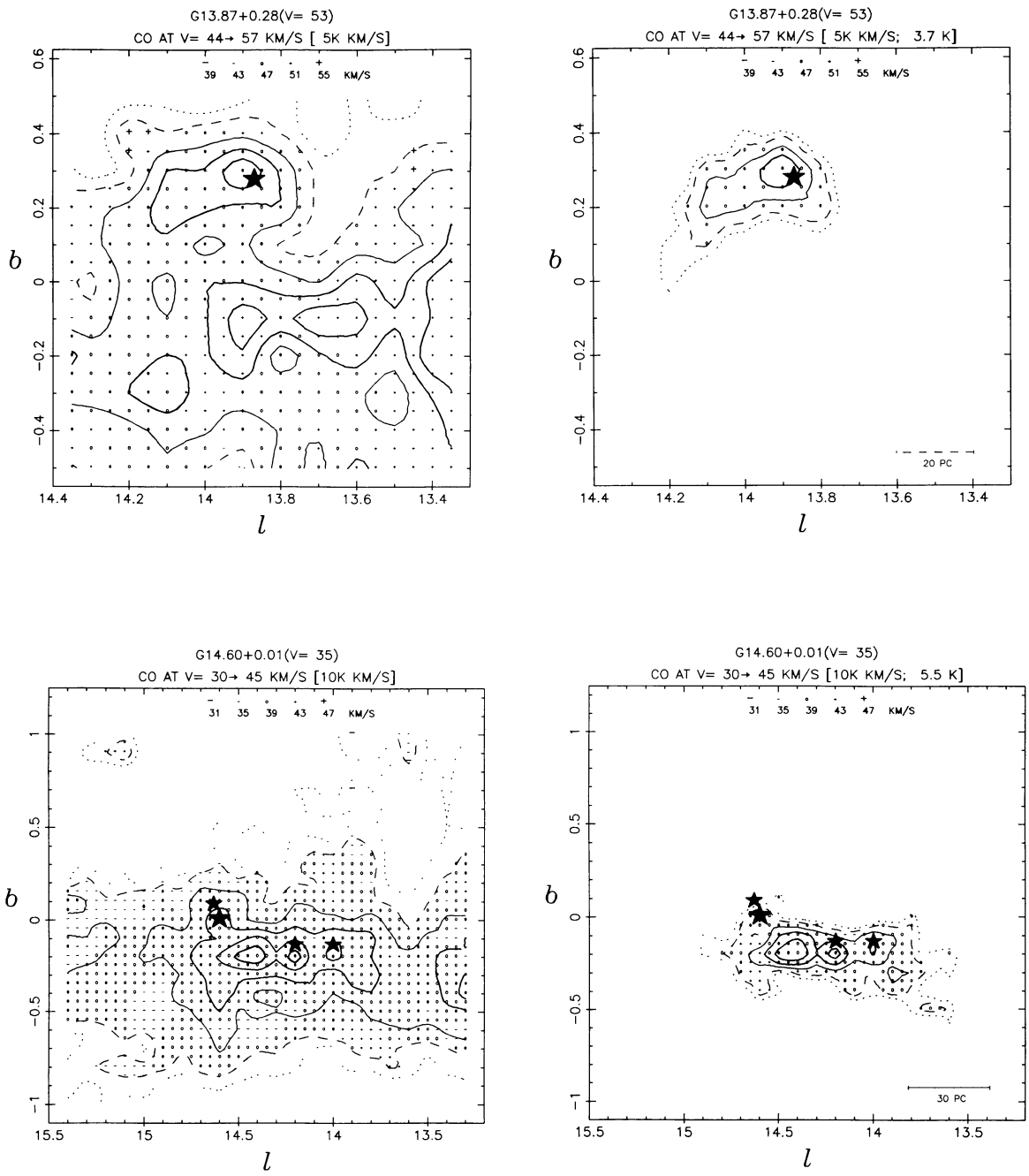

FIG. 13—*Continued*

© American Astronomical Society • Provided by the NASA Astrophysics Data System

1987ApJS...63..821S

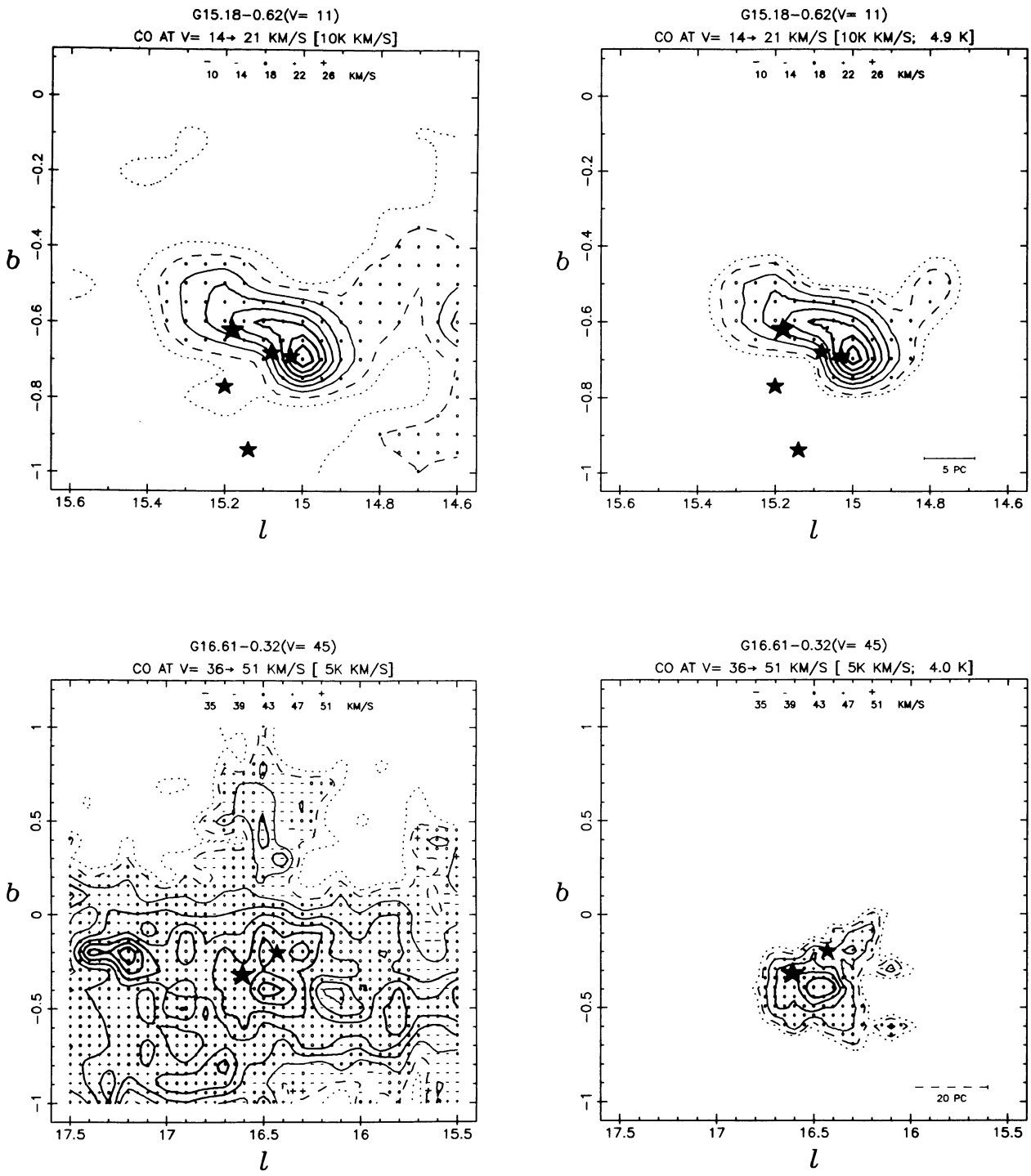

FIG. 13—*Continued*

© American Astronomical Society • Provided by the NASA Astrophysics Data System

1987ApJS...63..821S

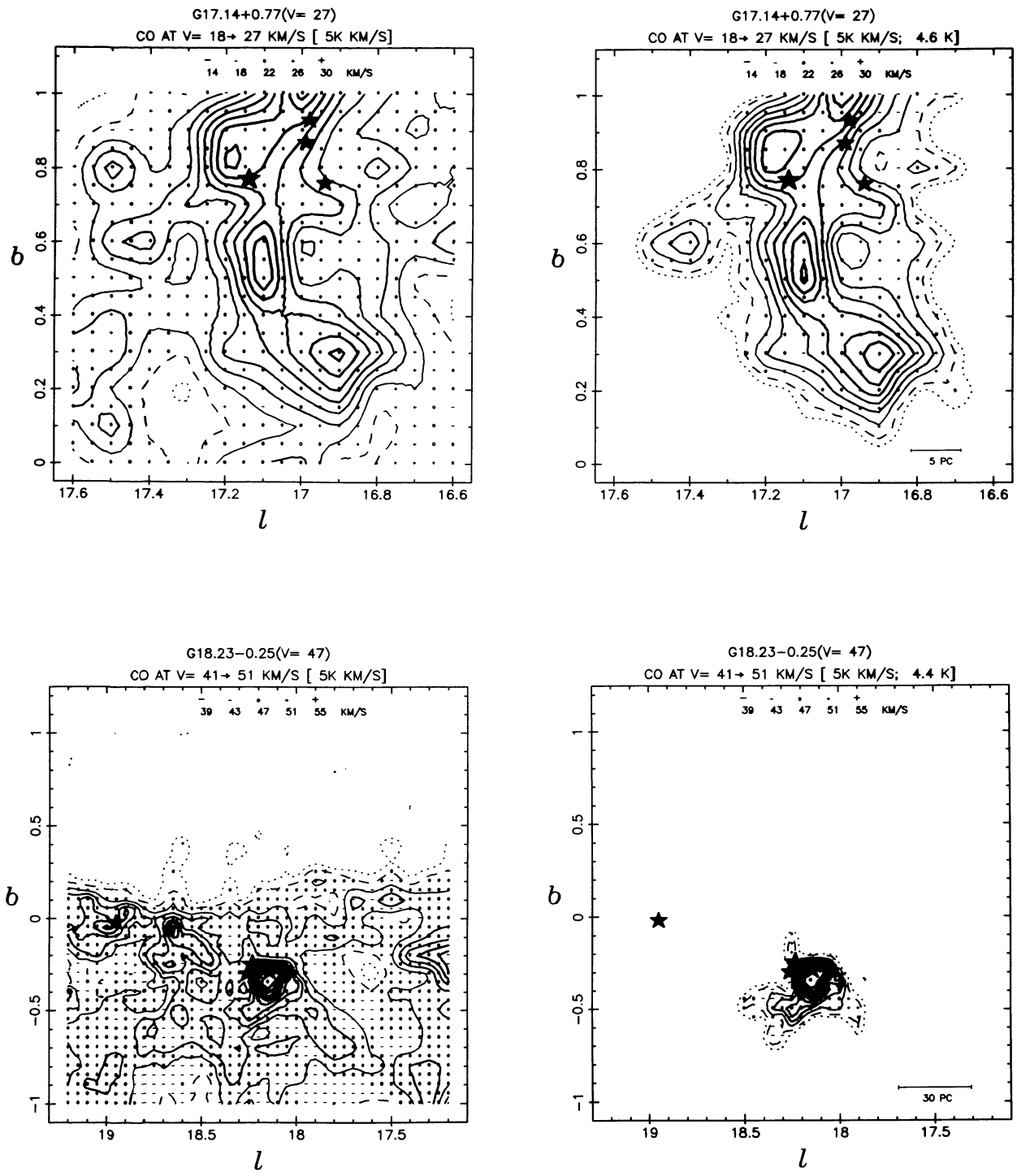

FIG. 13—*Continued*

© American Astronomical Society • Provided by the NASA Astrophysics Data System

1987ApJS...63..821S

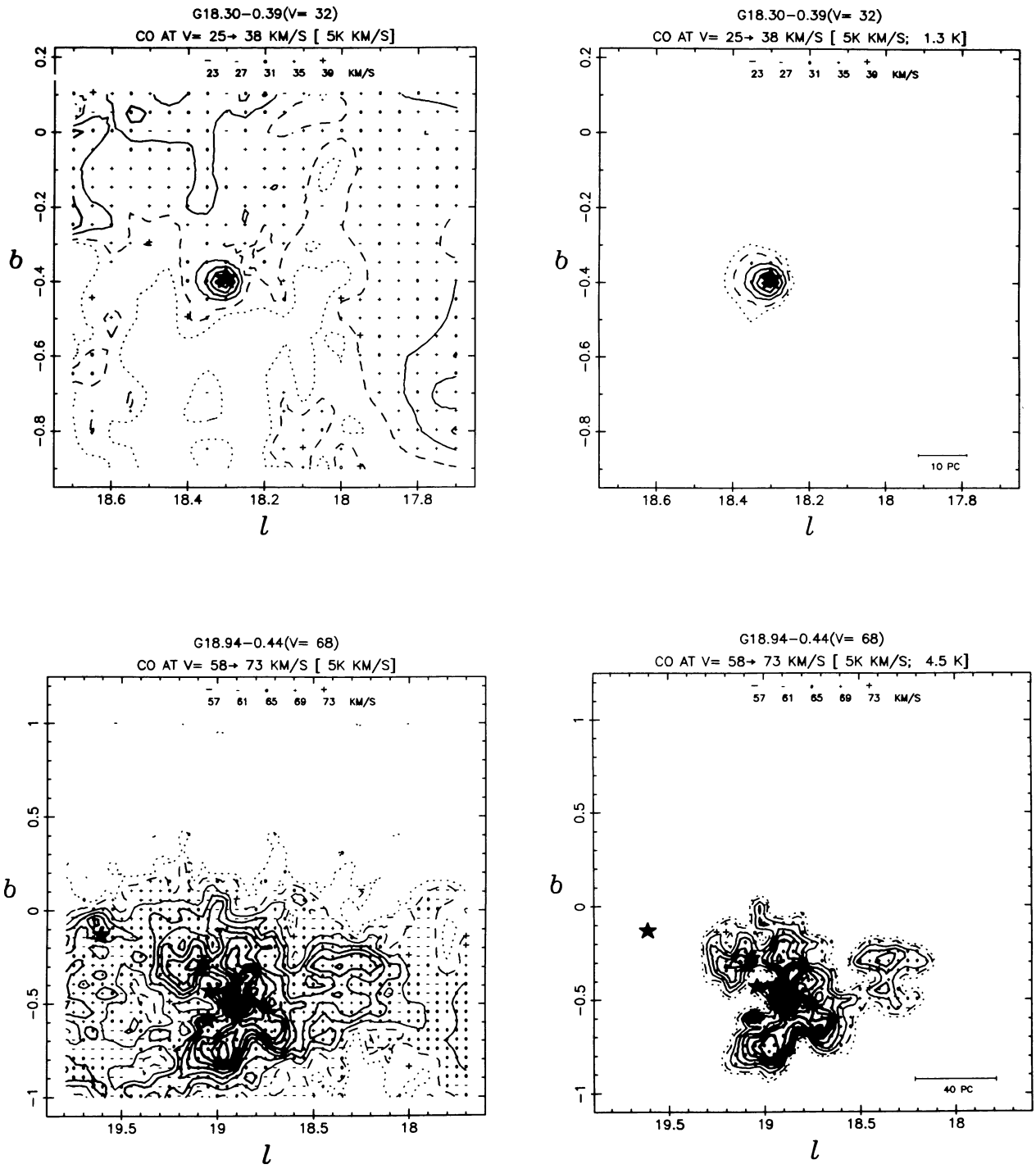

FIG. 13—*Continued*

© American Astronomical Society • Provided by the NASA Astrophysics Data System

1987ApJS...63..821S

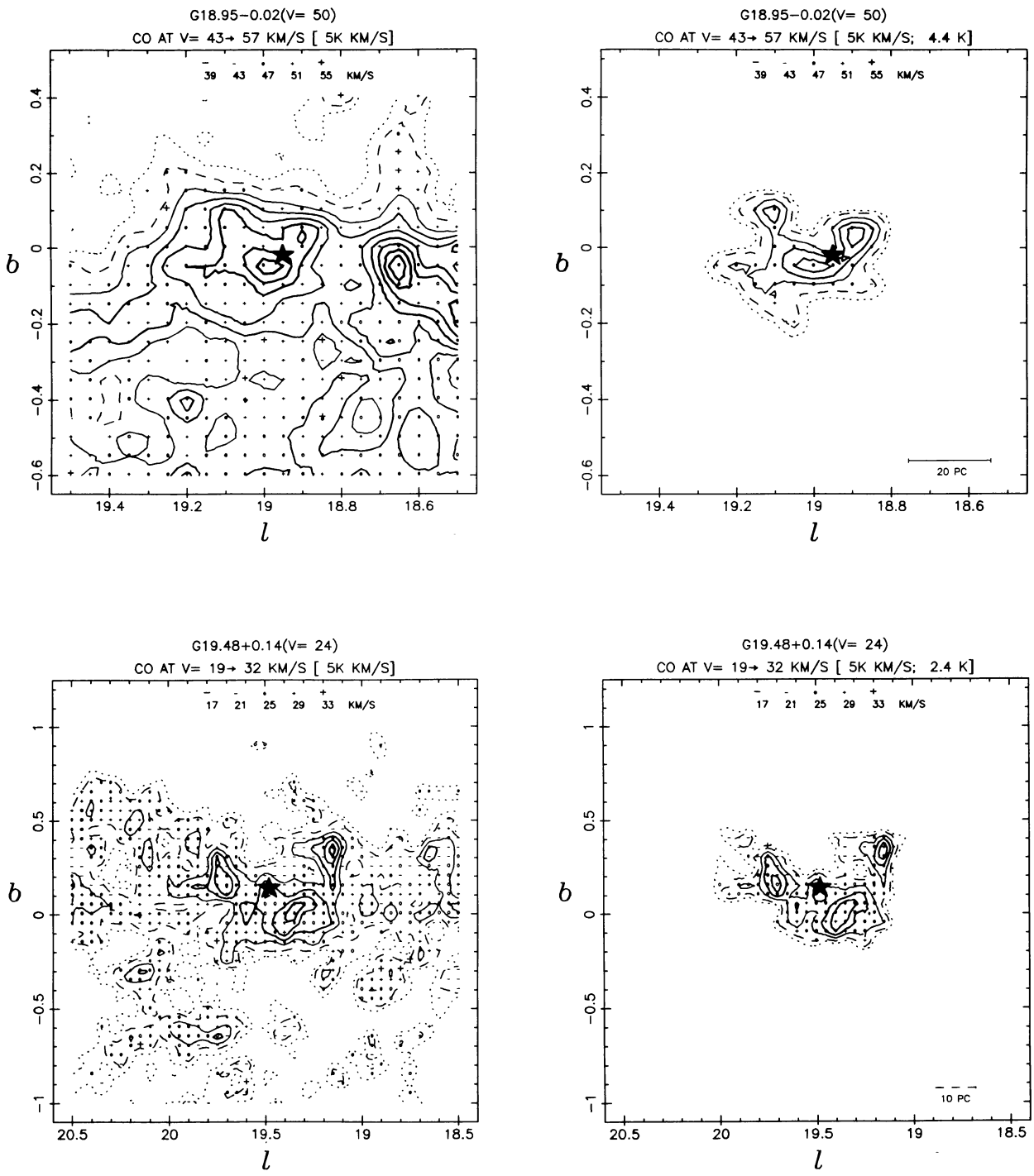

FIG. 13—*Continued*

© American Astronomical Society • Provided by the NASA Astrophysics Data System

1987ApJS...63..821S

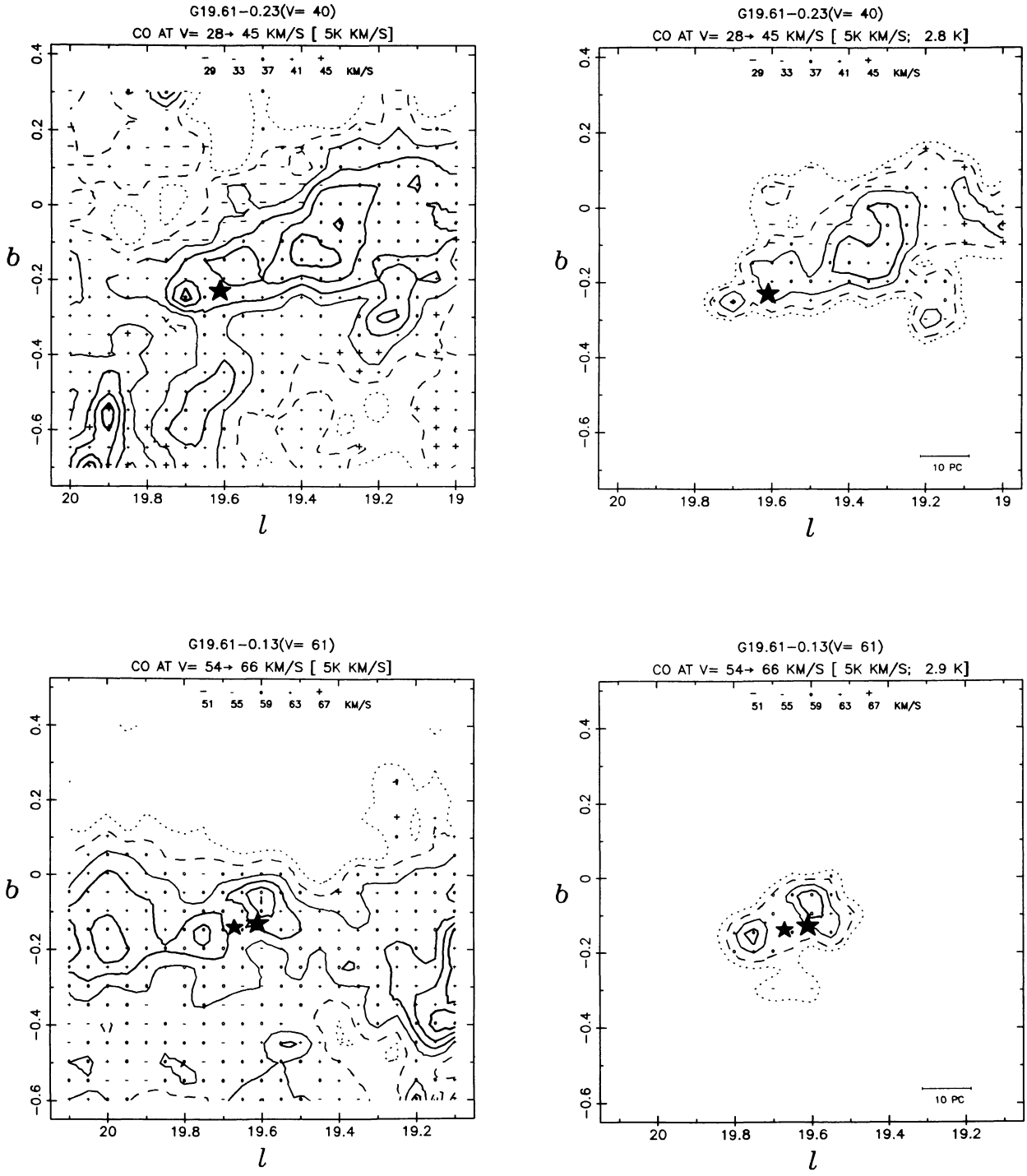

FIG. 13—*Continued*

© American Astronomical Society • Provided by the NASA Astrophysics Data System

1987ApJS...63..821S

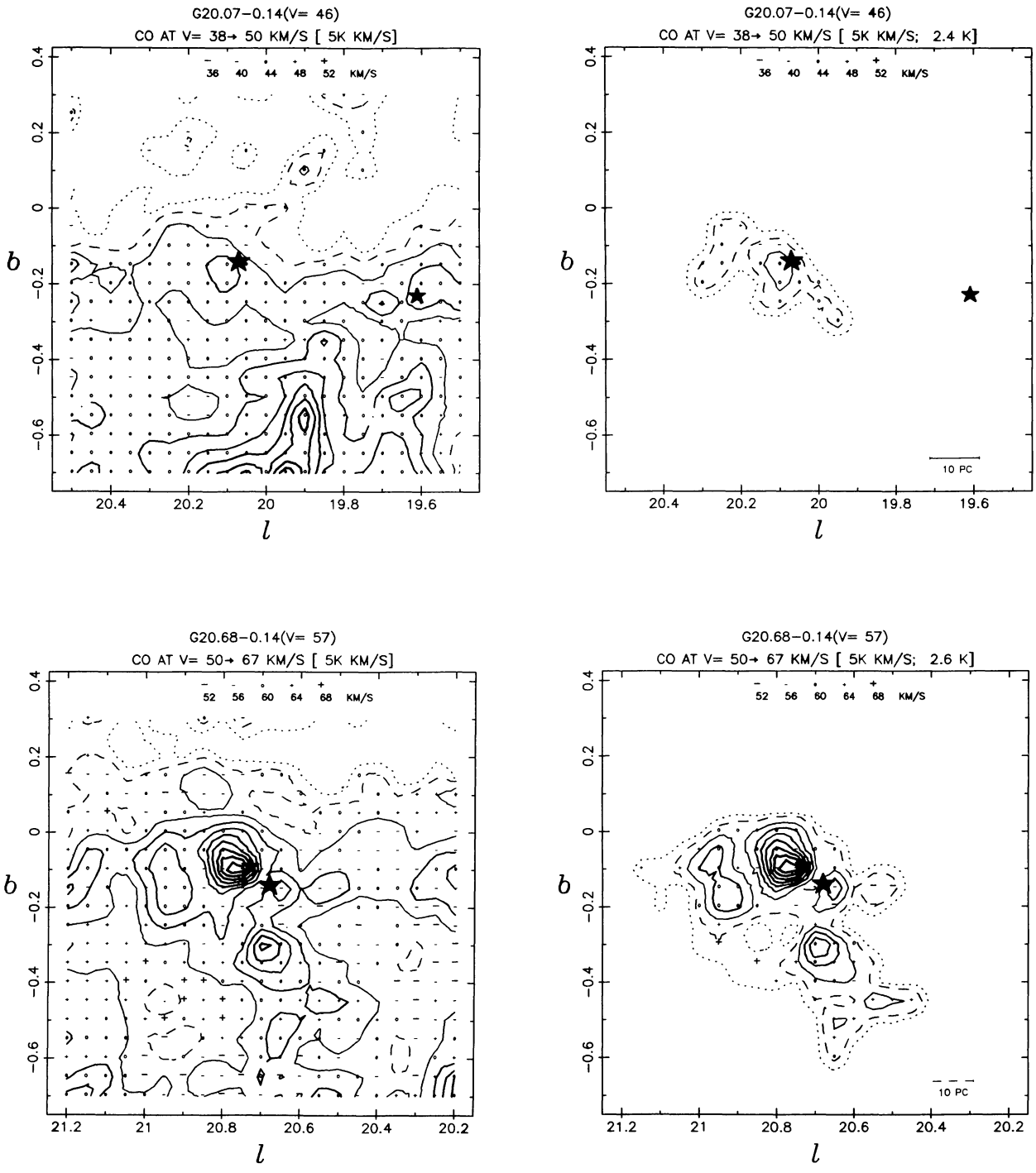

FIG. 13—*Continued*

© American Astronomical Society • Provided by the NASA Astrophysics Data System

1987ApJS...63..821S

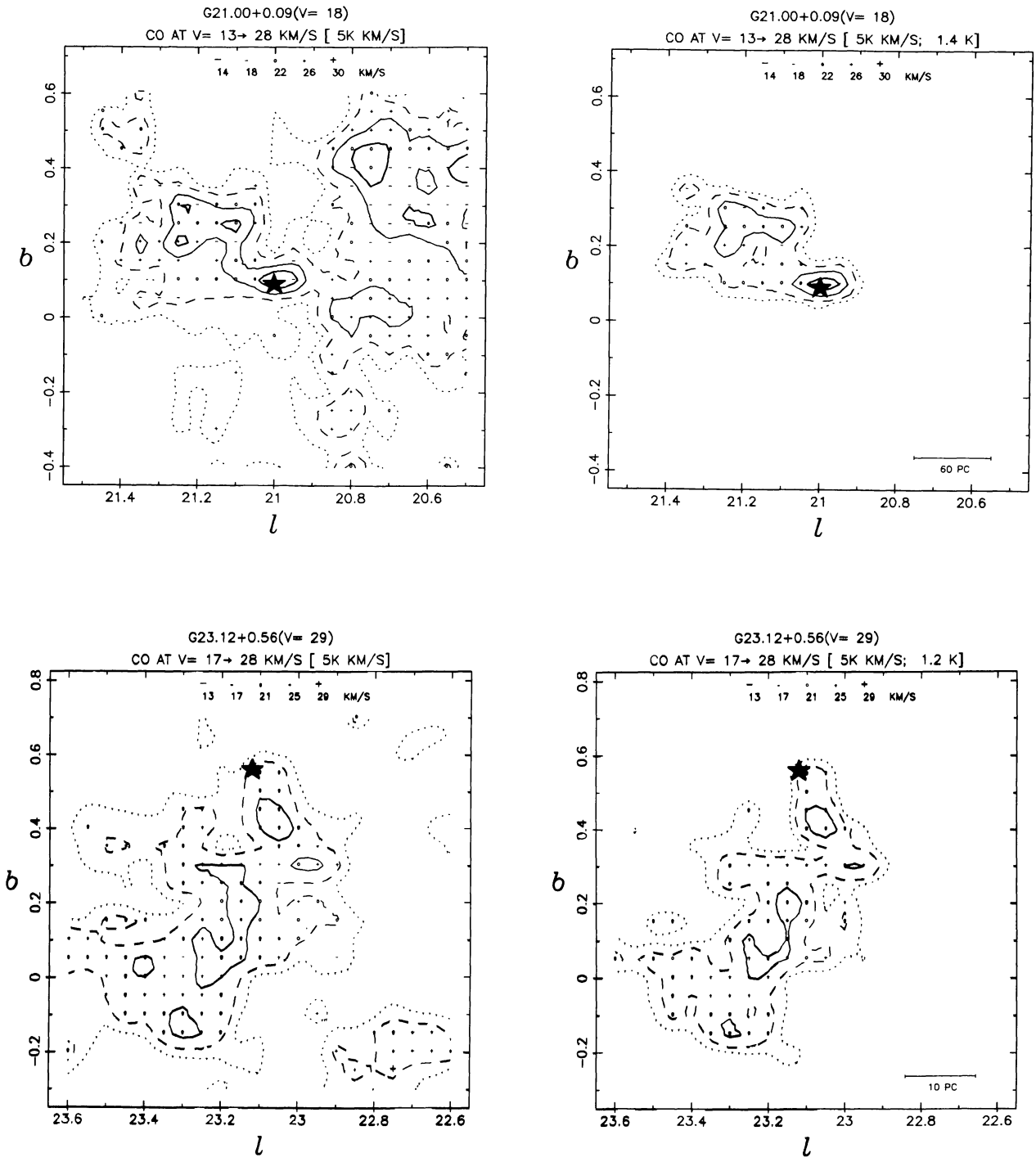

FIG. 13—*Continued*

© American Astronomical Society • Provided by the NASA Astrophysics Data System

1987ApJS...63..821S

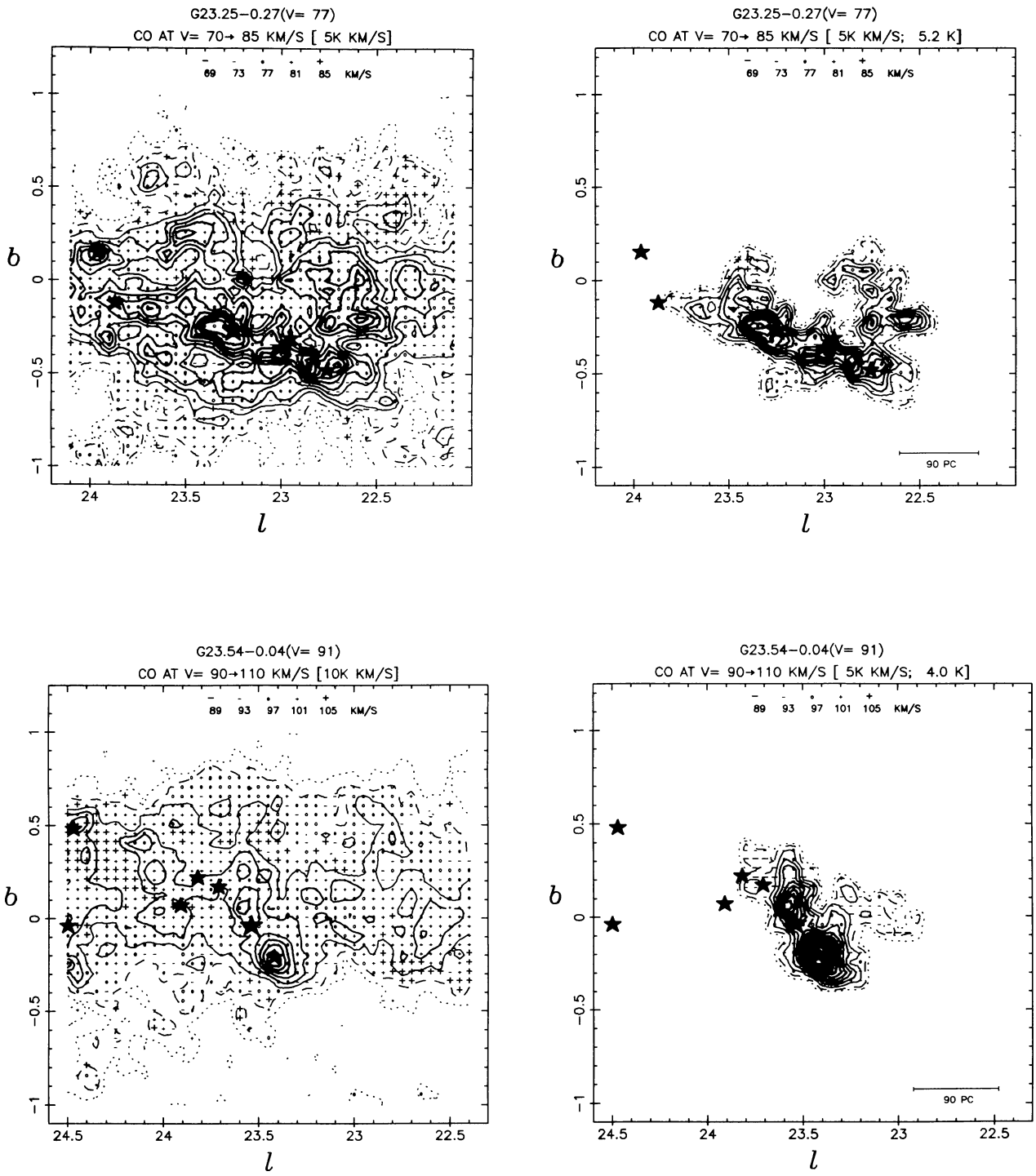

FIG. 13—*Continued*

© American Astronomical Society • Provided by the NASA Astrophysics Data System

1987ApJS...63..821S

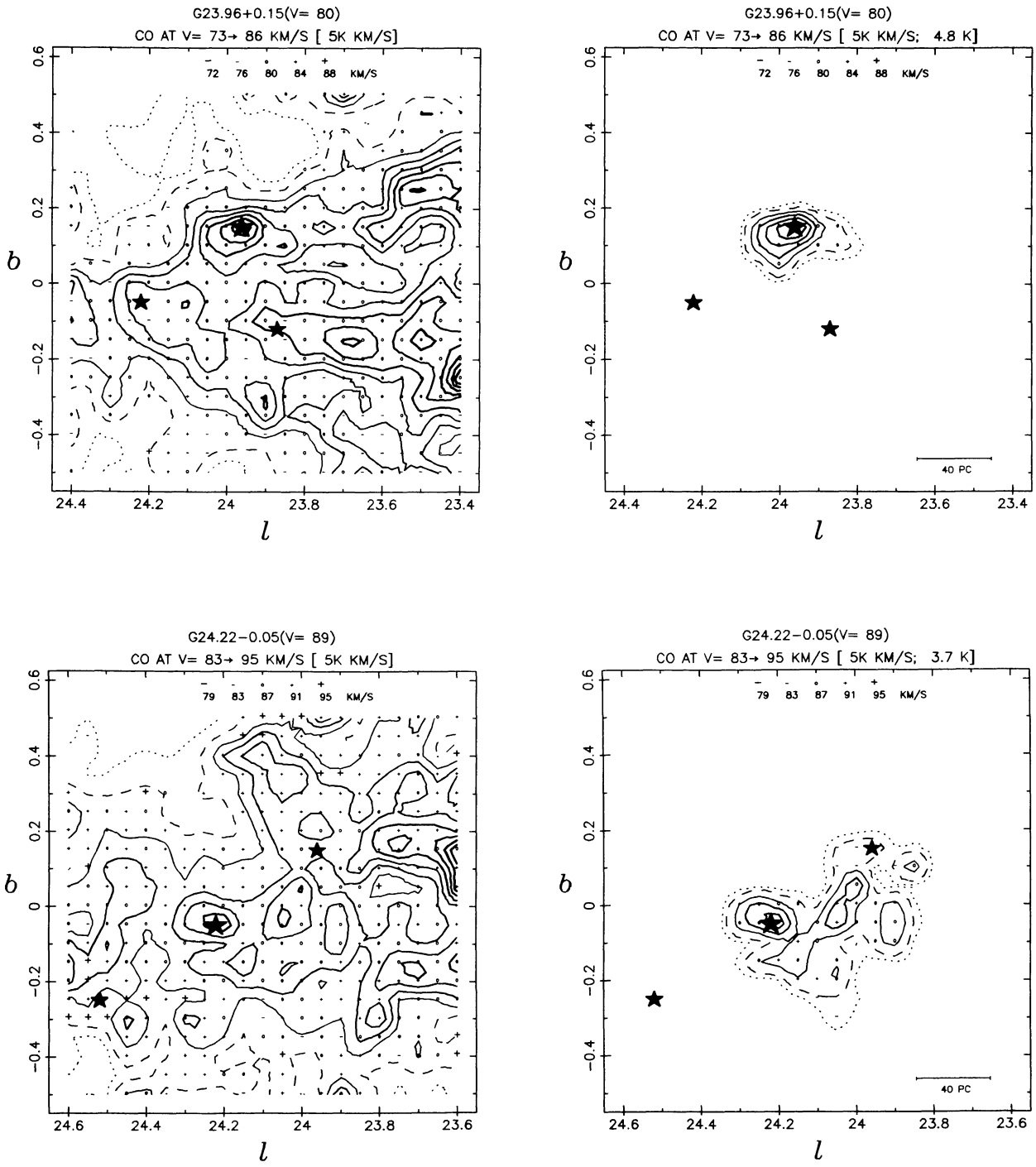

FIG. 13—*Continued*

© American Astronomical Society • Provided by the NASA Astrophysics Data System

1987ApJS...63..821S

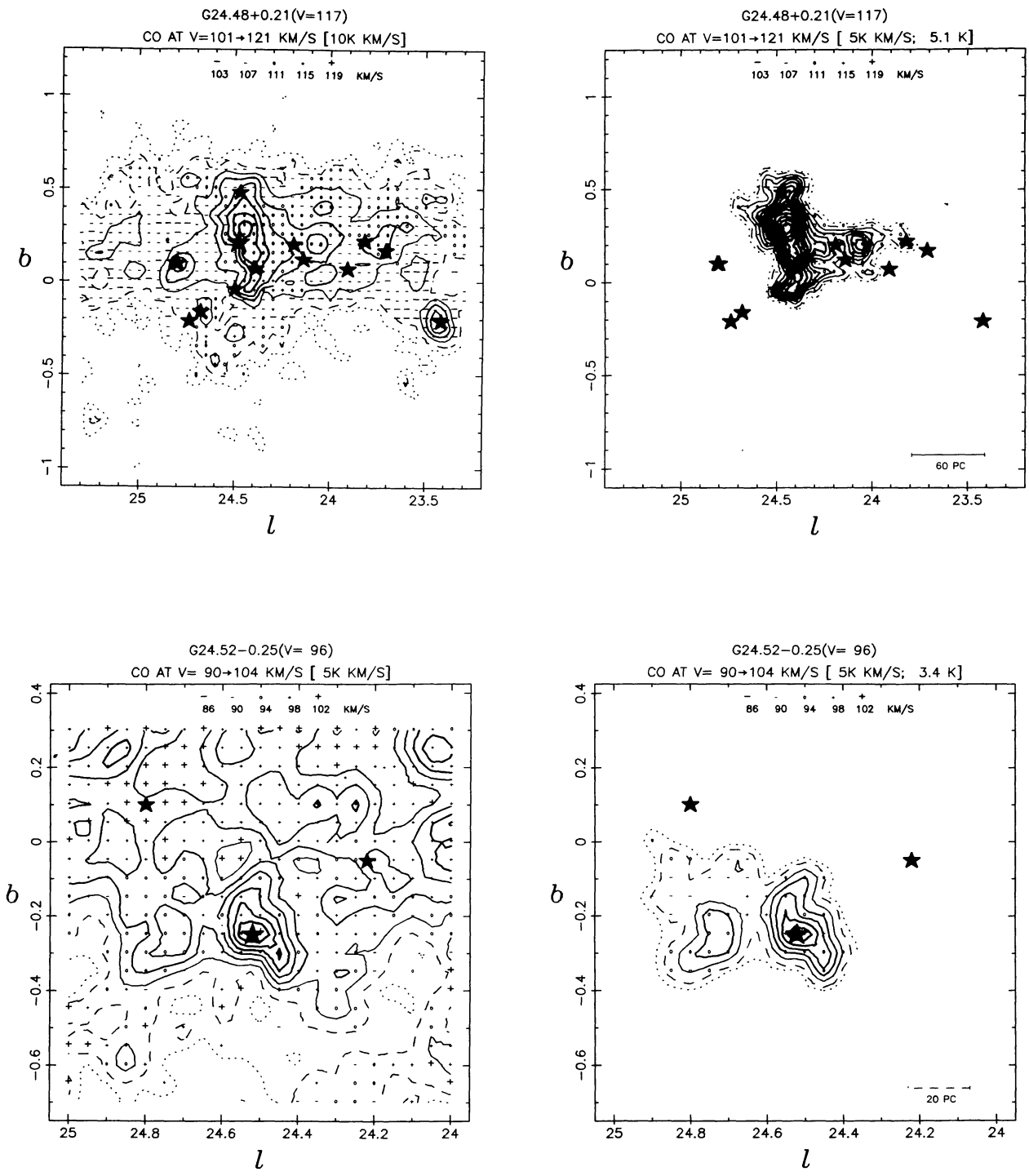

FIG. 13—*Continued*

© American Astronomical Society • Provided by the NASA Astrophysics Data System

1987ApJS...63..821S

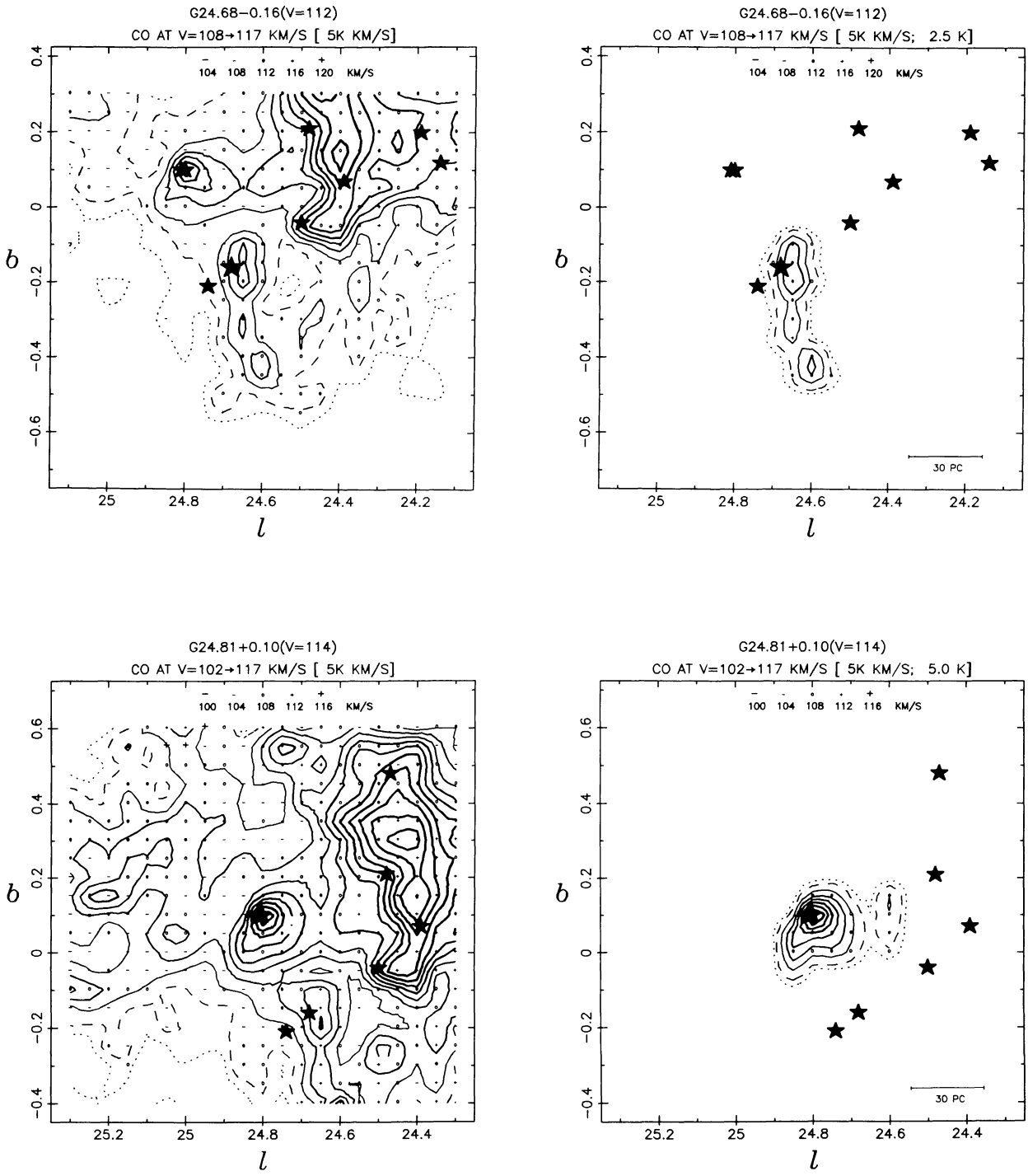

FIG. 13—*Continued*

© American Astronomical Society • Provided by the NASA Astrophysics Data System

1987ApJS...63..821S

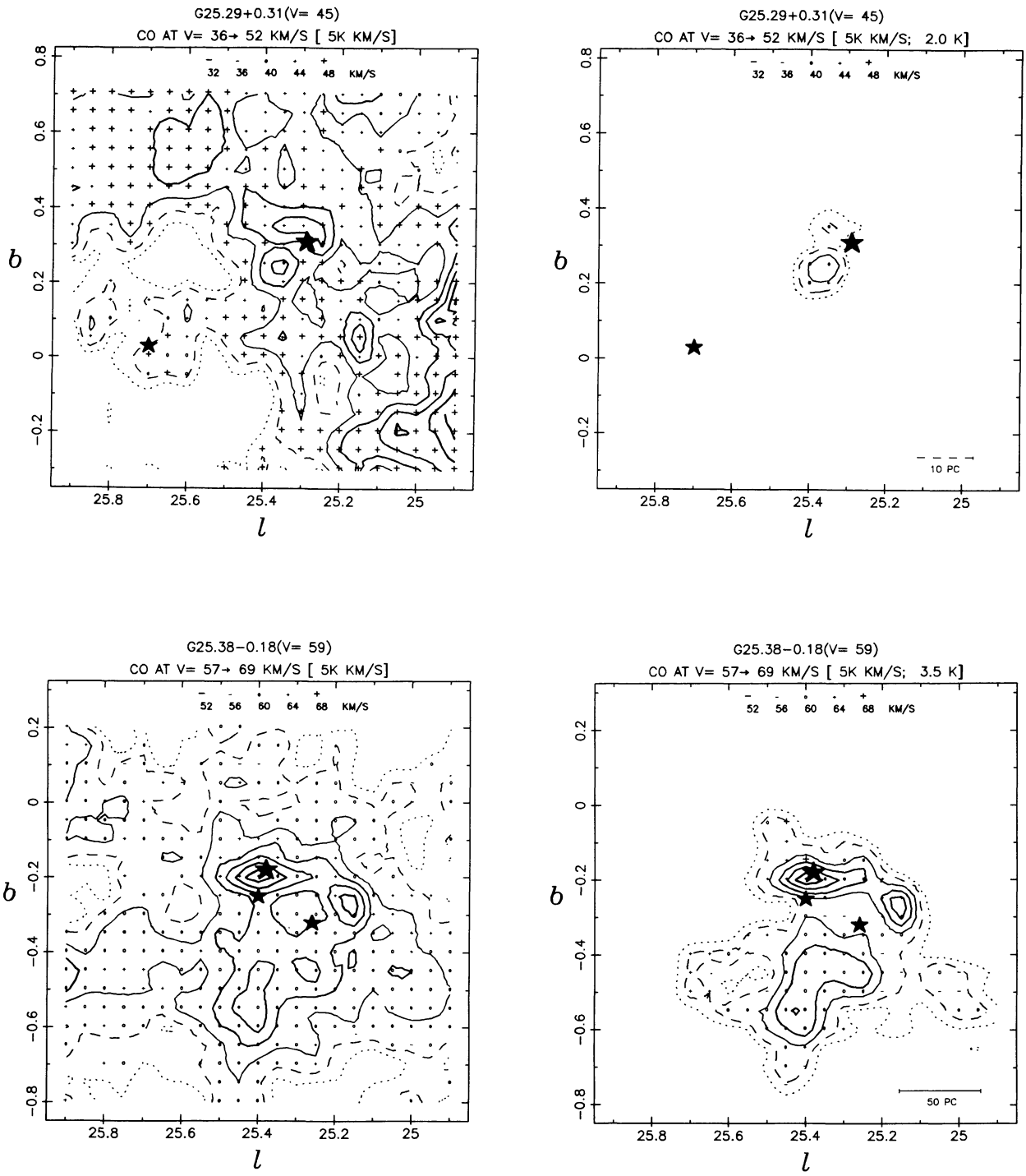

FIG. 13—*Continued*

© American Astronomical Society • Provided by the NASA Astrophysics Data System

1987ApJS...63..821S

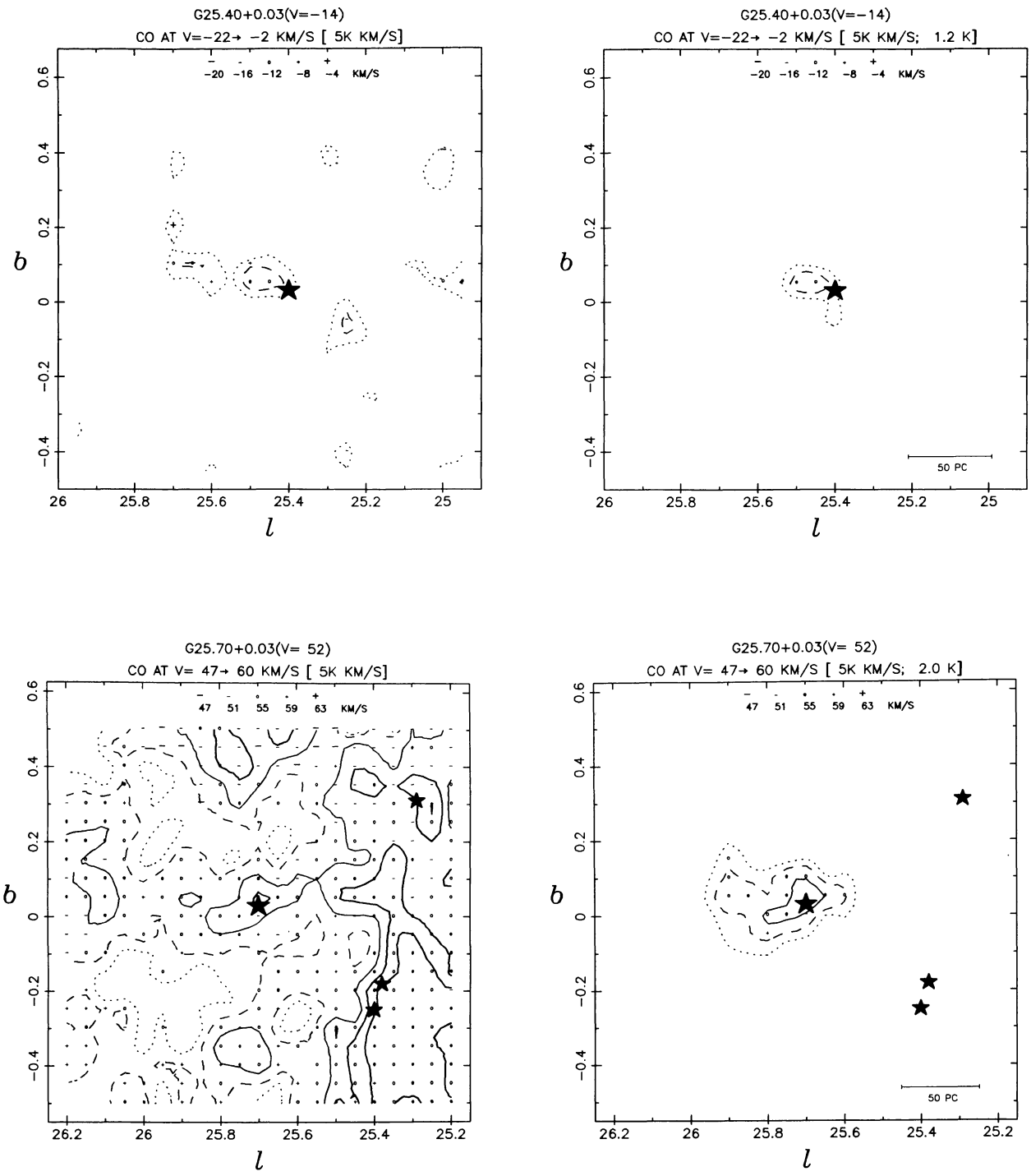

FIG. 13—*Continued*

© American Astronomical Society • Provided by the NASA Astrophysics Data System

1987ApJS...63..821S

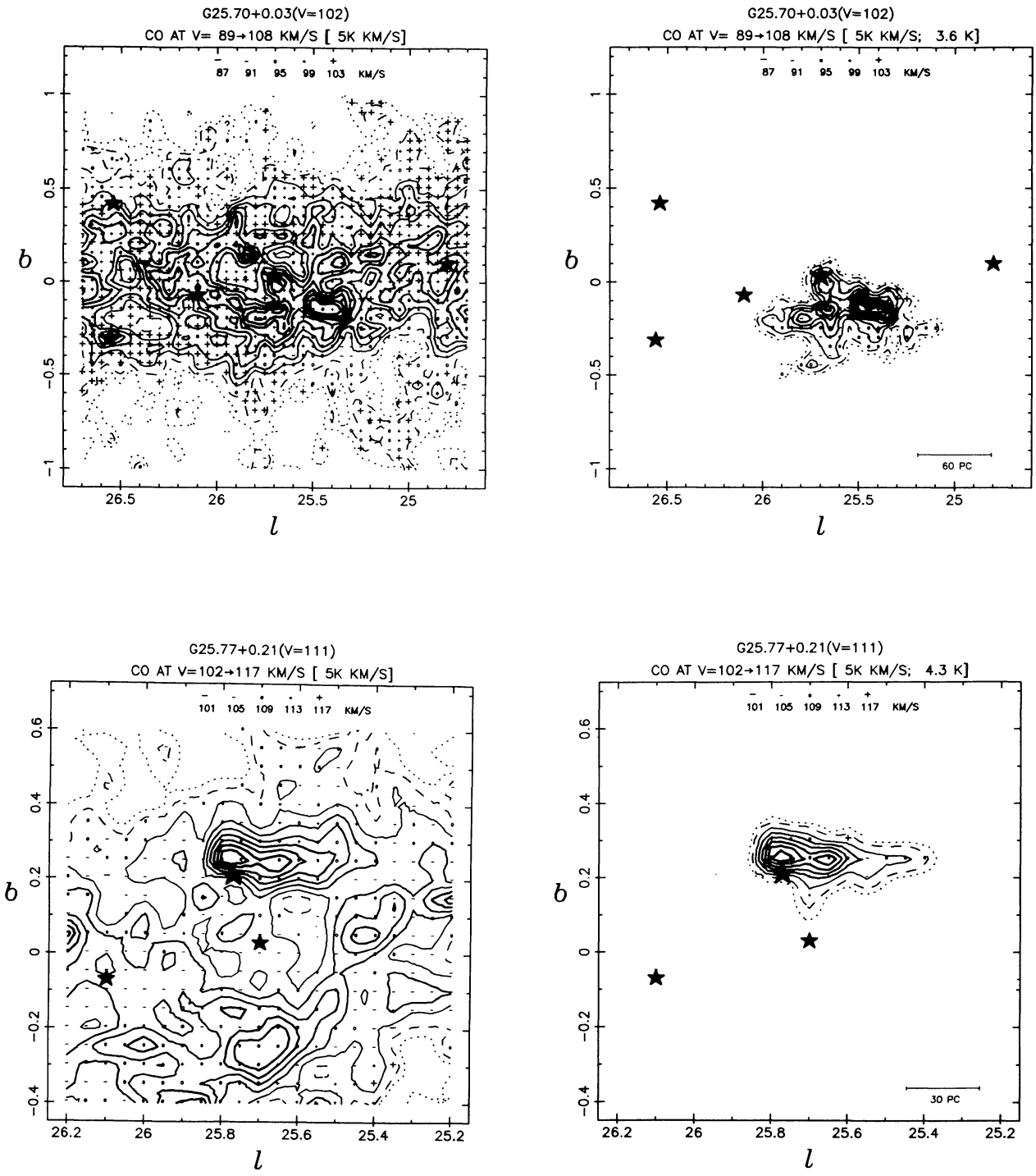

FIG. 13—*Continued*

© American Astronomical Society • Provided by the NASA Astrophysics Data System

1987ApJS...63..821S

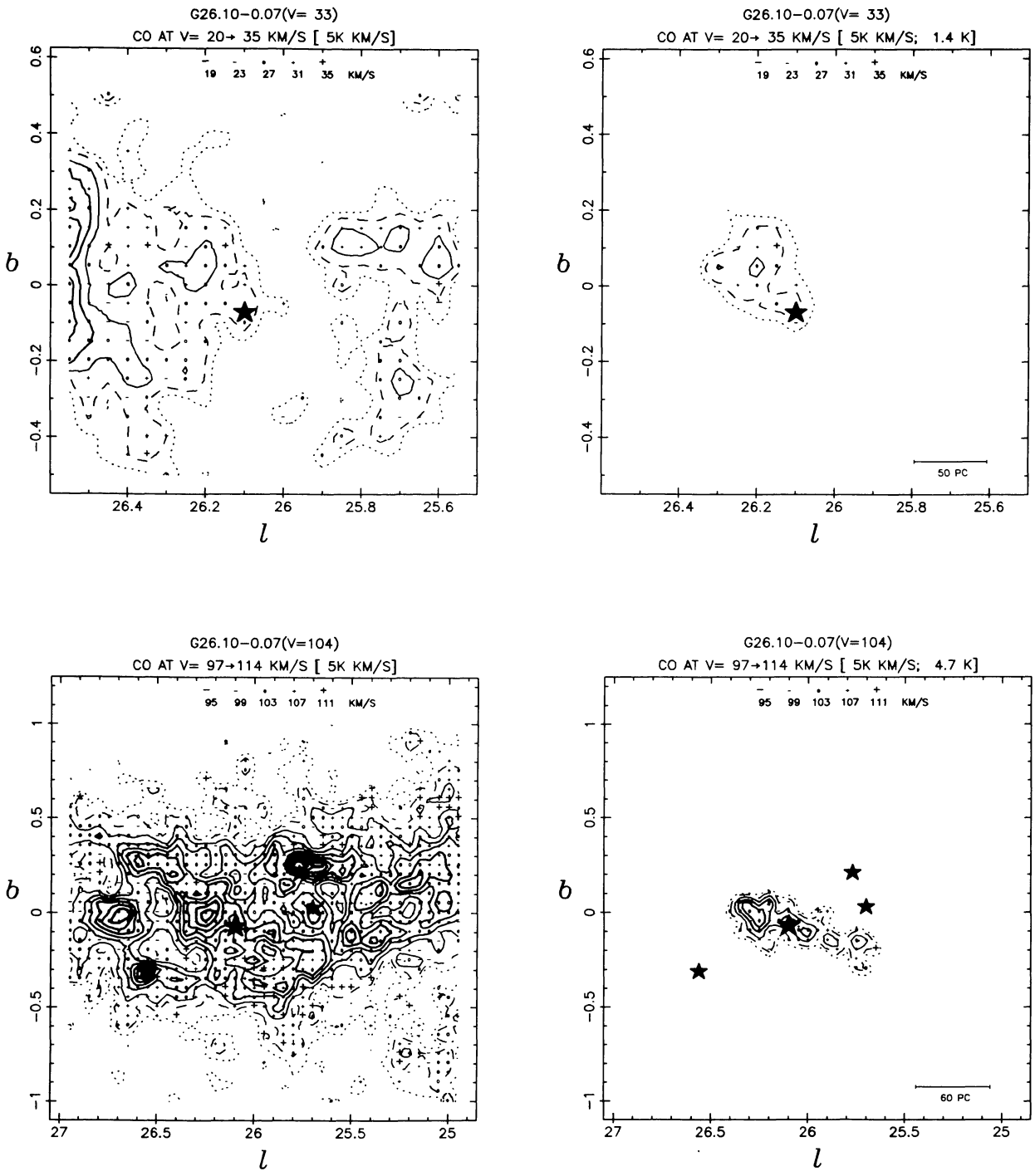

FIG. 13—*Continued*

© American Astronomical Society • Provided by the NASA Astrophysics Data System

1987ApJS...63..821S

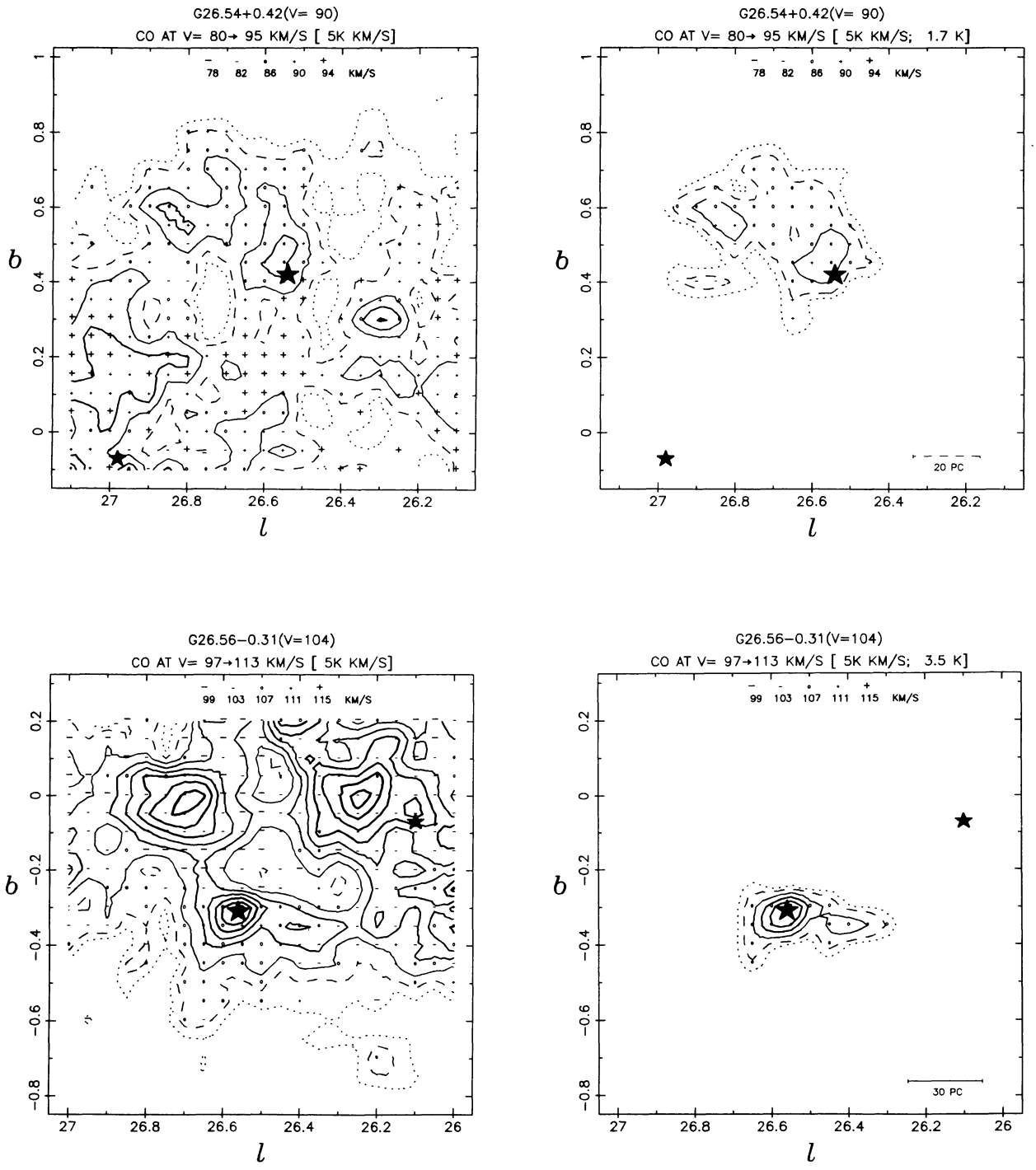

FIG. 13—*Continued*

© American Astronomical Society • Provided by the NASA Astrophysics Data System

1987ApJS...63..821S

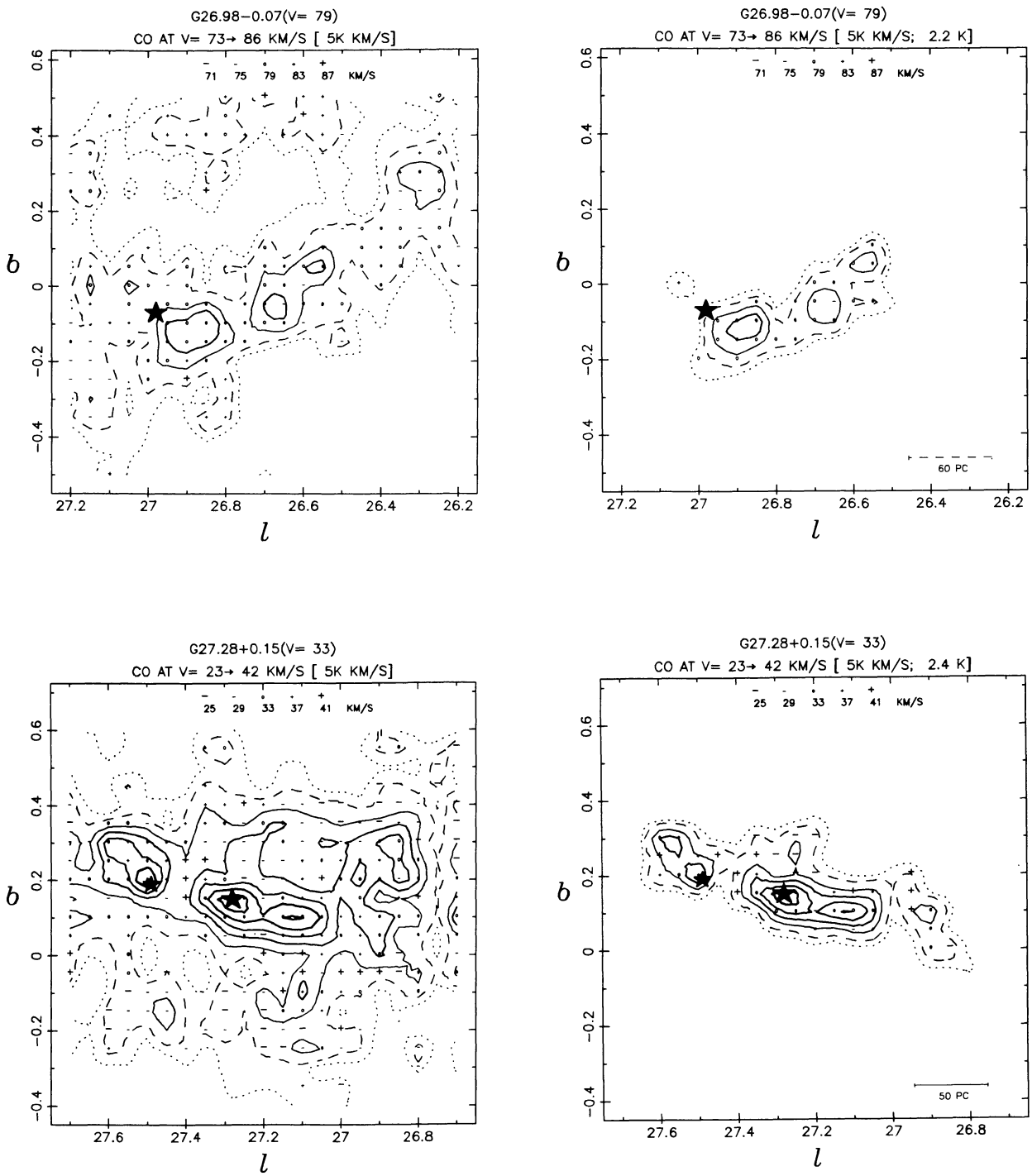

FIG. 13—*Continued*

© American Astronomical Society • Provided by the NASA Astrophysics Data System

1987ApJS...63..821S

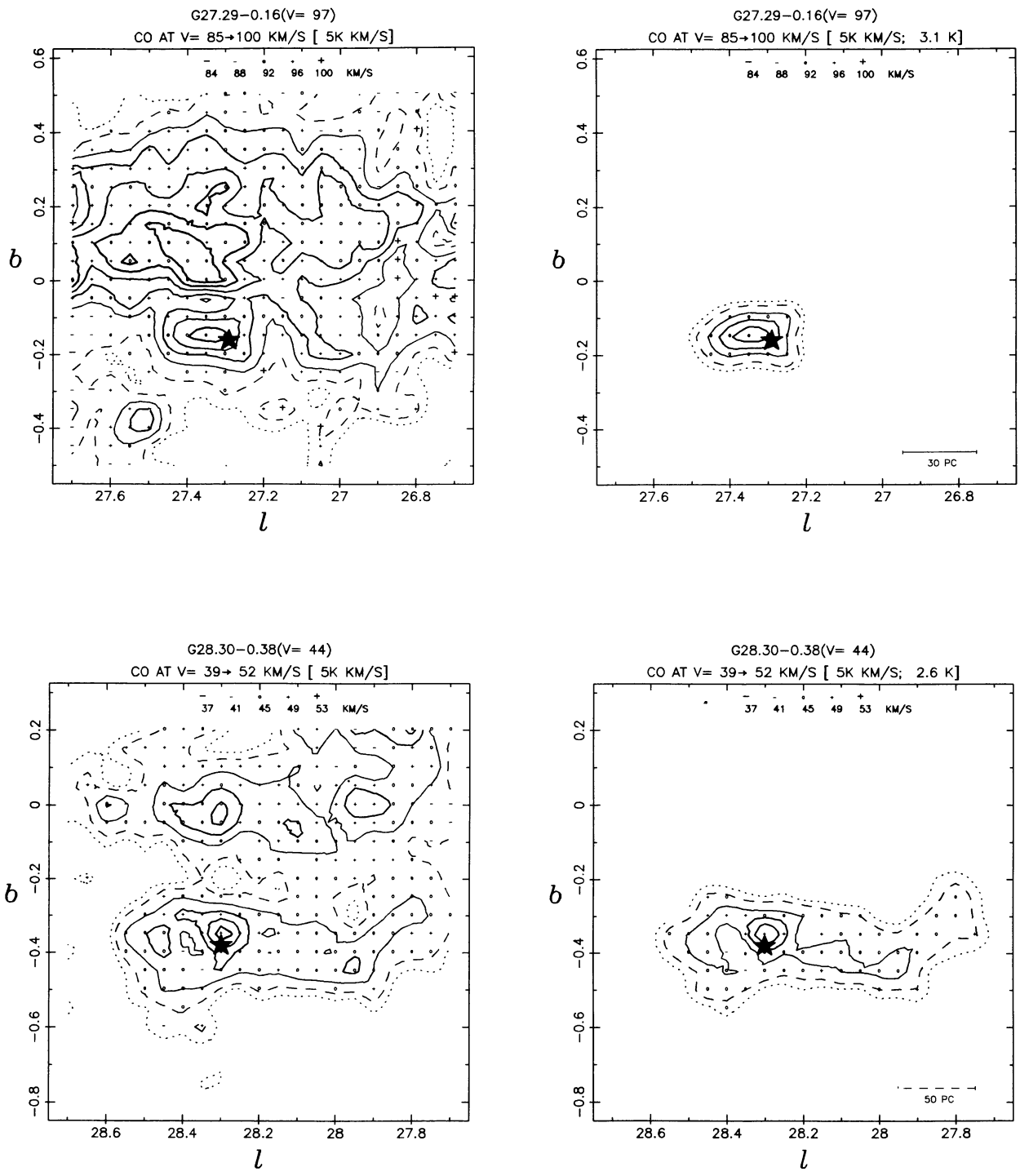

FIG. 13—*Continued*

© American Astronomical Society • Provided by the NASA Astrophysics Data System

1987ApJS...63..821S

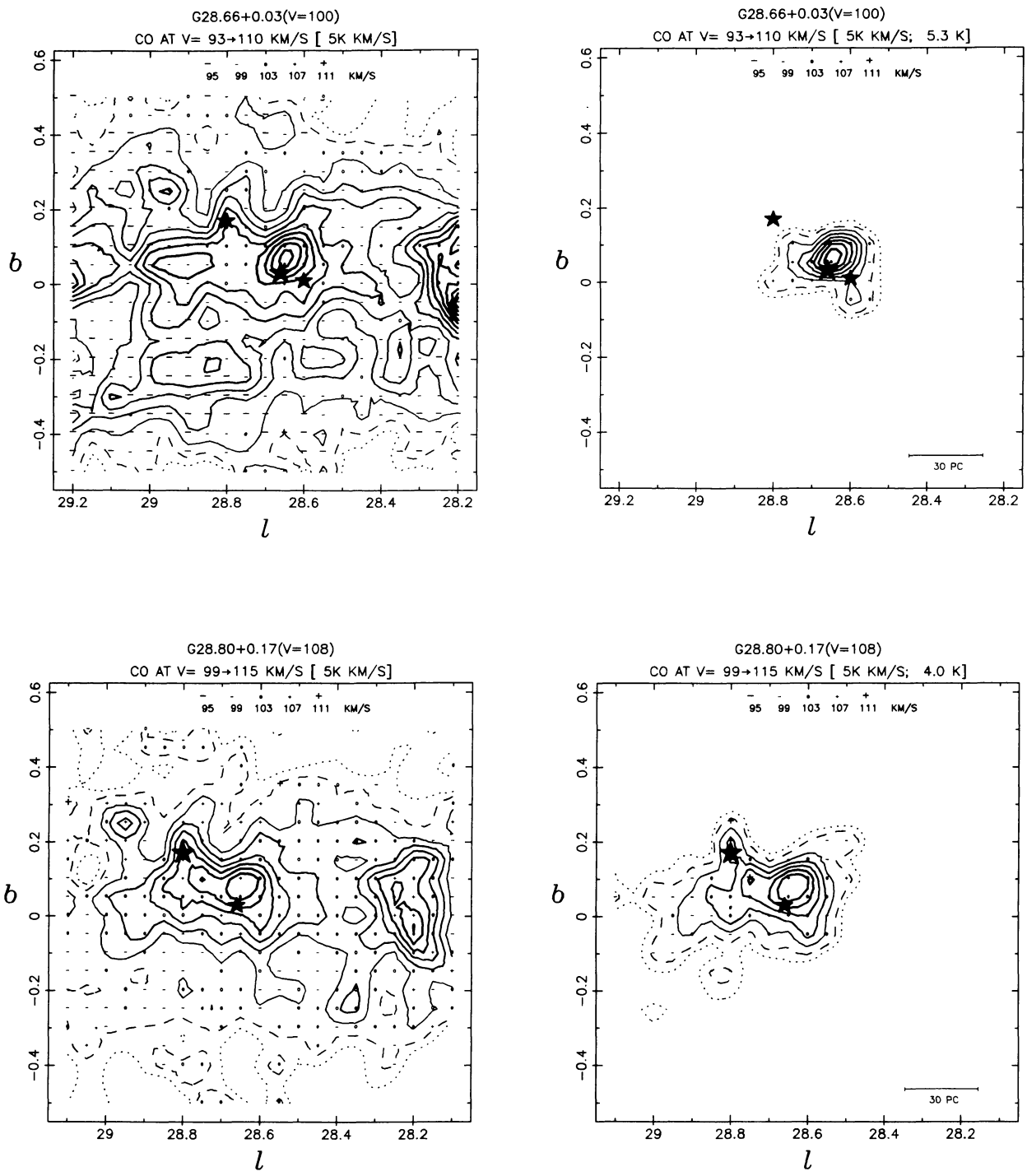

FIG. 13—*Continued*

© American Astronomical Society • Provided by the NASA Astrophysics Data System

1987ApJS...63..821S

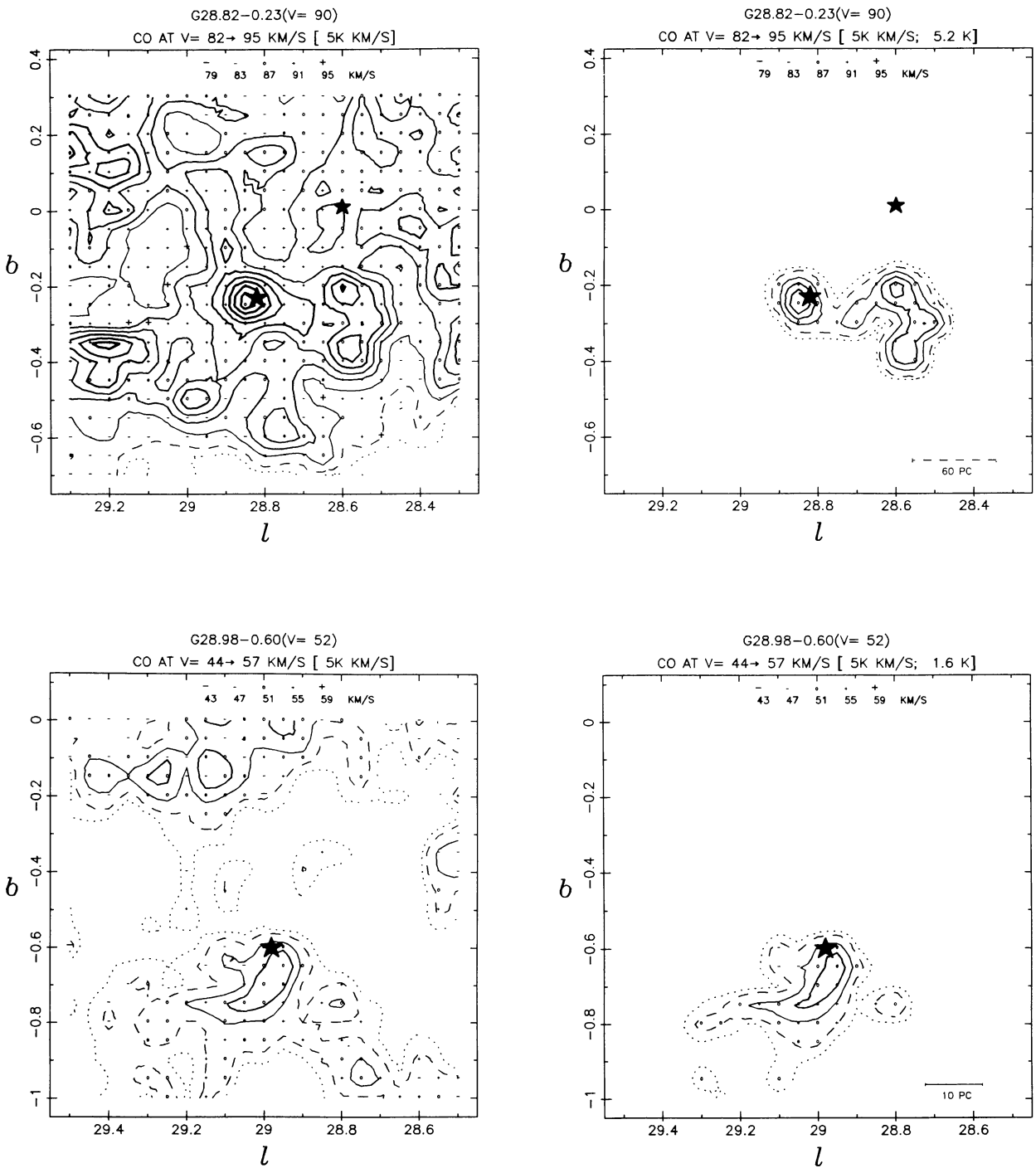

FIG. 13—*Continued*

© American Astronomical Society • Provided by the NASA Astrophysics Data System

1987ApJS...63..821S

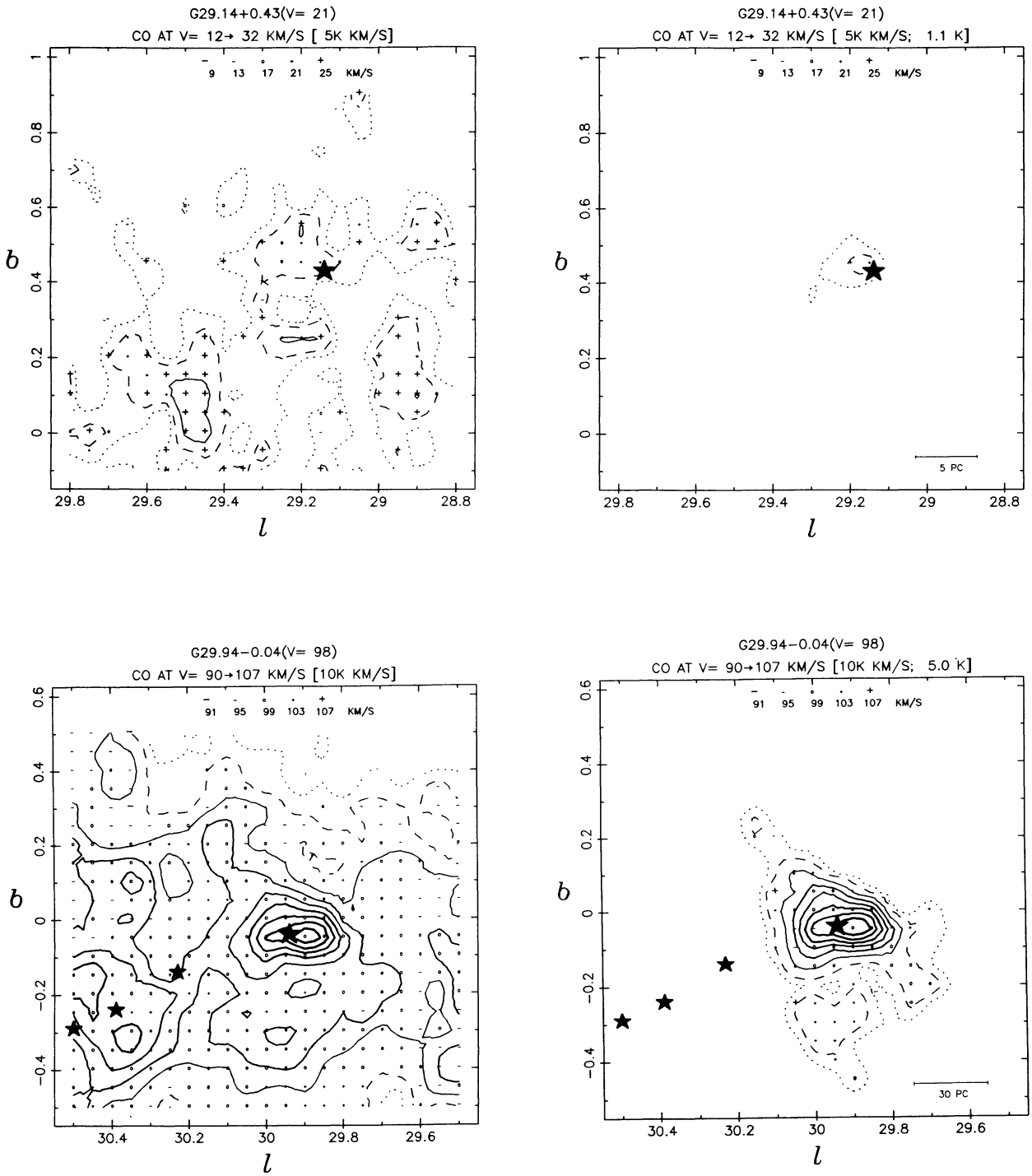

FIG. 13—*Continued*

© American Astronomical Society • Provided by the NASA Astrophysics Data System

1987ApJS...63..821S

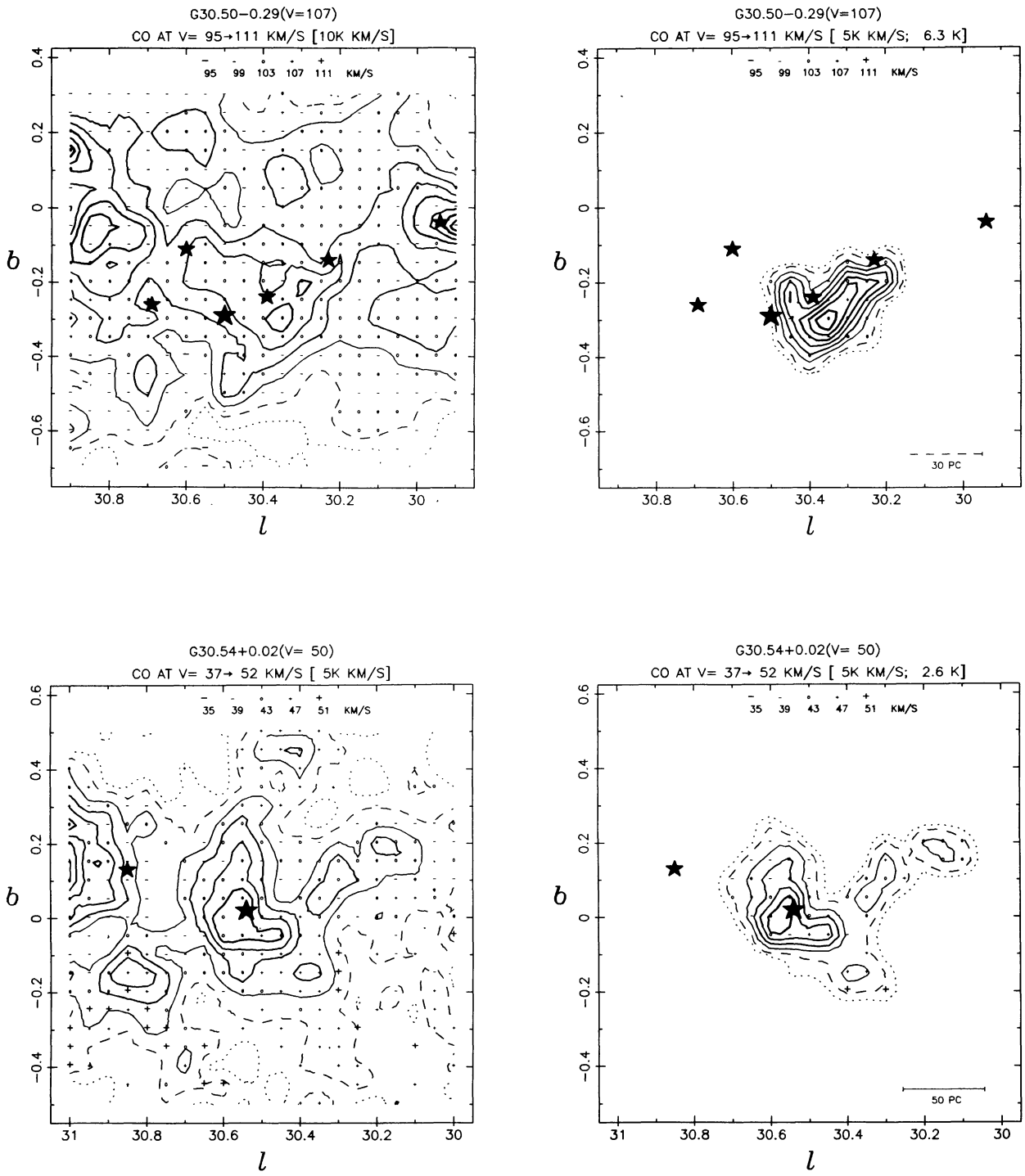

FIG. 13—*Continued*

© American Astronomical Society • Provided by the NASA Astrophysics Data System

1987ApJS...63..821S

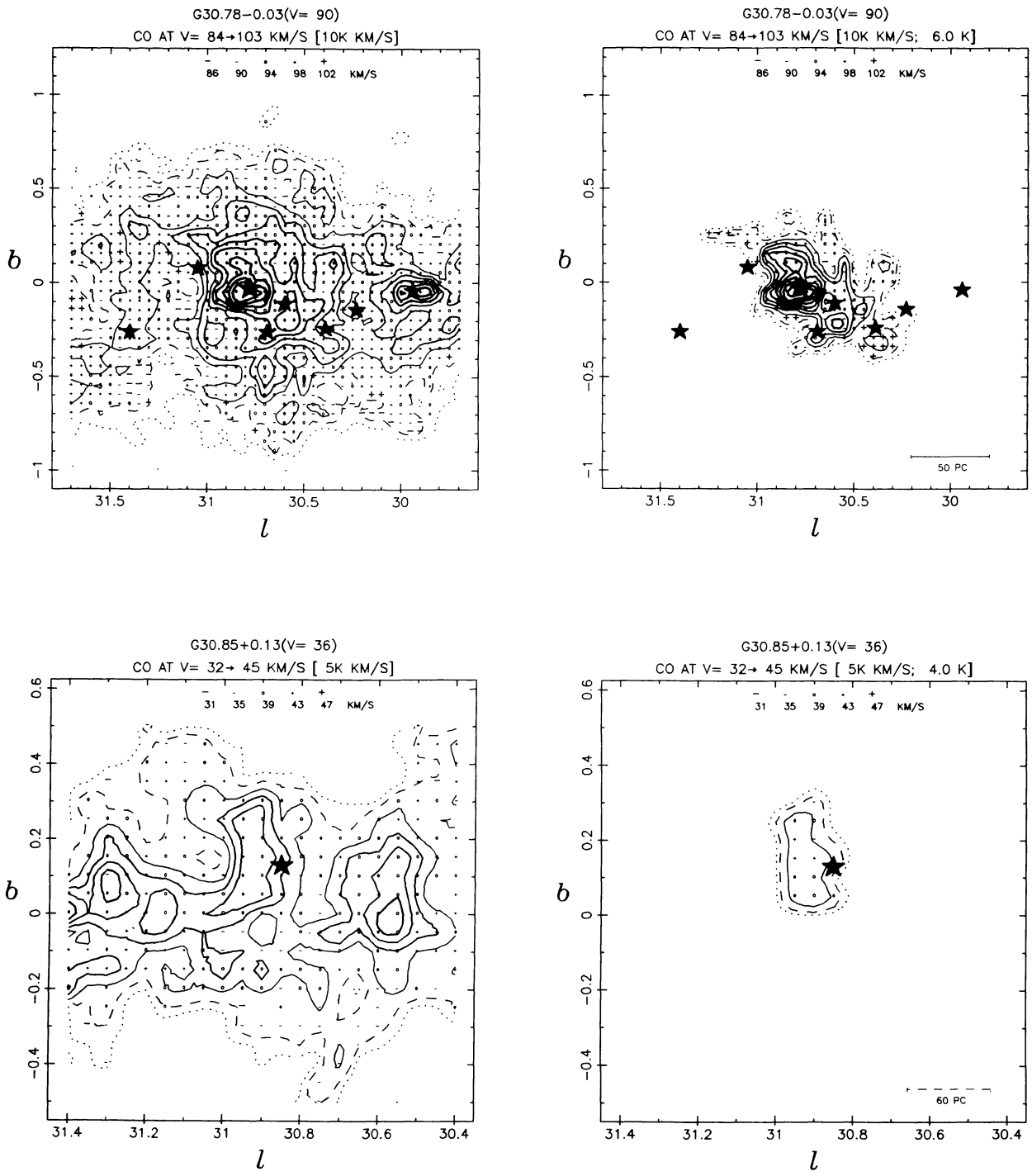

FIG. 13—*Continued*

© American Astronomical Society • Provided by the NASA Astrophysics Data System

1987ApJS...63..821S

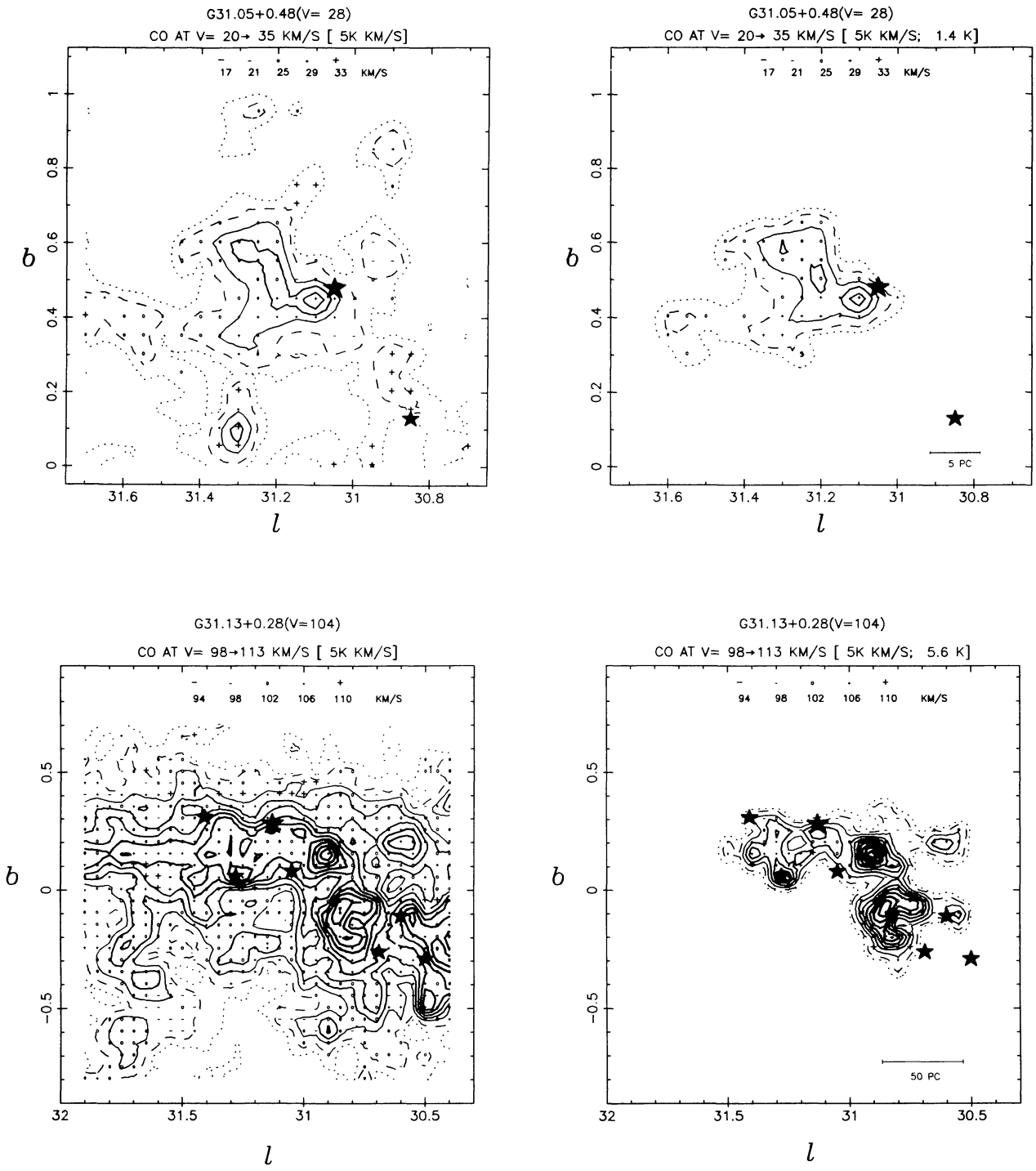

FIG. 13—*Continued*

© American Astronomical Society • Provided by the NASA Astrophysics Data System

1987ApJS...63..821S

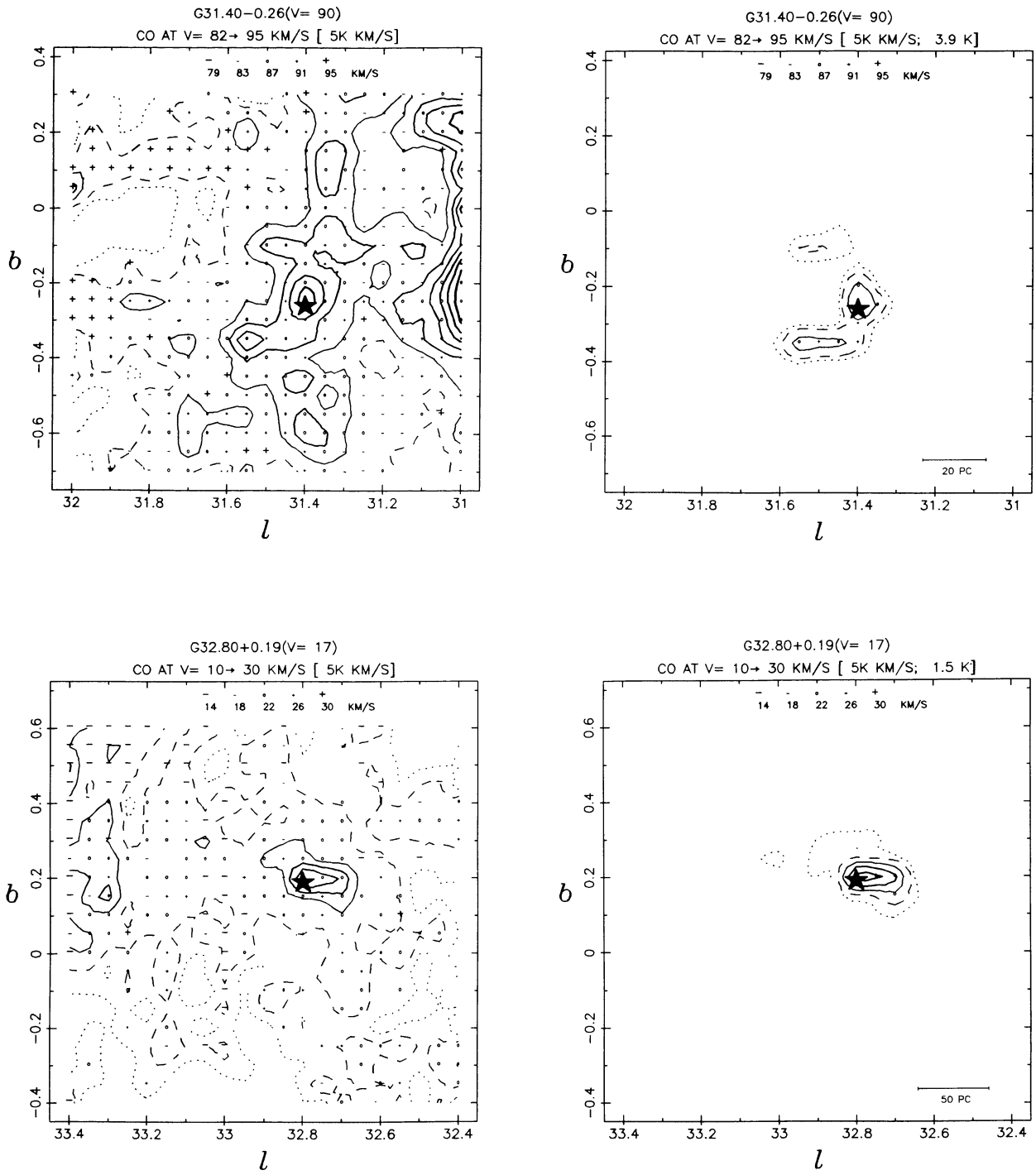

FIG. 13—*Continued*

© American Astronomical Society • Provided by the NASA Astrophysics Data System

1987ApJS...63..821S

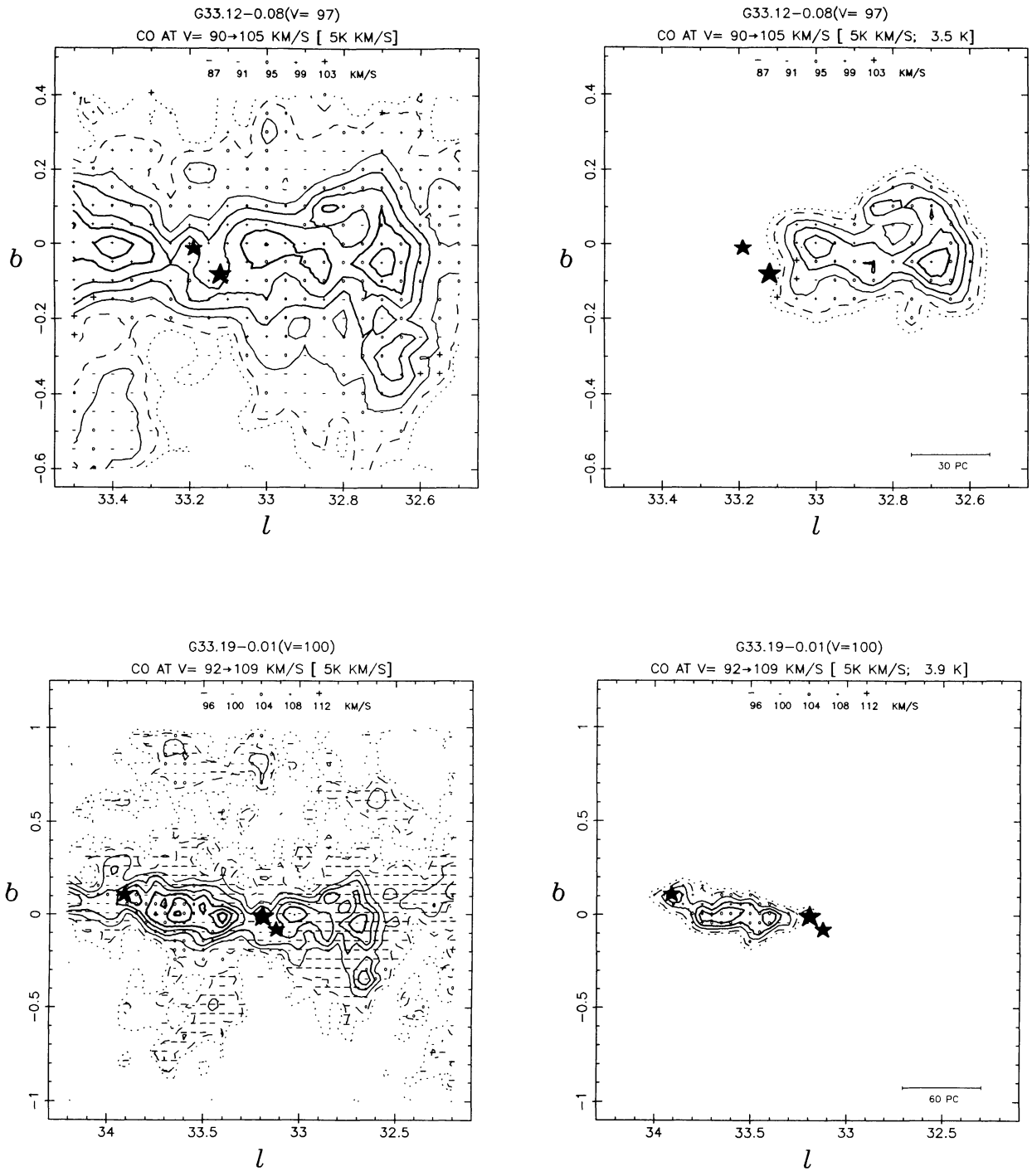

FIG. 13—*Continued*

© American Astronomical Society • Provided by the NASA Astrophysics Data System

1987ApJS...63..821S

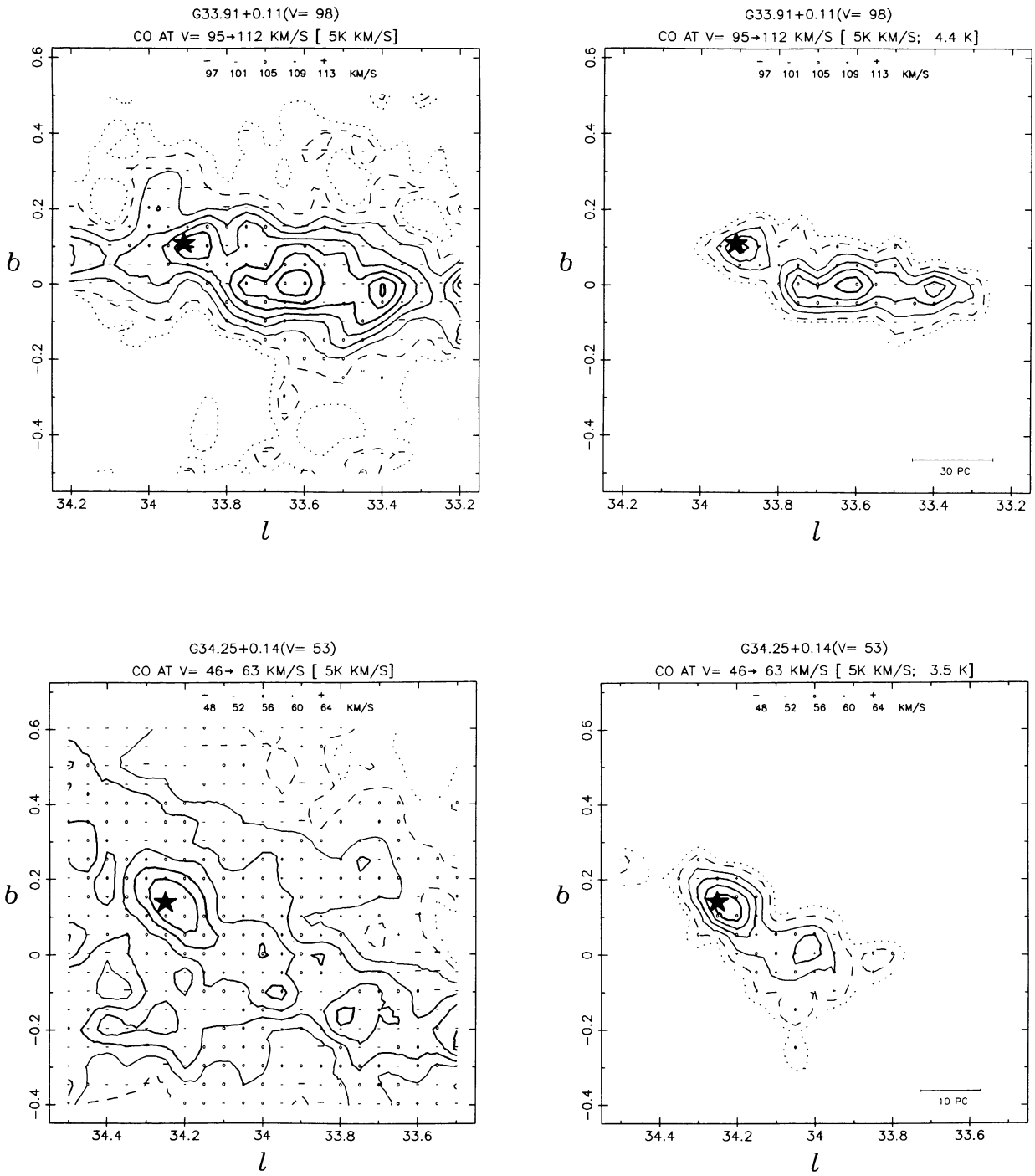

FIG. 13—*Continued*

© American Astronomical Society • Provided by the NASA Astrophysics Data System

1987ApJS...63..821S

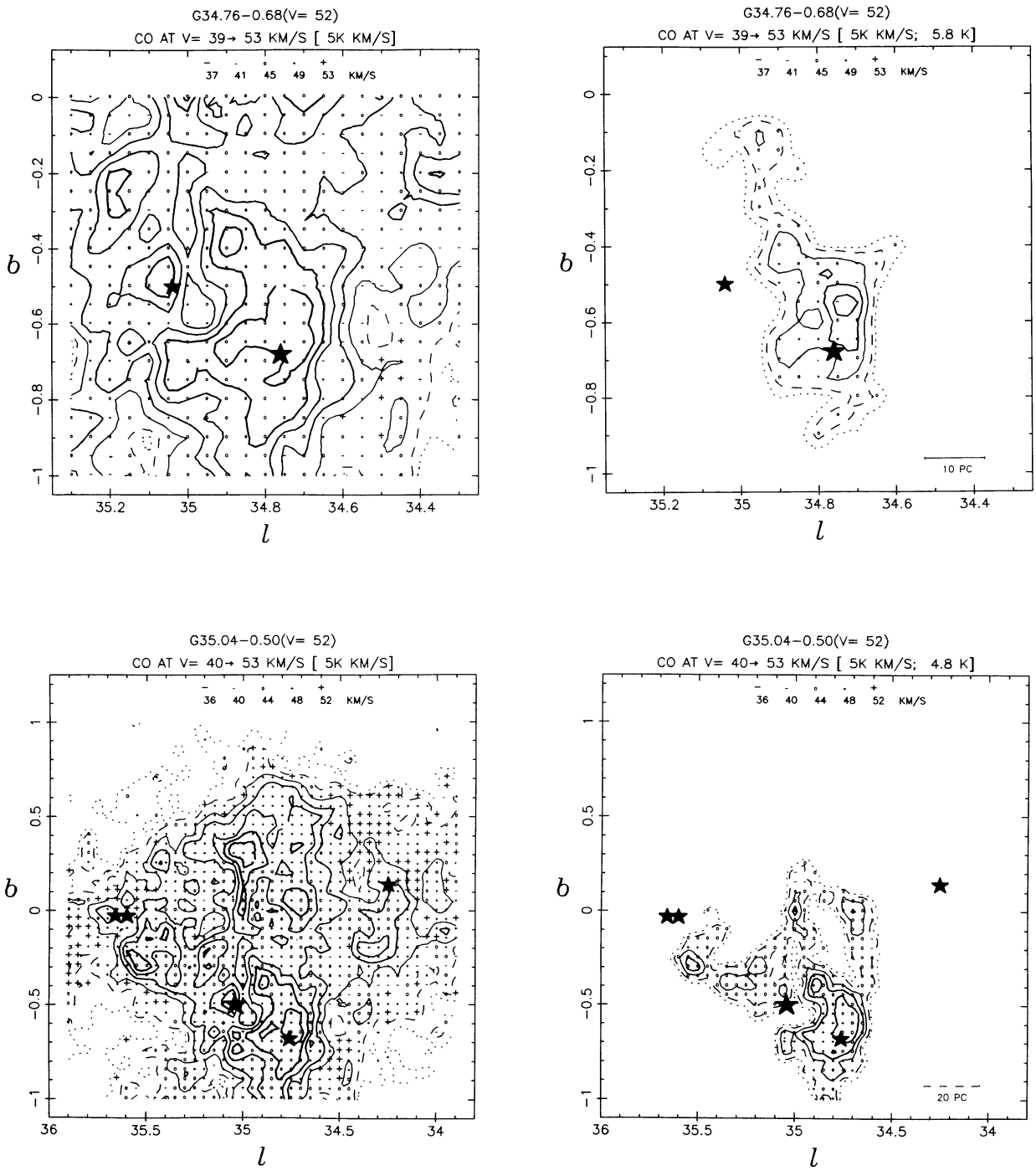

FIG. 13—*Continued*

© American Astronomical Society • Provided by the NASA Astrophysics Data System

1987ApJS...63..821S

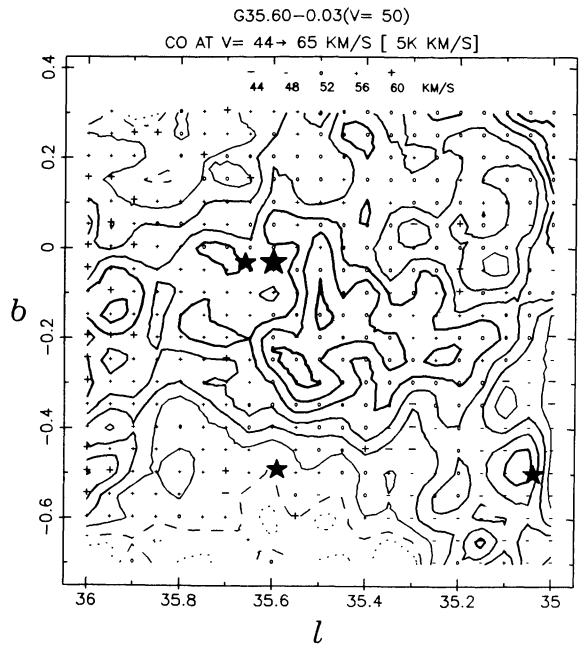

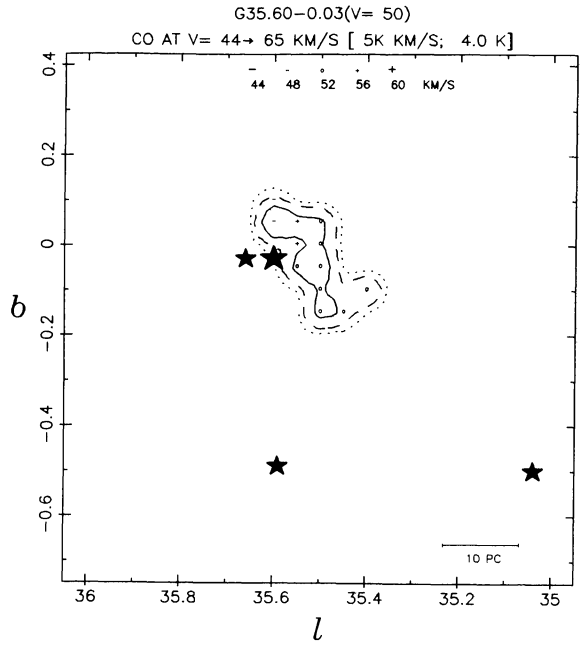

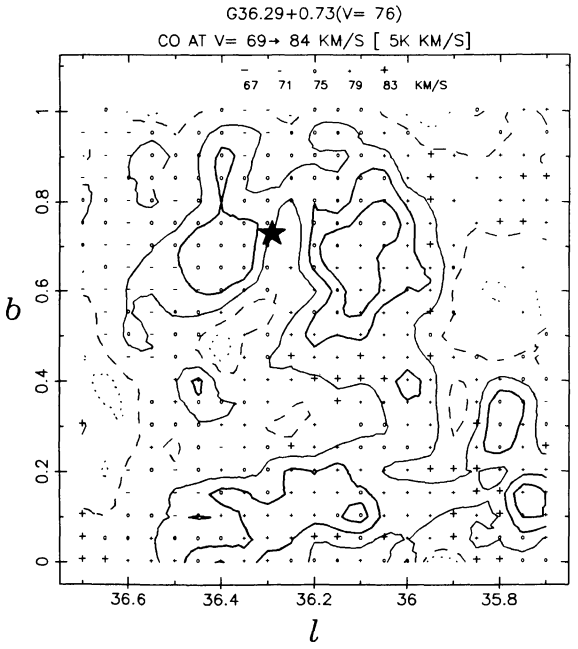

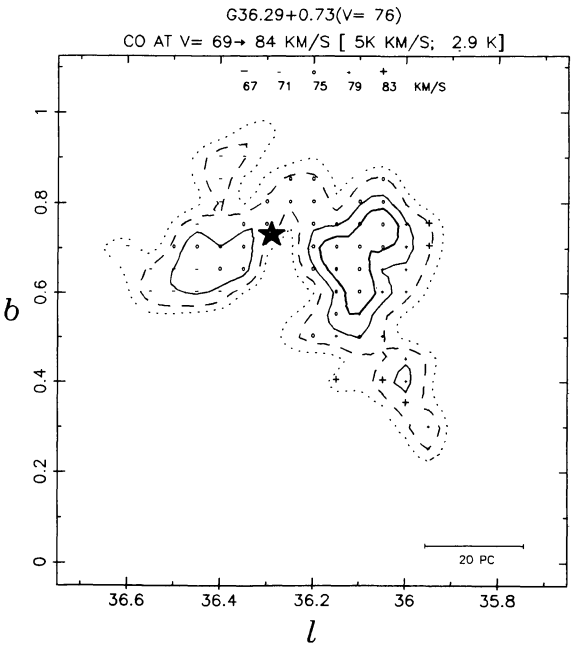

FIG. 13—*Continued*

© American Astronomical Society • Provided by the NASA Astrophysics Data System

1987ApJS...63..821S

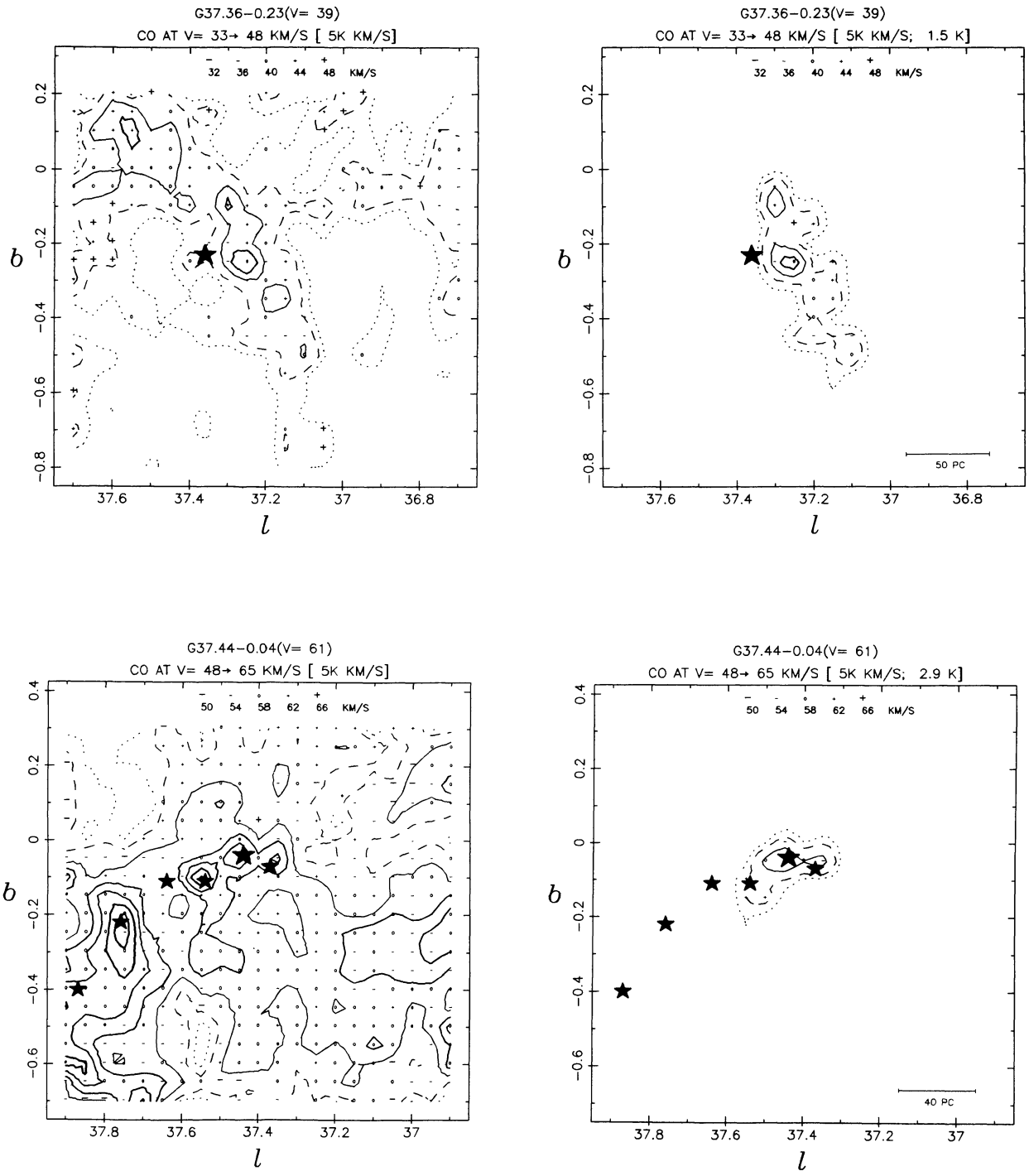

FIG. 13—*Continued*

© American Astronomical Society • Provided by the NASA Astrophysics Data System

1987ApJS...63..821S

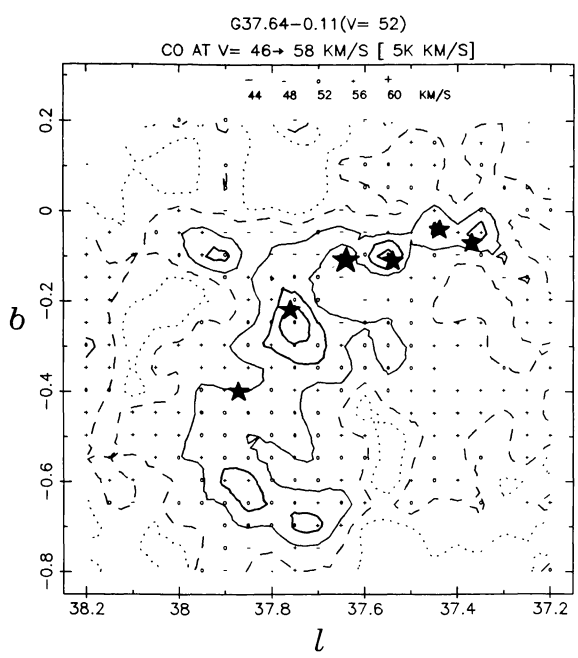

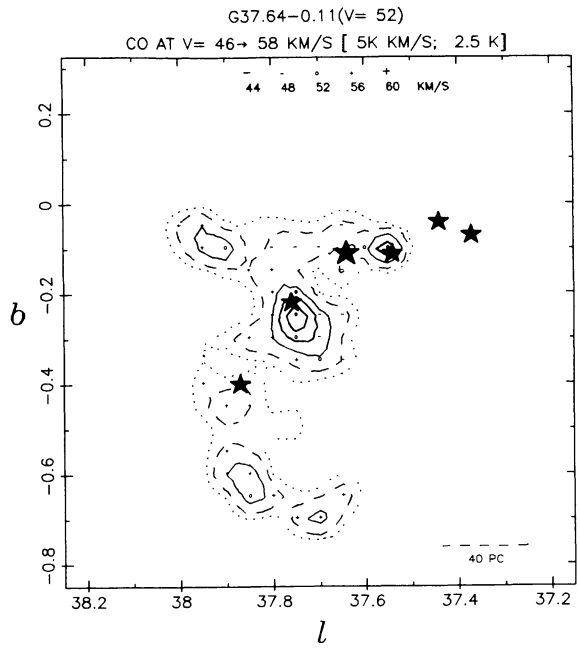

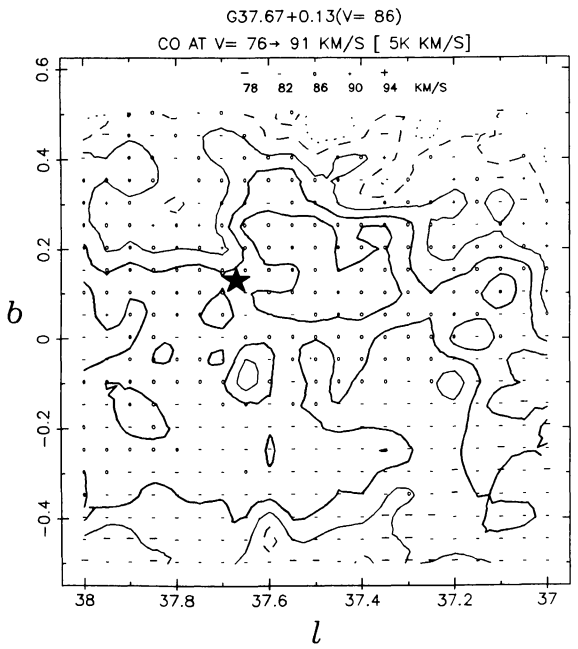

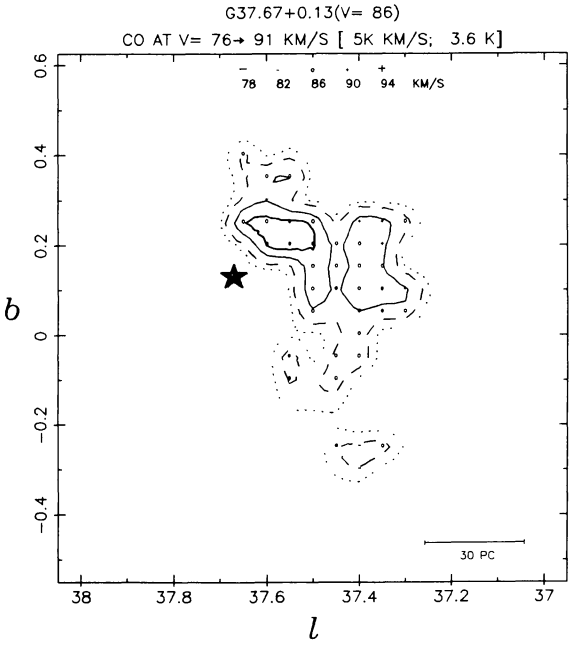

FIG. 13—*Continued*

© American Astronomical Society • Provided by the NASA Astrophysics Data System

1987ApJS...63..821S

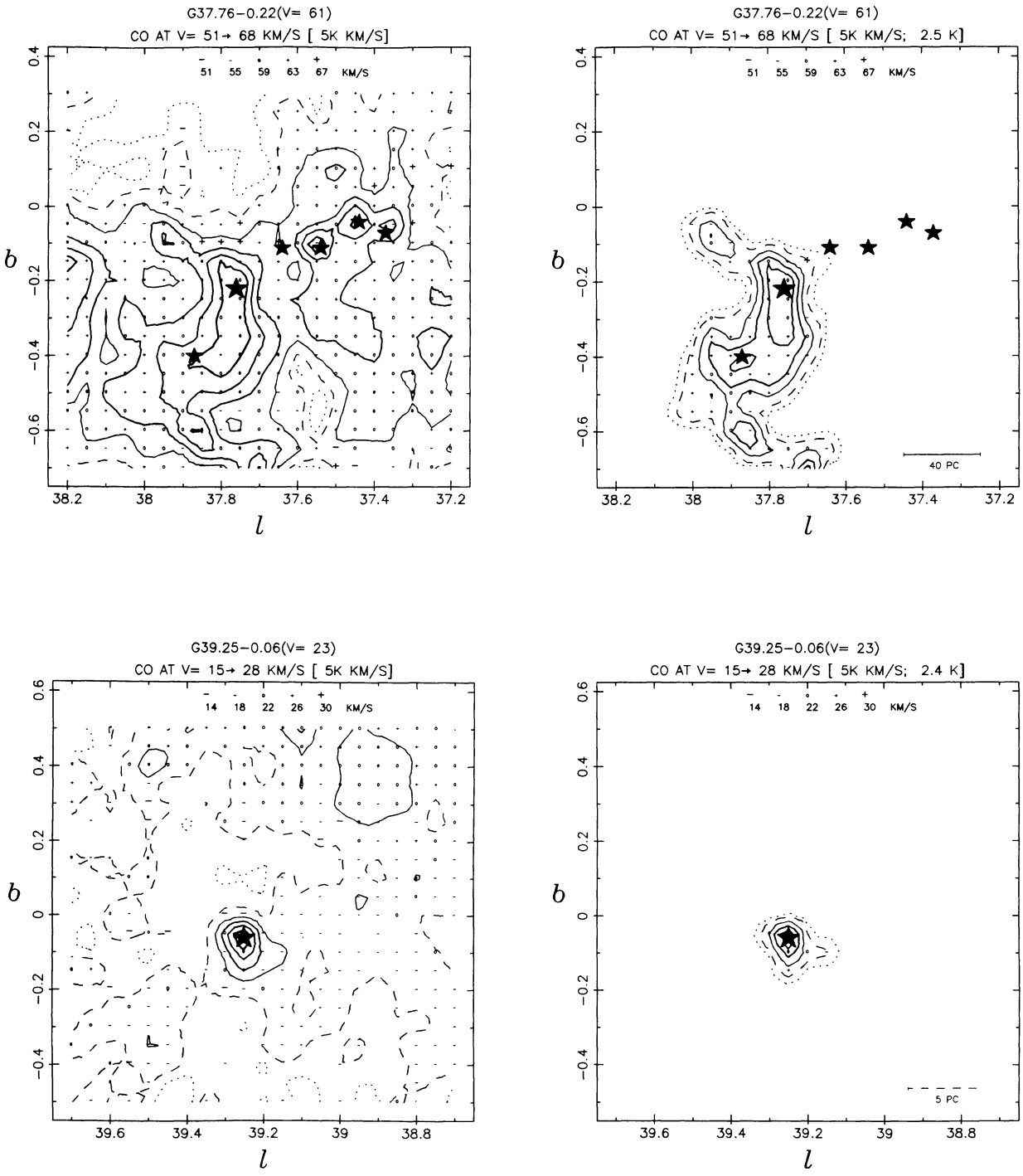

FIG. 13—*Continued*

© American Astronomical Society • Provided by the NASA Astrophysics Data System

1987ApJS...63..821S

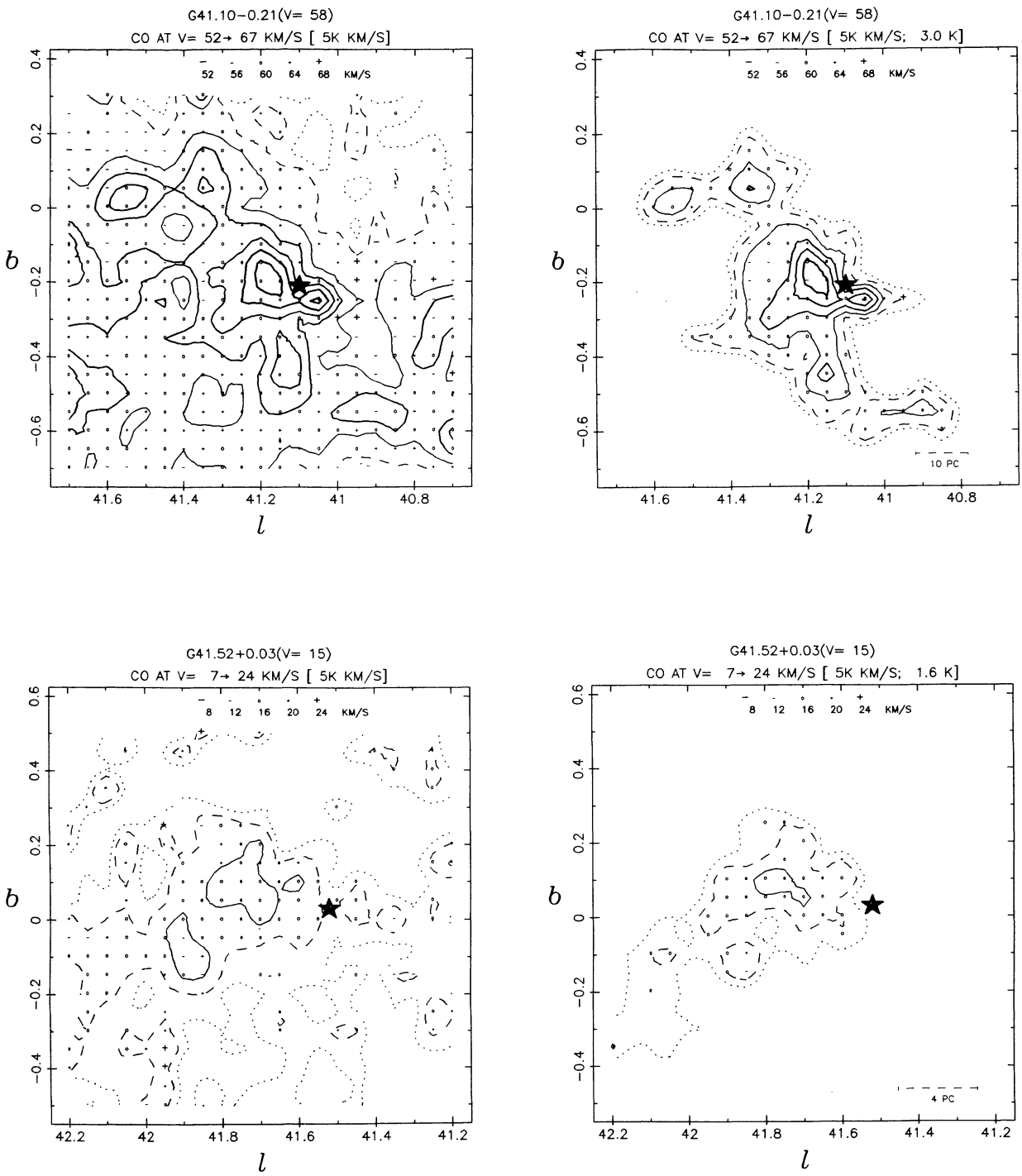

FIG. 13—*Continued*

© American Astronomical Society • Provided by the NASA Astrophysics Data System

1987ApJS...63..821S

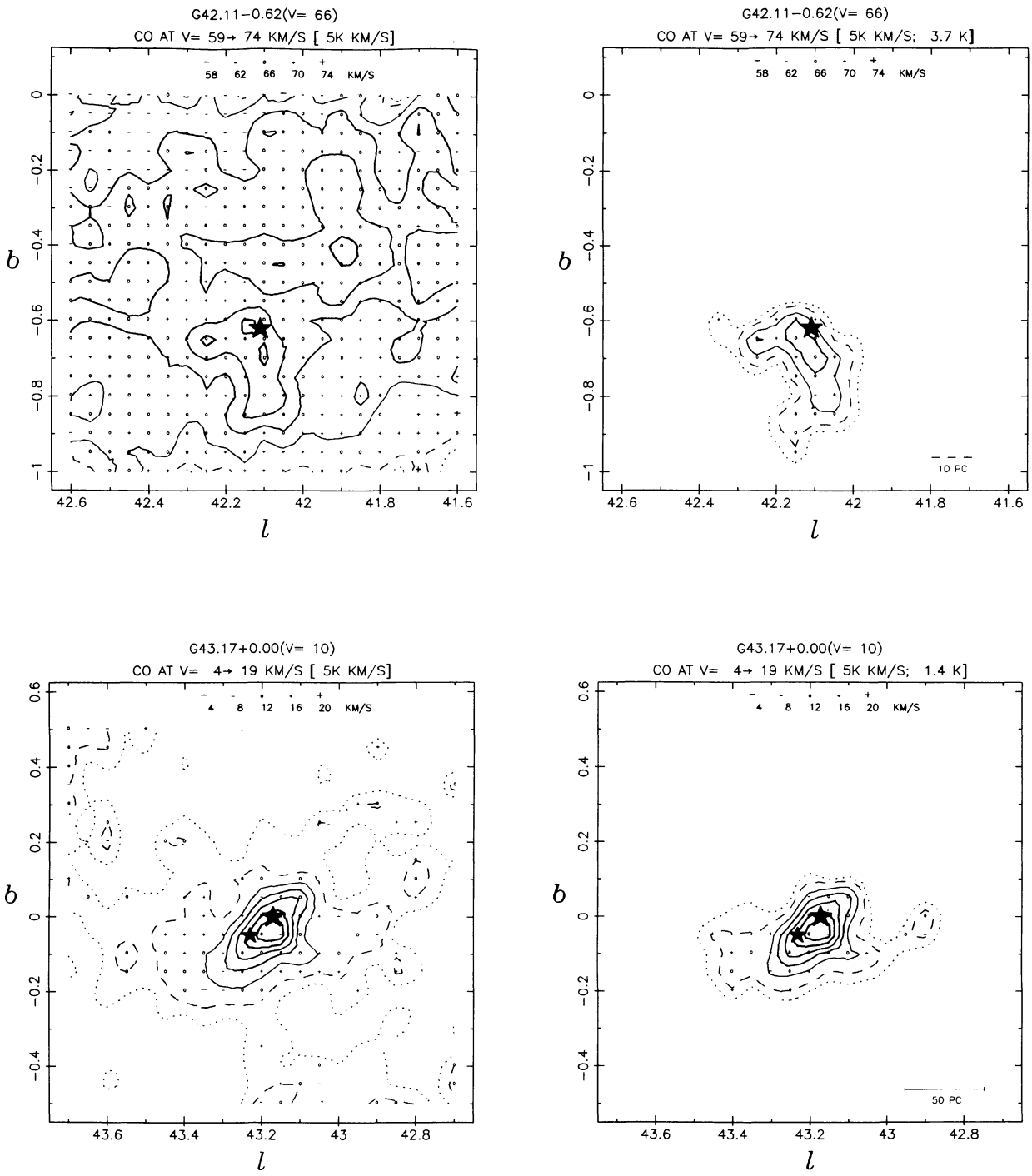

FIG. 13—*Continued*

© American Astronomical Society • Provided by the NASA Astrophysics Data System

1987ApJS...63..821S

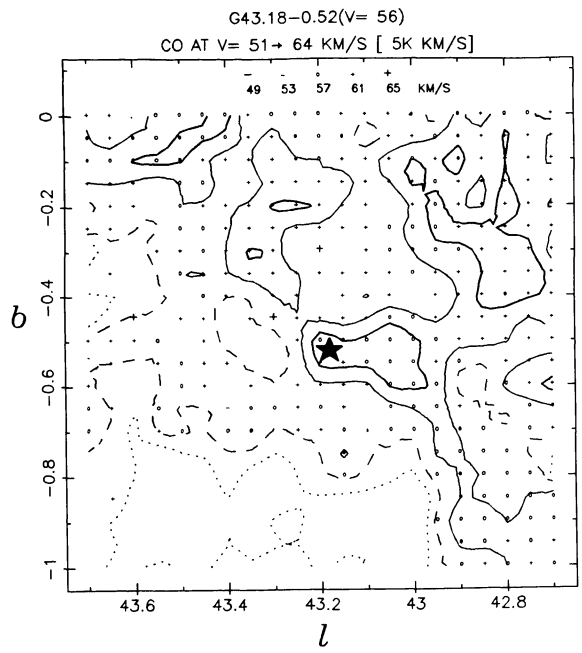

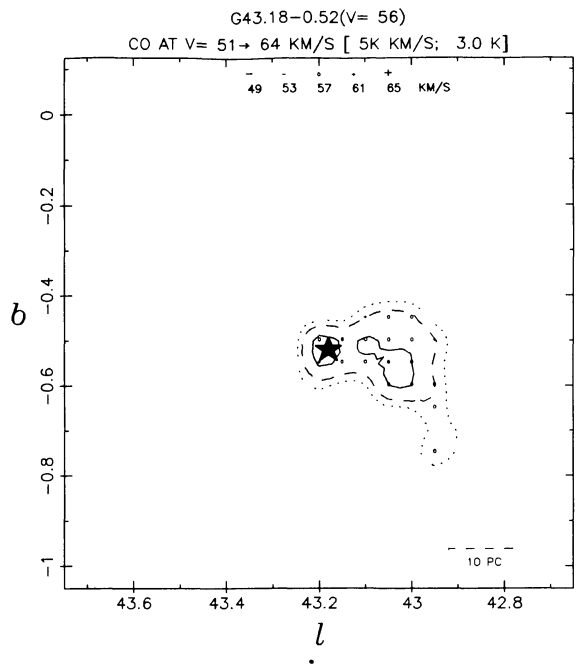

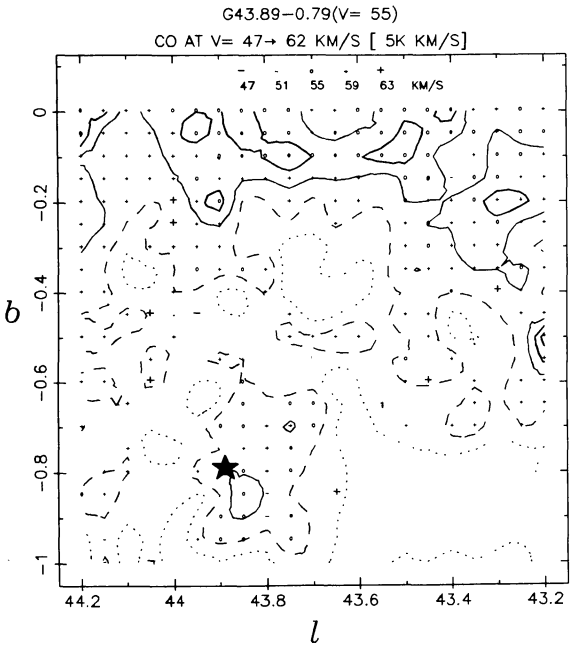

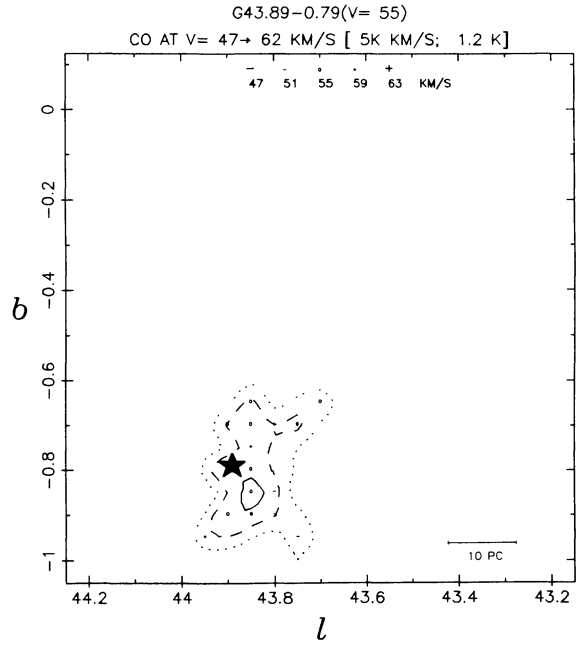

FIG. 13—*Continued*

© American Astronomical Society • Provided by the NASA Astrophysics Data System

1987ApJS...63..821S

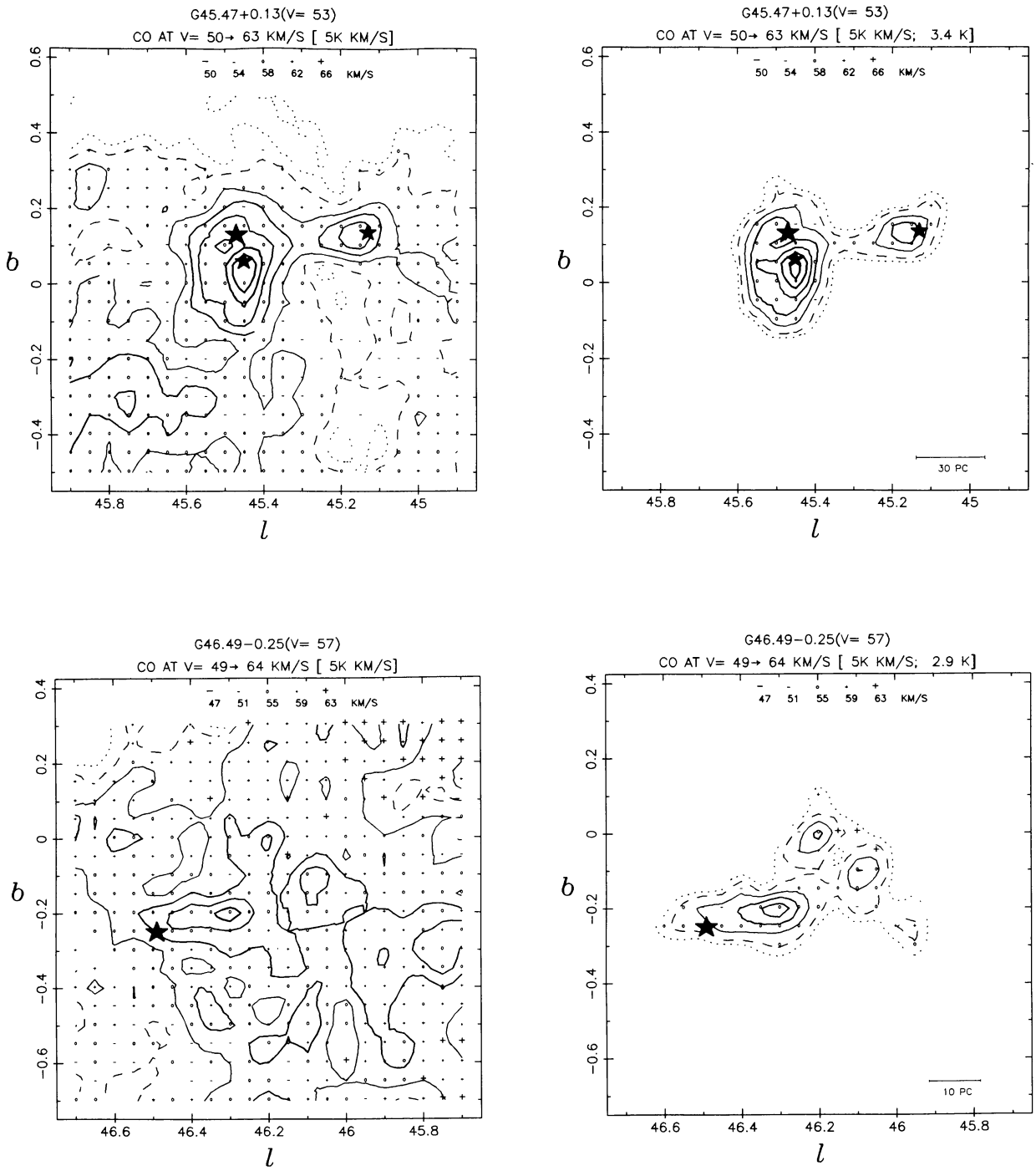

FIG. 13—*Continued*

© American Astronomical Society • Provided by the NASA Astrophysics Data System

1987ApJS...63..821S

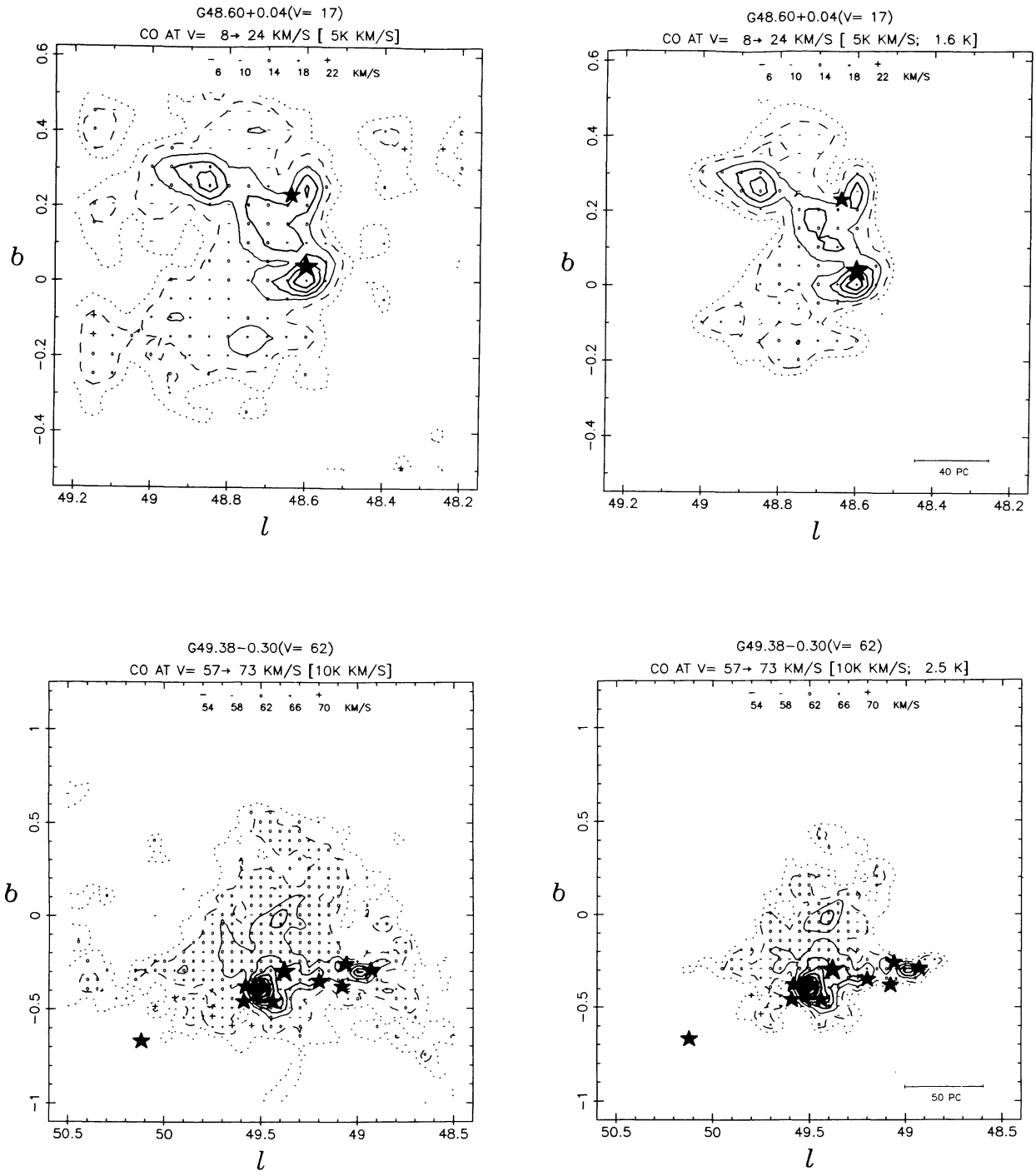

FIG. 13—*Continued*

© American Astronomical Society • Provided by the NASA Astrophysics Data System

1987ApJS...63..821S

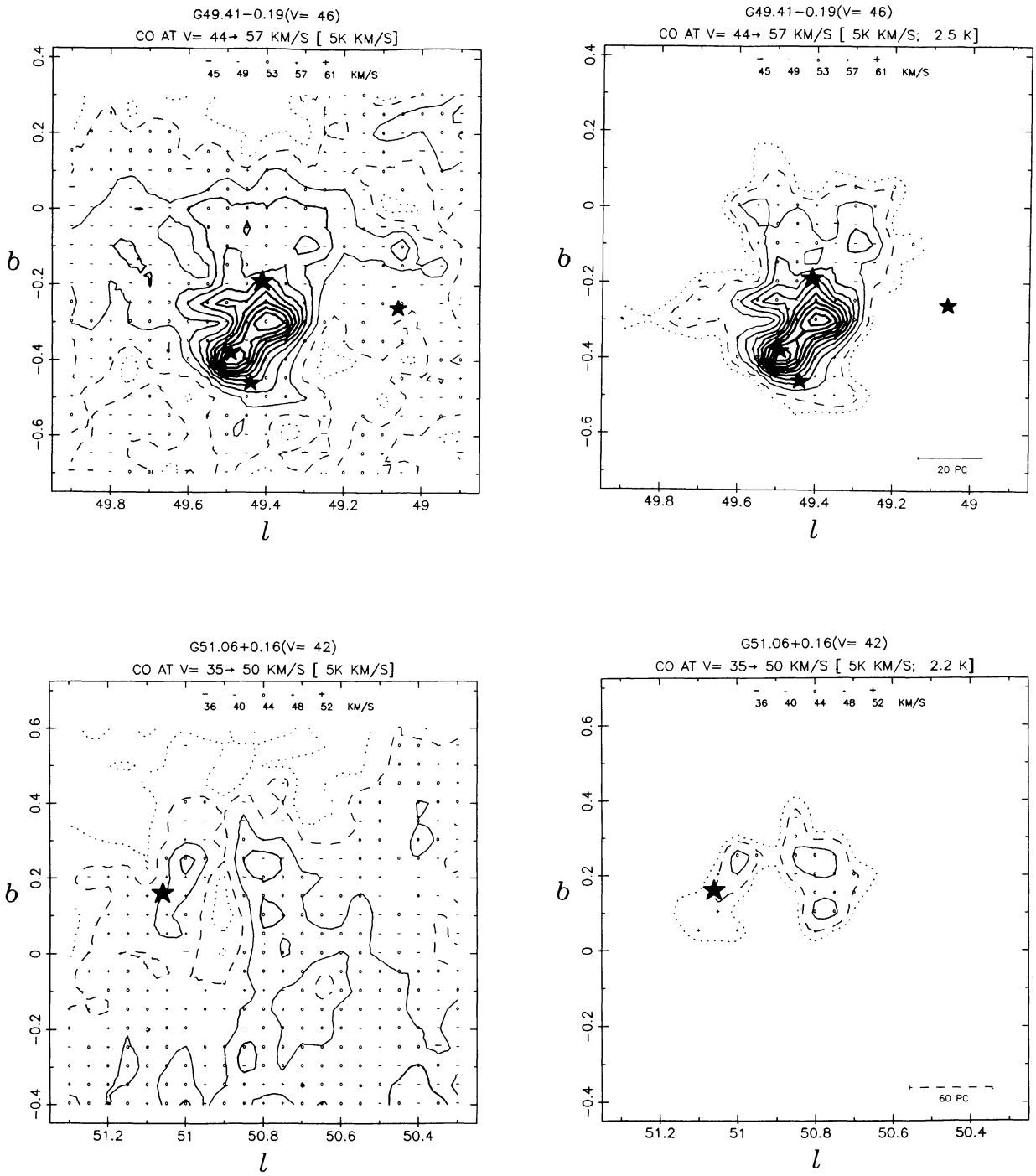

FIG. 13—*Continued*

© American Astronomical Society • Provided by the NASA Astrophysics Data System

1987ApJS...63..821S

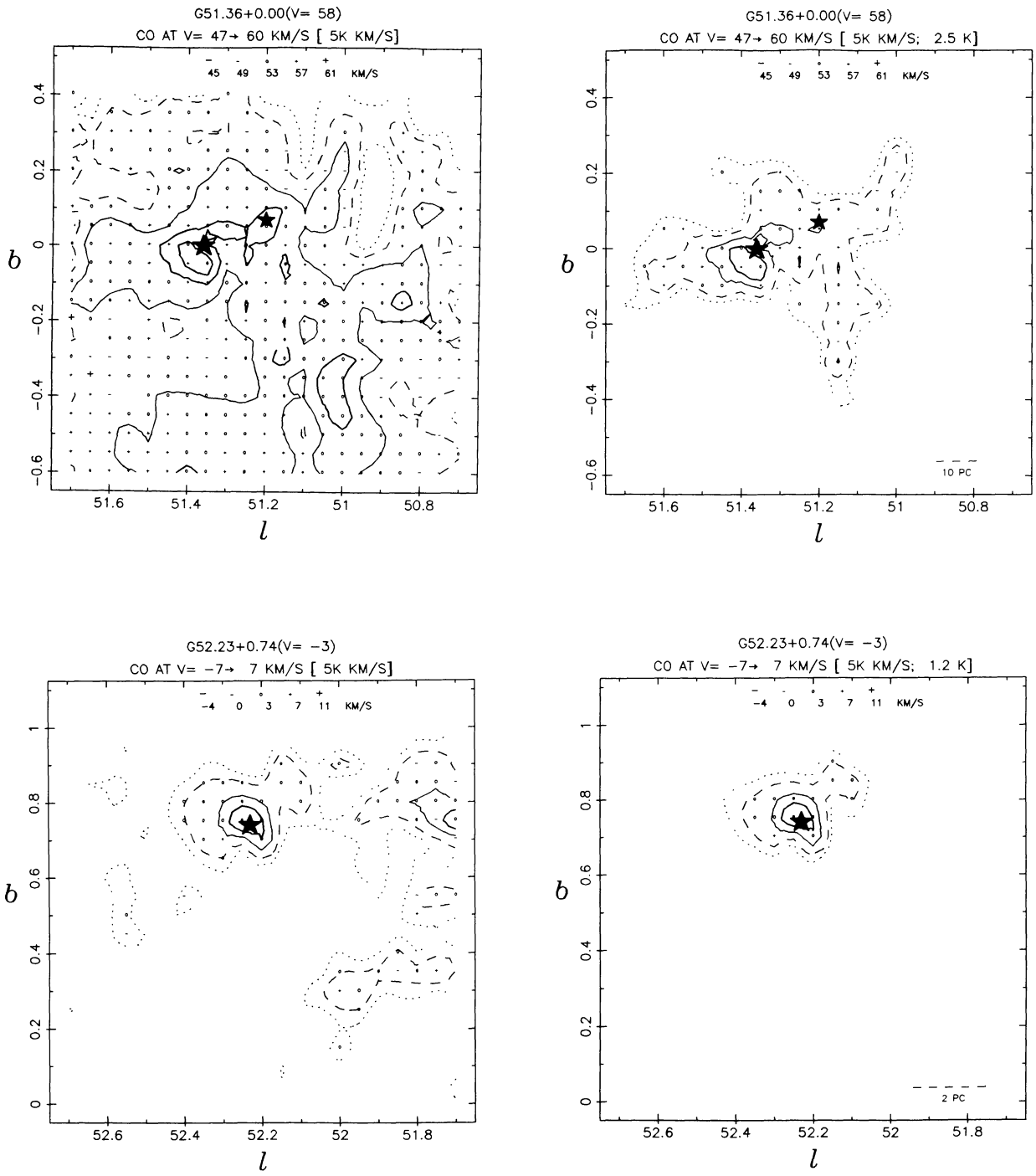

FIG. 13—*Continued*

© American Astronomical Society • Provided by the NASA Astrophysics Data System

1987ApJS...63..821S

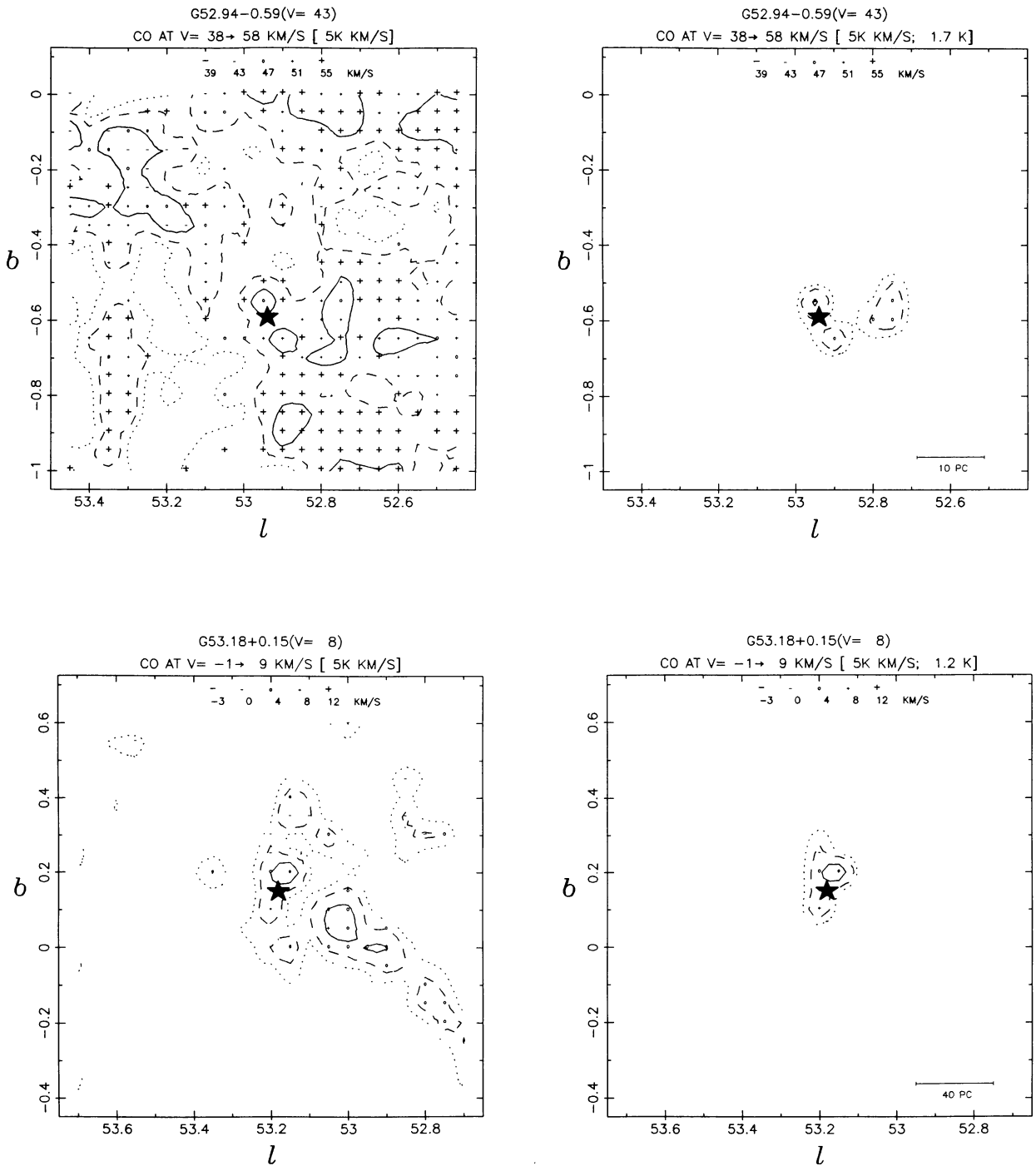

FIG. 13—*Continued*

© American Astronomical Society • Provided by the NASA Astrophysics Data System

1987ApJS...63..821S

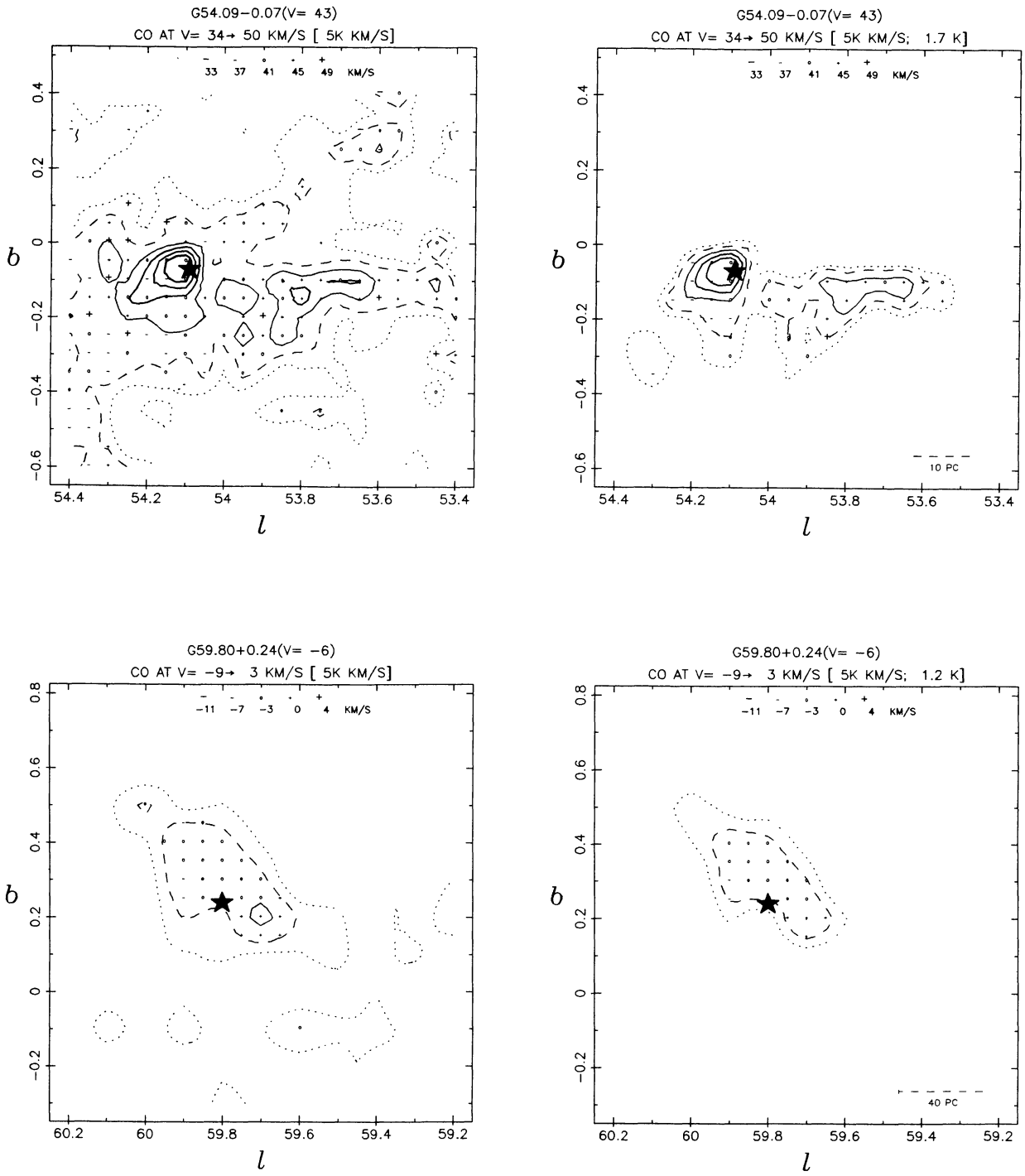

FIG. 13—*Continued*

© American Astronomical Society • Provided by the NASA Astrophysics Data System

TABLE 1

CO CLOUDS AND HOT CORES

CLOUD	l_p °	b_p °	v_p	T_p K	<l> °	<b> °	<v> km s^{-1}	<T> K	N	d_N kpc	d_P kpc	R kpc	<z> pc	Δl °	Δl, pc	Δb °	ΔB pc	σ_v km s^{-1}	NOTES
(1)	(2)	(3)	(4)	(5)	(6)	(7)	(8)	(9)	(10)	(11)	(12)	(13)	(14)	(15)	(16)	(17)	(18)	(19)	(20)
1	0.00	-0.50	37	7.8	0.01	-0.50	36.8	5.0	8	5.1	11.7	3.5	-44	0.10	8.9	0.15	13.3	0.65	
2	0.00	-0.50	128	5.8	0.12	-0.47	133.4	4.5	81	7.5	9.4	1.5	-61	0.25	32.6	0.25	32.6	4.23	TANG.
3	0.00	-0.50	32	9.7	0.01	-0.54	32.5	5.9	20	4.7	12.1	3.9	-44	0.10	8.2	0.25	20.5	1.18	
4	0.00	0.40	21	7.2	0.00	0.39	21.0	5.8	4	3.6	13.2	4.9	24	0.05	3.2	0.10	6.3	0.71	
5	0.30	-0.10	48	8.2	0.26	-0.12	47.7	5.4	31	5.7	11.1	3.0	-11	0.20	19.9	0.20	19.9	1.30	
6	0.30	0.40	20	5.4	0.30	0.42	20.3	4.8	3	3.5	13.4	5.1	25	0.05	3.0	0.10	6.0	0.47	
7	0.40	-0.60	11	7.4	0.41	-0.59	11.0	5.0	5	2.1	14.7	6.4	-22	0.10	3.7	0.10	3.7	0.61	
8	0.40	-0.30	37	17.0	0.84	-0.35	38.0	5.8	889	4.9	11.9	3.7	-30	1.40	119.6	0.80	68.4	2.42	NEAR
A	0.40	-0.30	37	17.0	0.44	-0.28	36.9	10.6	64				-23	0.35	29.9	0.35	29.9	1.27	
B	0.70	-0.40	40	9.8	0.71	-0.39	38.5	8.8	16				-33	0.25	21.4	0.15	12.8	1.27	
C	0.20	-0.20	43	10.0	0.22	-0.20	42.2	8.9	6				-17	0.10	8.5	0.05	4.3	1.05	
9	0.40	0.20	3	5.5	0.40	0.20	3.0	5.2	3	0.8	16.0	7.7	2	0.05	0.7	0.05	0.7	0.80	
10	0.50	-1.00	16	10.5	0.53	-0.29	18.2	5.1	2320	3.2	13.6	5.4	-15	1.40	77.3	1.85	102.1	3.13	NEAR
A	0.20	0.20	20	10.3	0.18	0.20	19.1	8.9	7				11	0.20	11.0	0.05	2.8	0.98	
B	0.50	-1.00	16	10.5	0.51	-0.98	15.8	9.4	6				-54	0.10	5.5	0.10	5.5	0.68	
C	0.60	-0.70	17	9.2	0.63	-0.70	17.1	8.3	12				-38	0.20	11.0	0.10	5.5	0.89	
D	0.60	-0.50	19	9.4	0.60	-0.54	19.3	8.8	4				-29	0.05	2.8	0.15	8.3	0.43	
11	0.50	0.70	15	6.7	0.50	0.71	15.0	4.7	9	2.7	14.1	5.8	33	0.10	4.8	0.20	9.6	0.64	NEAR
12	0.60	-0.30	30	5.8	0.61	-0.28	29.8	4.8	6	4.3	12.5	4.3	-21	0.10	7.5	0.10	7.5	0.68	
13	0.70	-0.10	37	6.0	0.79	-0.10	36.3	4.9	17	4.8	12.0	3.9	-8	0.25	20.8	0.10	8.3	1.00	
14	0.70	0.60	22	7.9	0.69	0.70	22.9	4.7	48	3.6	13.2	4.9	44	0.35	22.2	0.35	22.2	1.10	NEAR
15	0.90	-0.50	12	5.5	0.96	-0.54	9.6	4.4	32	1.8	15.0	6.7	-17	0.20	6.3	0.15	4.8	1.92	
16	0.90	0.70	26	8.6	0.90	0.71	25.6	5.6	9	3.8	13.0	4.7	47	0.15	10.1	0.15	10.1	0.50	NEAR
17	0.00	-0.20	26	11.2	0.00	-0.20	25.9	5.7	19	3.9	12.9	4.7	-13	0.15	10.1	0.15	10.1	0.80	
18	0.00	-0.20	-1	5.8	0.87	-0.11	0.9	4.5	407	4.6	4.6	3.4	-9	1.45	117.5	0.40	32.4	2.17	3 KPC
19	0.00	0.10	33	5.0	0.98	0.10	32.5	4.5	4	4.4	12.4	4.2	7	0.10	7.7	0.05	3.8	0.50	
20	0.10	-0.90	121	5.1	0.10	-0.90	121.4	4.6	4	7.2	9.6	1.8	-113	0.05	6.3	0.05	6.3	1.11	TANG.
21	0.10	-0.20	-11	6.0	0.13	-0.19	-11.6	4.5	8	21.2	21.2	12.9	-71	0.20	74.0	0.10	37.0	0.69	TANG.
22	0.10	0.20	30	5.6	0.05	0.20	30.0	4.9	3	4.2	12.6	4.4	14	0.15	11.0	0.05	3.7	0.00	
23	0.10	0.80	26	6.2	0.15	0.81	25.5	5.0	11	3.8	13.0	4.8	53	0.20	13.2	0.10	6.6	0.63	NEAR
24	0.30	-0.30	11	5.6	0.30	-0.31	11.0	4.8	4	2.0	14.8	6.6	-10	0.05	1.7	0.10	3.5	0.70	
25	0.30	0.00	31	7.6	0.28	0.06	32.7	4.9	77	4.3	12.4	4.3	4	0.30	22.8	0.30	22.8	1.42	
26	0.30	0.70	15	6.7	0.34	0.85	15.5	4.9	49	2.6	14.2	5.9	38	0.15	6.9	0.40	18.3	1.05	NEAR
27	0.40	-0.10	51	8.0	0.39	-0.09	50.9	5.3	7	5.6	11.2	3.1	-9	0.15	14.7	0.10	9.8	0.65	
28	0.50	-0.60	14	7.0	0.53	-0.59	14.5	4.9	24	2.4	14.3	6.1	-24	0.20	8.5	0.20	8.5	1.01	
29	0.50	0.30	25	5.7	0.51	0.23	25.1	4.7	18	3.7	13.1	4.9	14	0.25	15.9	0.20	12.8	0.78	
30	0.60	-0.20	25	5.2	0.60	-0.19	24.8	4.4	7	3.6	13.1	5.0	-11	0.05	3.2	0.10	6.3	1.21	
31	0.60	0.20	17	5.7	0.62	0.19	16.9	4.7	9	2.7	14.0	5.8	9	0.20	9.6	0.10	4.8	0.73	
32	0.60	0.80	26	6.6	0.82	0.80	28.7	4.4	197	3.9	12.8	4.7	54	0.65	44.3	0.45	30.7	3.10	NEAR
33	0.70	-0.80	15	5.1	0.71	-0.80	14.8	4.3	7	2.5	14.3	6.1	-34	0.20	8.6	0.05	2.1	0.63	
34	0.70	0.00	18	5.3	0.68	-0.02	17.5	4.4	6	2.8	14.0	5.8	0	0.10	4.9	0.10	4.9	0.50	
35	0.80	-0.80	28	8.8	0.91	-0.61	29.0	5.1	705	3.9	12.8	4.7	-41	0.95	64.8	0.85	58.0	3.16	NEAR
36	0.80	0.30	9	6.6	0.81	0.29	9.1	5.0	6	1.6	15.1	6.9	8	0.10	2.8	0.10	2.8	0.69	
37	0.90	-0.10	-4	7.7	0.90	-0.10	-3.6	5.3	9	4.7	4.7	3.4	-8	0.15	12.3	0.10	8.2	0.80	3 KPC
38	0.90	-0.10	6	5.4	0.88	-0.09	6.5	4.5	11	4.7	4.7	3.4	-7	0.15	12.2	0.10	8.2	1.21	3 KPC
39	0.90	-0.10	44	6.4	0.83	-0.17	43.7	4.5	17	5.1	11.7	3.6	-15	0.20	17.6	0.25	22.1	1.00	
40	10.00	-0.30	43	5.6	9.99	-0.27	42.7	4.7	6	4.9	11.8	3.8	-23	0.10	8.6	0.15	12.9	0.46	
41	10.00	-0.20	24	5.4	10.01	-0.20	24.4	4.4	7	3.5	13.3	5.1	-12	0.15	9.1	0.05	3.0	0.88	
42	10.00	0.00	48	5.5	10.00	0.00	48.0	4.9	3	5.3	11.4	3.4	0	0.05	4.6	0.05	4.6	0.79	
43	10.00	0.10	30	5.9	10.02	0.09	29.7	4.8	8	3.9	12.8	4.7	6	0.15	10.3	0.10	6.9	0.97	
44	10.10	0.00	42	5.7	10.10	0.00	42.1	5.2	3	4.8	11.9	3.8	0	0.05	4.2	0.05	4.2	0.80	
45	10.10	0.00	24	5.1	10.08	0.00	23.7	4.5	3	3.4	13.3	5.2	0	0.10	5.9	0.05	3.0	0.46	
46	10.30	-0.50	37	5.2	10.30	-0.50	37.0	4.8	3	4.4	12.3	4.2	-38	0.05	3.9	0.05	3.9	0.80	
47	10.30	-0.10	46	6.2	10.31	-0.10	45.2	4.8	11	5.0	11.7	3.7	-8	0.10	8.8	0.05	4.4	2.04	
48	10.40	0.10	68	5.0	10.43	0.03	67.7	4.5	18	6.1	10.7	2.8	2	0.20	21.2	0.15	15.9	1.26	
49	10.50	-0.60	42	5.3	10.52	-0.60	42.5	4.6	4	4.8	12.0	3.9	-49	0.10	8.3	0.05	4.2	0.50	
50	10.60	0.20	10	5.1	10.60	0.20	10.5	4.6	4	1.7	15.0	6.8	5	0.05	1.5	0.05	1.5	1.00	
51	10.60	0.50	36	5.6	10.60	0.49	37.2	4.8	7	4.4	12.3	4.3	37	0.05	3.8	0.10	7.6	1.65	
52	10.60	1.00	19	5.4	10.60	1.00	19.0	5.0	3	2.8	13.9	5.8	48	0.05	2.4	0.05	2.4	0.80	NEAR
53	10.70	-0.10	51	5.7	10.70	-0.09	51.8	4.8	6	5.4	11.3	3.4	-8	0.05	4.7	0.10	9.4	1.29	

© American Astronomical Society • Provided by the NASA Astrophysics Data System

TABLE 1—*Continued*

CLOUD	l_p	b_p	v_p	T_p	<l>	<b>	<v>	<T>	N	d_N	d_F	R	<z>	Δl	ΔL	Δb	ΔB	σ_v	NOTES
	°	°		K	°	°	km s^{-1}	K		kpc	kpc	kpc	pc	°	pc	°	pc	km s^{-1}	
(1)	(2)	(3)	(4)	(5)	(6)	(7)	(8)	(9)	(10)	(11)	(12)	(13)	(14)	(15)	(16)	(17)	(18)	(19)	(20)
54	10.80	-0.10	67	8.0	10.80	-0.13	65.7	5.3	20	6.0	10.7	2.9	-13	0.15	15.6	0.15	15.6	1.67	
55	10.80	0.00	37	5.5	10.80	0.03	36.8	4.4	10	4.3	12.4	4.3	2	0.10	7.5	0.20	15.0	0.74	
56	10.90	0.50	28	5.4	10.90	0.55	28.8	4.8	6	3.7	13.0	4.9	35	0.05	3.2	0.15	9.7	0.67	NEAR
57	11.00	-0.10	39	5.3	11.00	-0.10	39.0	4.8	3	4.4	12.3	4.2	-7	0.05	3.9	0.05	3.9	0.79	
58	11.00	0.10	21	5.7	11.01	0.06	20.6	4.6	9	2.9	13.8	5.7	2	0.10	5.1	0.15	7.6	0.82	
59	11.10	-0.40	-2	12.9	11.11	-0.38	-0.2	5.7	91	0.5	16.5	8.3	-3	0.40	3.5	0.25	2.2	2.11	
A	11.10	-0.40	-2	12.9	11.10	-0.39	-1.8	10.5	6				-3	0.05	0.4	0.10	0.9	1.28	
60	11.10	0.00	25	5.2	11.10	0.00	25.5	5.1	4	3.4	13.3	5.2	0	0.05	2.9	0.05	2.9	1.11	
61	11.40	-0.30	49	6.1	11.46	-0.28	48.2	4.8	19	4.9	11.7	3.8	-24	0.25	21.5	0.10	8.6	0.96	
62	11.40	0.00	49	6.3	11.42	0.00	49.6	4.7	13	5.0	11.6	3.7	0	0.20	17.6	0.15	13.2	0.89	
63	11.40	0.40	30	6.5	11.39	0.36	31.1	4.6	15	3.8	12.9	4.8	23	0.20	13.2	0.20	13.2	1.10	
64	11.50	0.20	28	5.8	11.50	0.25	28.4	4.5	6	3.6	13.1	5.1	15	0.05	3.1	0.15	9.3	0.94	
65	11.60	0.00	94	5.1	11.60	0.00	94.0	4.6	3	6.6	10.0	2.4	0	0.05	5.8	0.05	5.8	0.79	
66	11.60	0.00	34	5.8	11.57	0.00	34.0	4.6	9	4.0	12.7	4.7	0	0.15	10.4	0.15	10.4	0.66	
67	11.70	-0.30	47	6.8	11.69	-0.28	48.7	4.7	36	4.9	11.7	3.8	-23	0.25	21.4	0.25	21.4	1.48	
68	11.70	0.10	33	6.1	11.69	0.10	33.0	5.1	4	3.9	12.8	4.8	6	0.10	6.8	0.05	3.4	0.70	
69	11.80	-0.10	48	5.2	11.80	-0.10	48.0	4.7	3	4.8	11.8	3.9	-8	0.05	4.2	0.05	4.2	0.80	
70	11.90	-0.10	42	6.0	11.96	-0.14	41.0	4.5	31	4.4	12.3	4.3	-10	0.25	19.0	0.15	11.4	1.73	
71	11.90	0.80	26	10.5	11.79	0.75	25.6	5.2	169	3.3	13.4	5.4	42	0.50	28.4	0.50	28.4	1.33	NEAR
A	11.90	0.80	26	10.5	11.87	0.80	25.5	9.0	10				45	0.15	8.5	0.15	8.5	0.79	
72	12.00	-0.20	50	7.5	12.02	-0.19	49.1	5.0	13	4.9	11.8	3.9	-16	0.20	17.0	0.10	8.5	1.01	
73	12.10	-0.20	34	5.5	12.11	-0.19	33.7	4.6	6	3.9	12.8	4.8	-12	0.10	6.7	0.15	10.1	0.47	
74	12.10	0.70	17	5.4	12.07	0.70	16.7	4.5	6	2.3	14.3	6.3	27	0.15	6.0	0.05	2.0	0.73	NEAR
75	12.20	-0.10	23	10.1	12.20	-0.10	25.6	5.8	46	4.8	4.8	3.4	-8	0.15	12.5	0.15	12.5	2.56	3 KPC
A	12.20	-0.10	23	10.1	12.20	-0.10	25.5	9.1	8				-8	0.05	4.2	0.05	4.2	2.24	
76	12.20	0.00	48	5.7	12.21	0.01	48.6	4.7	8	4.8	11.8	4.0	0	0.15	12.5	0.10	8.4	0.68	
77	12.20	0.50	20	5.5	12.10	0.54	27.7	4.5	20	3.4	13.2	5.2	32	0.25	14.8	0.30	17.7	0.63	NEAR
78	12.30	-0.70	45	6.9	12.32	-0.65	44.8	5.2	14	4.5	12.1	4.2	-51	0.20	15.8	0.15	11.9	0.67	
79	12.30	-0.10	67	6.6	12.31	-0.10	66.0	5.2	10	5.8	10.8	3.1	-10	0.10	10.1	0.05	5.0	1.68	
80	12.30	0.30	30	5.1	12.32	0.30	29.5	4.6	4	3.5	13.1	5.1	18	0.10	6.1	0.05	3.1	0.50	
81	12.40	-0.70	25	6.3	12.41	-0.68	24.7	4.6	24	3.1	13.5	5.5	-36	0.20	10.7	0.20	10.7	1.09	
82	12.40	-0.60	16	6.3	12.42	-0.58	16.6	4.9	22	4.8	4.8	3.4	-48	0.15	12.6	0.15	12.6	2.01	3 KPC
83	12.40	0.20	20	5.2	12.41	0.20	19.8	4.5	4	2.6	14.0	6.0	9	0.10	4.5	0.05	2.3	0.81	
84	12.40	0.40	11	5.0	12.42	0.40	10.4	4.8	3	1.5	15.1	7.0	10	0.10	2.6	0.05	1.3	0.48	
85	12.60	-0.80	26	6.0	12.60	-0.79	26.3	4.6	5	3.2	13.4	5.4	-44	0.05	2.8	0.10	5.6	0.98	
86	12.60	-0.30	13	5.5	12.60	-0.28	12.8	4.7	5	4.8	4.8	3.4	-23	0.05	4.2	0.10	8.4	0.73	3 KPC
87	12.60	-0.20	7	5.5	12.61	-0.20	7.4	4.4	5	1.1	15.5	7.4	-3	0.10	2.0	0.05	1.0	0.99	
88	12.70	-0.60	8	5.2	12.69	-0.56	6.7	4.4	10	1.0	15.5	7.5	-10	0.20	3.7	0.15	2.7	0.79	
89	12.70	-0.10	56	9.8	12.69	-0.12	55.8	5.4	26	5.2	11.4	3.7	-10	0.20	18.0	0.20	18.0	1.87	
90	12.80	-0.20	32	22.5	12.36	-0.29	34.4	5.3	9651	3.9	12.7	4.8	-19	5.30	356.8	1.70	114.5	11.27	NEAR
A	10.20	-0.30	8	10.9	10.21	-0.29	9.6	8.9	13				-19	0.10	6.7	0.10	6.7	1.65	
B	10.30	-0.10	11	10.2	10.32	-0.10	10.8	8.9	5				-6	0.10	6.7	0.05	3.4	0.75	
C	10.60	-0.40	-2	16.8	10.61	-0.37	-2.8	10.3	43				-24	0.25	16.8	0.20	13.5	1.41	
D	12.80	-0.20	32	22.5	12.83	-0.23	35.7	10.7	166				-15	0.70	47.1	0.30	20.2	3.17	
E	13.00	-0.10	47	10.6	13.00	-0.10	47.0	9.4	3				-6	0.05	3.4	0.05	3.4	0.79	
F	13.10	-0.10	36	9.5	13.13	-0.10	35.8	8.7	10				-6	0.15	10.1	0.15	10.1	0.75	
G	13.30	0.00	54	10.1	13.23	-0.05	53.7	8.6	30				-3	0.25	16.8	0.20	13.5	1.55	
H	14.20	-0.20	39	15.6	14.21	-0.19	40.3	9.4	178				-12	0.85	57.2	0.30	20.2	2.12	
I	14.40	-0.20	35	9.1	14.44	-0.20	35.7	8.3	4				-13	0.15	10.1	0.05	3.4	0.45	
J	14.60	0.00	38	9.3	14.60	0.00	38.0	8.9	3				0	0.05	3.4	0.05	3.4	0.81	
91	12.90	-0.40	58	5.2	12.90	-0.40	58.0	4.4	3	5.3	11.3	3.6	-36	0.05	4.6	0.05	4.6	0.78	
92	13.00	-0.50	22	6.6	13.01	-0.49	22.5	4.9	15	4.8	4.8	3.4	-41	0.20	16.9	0.15	12.6	0.85	3 KPC
93	13.00	0.40	32	9.1	12.79	0.46	31.1	4.8	131	3.5	13.0	5.1	28	0.70	43.4	0.50	31.0	2.21	
94	13.10	0.70	26	6.0	13.07	0.71	25.7	4.6	7	3.1	13.5	5.6	37	0.15	8.0	0.10	5.3	0.69	NEAR
95	13.30	1.00	29	5.2	13.34	1.00	28.9	4.7	8	3.3	13.3	5.4	57	0.15	8.6	0.05	2.9	0.76	NEAR
96	13.40	-0.50	24	7.2	13.38	-0.52	23.2	4.9	20	4.8	4.8	3.4	-44	0.20	16.9	0.20	16.9	0.79	3 KPC
97	13.50	-0.30	59	5.3	13.49	-0.31	59.6	4.7	5	5.2	11.3	3.6	-28	0.10	9.1	0.10	9.1	0.79	
98	13.60	-0.50	50	6.1	13.60	-0.49	50.0	4.8	4	4.6	11.9	4.2	-39	0.05	4.0	0.10	8.1	0.68	
99	13.60	0.50	21	5.0	13.60	0.50	21.0	4.6	3	2.5	14.0	6.1	22	0.05	2.2	0.05	2.2	0.80	NEAR
100	13.60	0.80	31	5.9	13.65	0.78	29.9	4.5	19	3.3	13.2	5.3	45	0.20	11.6	0.25	14.5	1.00	NEAR

© American Astronomical Society • Provided by the NASA Astrophysics Data System

TABLE 1—*Continued*

CLOUD (1)	l_p ° (2)	b_p ° (3)	v_p (4)	T_p K (5)	<l> ° (6)	<b> ° (7)	<v> km s^{-1} (8)	<T> K (9)	N (10)	d_N kpc (11)	d_P kpc (12)	R kpc (13)	<z> pc (14)	Δl ° (15)	ΔL pc (16)	Δb ° (17)	ΔB pc (18)	σ_v km s^{-1} (19)	NOTES (20)
101	13.70	-0.60	49	5.3	13.70	-0.60	49.0	4.8	3	4.5	12.0	4.2	-47	0.05	4.0	0.05	4.0	0.80	
102	13.70	-0.20	101	5.9	13.71	-0.20	99.9	5.0	6	6.7	9.9	2.6	-23	0.10	11.6	0.05	5.8	1.33	
103	13.70	-0.10	48	7.5	13.72	-0.10	49.3	4.8	49	4.6	12.0	4.2	-7	0.40	31.8	0.20	15.9	1.60	
104	13.80	0.10	22	5.5	13.79	0.10	21.5	4.7	6	2.6	14.0	6.0	4	0.10	4.5	0.15	6.7	0.77	
105	13.90	0.30	49	9.0	13.97	0.24	47.2	5.1	126	4.4	12.1	4.4	18	0.50	38.4	0.45	34.6	1.56	
A	13.90	0.30	49	9.0	13.90	0.30	48.0	8.8	3				23	0.05	3.8	0.05	3.8	0.81	
106	13.90	0.90	27	5.3	13.98	0.88	26.5	4.3	64	3.0	13.5	5.6	46	0.40	20.9	0.35	18.3	1.65	NEAR
107	14.00	-1.00	14	8.1	13.99	-0.98	15.4	5.4	15	1.9	14.6	6.7	-32	0.15	5.0	0.15	5.0	1.35	
108	14.00	-0.10	26	5.8	14.14	-0.13	25.4	4.3	30	4.9	4.9	3.4	-11	0.35	29.9	0.30	25.6	1.21	3 KPC
109	14.10	0.10	10	6.2	14.09	0.10	8.9	5.3	14	1.2	15.3	7.3	2	0.10	2.1	0.05	1.1	3.51	
110	14.30	-0.50	36	5.5	14.30	-0.51	35.5	4.6	8	4.9	4.9	3.4	-43	0.15	12.8	0.10	8.6	0.50	3 KPC
111	14.40	-0.50	57	5.4	14.40	-0.50	57.1	4.8	3	4.9	11.6	4.0	-42	0.05	4.3	0.05	4.3	0.79	
112	14.40	-0.50	33	6.4	14.41	-0.50	33.0	4.8	6	4.9	4.9	3.4	-42	0.10	8.6	0.15	12.9	0.59	3 KPC
113	14.40	0.50	20	6.7	14.40	0.49	19.0	5.0	15	2.2	14.2	6.4	19	0.15	5.9	0.10	3.9	2.39	NEAR
114	14.40	1.00	24	5.7	14.40	1.00	24.9	5.1	3	2.8	13.7	5.8	48	0.05	2.4	0.05	2.4	0.80	NEAR
115	14.50	-0.30	59	5.8	14.50	-0.30	58.7	4.9	6	5.0	11.5	3.9	-26	0.05	4.3	0.15	13.0	0.92	
116	14.60	-0.60	37	6.6	14.57	-0.64	37.0	4.7	62	4.9	4.9	3.4	-55	0.35	30.1	0.40	34.4	0.91	3 KPC
117	14.60	0.80	28	5.7	14.67	0.78	28.5	4.6	11	3.1	13.4	5.6	41	0.20	10.7	0.15	8.0	0.79	NEAR
118	14.70	-0.30	60	6.1	14.71	-0.31	59.7	4.8	21	5.0	11.5	3.9	-26	0.15	13.1	0.35	30.5	0.97	
119	14.70	0.20	27	5.3	14.69	0.21	26.8	4.5	6	2.9	13.5	5.7	10	0.10	5.1	0.10	5.1	0.68	
120	14.90	-1.00	22	6.4	14.90	-1.00	21.1	5.4	5	2.4	14.0	6.2	-41	0.05	2.1	0.05	2.1	1.35	
121	14.90	-0.40	62	13.7	14.90	-0.40	61.6	6.6	24	5.1	11.4	3.8	-35	0.15	13.3	0.15	13.3	1.06	
A	14.90	-0.40	62	13.7	14.90	-0.40	61.5	11.1	4				-35	0.05	4.4	0.05	4.4	1.02	
122	15.00	-0.70	20	42.6	13.90	-0.31	19.6	6.3	4845	2.4	14.1	6.2	-12	3.30	135.7	2.05	84.3	3.27	NEAR
A	12.40	0.50	18	12.2	12.40	0.51	18.7	9.8	10				20	0.15	6.2	0.10	4.1	0.91	
B	12.60	0.40	18	9.9	12.62	0.40	18.3	8.9	3				16	0.10	4.1	0.05	2.1	0.46	
C	12.70	0.70	18	16.2	12.76	0.58	18.8	9.5	57				23	0.35	14.4	0.35	14.4	0.96	
D	13.40	-0.20	16	10.4	13.42	-0.25	16.4	9.1	22				-10	0.15	6.2	0.30	12.3	1.01	
E	13.40	-0.20	20	10.6	13.43	-0.23	20.1	8.7	13				-9	0.25	10.3	0.15	6.2	0.61	
F	13.50	0.00	17	11.2	13.50	0.01	15.9	9.4	15				0	0.05	2.1	0.15	6.2	2.04	
G	13.60	0.10	13	9.9	13.60	0.10	12.6	8.8	6				4	0.05	2.1	0.05	2.1	1.67	
H	13.70	-0.70	15	11.1	13.72	-0.70	14.7	9.5	7				-28	0.10	4.1	0.05	2.1	1.02	
I	13.70	-0.30	17	13.2	13.68	-0.28	17.9	9.3	34				-11	0.25	10.3	0.20	8.2	1.41	
J	14.00	-0.60	18	15.3	14.08	-0.56	19.7	9.6	361				-23	0.95	39.1	0.50	20.6	1.52	
K	14.80	-0.50	21	9.9	14.79	-0.51	20.8	8.9	6				-20	0.10	4.1	0.10	4.1	1.08	
L	15.00	-0.70	20	42.6	15.06	-0.64	19.5	13.9	182				-26	0.45	18.5	0.30	12.3	1.95	
M	15.20	-0.50	16	11.2	15.22	-0.50	15.7	9.3	3				-20	0.10	4.1	0.05	2.1	0.46	
123	15.10	0.90	43	9.5	15.16	0.91	42.6	5.8	26	4.0	12.4	4.8	63	0.30	20.8	0.15	10.4	1.19	NEAR
124	15.30	-0.20	78	6.0	15.30	-0.18	77.9	4.8	5	5.9	10.5	3.2	-18	0.05	5.1	0.10	10.3	0.75	
125	15.30	-0.20	61	6.6	15.30	-0.20	61.0	5.3	3	5.0	11.4	3.9	-17	0.05	4.3	0.05	4.3	0.77	
126	15.30	0.00	32	6.7	15.32	-0.06	32.1	4.9	78	3.3	13.1	5.4	-3	0.30	17.1	0.50	28.5	0.89	
127	15.40	-0.20	22	5.2	15.40	-0.20	22.0	4.7	3	2.4	14.0	6.2	-8	0.05	2.1	0.05	2.1	0.79	
128	15.50	-1.00	58	5.2	15.35	-1.00	57.5	4.4	16	4.8	11.6	4.1	-83	0.35	29.1	0.10	8.3	0.70	
129	15.50	-0.60	44	5.1	15.50	-0.61	44.2	4.4	8	5.0	5.0	3.4	-53	0.05	4.4	0.20	17.4	0.65	3 KPC
130	15.50	-0.50	57	6.7	15.46	-0.52	57.3	4.9	20	4.7	11.6	4.1	-43	0.20	16.6	0.15	12.4	0.97	
131	15.50	-0.20	60	8.2	15.50	-0.20	59.8	5.2	9	4.9	11.5	4.0	-17	0.15	12.8	0.15	12.8	0.63	
132	15.50	-0.10	50	5.3	15.48	-0.10	49.5	4.7	4	5.0	5.0	3.4	-8	0.10	8.7	0.05	4.4	0.50	3 KPC
133	15.50	0.30	49	6.9	15.50	0.28	49.0	5.2	10	4.3	12.1	4.5	20	0.10	7.5	0.25	18.8	0.61	
134	15.50	0.70	28	5.8	15.47	0.69	27.5	4.7	17	2.9	13.5	5.8	34	0.25	12.6	0.20	10.1	0.68	NEAR
135	15.70	-0.50	51	6.1	15.71	-0.51	50.9	4.9	6	5.0	5.0	3.4	-44	0.10	8.7	0.10	8.7	0.69	3 KPC
136	15.70	-0.40	59	6.8	15.70	-0.41	59.2	5.6	6	4.8	11.6	4.1	-34	0.05	4.2	0.10	8.4	1.04	
137	15.70	-0.20	57	7.0	15.74	-0.20	57.9	4.9	24	4.7	11.6	4.1	-16	0.25	20.7	0.30	24.8	0.78	
138	15.80	-0.60	48	7.1	15.76	-0.51	43.9	4.7	146	5.0	5.0	3.4	-44	0.65	56.9	0.45	39.4	2.60	3 KPC
139	15.80	-0.20	44	5.2	15.80	-0.19	43.4	4.6	5	5.0	5.0	3.4	-16	0.05	4.4	0.10	8.8	0.99	3 KPC
140	15.90	-1.00	58	5.2	15.90	-0.95	57.9	4.4	26	4.7	11.6	4.2	-78	0.30	24.7	0.25	20.6	0.56	
141	15.90	-0.60	52	6.2	15.89	-0.60	51.8	4.6	13	5.0	5.0	3.4	-53	0.10	8.8	0.20	17.5	1.17	3 KPC
142	15.90	-0.60	19	12.7	16.00	-0.70	19.0	5.9	245	2.1	14.3	6.5	-25	0.95	34.4	0.45	16.3	1.35	
A	15.90	-0.60	19	12.7	15.87	-0.64	18.2	9.6	23				-23	0.30	10.8	0.25	9.0	0.83	
B	16.30	-0.70	20	9.3	16.26	-0.70	19.4	8.6	5				-25	0.15	5.4	0.05	1.8	0.49	
143	15.90	-0.30	60	5.4	15.90	-0.29	61.1	4.7	6	4.9	11.5	4.0	-24	0.05	4.3	0.10	8.5	1.34	

© American Astronomical Society • Provided by the NASA Astrophysics Data System

TABLE 1—*Continued*

CLOUD (1)	l_p ° (2)	b_p ° (3)	v_p (4)	T_p K (5)	<l> ° (6)	<b> ° (7)	<v> km s^{-1} (8)	<T> K (9)	N (10)	d_N kpc (11)	d_F kpc (12)	R kpc (13)	<z> pc (14)	Δl ° (15)	ΔL pc (16)	Δb ° (17)	ΔB pc (18)	σ_v km s^{-1} (19)	NOTES (20)
144	15.90	-0.30	53	6.8	15.86	-0.36	52.2	4.9	23	5.0	5.0	3.4	-31	0.20	17.5	0.25	21.9	0.97	3 KPC
145	15.90	0.00	25	7.1	15.90	-0.03	25.7	5.2	8	2.7	13.7	6.0	-1	0.05	2.3	0.20	9.4	0.65	
146	15.90	0.30	19	6.9	16.11	0.38	18.8	4.7	72	2.0	14.3	6.6	13	0.55	19.6	0.35	12.5	1.20	
147	16.00	0.50	26	8.1	16.01	0.50	25.5	5.7	9	2.6	13.7	6.0	23	0.15	6.9	0.05	2.3	1.20	
148	16.10	-0.50	22	5.7	16.12	-0.51	21.6	4.7	5	2.3	14.0	6.3	-20	0.10	4.0	0.10	4.0	0.49	
149	16.20	-0.80	56	6.1	16.23	-0.83	57.2	4.5	29	4.6	11.7	4.2	-67	0.15	12.2	0.20	16.2	1.07	
150	16.20	0.90	25	7.2	16.21	0.89	25.7	5.2	7	2.6	13.7	6.0	40	0.10	4.6	0.10	4.6	0.68	NEAR
151	16.30	-0.60	24	5.9	16.36	-0.58	23.5	4.6	14	2.4	13.9	6.2	-24	0.25	10.7	0.15	6.4	0.50	
152	16.30	-0.40	19	8.6	16.29	-0.33	18.5	5.2	26	2.0	14.3	6.6	-11	0.20	7.0	0.30	10.4	1.13	
153	16.30	-0.10	27	5.9	16.30	-0.11	26.8	4.7	6	2.7	13.6	5.9	-5	0.05	2.4	0.15	7.2	0.68	
154	16.30	0.00	24	5.2	16.25	0.00	24.5	4.5	8	2.5	13.8	6.1	0	0.15	6.6	0.05	2.2	0.86	
155	16.30	0.40	28	10.0	16.30	0.58	27.8	5.5	133	2.8	13.5	5.9	28	0.35	17.2	0.60	29.5	1.12	NEAR
A	16.30	0.40	28	10.0	16.27	0.47	27.6	9.1	11				23	0.15	7.4	0.20	9.8	0.48	
156	16.40	0.30	36	5.8	16.48	0.28	32.5	4.6	60	3.2	13.1	5.5	15	0.30	16.5	0.35	19.3	2.89	
157	16.40	0.90	20	7.0	16.40	0.94	19.7	4.8	36	2.1	14.2	6.5	34	0.30	11.0	0.25	9.1	0.80	NEAR
158	16.50	-0.50	20	5.7	16.51	-0.46	20.0	4.4	13	2.1	14.2	6.5	-16	0.15	5.5	0.15	5.5	0.67	
159	16.50	-0.10	39	9.2	16.51	-0.10	38.2	5.1	37	5.1	5.1	3.4	-9	0.20	17.7	0.25	22.2	1.45	3 KPC
160	16.50	0.40	38	6.8	16.49	0.40	38.4	5.0	8	3.6	12.7	5.2	24	0.10	6.2	0.15	9.3	0.48	
161	16.70	-0.80	43	5.5	16.71	-0.81	43.4	4.4	20	3.8	12.4	4.9	-54	0.15	10.1	0.15	10.1	1.49	
162	16.70	-0.70	27	5.6	16.70	-0.70	27.0	4.8	3	2.7	13.6	6.0	-33	0.05	2.4	0.05	2.4	0.78	
163	16.70	-0.60	33	5.4	16.70	-0.62	33.0	4.5	10	3.2	13.1	5.5	-34	0.05	2.8	0.20	11.1	0.76	
164	16.70	-0.50	43	9.9	16.44	-0.38	44.0	5.2	636	5.1	5.1	3.4	-33	0.90	79.7	0.75	66.4	2.87	3 KPC
A	16.70	-0.50	43	9.9	16.57	-0.43	44.6	8.8	16				-38	0.25	22.1	0.25	22.1	0.92	
165	16.70	-0.10	60	8.8	16.65	-0.13	57.7	4.8	93	5.1	5.1	3.4	-11	0.55	48.9	0.35	31.1	2.00	3 KPC
166	16.80	-0.30	52	7.8	16.80	-0.30	51.5	5.1	20	5.1	5.1	3.4	-26	0.15	13.4	0.15	13.4	1.25	3 KPC
167	16.90	-0.50	47	7.4	16.90	-0.50	47.0	5.0	16	5.1	5.1	3.4	-44	0.15	13.4	0.15	13.4	1.01	3 KPC
168	16.90	0.30	24	18.1	17.00	0.41	23.4	6.4	1622	2.4	13.9	6.3	16	1.10	45.4	1.75	72.2	3.17	NEAR
A	16.80	-0.30	23	10.3	16.80	-0.29	23.3	9.1	3				-11	0.05	2.1	0.10	4.1	0.47	
B	16.80	0.10	30	12.6	16.80	0.08	30.2	10.2	5				3	0.05	2.1	0.10	4.1	0.73	
C	16.80	0.60	25	9.7	16.82	0.60	24.7	8.8	3				24	0.10	4.1	0.05	2.1	0.47	
D	16.90	0.30	24	18.1	17.04	0.59	22.7	10.2	329				24	0.60	24.8	0.95	39.2	1.83	
E	16.90	0.70	24	9.9	16.92	0.69	23.6	8.7	5				28	0.10	4.1	0.10	4.1	0.49	
F	17.40	0.60	22	12.5	17.42	0.60	22.7	10.7	5				24	0.10	4.1	0.05	2.1	0.72	
169	17.00	0.00	22	6.9	17.01	0.00	21.8	4.8	11	2.2	14.0	6.4	0	0.10	3.9	0.15	5.8	0.90	
170	17.10	-0.30	50	5.3	17.11	-0.30	49.9	4.6	4	5.1	5.1	3.4	-26	0.10	9.0	0.05	4.5	0.70	3 KPC
171	17.10	-0.20	32	5.6	17.10	-0.22	33.3	4.5	14	3.1	13.1	5.6	-11	0.20	11.0	0.15	8.2	1.40	
172	17.20	-0.90	20	5.2	17.20	-0.90	20.6	4.7	8	2.1	14.1	6.5	-33	0.05	1.8	0.05	1.8	2.23	
173	17.20	-0.80	55	7.7	17.21	-0.80	55.1	5.1	17	4.4	11.8	4.5	-61	0.15	11.6	0.15	11.6	1.24	
174	17.20	-0.50	50	6.5	17.21	-0.51	50.3	5.0	7	5.1	5.1	3.4	-45	0.15	13.5	0.10	9.0	0.67	3 KPC
175	17.20	-0.20	55	7.6	17.21	-0.21	54.6	5.1	10	5.1	5.1	3.4	-18	0.10	9.0	0.15	13.5	0.65	3 KPC
176	17.20	-0.20	43	13.0	17.18	-0.21	44.4	5.6	200	5.1	5.1	3.4	-18	0.70	62.8	0.40	35.9	2.37	3 KPC
A	17.20	-0.20	43	13.0	17.21	-0.22	43.5	9.4	20				-19	0.20	18.0	0.20	18.0	1.06	
177	17.30	-0.90	46	7.9	17.31	-0.90	45.5	5.0	29	3.9	12.3	4.9	-61	0.20	13.6	0.25	17.0	1.45	
178	17.30	-0.40	57	5.3	17.30	-0.38	57.8	4.7	5	5.2	5.2	3.4	-34	0.05	4.5	0.10	9.0	0.73	3 KPC
179	17.40	-0.20	37	5.1	17.40	-0.22	36.3	4.5	6	3.3	12.9	5.4	-12	0.05	2.9	0.10	5.8	1.09	
180	17.50	0.10	46	6.7	17.48	0.10	45.2	4.9	17	3.9	12.3	4.9	6	0.25	16.9	0.15	10.1	0.96	
181	17.50	0.80	24	11.7	17.50	0.80	23.4	6.1	20	2.3	13.9	6.3	32	0.15	6.1	0.15	6.1	1.00	NEAR
A	17.50	0.80	24	11.7	17.50	0.80	23.1	10.3	3				32	0.05	2.0	0.05	2.0	0.79	
182	17.50	0.90	18	5.7	17.50	0.85	18.0	5.1	3	1.9	14.4	6.8	27	0.05	1.6	0.15	4.9	0.00	NEAR
183	17.60	-0.50	35	6.3	17.61	-0.51	35.0	5.1	5	3.2	13.0	5.5	-28	0.10	5.6	0.10	5.6	0.65	
184	17.60	-0.20	21	7.6	17.61	-0.20	21.0	5.2	6	2.1	14.1	6.5	-7	0.10	3.7	0.15	5.5	0.58	
185	17.60	0.00	35	6.1	17.57	0.02	35.0	5.2	13	3.2	13.0	5.5	1	0.15	8.4	0.15	8.4	0.88	
186	17.60	0.70	26	5.3	17.60	0.71	26.3	4.8	3	2.6	13.7	6.1	31	0.05	2.2	0.10	4.5	0.47	NEAR
187	17.70	-0.60	65	5.2	17.68	-0.60	65.4	4.4	20	5.2	5.2	3.4	-54	0.20	18.1	0.25	22.7	0.85	3 KPC
188	17.70	0.10	41	7.0	17.68	0.09	41.9	5.0	19	3.7	12.5	5.1	5	0.15	9.6	0.15	9.6	2.17	
189	17.70	0.30	22	8.2	17.67	0.26	23.5	5.4	272	2.3	13.9	6.3	10	0.70	28.2	0.45	18.2	1.84	
190	17.80	-0.70	45	5.2	17.80	-0.70	44.5	4.5	6	3.8	12.4	5.0	-46	0.15	9.9	0.05	3.3	0.94	
191	17.80	-0.10	48	5.1	17.80	-0.10	47.0	4.8	5	3.9	12.2	4.9	-6	0.05	3.4	0.05	3.4	1.38	
192	17.80	0.00	17	7.2	17.79	0.01	17.0	5.4	3	1.7	14.4	6.9	0	0.10	3.0	0.10	3.0	0.00	
193	17.80	0.50	23	8.7	17.80	0.50	23.0	5.3	7	2.3	13.9	6.4	19	0.15	5.9	0.15	5.9	0.52	NEAR

© American Astronomical Society • Provided by the NASA Astrophysics Data System

TABLE 1—*Continued*

CLOUD	l_p	b_p	v_p	T_p	<l>	<b>	<v>	<T>	N	d_N	d_F	R	<z>	Δl	ΔL	Δb	ΔB	σ_v	NOTES
	°	°		K	°	°	km s^{-1}	K		kpc	kpc	kpc	pc	°	pc	°	pc	km s^{-1}	
(1)	(2)	(3)	(4)	(5)	(6)	(7)	(8)	(9)	(10)	(11)	(12)	(13)	(14)	(15)	(16)	(17)	(18)	(19)	(20)
194	17.90	-1.00	39	5.2	17.92	-1.00	38.6	4.7	4	3.4	12.8	5.4	-59	0.10	6.0	0.05	3.0	0.50	
195	17.90	-0.70	41	5.4	17.93	-0.61	41.2	4.4	47	3.6	12.6	5.2	-37	0.20	12.5	0.25	15.7	1.48	
196	17.95	-0.20	53	5.9	17.91	-0.20	53.6	4.7	12	5.2	5.2	3.4	-18	0.15	13.7	0.05	4.6	1.40	3 KPC
197	17.95	0.00	52	6.8	17.92	-0.02	52.6	5.1	15	4.2	11.9	4.7	-1	0.15	11.1	0.10	7.4	1.00	
198	17.95	0.20	48	6.0	17.92	0.20	48.0	5.0	7	4.0	12.2	4.9	13	0.15	10.4	0.05	3.5	0.73	
199	18.00	-0.25	24	5.8	18.03	-0.24	24.0	5.1	3	2.3	13.8	6.3	-9	0.10	4.1	0.10	4.1	0.00	
200	18.05	0.30	23	5.4	18.11	0.38	23.2	4.7	18	2.2	13.9	6.4	15	0.15	5.9	0.30	11.8	0.68	
201	18.10	-0.90	40	6.4	18.11	-0.87	38.6	5.2	10	3.4	12.8	5.4	-51	0.10	5.9	0.10	5.9	1.45	
202	18.10	-0.15	112	5.9	18.10	-0.15	112.0	5.0	3	7.1	9.1	2.8	-18	0.05	6.2	0.05	6.2	0.78	TANG.
203	18.10	0.05	52	6.5	18.14	0.01	50.9	4.7	28	4.1	12.0	4.8	0	0.15	10.8	0.20	14.4	2.03	
204	18.15	-0.30	54	25.4	18.43	-0.28	47.9	6.2	1127	3.9	12.2	4.9	-19	1.45	99.4	0.95	65.1	4.02	NEAR
A	17.95	-0.50	53	9.2	17.92	-0.50	52.5	8.8	4				-34	0.10	6.9	0.05	3.4	0.50	
B	18.00	-0.35	42	10.9	18.00	-0.35	41.9	9.6	3				-23	0.05	3.4	0.05	3.4	0.79	
C	18.10	-0.35	55	13.2	18.10	-0.35	55.0	11.4	3				-23	0.05	3.4	0.05	3.4	0.78	
D	18.15	-0.30	54	25.4	18.15	-0.32	49.7	11.8	99				-21	0.25	17.1	0.35	24.0	3.02	
E	18.45	-0.20	52	11.3	18.46	-0.21	51.2	9.6	11				-14	0.15	10.3	0.15	10.3	1.05	
F	18.65	-0.05	45	15.2	18.65	-0.07	46.3	10.4	10				-4	0.10	6.9	0.15	10.3	1.36	
G	18.85	0.05	50	11.7	18.88	0.04	49.5	9.2	8				2	0.10	6.9	0.10	6.9	0.86	
H	19.00	-0.05	45	11.1	18.98	-0.05	45.5	9.6	6				-3	0.10	6.9	0.05	3.4	0.96	
I	19.10	0.10	46	11.6	19.10	0.08	46.1	9.8	6				5	0.05	3.4	0.10	6.9	1.03	
205	18.15	0.20	11	5.2	18.14	0.20	10.6	4.8	3	1.2	15.0	7.4	4	0.10	2.1	0.05	1.0	0.48	
206	18.20	-0.70	47	5.6	18.20	-0.70	47.9	4.7	3	3.9	12.2	4.9	-48	0.05	3.4	0.05	3.4	0.82	
207	18.25	0.75	38	5.4	18.25	0.70	38.5	4.6	6	3.4	12.8	5.4	41	0.05	3.0	0.15	8.9	0.50	NEAR
208	18.30	-0.85	39	10.2	18.31	-0.85	39.0	6.5	4	3.4	12.7	5.4	-50	0.10	5.9	0.05	3.0	0.67	
209	18.30	-0.40	34	11.3	18.31	-0.39	32.8	6.8	16	3.0	13.2	5.7	-20	0.10	5.2	0.10	5.2	2.13	
A	18.30	-0.40	34	11.3	18.30	-0.40	33.6	10.1	4				-20	0.05	2.6	0.05	2.6	1.09	
210	18.30	-0.25	46	5.5	18.30	-0.26	45.3	4.7	5	3.8	12.3	5.0	-17	0.05	3.3	0.10	6.6	1.14	
211	18.35	-1.05	48	5.0	18.35	-1.03	49.0	4.4	6	4.0	12.1	4.9	-71	0.05	3.5	0.10	7.0	1.26	
212	18.35	-0.20	36	8.1	18.37	-0.20	35.8	5.5	5	3.2	12.9	5.6	-11	0.10	5.6	0.05	2.8	0.72	
213	18.45	-0.70	52	7.3	18.34	-0.78	50.6	5.0	68	4.1	12.1	4.8	-55	0.25	17.8	0.30	21.4	2.41	
214	18.50	-0.60	49	7.0	18.52	-0.61	49.7	5.2	10	4.0	12.1	4.9	-42	0.10	7.0	0.10	7.0	1.06	
215	18.50	0.00	44	7.1	18.50	0.00	44.8	5.9	3	3.7	12.4	5.1	0	0.05	3.3	0.05	3.3	0.78	
216	18.50	0.00	25	7.2	18.48	0.02	24.4	5.2	8	2.3	13.8	6.3	0	0.15	6.1	0.10	4.0	0.80	
217	18.55	-0.35	19	6.8	18.55	-0.34	18.6	4.9	5	1.8	14.3	6.8	-10	0.05	1.6	0.10	3.2	0.94	
218	18.65	0.00	61	5.0	18.67	0.00	61.3	4.6	3	4.6	11.5	4.4	0	0.10	8.0	0.05	4.0	0.47	
219	18.65	0.00	27	5.3	18.67	0.00	27.0	4.7	6	2.5	13.6	6.2	0	0.10	4.4	0.05	2.2	0.80	
220	18.65	0.30	21	7.1	18.65	0.31	20.1	5.2	25	1.9	14.2	6.7	10	0.25	8.5	0.15	5.1	2.39	
221	18.70	0.00	79	6.4	18.67	0.03	79.2	5.0	16	5.5	10.6	3.7	2	0.15	14.4	0.10	9.6	1.77	
222	18.75	-0.05	63	5.0	18.75	-0.05	63.0	4.6	3	5.3	5.3	3.4	-4	0.05	4.6	0.05	4.6	0.80	3 KPC
223	18.80	-0.90	63	5.9	18.81	-0.90	62.4	4.7	11	4.6	11.5	4.4	-72	0.10	8.1	0.15	12.1	1.19	
224	18.80	0.20	18	5.2	18.80	0.20	17.5	4.8	4	1.7	14.4	6.9	6	0.05	1.5	0.05	1.5	1.09	
225	18.85	-0.80	75	5.5	18.85	-0.80	75.5	4.7	4	5.3	10.8	3.9	-73	0.05	4.6	0.05	4.6	1.06	
226	18.85	-0.50	66	17.9	18.81	-0.48	65.9	6.0	1601	5.3	5.3	3.4	-44	1.35	125.4	1.20	111.5	3.71	3 KPC
A	18.65	-0.60	66	9.0	18.65	-0.62	64.8	8.5	9				-57	0.05	4.6	0.10	9.3	1.30	
B	18.65	-0.50	71	11.3	18.65	-0.50	71.0	10.6	3				-46	0.05	4.6	0.05	4.6	0.80	
C	18.80	-0.35	60	9.8	18.80	-0.35	58.6	8.9	6				-32	0.05	4.6	0.05	4.6	1.68	
D	18.85	-0.50	66	17.9	18.83	-0.50	66.1	10.8	78				-46	0.25	23.2	0.30	27.9	2.27	
E	18.90	-0.15	65	10.9	18.86	-0.19	64.4	9.4	11				-17	0.10	9.3	0.15	13.9	0.86	
F	18.95	-0.80	64	10.4	18.92	-0.73	65.1	8.9	43				-67	0.20	18.6	0.20	18.6	1.83	
G	18.95	-0.10	64	10.1	18.95	-0.10	64.0	9.0	3				-9	0.05	4.6	0.05	4.6	0.79	
H	19.05	-0.60	65	9.8	19.02	-0.60	66.9	8.9	11				-55	0.15	13.9	0.05	4.6	1.50	
227	18.85	-0.30	42	5.5	18.85	-0.30	42.9	5.0	3	3.6	12.5	5.2	-18	0.05	3.1	0.05	3.1	0.80	
228	18.85	-0.15	58	6.0	18.85	-0.13	57.8	5.1	6	5.3	5.3	3.4	-12	0.05	4.7	0.10	9.3	1.30	3 KPC
229	18.85	0.00	28	5.1	18.85	0.00	27.1	4.6	5	2.5	13.6	6.2	0	0.05	2.2	0.05	2.2	1.38	
230	18.90	-0.20	51	6.5	18.91	-0.19	51.5	5.0	8	4.1	12.0	4.8	-13	0.10	7.1	0.10	7.1	1.07	
231	18.95	-0.75	47	5.5	18.96	-0.75	47.3	4.5	9	3.8	12.2	5.0	-50	0.10	6.7	0.05	3.4	1.82	
232	18.95	-0.40	26	5.7	18.97	-0.40	25.5	4.7	4	2.4	13.7	6.3	-16	0.10	4.1	0.05	2.1	0.50	
233	18.95	-0.15	59	8.8	18.95	-0.15	59.5	7.5	4	5.3	5.3	3.4	-13	0.05	4.7	0.05	4.7	1.04	3 KPC
234	19.05	0.05	53	5.7	19.04	0.03	53.4	5.0	5	4.2	11.9	4.8	2	0.10	7.3	0.10	7.3	0.80	
235	19.10	-0.65	52	5.7	19.10	-0.65	50.6	5.1	6	4.0	12.1	4.9	-45	0.05	3.5	0.05	3.5	1.66	

© American Astronomical Society • Provided by the NASA Astrophysics Data System

TABLE 1—*Continued*

CLOUD	l_p °	b_p °	v_p	T_p K	<l> °	<b> °	<v> km s^{-1}	<T> K	N	d_N kpc	d_P kpc	R kpc	<z> pc	Δl °	ΔL pc	Δb °	ΔB pc	σ_v km s^{-1}	NOTES
(1)	(2)	(3)	(4)	(5)	(6)	(7)	(8)	(9)	(10)	(11)	(12)	(13)	(14)	(15)	(16)	(17)	(18)	(19)	(20)
236	19.10	0.45	19	6.2	19.10	0.47	19.3	5.1	3	1.9	14.2	6.8	15	0.05	1.6	0.10	3.2	0.45	
237	19.15	-0.20	99	5.2	19.13	-0.25	100.1	4.5	13	6.6	9.5	3.1	-28	0.10	11.5	0.15	17.2	1.05	
238	19.15	0.35	28	9.8	19.16	0.34	26.6	5.6	23	2.4	13.6	6.2	14	0.15	6.4	0.20	8.5	2.06	
A	19.15	0.35	28	9.8	19.15	0.35	27.5	9.1	4				14	0.05	2.1	0.05	2.1	1.08	
239	19.20	-0.60	56	5.5	19.20	-0.60	56.0	5.0	3	4.3	11.8	4.7	-44	0.05	3.7	0.05	3.7	0.79	
240	19.20	-0.40	44	7.0	19.20	-0.40	44.0	5.8	3	3.6	12.4	5.2	-25	0.05	3.2	0.05	3.2	0.77	
241	19.20	-0.30	33	6.4	19.20	-0.30	33.5	5.5	4	2.9	13.1	5.8	-15	0.05	2.6	0.05	2.6	1.09	
242	19.20	0.30	20	6.2	19.20	0.30	19.6	5.0	4	1.9	14.2	6.8	9	0.05	1.6	0.05	1.6	1.07	
243	19.25	-0.45	71	5.6	19.25	-0.48	71.0	4.5	7	5.4	5.4	3.4	-45	0.05	4.7	0.15	14.1	0.73	3 KPC
244	19.25	0.05	26	8.1	19.34	0.02	26.4	5.3	169	2.4	13.6	6.3	0	0.45	18.9	0.40	16.8	1.66	
245	19.25	0.35	20	5.6	19.30	0.36	20.1	4.6	20	1.9	14.1	6.7	11	0.20	6.7	0.15	5.0	1.30	
246	19.30	-0.65	63	7.6	19.28	-0.65	62.6	5.9	9	5.4	5.4	3.4	-61	0.10	9.4	0.10	9.4	1.43	3 KPC
247	19.30	-0.35	66	5.2	19.30	-0.35	66.1	4.7	3	5.4	5.4	3.4	-32	0.05	4.7	0.05	4.7	0.79	3 KPC
248	19.30	0.00	41	5.0	19.30	-0.01	41.4	4.7	5	3.5	12.6	5.4	0	0.05	3.0	0.10	6.1	1.01	
249	19.40	-0.95	44	5.0	19.38	-0.94	42.8	4.4	10	3.5	12.5	5.3	-58	0.15	9.3	0.10	6.2	1.24	
250	19.40	-0.60	22	7.6	19.38	-0.60	21.5	5.7	5	2.0	14.0	6.6	-21	0.10	3.5	0.05	1.8	0.96	
251	19.45	0.15	113	6.3	19.45	0.15	112.9	5.3	3	7.2	8.8	2.9	18	0.05	6.3	0.05	6.3	0.77	TANG.
252	19.50	-0.45	63	9.4	19.52	-0.45	63.2	7.1	7	5.4	5.4	3.4	-42	0.10	9.5	0.05	4.7	1.17	3 KPC
253	19.55	-0.95	64	6.4	19.55	-0.93	62.6	5.2	5	4.6	11.4	4.5	-74	0.05	4.0	0.10	8.0	1.03	
254	19.55	-0.15	62	5.3	19.54	-0.12	62.6	4.7	7	5.4	5.4	3.4	-11	0.10	9.5	0.10	9.5	0.89	3 KPC
255	19.55	0.10	122	6.0	19.56	0.08	123.2	4.9	10	8.0	8.0	2.8	11	0.10	14.0	0.10	14.0	1.40	TANG.
256	19.55	0.25	5	7.1	19.53	0.27	5.6	4.6	34	0.7	15.3	7.8	3	0.40	5.0	0.30	3.7	0.58	
257	19.60	-0.90	35	6.5	19.60	-0.90	35.0	5.7	7	3.0	13.0	5.7	-47	0.05	2.6	0.05	2.6	1.87	
258	19.60	-0.80	21	8.1	19.62	-0.81	21.7	6.7	5	2.0	14.0	6.6	-28	0.10	3.5	0.10	3.5	0.74	
259	19.60	-0.45	42	5.7	19.62	-0.49	42.1	4.8	17	3.5	12.5	5.4	-29	0.10	6.1	0.15	9.1	1.47	
260	19.60	-0.20	41	5.4	19.58	-0.21	40.2	4.6	9	3.4	12.7	5.4	-12	0.10	5.9	0.10	5.9	1.32	
261	19.60	-0.05	58	8.3	19.60	-0.06	59.7	5.8	18	4.4	11.6	4.6	-4	0.15	11.6	0.15	11.6	1.93	
262	19.65	-0.65	55	6.4	19.62	-0.68	56.8	4.7	41	4.3	11.7	4.7	-51	0.25	18.7	0.20	15.0	2.17	
263	19.70	-0.30	71	5.6	19.70	-0.30	71.4	5.0	4	5.4	5.4	3.4	-28	0.05	4.8	0.05	4.8	1.09	3 KPC
264	19.70	-0.25	39	7.3	19.71	-0.25	40.5	5.6	11	3.4	12.6	5.4	-14	0.10	5.9	0.05	2.9	1.94	
265	19.70	0.10	26	7.0	19.74	0.17	25.0	4.9	61	2.3	13.7	6.4	6	0.35	13.8	0.30	11.8	2.04	
266	19.75	-0.85	64	7.2	19.74	-0.86	63.7	5.1	15	4.6	11.4	4.4	-69	0.20	16.1	0.15	12.1	0.92	
267	19.75	-0.65	24	10.2	19.86	-0.64	23.6	6.1	38	2.1	13.8	6.5	-23	0.35	13.1	0.25	9.4	1.07	
A	19.75	-0.65	24	10.2	19.73	-0.65	23.4	9.1	5				-24	0.10	3.8	0.05	1.9	1.00	
268	19.75	-0.15	58	5.1	19.76	-0.15	59.9	4.7	8	4.4	11.6	4.6	-11	0.10	7.7	0.05	3.9	1.76	
269	19.75	0.30	32	6.7	19.75	0.31	31.4	5.6	3	2.7	13.3	6.0	14	0.05	2.4	0.10	4.8	0.49	
270	19.80	-0.50	25	6.8	19.80	-0.52	24.5	6.1	4	2.2	13.8	6.5	-20	0.05	1.9	0.10	3.9	0.50	
271	19.80	-0.45	69	10.4	19.93	-0.24	69.1	5.1	252	5.5	5.5	3.4	-22	0.50	47.8	0.65	62.2	2.72	3 KPC
A	19.80	-0.45	69	10.4	19.80	-0.45	69.0	9.2	3				-43	0.05	4.8	0.05	4.8	0.79	
272	19.85	-0.35	45	14.0	19.84	-0.35	44.7	9.1	5	3.6	12.4	5.2	-22	0.10	6.3	0.05	3.2	0.92	
A	19.85	-0.35	45	14.0	19.85	-0.35	45.0	11.6	3				-22	0.05	3.2	0.05	3.2	0.77	
273	19.90	-0.55	44	17.8	19.95	-0.74	43.8	5.8	617	3.6	12.4	5.3	-45	0.85	52.7	0.70	43.4	2.89	NEAR
A	19.85	-0.90	43	11.6	19.85	-0.91	43.6	9.4	3				-56	0.05	3.1	0.10	6.2	0.49	
B	19.90	-0.55	44	17.8	19.97	-0.75	41.9	10.5	83				-46	0.40	24.8	0.50	31.0	1.73	
274	19.90	0.10	46	11.0	19.90	0.10	45.6	7.7	4	3.7	12.3	5.2	6	0.05	3.2	0.05	3.2	0.95	
275	19.90	0.25	114	5.8	19.91	0.25	113.7	4.6	3	7.4	8.6	3.0	32	0.10	12.9	0.05	6.4	0.46	TANG.
276	20.00	-0.25	46	6.1	20.00	-0.23	45.5	5.1	4	3.7	12.3	5.2	-14	0.05	3.2	0.10	6.4	0.50	
277	20.00	-0.20	55	6.1	20.01	-0.19	54.6	4.9	8	4.1	11.8	4.8	-13	0.10	7.2	0.10	7.2	1.09	
278	20.05	-0.45	46	5.1	20.05	-0.45	47.0	4.9	3	3.7	12.2	5.2	-29	0.05	3.3	0.05	3.3	0.81	
279	20.05	0.20	17	5.7	20.05	0.20	17.5	5.0	4	1.7	14.3	7.0	5	0.05	1.4	0.05	1.4	1.08	
280	20.10	-0.50	23	7.3	20.10	-0.50	22.9	5.8	3	2.1	13.9	6.6	-18	0.05	1.8	0.05	1.8	0.76	
281	20.20	-0.60	67	6.1	20.21	-0.69	65.6	4.6	45	4.7	11.3	4.4	-56	0.15	12.2	0.30	24.4	2.37	
282	20.20	-0.05	47	7.7	20.22	-0.05	46.8	6.2	5	3.7	12.2	5.2	-3	0.10	6.5	0.05	3.2	0.70	
283	20.20	0.00	77	6.1	20.19	0.00	81.0	4.6	13	5.4	10.5	3.9	0	0.10	9.5	0.05	4.7	2.34	
284	20.20	0.50	41	5.7	20.20	0.50	41.0	5.3	3	3.4	12.6	5.5	29	0.05	2.9	0.05	2.9	0.80	
285	20.30	-0.20	96	6.6	20.30	-0.20	95.9	5.7	3	6.3	9.6	3.4	-21	0.05	5.5	0.05	5.5	0.78	
286	20.30	-0.20	44	6.0	20.30	-0.20	43.9	5.0	3	3.5	12.4	5.3	-12	0.05	3.1	0.05	3.1	0.78	
287	20.35	-0.70	63	6.3	20.35	-0.71	62.8	5.1	6	4.5	11.4	4.5	-56	0.05	3.9	0.10	7.9	1.04	
288	20.35	0.05	24	5.6	20.37	0.05	24.5	4.6	6	2.2	13.8	6.5	1	0.10	3.8	0.05	1.9	0.95	
289	20.40	0.60	7	5.2	20.38	0.58	6.9	4.4	16	0.8	15.1	7.8	8	0.30	4.2	0.30	4.2	0.33	NEAR

© American Astronomical Society • Provided by the NASA Astrophysics Data System

TABLE 1—*Continued*

CLOUD	l_p	b_p	v_p	T_p	<l>	<b>	<v>	<T>	N	d_N	d_F	R	<z>	Δl	ΔL	Δb	ΔB	σ_v	NOTES
	°	°		K	°	°	km s^{-1}	K		kpc	kpc	kpc	pc	°	pc	°	pc	km s^{-1}	
(1)	(2)	(3)	(4)	(5)	(6)	(7)	(8)	(9)	(10)	(11)	(12)	(13)	(14)	(15)	(16)	(17)	(18)	(19)	(20)
290	20.45	-0.55	47	5.0	20.49	-0.55	47.0	4.6	7	3.7	12.2	5.2	-35	0.15	9.7	0.05	3.2	0.75	
291	20.45	-0.45	62	5.6	20.45	-0.45	62.0	4.7	3	4.5	11.4	4.6	-35	0.05	3.9	0.05	3.9	0.78	
292	20.50	-0.80	51	5.9	20.49	-0.80	50.3	4.9	5	3.9	12.0	5.1	-54	0.10	6.8	0.05	3.4	1.11	
293	20.55	-0.45	67	8.8	20.54	-0.45	65.3	5.7	12	4.6	11.3	4.5	-36	0.10	8.1	0.05	4.0	2.17	
294	20.55	-0.15	51	7.3	20.54	-0.16	50.9	5.1	9	3.9	12.0	5.0	-11	0.10	6.8	0.10	6.8	0.97	
295	20.65	-0.75	59	5.3	20.65	-0.74	59.3	4.7	4	4.3	11.6	4.7	-55	0.05	3.8	0.10	7.6	0.80	
296	20.65	-0.50	63	6.3	20.63	-0.50	64.0	5.1	9	4.6	11.3	4.5	-40	0.10	8.0	0.10	8.0	1.75	
297	20.65	0.05	82	5.8	20.65	0.05	82.0	5.1	3	5.4	10.5	3.9	4	0.05	4.7	0.05	4.7	0.79	
298	20.70	-0.65	59	5.7	20.70	-0.65	59.9	5.1	3	4.4	11.5	4.7	-49	0.05	3.8	0.05	3.8	0.79	
299	20.70	-0.55	70	5.1	20.70	-0.55	69.1	4.7	3	4.8	11.1	4.4	-46	0.05	4.2	0.05	4.2	0.81	
300	20.70	-0.30	63	14.4	20.67	-0.32	62.3	5.8	36	4.5	11.4	4.6	-24	0.25	19.5	0.20	15.6	1.65	
A	20.70	-0.30	63	14.4	20.70	-0.30	62.6	11.9	4				-23	0.05	3.9	0.05	3.9	1.05	
301	20.70	-0.25	34	5.7	20.70	-0.25	33.5	5.0	4	2.8	13.1	5.9	-12	0.05	2.5	0.05	2.5	1.07	
302	20.70	-0.05	82	5.3	20.72	-0.05	82.5	4.5	4	5.4	10.5	3.9	-4	0.10	9.5	0.05	4.8	0.50	
303	20.70	0.30	77	5.0	20.70	0.30	77.0	4.7	3	5.2	10.7	4.1	26	0.05	4.5	0.15	13.5	0.00	
304	20.70	0.80	7	5.8	20.63	0.78	6.4	4.6	18	0.8	15.2	7.8	10	0.25	3.3	0.25	3.3	0.49	NEAR
305	20.75	-0.10	105	5.2	20.72	-0.10	104.8	4.9	5	6.8	9.1	3.2	-11	0.10	11.9	0.05	5.9	0.73	TANG.
306	20.75	-0.10	59	15.9	20.75	-0.09	57.7	7.0	76	4.2	11.7	4.8	-6	0.30	22.2	0.25	18.5	2.94	
A	20.75	-0.10	59	15.9	20.78	-0.09	58.0	11.7	17				-6	0.10	7.4	0.10	7.4	2.12	
307	20.75	0.10	77	6.6	20.74	0.03	77.2	4.6	32	5.2	10.7	4.1	2	0.30	27.1	0.25	22.6	1.69	
308	20.75	0.55	27	5.1	20.76	0.49	29.0	4.4	21	2.5	13.4	6.2	21	0.10	4.4	0.25	10.9	1.31	
309	20.85	0.00	30	6.8	20.86	-0.01	30.5	4.8	69	2.6	13.3	6.1	0	0.35	15.9	0.20	9.1	2.67	
310	20.90	-0.40	71	5.1	20.91	-0.40	70.8	4.4	4	4.9	11.0	4.3	-33	0.10	8.5	0.05	4.2	0.81	
311	20.90	-0.15	61	5.2	20.90	-0.17	61.3	4.4	13	4.4	11.5	4.7	-13	0.15	11.6	0.10	7.7	1.77	
312	20.90	0.00	38	5.7	20.90	0.00	38.1	5.1	3	3.1	12.8	5.7	0	0.05	2.7	0.05	2.7	0.79	
313	20.95	-0.65	70	6.8	20.96	-0.65	70.3	5.3	7	4.8	11.0	4.3	-54	0.10	8.4	0.05	4.2	1.32	
314	20.95	0.05	73	5.9	20.95	0.05	73.0	5.2	3	5.0	10.9	4.3	4	0.05	4.3	0.05	4.3	0.79	
315	21.00	-1.00	6	6.0	20.95	-1.02	8.0	4.6	18	0.9	15.0	7.7	-15	0.20	3.1	0.10	1.5	1.50	
316	21.00	-0.05	66	5.6	21.01	-0.05	65.7	4.8	3	4.6	11.3	4.5	-4	0.10	8.1	0.05	4.0	0.47	
317	21.00	0.10	21	9.7	21.00	0.10	20.6	6.0	15	1.8	14.0	6.8	3	0.20	6.4	0.05	1.6	1.79	
A	21.00	0.10	21	9.7	21.00	0.10	21.0	8.8	3				3	0.05	1.6	0.05	1.6	0.79	
318	21.10	-0.25	36	8.1	21.10	-0.25	36.1	6.8	3	3.0	12.9	5.8	-12	0.05	2.6	0.05	2.6	0.77	
319	21.10	0.25	26	7.4	21.08	0.25	25.5	6.1	4	2.2	13.7	6.5	9	0.10	3.9	0.05	1.9	0.50	
320	21.15	-0.45	77	5.7	21.15	-0.44	77.1	4.5	7	5.1	10.7	4.1	-39	0.05	4.5	0.15	13.5	0.96	
321	21.15	-0.30	35	5.6	21.17	-0.32	37.0	4.5	12	3.0	12.8	5.8	-16	0.10	5.3	0.10	5.3	1.60	
322	21.20	-0.90	55	8.6	21.20	-0.90	55.1	6.7	3	4.1	11.8	4.9	-64	0.05	3.6	0.05	3.6	0.76	
323	21.20	0.35	82	5.6	21.20	0.35	82.0	4.7	3	5.4	10.5	4.0	32	0.05	4.7	0.05	4.7	0.78	
324	21.25	0.10	70	5.8	21.25	0.11	70.0	4.9	4	4.8	11.0	4.4	9	0.05	4.2	0.10	8.4	0.67	
325	21.25	0.20	26	9.6	21.29	0.19	25.9	5.9	17	2.2	13.6	6.5	7	0.25	9.7	0.10	3.9	1.05	
326	21.30	-0.15	67	5.8	21.32	-0.16	66.4	4.9	17	4.6	11.2	4.5	-13	0.20	16.2	0.10	8.1	1.52	
327	21.30	0.10	113	5.4	21.30	0.09	112.8	4.9	4	7.6	8.3	3.1	11	0.05	6.6	0.10	13.2	0.83	TANG.
328	21.35	0.35	8	7.4	21.25	0.29	7.6	4.8	352	0.8	15.0	7.7	4	1.35	19.7	0.85	12.4	0.84	NEAR
329	21.35	0.85	35	5.5	21.34	0.86	35.5	4.9	4	2.9	12.9	5.9	43	0.10	5.1	0.10	5.1	0.50	NEAR
330	21.40	-0.65	55	10.1	21.79	-0.54	53.5	5.2	322	4.0	11.8	5.0	-37	1.25	86.3	0.45	31.1	1.69	
A	21.40	-0.65	55	10.1	21.42	-0.68	55.4	9.3	5				-46	0.10	6.9	0.10	6.9	0.49	
331	21.40	-0.10	76	7.7	21.40	-0.10	76.0	6.0	3	5.1	10.8	4.2	-8	0.05	4.4	0.05	4.4	0.76	
332	21.40	0.00	75	10.1	21.29	0.01	74.1	5.6	80	5.0	10.8	4.3	0	0.40	34.9	0.25	21.8	1.54	
A	21.40	0.00	75	10.1	21.40	0.00	75.5	9.6	4				0	0.05	4.4	0.05	4.4	1.11	
333	21.40	0.40	46	7.4	21.42	0.43	46.7	5.6	8	3.6	12.2	5.3	27	0.10	6.3	0.10	6.3	0.98	
334	21.45	-0.65	6	5.0	21.43	-0.61	6.4	4.5	7	0.7	15.1	7.8	-7	0.10	1.3	0.10	1.3	0.90	
335	21.45	-0.35	113	5.6	21.46	-0.28	112.4	5.0	8	7.5	8.3	3.1	-37	0.10	13.2	0.15	19.7	0.68	TANG.
336	21.45	0.85	35	5.2	21.46	0.85	34.7	4.5	3	2.8	13.0	5.9	42	0.10	5.0	0.05	2.5	0.46	NEAR
337	21.50	0.25	77	7.4	21.50	0.27	77.8	5.2	22	5.2	10.7	4.2	24	0.20	18.0	0.15	13.5	1.35	
338	21.55	-0.15	120	7.4	21.56	-0.12	120.4	5.5	13	7.9	7.9	3.1	-16	0.10	13.8	0.15	20.7	1.03	TANG.
339	21.55	-0.10	73	7.1	21.54	-0.12	73.2	5.3	8	4.9	10.9	4.3	-9	0.15	12.9	0.10	8.6	0.57	
340	21.55	-0.05	114	5.5	21.56	-0.05	114.0	4.9	4	7.9	7.9	3.1	-6	0.10	13.8	0.05	6.9	0.70	TANG.
341	21.55	0.90	33	5.7	21.57	0.90	33.9	4.8	4	2.8	13.0	6.0	43	0.10	4.9	0.05	2.4	0.70	NEAR
342	21.60	-0.25	69	5.8	21.62	-0.25	69.4	4.6	8	4.7	11.1	4.4	-20	0.10	8.3	0.15	12.4	0.95	
343	21.60	-0.05	103	6.1	21.62	-0.08	103.1	4.8	6	6.7	9.1	3.4	-9	0.10	11.7	0.10	11.7	0.70	TANG.
344	21.60	0.10	119	5.2	21.60	0.10	119.1	4.6	3	7.9	7.9	3.1	13	0.05	6.9	0.05	6.9	0.79	TANG.

© American Astronomical Society • Provided by the NASA Astrophysics Data System

TABLE 1—*Continued*

CLOUD	l_p	b_p	v_p	T_p	<l>	<b>	<v>	<T>	N	d_N	d_F	R	<z>	Δl	ΔL	Δb	ΔB	σ_v	NOTES
	°	°		K	°	°	km s^{-1}	K		kpc	kpc	kpc	pc	°	pc	°	pc	km s^{-1}	
(1)	(2)	(3)	(4)	(5)	(6)	(7)	(8)	(9)	(10)	(11)	(12)	(13)	(14)	(15)	(16)	(17)	(18)	(19)	(20)
345	21.65	-0.35	86	6.0	21.65	-0.35	86.4	5.6	4	5.6	10.2	3.9	-34	0.05	4.9	0.05	4.9	1.09	
346	21.65	0.10	51	7.6	21.67	0.10	50.5	5.5	6	3.8	12.0	5.2	6	0.10	6.6	0.05	3.3	0.89	
347	21.65	0.15	24	9.6	21.64	0.14	24.2	6.2	5	2.1	13.7	6.6	5	0.10	3.6	0.10	3.6	0.72	
348	21.65	0.55	32	8.4	21.66	0.57	32.0	5.6	8	2.6	13.2	6.1	26	0.10	4.6	0.10	4.6	0.94	NEAR
349	21.70	-0.30	85	7.1	21.70	-0.30	84.5	6.1	4	5.5	10.3	4.0	-28	0.05	4.8	0.05	4.8	1.05	
350	21.70	-0.05	41	5.1	21.70	-0.05	41.0	4.7	3	3.2	12.6	5.6	-2	0.05	2.8	0.05	2.8	0.80	
351	21.70	-0.05	91	5.6	21.71	-0.06	90.8	4.7	18	5.8	10.0	3.8	-5	0.20	20.4	0.10	10.2	1.63	
352	21.75	-0.35	72	5.9	21.75	-0.44	71.4	4.7	23	4.8	11.0	4.4	-36	0.15	12.7	0.20	16.9	1.21	
353	21.75	-0.05	25	5.8	21.68	-0.01	22.4	5.0	15	1.9	13.9	6.7	0	0.15	5.1	0.15	5.1	1.55	
354	21.75	0.00	67	9.2	21.63	-0.03	67.8	5.3	78	4.7	11.1	4.5	-2	0.40	32.6	0.20	16.3	2.08	
355	21.75	0.10	96	6.4	21.74	0.10	95.8	5.3	7	6.2	9.6	3.6	10	0.10	10.8	0.05	5.4	1.21	
356	21.90	-0.35	82	10.6	21.81	-0.41	82.3	5.2	185	5.4	10.4	4.1	-38	0.45	42.1	0.55	51.4	2.99	
A	21.90	-0.35	82	10.6	21.90	-0.35	82.0	9.5	3				-32	0.05	4.7	0.05	4.7	0.79	
357	21.90	-0.10	118	5.7	21.90	-0.10	118.9	5.3	3	7.9	7.9	3.2	-13	0.05	6.9	0.05	6.9	0.80	TANG.
358	21.90	-0.10	68	6.2	21.90	-0.10	67.5	5.4	6	4.6	11.1	4.5	-8	0.05	4.1	0.05	4.1	1.63	
359	22.00	-0.20	87	5.8	22.00	-0.20	87.0	5.3	3	5.6	10.2	3.9	-19	0.05	4.9	0.05	4.9	0.80	
360	22.00	-0.05	93	6.8	22.00	-0.05	91.5	5.8	12	5.9	9.9	3.8	-5	0.05	5.1	0.05	5.1	3.23	
361	22.05	0.20	50	10.3	22.04	0.24	51.1	5.2	251	3.8	11.9	5.2	15	0.60	39.9	0.75	49.9	2.37	NEAR
A	22.05	0.20	50	10.3	22.03	0.20	50.6	9.4	3				13	0.10	6.7	0.05	3.3	0.48	
362	22.05	0.40	91	5.7	22.05	0.40	90.9	5.1	3	5.8	9.9	3.8	40	0.05	5.1	0.05	5.1	0.79	
363	22.05	0.40	87	5.9	22.05	0.45	87.6	5.1	9	5.6	10.1	3.9	44	0.05	4.9	0.15	14.7	0.91	
364	22.10	-0.30	53	5.1	22.10	-0.32	52.7	4.4	3	3.9	11.9	5.1	-21	0.05	3.4	0.10	6.8	0.46	
365	22.10	-0.15	65	5.2	22.10	-0.15	65.0	4.9	3	4.5	11.2	4.6	-11	0.05	3.9	0.05	3.9	0.80	
366	22.10	-0.05	74	7.8	22.10	-0.05	74.1	6.1	5	4.9	10.8	4.3	-4	0.05	4.3	0.05	4.3	1.27	
367	22.15	-0.80	70	5.7	22.15	-0.82	70.6	4.6	9	4.8	11.0	4.5	-68	0.15	12.5	0.10	8.3	0.81	
368	22.20	-0.35	67	5.1	22.20	-0.35	67.5	4.4	4	4.6	11.1	4.6	-28	0.05	4.0	0.05	4.0	1.09	
369	22.25	-0.90	66	5.5	22.26	-0.90	66.0	4.9	4	4.6	11.2	4.6	-71	0.10	7.9	0.05	4.0	0.72	
370	22.25	-0.25	75	5.1	22.25	-0.20	75.7	4.5	7	5.0	10.7	4.3	-17	0.05	4.4	0.15	13.1	1.01	
371	22.25	-0.25	70	5.9	22.25	-0.25	70.0	5.0	3	4.7	11.0	4.5	-20	0.05	4.1	0.05	4.1	0.78	
372	22.25	-0.10	84	5.6	22.25	-0.10	84.5	5.1	4	5.4	10.3	4.0	-9	0.05	4.7	0.05	4.7	1.08	
373	22.35	0.10	85	9.8	22.32	0.02	83.6	4.8	119	5.4	10.3	4.1	2	0.25	23.5	0.30	28.2	5.14	
A	22.35	0.10	85	9.8	22.35	0.10	85.0	9.1	3				9	0.05	4.7	0.05	4.7	0.80	
374	22.35	0.60	83	6.5	22.33	0.60	83.5	5.1	6	5.4	10.3	4.1	56	0.10	9.4	0.05	4.7	0.91	
375	22.40	-0.75	69	7.5	22.40	-0.75	69.0	6.2	3	4.7	11.0	4.5	-61	0.05	4.1	0.05	4.1	0.77	
376	22.40	0.30	84	15.1	22.38	0.34	84.9	6.3	62	5.5	10.3	4.0	32	0.30	28.6	0.35	33.3	1.58	
A	22.40	0.30	84	15.1	22.41	0.33	84.4	10.4	10				31	0.10	9.5	0.10	9.5	0.98	
377	22.40	0.45	53	7.1	22.42	0.45	53.0	5.8	4	3.9	11.8	5.1	30	0.10	6.8	0.05	3.4	0.68	
378	22.50	0.00	114	8.2	22.58	-0.09	110.3	4.9	157	7.4	8.3	3.3	-11	0.55	71.3	0.50	64.9	4.50	TANG.
379	22.50	0.25	56	5.4	22.48	0.29	57.1	4.7	14	4.1	11.6	5.0	20	0.15	10.7	0.15	10.7	0.88	
380	22.55	-0.35	82	6.8	22.55	-0.35	82.0	5.7	3	5.3	10.4	4.1	-32	0.05	4.6	0.05	4.6	0.78	
381	22.55	-0.35	65	5.2	22.53	-0.36	63.2	4.5	19	4.4	11.3	4.7	-27	0.20	15.4	0.10	7.7	1.54	
382	22.55	-0.05	115	9.7	22.55	-0.05	114.6	7.0	4	7.8	7.9	3.3	-6	0.05	6.8	0.05	6.8	0.97	TANG.
383	22.55	0.00	70	10.0	22.54	-0.03	70.1	6.7	12	4.7	11.0	4.5	-2	0.15	12.4	0.10	8.3	0.80	
A	22.55	0.00	70	10.0	22.53	-0.03	70.0	9.4	3				-2	0.10	8.3	0.10	8.3	0.00	
384	22.60	0.50	84	6.2	22.60	0.50	84.5	5.5	4	5.4	10.3	4.1	47	0.05	4.7	0.05	4.7	1.10	
385	22.70	-0.20	88	5.1	22.73	-0.20	87.5	4.4	9	5.6	10.1	4.0	-19	0.10	9.7	0.05	4.9	1.55	
386	22.75	0.55	85	7.1	22.76	0.58	85.4	5.4	10	5.5	10.2	4.1	54	0.10	9.5	0.10	9.5	0.99	
387	22.80	0.40	92	7.2	22.85	0.52	95.7	5.0	62	6.1	9.6	3.7	54	0.20	21.1	0.30	31.7	2.77	
388	22.80	0.70	87	5.2	22.80	0.70	87.0	4.7	3	5.5	10.1	4.0	67	0.05	4.8	0.05	4.8	0.79	NEAR
389	22.85	-0.45	63	6.7	22.85	-0.45	62.6	5.6	4	4.4	11.3	4.8	-34	0.05	3.8	0.05	3.8	1.04	
390	22.85	0.20	86	9.4	22.85	0.20	86.0	5.5	19	5.5	10.2	4.0	19	0.15	14.4	0.15	14.4	1.52	
391	22.85	0.40	114	7.4	22.81	0.40	114.2	5.0	27	7.8	7.8	3.3	54	0.25	34.2	0.05	6.8	2.01	TANG.
392	22.85	0.80	37	8.0	22.90	0.82	37.3	5.9	8	2.9	12.7	5.9	41	0.15	7.6	0.10	5.1	0.48	NEAR
393	22.90	-0.15	104	6.1	22.91	-0.19	102.5	5.1	13	6.6	9.1	3.5	-22	0.10	11.5	0.15	17.2	1.18	TANG.
394	22.90	0.35	86	5.3	22.90	0.33	88.5	4.6	7	5.6	10.0	4.0	32	0.05	4.9	0.10	9.8	1.62	
395	22.95	-0.25	52	6.4	23.18	-0.12	53.6	4.6	169	3.9	11.8	5.2	-7	0.75	50.7	0.55	37.2	1.81	
396	23.00	-0.15	104	7.4	23.03	-0.09	103.1	5.3	26	6.6	9.0	3.5	-10	0.20	23.1	0.15	17.3	2.34	TANG.
397	23.00	0.60	38	5.0	22.97	0.60	37.7	4.7	3	2.9	12.7	5.9	30	0.10	5.1	0.05	2.6	0.47	NEAR
398	23.05	-0.30	59	5.7	23.07	-0.28	58.6	4.8	9	4.1	11.5	5.0	-20	0.10	7.2	0.15	10.8	1.05	
399	23.05	-0.05	79	6.8	23.05	-0.05	79.0	5.5	3	5.1	10.5	4.3	-4	0.05	4.5	0.05	4.5	0.77	

© American Astronomical Society • Provided by the NASA Astrophysics Data System

TABLE 1—*Continued*

CLOUD (1)	l_p ° (2)	b_p ° (3)	v_p (4)	T_p K (5)	<l> ° (6)	<b> ° (7)	<v> km s^{-1} (8)	<T> K (9)	N (10)	d_N kpc (11)	d_F kpc (12)	R kpc (13)	<z> pc (14)	Δl ° (15)	ΔL pc (16)	Δb ° (17)	ΔB pc (18)	σ_v km s^{-1} (19)	NOTES (20)
400	23.05	-0.05	66	8.0	23.00	-0.03	64.8	5.3	17	4.5	11.2	4.7	-2	0.20	15.6	0.10	7.8	1.51	
401	23.05	0.20	106	9.3	23.13	0.19	108.1	4.9	97	7.2	8.5	3.4	23	0.55	68.6	0.25	31.2	2.41	TANG.
402	23.05	0.25	76	7.2	22.98	0.25	74.5	5.0	47	4.9	10.7	4.4	21	0.35	30.0	0.30	25.7	1.96	
403	23.10	-0.15	66	7.8	23.10	-0.11	67.3	6.1	19	4.6	11.1	4.7	-8	0.10	8.0	0.15	12.0	2.32	
404	23.10	0.60	38	12.0	23.08	0.56	38.3	6.6	16	3.0	12.7	5.9	29	0.10	5.2	0.20	10.4	1.26	NEAR
405	23.15	0.20	19	5.5	23.15	0.20	19.4	5.1	4	1.7	14.0	7.0	5	0.05	1.4	0.05	1.4	1.00	
406	23.15	0.45	99	5.4	23.15	0.45	100.0	4.9	5	6.4	9.3	3.6	49	0.05	5.5	0.05	5.5	1.37	
407	23.15	0.65	84	5.1	23.15	0.65	84.5	4.7	4	5.4	10.2	4.1	61	0.05	4.7	0.05	4.7	1.00	
408	23.15	0.70	37	6.3	23.12	0.70	36.6	5.5	4	2.9	12.8	6.0	34	0.10	5.0	0.05	2.5	0.50	NEAR
409	23.20	-0.70	72	5.3	23.20	-0.70	72.0	4.7	3	4.8	10.8	4.5	-58	0.05	4.2	0.05	4.2	0.79	
410	23.20	0.00	77	10.9	23.22	0.00	76.9	7.4	14	5.0	10.6	4.4	0	0.10	8.8	0.05	4.4	1.90	
A	23.20	0.00	77	10.9	23.20	0.00	77.0	10.1	5				0	0.05	4.4	0.05	4.4	1.36	
411	23.20	0.30	88	6.5	23.15	0.26	88.0	4.8	36	5.6	10.1	4.0	25	0.15	14.6	0.20	19.5	1.53	
412	23.25	0.10	66	5.5	23.25	0.10	65.9	4.8	3	4.5	11.1	4.7	7	0.05	3.9	0.05	3.9	0.79	
413	23.30	-0.80	53	5.1	23.30	-0.80	53.0	4.9	3	3.8	11.8	5.2	-53	0.05	3.3	0.05	3.3	0.81	
414	23.30	-0.70	62	5.5	23.41	-0.71	61.0	4.4	27	4.2	11.4	4.9	-52	0.35	25.9	0.15	11.1	1.29	
415	23.30	0.45	99	5.2	23.30	0.42	98.2	4.6	5	6.2	9.4	3.7	45	0.05	5.4	0.10	10.8	0.73	
416	23.35	-0.30	55	5.9	23.33	-0.30	55.5	4.7	5	4.0	11.6	5.1	-20	0.10	6.9	0.05	3.5	0.99	
417	23.35	0.45	80	7.4	23.35	0.45	80.1	6.3	3	5.2	10.4	4.3	40	0.05	4.5	0.05	4.5	0.77	
418	23.40	0.45	108	8.3	23.42	0.45	107.6	5.6	18	7.1	8.5	3.5	55	0.15	18.6	0.15	18.6	1.57	TANG.
419	23.45	-0.30	70	5.3	23.45	-0.28	69.5	4.7	6	4.7	10.9	4.6	-23	0.05	4.1	0.10	8.1	0.95	
420	23.45	0.25	108	6.8	23.45	0.25	108.4	5.6	4	7.2	8.4	3.4	31	0.05	6.3	0.05	6.3	1.04	TANG.
421	23.50	-0.60	65	5.2	23.50	-0.60	63.6	4.8	4	4.4	11.2	4.8	-45	0.05	3.8	0.05	3.8	1.11	
422	23.50	-0.25	57	5.1	23.50	-0.25	58.0	4.9	3	4.1	11.5	5.0	-17	0.05	3.6	0.05	3.6	0.81	
423	23.50	0.45	82	7.0	23.50	0.45	81.9	5.7	3	5.3	10.3	4.2	41	0.05	4.6	0.05	4.6	0.76	
424	23.50	0.60	83	6.4	23.52	0.60	83.9	5.1	6	5.3	10.2	4.2	56	0.10	9.3	0.05	4.7	1.27	
425	23.50	0.70	82	5.6	23.50	0.70	82.0	4.9	3	5.3	10.3	4.2	64	0.05	4.6	0.05	4.6	0.79	NEAR
426	23.55	0.55	103	6.1	23.53	0.54	100.6	4.9	14	6.4	9.2	3.7	59	0.10	11.1	0.10	11.1	1.81	
427	23.60	-0.50	56	5.1	23.60	-0.50	56.0	4.5	3	4.0	11.6	5.1	-34	0.05	3.5	0.05	3.5	0.79	
428	23.60	-0.35	98	5.2	23.60	-0.35	98.0	4.6	3	6.2	9.4	3.8	-37	0.05	5.4	0.05	5.4	0.79	
429	23.60	0.45	96	5.1	23.60	0.47	96.6	4.8	3	6.1	9.5	3.8	49	0.05	5.3	0.10	10.6	0.48	
430	23.70	0.50	82	8.9	23.67	0.55	83.0	5.7	29	5.3	10.3	4.2	50	0.15	13.9	0.15	13.9	1.71	
431	23.75	-0.10	100	7.3	23.72	-0.11	100.1	5.7	11	6.3	9.2	3.7	-12	0.10	11.0	0.10	11.0	1.35	
432	23.75	0.25	80	7.9	23.71	0.25	79.5	5.5	7	5.1	10.4	4.3	22	0.15	13.4	0.05	4.5	0.92	
433	23.80	-0.30	90	7.0	23.78	-0.23	92.7	5.0	33	5.8	9.7	4.0	-23	0.20	20.3	0.20	20.3	2.86	
434	23.80	0.55	10	5.4	23.79	0.66	9.3	4.4	82	0.9	14.6	7.7	10	0.70	11.2	0.55	8.8	0.77	NEAR
435	23.85	-0.60	77	5.9	23.85	-0.59	76.7	5.2	3	5.0	10.6	4.4	-50	0.05	4.3	0.10	8.7	0.47	
436	23.85	0.15	103	5.3	23.83	0.15	102.3	4.4	16	6.5	9.0	3.7	17	0.25	28.4	0.10	11.4	1.14	TANG.
437	23.90	-0.50	89	5.9	23.90	-0.50	89.1	5.3	5	5.6	9.9	4.1	-48	0.05	4.9	0.05	4.9	1.35	
438	23.90	-0.15	98	5.9	23.90	-0.15	97.6	5.4	4	6.1	9.4	3.8	-16	0.05	5.3	0.05	5.3	1.09	
439	23.90	0.05	38	7.3	23.90	0.07	38.1	5.6	9	2.9	12.6	6.0	3	0.10	5.1	0.10	5.1	1.14	
440	23.90	0.40	101	7.6	23.91	0.41	101.5	6.1	8	6.4	9.1	3.7	46	0.10	11.2	0.10	11.2	1.09	
441	23.90	0.60	87	5.1	23.90	0.59	86.7	4.8	4	5.5	10.1	4.1	56	0.05	4.8	0.10	9.6	0.81	
442	23.95	0.15	79	15.3	23.23	-0.17	80.9	5.7	4598	5.2	10.4	4.2	-15	1.90	172.9	1.15	104.6	10.69	NEAR
A	22.55	-0.20	77	10.3	22.57	-0.20	78.2	8.9	15				-18	0.15	13.6	0.15	13.6	1.38	
B	22.75	-0.25	72	12.2	22.76	-0.23	71.9	9.9	7				-20	0.10	9.1	0.10	9.1	0.75	
C	22.85	-0.45	87	9.2	22.85	-0.45	86.5	8.9	6				-40	0.05	4.5	0.05	4.5	1.69	
D	22.95	-0.10	66	11.5	22.95	-0.22	64.6	9.3	25				-20	0.15	13.6	0.30	27.3	1.04	
E	23.00	-0.40	74	13.6	23.11	-0.35	76.8	9.3	217				-31	0.90	81.9	0.35	31.8	2.77	
F	23.30	-0.10	81	9.1	23.30	-0.10	81.0	8.8	3				-9	0.05	4.5	0.05	4.5	0.81	
G	23.40	-0.25	102	13.4	23.43	-0.22	102.0	9.9	65				-20	0.20	18.2	0.20	18.2	3.01	
H	23.45	0.00	82	9.1	23.45	0.00	82.5	8.8	4				0	0.05	4.5	0.05	4.5	1.11	
I	23.55	0.00	105	13.1	23.55	0.00	105.5	10.7	4				0	0.05	4.5	0.05	4.5	1.02	
J	23.55	0.20	82	10.4	23.53	0.23	82.7	9.2	8				20	0.10	9.1	0.10	9.1	0.97	
K	23.60	0.05	105	9.3	23.60	0.05	104.1	8.7	5				4	0.05	4.5	0.05	4.5	1.41	
L	23.60	0.05	93	12.0	23.60	0.05	93.0	10.6	3				4	0.05	4.5	0.05	4.5	0.79	
M	23.95	0.15	79	15.3	23.98	0.15	79.8	10.4	9				13	0.15	13.6	0.05	4.5	1.61	
443	23.95	0.55	50	5.2	23.95	0.55	50.0	4.8	3	3.6	11.9	5.4	34	0.05	3.2	0.05	3.2	0.80	
444	24.00	-0.30	91	6.2	24.00	-0.30	91.0	5.1	3	5.7	9.8	4.0	-29	0.05	5.0	0.05	5.0	0.77	
445	24.00	0.05	35	5.1	24.00	0.05	34.5	4.6	4	2.7	12.9	6.2	2	0.05	2.3	0.05	2.3	1.09	

© American Astronomical Society • Provided by the NASA Astrophysics Data System

TABLE 1—*Continued*

CLOUD (1)	l_p ° (2)	b_p ° (3)	v_p (4)	T_p K (5)	<l> ° (6)	<b> ° (7)	<v> km s^{-1} (8)	<T> K (9)	N (10)	d_N kpc (11)	d_F kpc (12)	R kpc (13)	<z> pc (14)	Δl ° (15)	ΔL pc (16)	Δb ° (17)	ΔB pc (18)	σ_v km s^{-1} (19)	NOTES (20)
446	24.00	0.40	116	5.3	24.00	0.40	116.0	4.8	3	7.8	7.8	3.5	54	0.05	6.8	0.05	6.8	0.80	TANG.
447	24.00	0.60	91	7.4	24.00	0.60	90.6	6.7	4	5.7	9.8	4.0	59	0.05	5.0	0.05	5.0	1.08	
448	24.05	0.10	67	5.5	24.05	0.11	66.7	4.8	3	4.5	11.0	4.8	8	0.05	3.9	0.10	7.8	0.47	
449	24.10	-0.65	45	6.9	24.11	-0.62	44.1	5.3	20	3.3	12.2	5.7	-35	0.20	11.4	0.15	8.6	1.81	
450	24.10	-0.65	52	6.1	24.08	-0.65	51.5	5.0	6	3.7	11.8	5.3	-42	0.10	6.5	0.05	3.2	0.94	
451	24.10	0.45	95	12.7	23.99	0.39	94.4	5.4	217	5.9	9.6	3.9	40	0.60	61.8	0.55	56.7	2.73	
A	24.10	0.45	95	12.7	24.13	0.42	95.1	9.3	12				43	0.15	15.5	0.10	10.3	1.05	
452	24.15	0.10	89	5.2	24.13	0.10	88.0	4.8	4	5.5	10.0	4.1	9	0.10	9.7	0.05	4.8	0.71	
453	24.20	-0.30	89	6.1	24.23	-0.33	89.7	5.0	10	5.6	9.9	4.1	-31	0.10	9.8	0.10	9.8	1.12	
454	24.20	-0.25	93	7.5	24.20	-0.25	93.1	6.5	3	5.8	9.7	4.0	-25	0.05	5.1	0.05	5.1	0.77	
455	24.20	-0.05	88	8.7	24.24	-0.03	88.6	6.2	35	5.6	9.9	4.1	-2	0.20	19.4	0.10	9.7	1.90	
456	24.20	0.10	37	5.6	24.20	0.10	36.1	4.9	5	2.8	12.8	6.1	4	0.05	2.4	0.05	2.4	1.42	
457	24.20	0.30	34	5.8	24.20	0.30	34.4	5.1	6	2.6	12.9	6.2	13	0.05	2.3	0.05	2.3	1.62	
458	24.25	-0.60	90	5.4	24.25	-0.60	89.5	4.7	4	5.6	9.9	4.1	-58	0.05	4.9	0.05	4.9	1.06	
459	24.25	0.10	100	8.4	24.25	0.10	99.3	5.8	13	6.2	9.3	3.8	10	0.10	10.9	0.15	16.3	1.38	
460	24.30	-0.90	61	5.2	24.28	-0.89	60.8	4.6	6	4.2	11.3	5.0	-65	0.10	7.3	0.10	7.3	0.69	
461	24.30	-0.55	58	6.5	24.30	-0.55	58.2	4.8	8	4.1	11.4	5.1	-38	0.05	3.5	0.15	10.6	0.93	
462	24.30	-0.30	86	6.5	24.30	-0.30	85.1	5.5	7	5.4	10.1	4.2	-28	0.05	4.7	0.05	4.7	1.87	
463	24.30	-0.15	101	10.4	24.30	-0.15	101.0	6.8	5	6.4	9.1	3.8	-16	0.05	5.6	0.05	5.6	1.19	
464	24.35	-0.30	98	6.5	24.35	-0.30	98.1	6.1	3	6.1	9.4	3.9	-32	0.05	5.4	0.05	5.4	0.80	
465	24.35	-0.20	112	7.1	24.35	-0.22	112.0	5.5	8	7.7	7.7	3.5	-30	0.05	6.8	0.10	13.5	1.14	TANG.
466	24.35	-0.15	79	6.7	24.35	-0.15	78.6	5.5	4	5.1	10.4	4.4	-13	0.05	4.4	0.05	4.4	1.07	
467	24.35	0.10	101	5.3	24.35	0.10	98.2	4.6	9	6.1	9.3	3.9	10	0.05	5.4	0.05	5.4	2.59	
468	24.40	-0.80	49	5.1	24.40	-0.80	49.0	4.4	3	3.5	11.9	5.5	-49	0.05	3.1	0.05	3.1	0.79	
469	24.40	0.00	88	6.4	24.45	0.02	88.1	4.8	27	5.5	9.9	4.2	1	0.30	29.0	0.10	9.7	1.20	
470	24.40	0.00	76	8.2	24.39	-0.02	76.1	5.5	10	4.9	10.5	4.5	-1	0.10	8.6	0.10	8.6	1.11	
471	24.45	-0.80	57	5.2	24.47	-0.81	57.8	4.4	28	4.0	11.4	5.1	-56	0.20	14.1	0.20	14.1	1.65	
472	24.45	-0.30	112	5.0	24.45	-0.27	111.6	4.5	5	7.7	7.7	3.5	-36	0.05	6.8	0.10	13.5	0.99	TANG.
473	24.45	-0.20	75	5.3	24.45	-0.20	74.9	4.8	3	4.9	10.6	4.5	-17	0.05	4.3	0.05	4.3	0.80	
474	24.45	0.20	80	5.9	24.45	0.18	79.7	5.4	5	5.1	10.4	4.4	15	0.05	4.5	0.10	8.9	0.70	
475	24.45	0.25	120	16.6	24.33	0.22	109.8	5.8	1823	7.7	7.7	3.5	29	1.40	189.2	0.75	101.4	5.18	TANG.
A	23.70	0.15	114	9.8	23.72	0.15	114.0	8.9	4				20	0.10	13.5	0.05	6.8	0.71	
B	24.05	0.20	113	11.0	24.05	0.19	112.4	9.2	7				25	0.05	6.8	0.10	13.5	1.63	
C	24.20	0.25	114	10.6	24.18	0.25	113.7	9.4	3				33	0.10	13.5	0.05	6.8	0.47	
D	24.25	0.15	115	9.1	24.25	0.18	114.0	8.9	4				24	0.05	6.8	0.10	13.5	0.71	
E	24.45	-0.05	109	10.1	24.47	-0.05	109.9	9.3	8				-6	0.10	13.5	0.05	6.8	1.20	
F	24.45	0.25	120	16.6	24.43	0.18	115.1	9.5	108				24	0.30	40.5	0.45	60.8	3.19	
G	24.45	0.50	101	13.3	24.46	0.48	102.6	9.9	18				64	0.15	20.3	0.10	13.5	1.72	
H	24.80	0.10	113	12.8	24.80	0.10	112.9	10.7	5				13	0.05	6.8	0.05	6.8	1.32	
I	24.80	0.10	107	10.6	24.78	0.08	108.4	8.9	11				10	0.10	13.5	0.10	13.5	2.11	
476	24.50	-0.70	47	6.7	24.47	-0.73	48.9	4.7	53	3.5	11.9	5.5	-44	0.35	21.6	0.30	18.5	1.45	
477	24.50	-0.60	52	5.8	24.50	-0.57	52.3	4.8	3	3.7	11.7	5.3	-37	0.05	3.3	0.10	6.5	0.47	
478	24.50	-0.40	111	6.1	24.50	-0.38	111.0	4.8	6	7.7	7.7	3.5	-50	0.05	6.7	0.10	13.5	0.79	TANG.
479	24.50	-0.30	118	7.1	24.53	-0.30	117.8	5.5	7	7.7	7.7	3.5	-40	0.10	13.5	0.05	6.7	0.97	TANG.
480	24.50	-0.25	101	17.8	24.64	-0.20	91.7	5.9	274	5.7	9.7	4.1	-20	0.55	55.0	0.35	35.0	6.42	
A	24.45	-0.30	97	9.9	24.45	-0.28	96.7	9.1	3				-27	0.05	5.0	0.10	10.0	0.47	
B	24.50	-0.25	101	17.8	24.52	-0.25	99.7	12.8	11				-24	0.10	10.0	0.10	10.0	1.62	
C	24.50	-0.10	95	10.5	24.50	-0.10	95.0	9.5	3				-9	0.05	5.0	0.05	5.0	0.79	
D	24.55	-0.15	95	11.2	24.55	-0.15	95.4	9.6	4				-14	0.05	5.0	0.05	5.0	1.08	
E	24.60	-0.15	83	9.1	24.60	-0.14	83.0	8.6	4				-13	0.05	5.0	0.10	10.0	0.69	
481	24.50	0.20	38	8.5	24.52	0.20	37.2	5.3	34	2.8	12.7	6.1	9	0.20	9.8	0.30	14.7	1.96	
482	24.55	-0.80	100	5.4	24.54	-0.80	100.6	4.5	5	6.3	9.1	3.8	-88	0.10	11.0	0.05	5.5	0.98	
483	24.55	0.30	61	5.7	24.58	0.28	61.1	5.0	10	4.2	11.3	5.0	20	0.10	7.3	0.20	14.6	0.95	
484	24.60	-0.40	113	7.3	24.60	-0.43	113.4	5.7	16	7.7	7.7	3.5	-57	0.15	20.2	0.10	13.5	1.50	TANG.
485	24.60	-0.25	38	5.1	24.60	-0.23	38.0	4.5	6	2.9	12.6	6.0	-11	0.05	2.5	0.10	5.0	0.80	
486	24.65	-0.10	114	9.3	24.65	-0.20	112.9	6.3	33	7.7	7.7	3.5	-27	0.10	13.5	0.30	40.4	1.93	TANG.
A	24.65	-0.10	114	9.3	24.65	-0.10	114.0	8.9	3				-13	0.05	6.7	0.05	6.7	0.81	
487	24.70	-0.50	53	5.2	24.70	-0.50	52.1	4.7	3	3.7	11.7	5.4	-32	0.05	3.2	0.05	3.2	0.81	
488	24.70	-0.10	107	5.9	24.74	-0.12	106.0	4.8	11	6.9	8.6	3.7	-14	0.15	18.0	0.10	12.0	0.95	TANG.
489	24.70	0.55	103	6.5	24.70	0.55	103.5	5.6	4	6.6	8.9	3.7	63	0.05	5.7	0.05	5.7	1.05	TANG.

© American Astronomical Society • Provided by the NASA Astrophysics Data System

TABLE 1—*Continued*

CLOUD	l_p	b_p	v_p	T_p	<l>	<b>	<v>	<T>	N	d_N	d_F	R	<z>	Δl	ΔL	Δb	ΔB	σ_v	NOTES
	°	°		K	°	°	km s^{-1}	K		kpc	kpc	kpc	pc	°	pc	°	pc	km s^{-1}	
(1)	(2)	(3)	(4)	(5)	(6)	(7)	(8)	(9)	(10)	(11)	(12)	(13)	(14)	(15)	(16)	(17)	(18)	(19)	(20)
490	24.70	0.65	105	5.8	24.70	0.65	104.5	5.3	4	6.7	8.8	3.7	75	0.05	5.8	0.05	5.8	1.10	TANG.
491	24.75	-0.40	42	5.9	24.75	-0.40	42.4	5.0	4	3.1	12.3	5.8	-21	0.05	2.7	0.05	2.7	1.07	
492	24.75	0.50	106	7.1	24.76	0.51	105.8	5.2	7	6.8	8.6	3.7	60	0.10	11.9	0.10	11.9	0.97	TANG.
493	24.80	-0.70	53	5.7	24.80	-0.70	53.0	4.7	3	3.7	11.7	5.3	-45	0.05	3.3	0.05	3.3	0.77	
494	24.80	-0.15	82	6.9	24.80	-0.13	81.5	5.8	7	5.2	10.2	4.4	-12	0.05	4.5	0.10	9.1	1.31	
495	24.85	-0.60	95	5.1	24.85	-0.60	95.0	4.9	3	5.9	9.5	4.0	-62	0.05	5.2	0.05	5.2	0.81	
496	24.85	-0.30	107	5.5	24.85	-0.30	107.0	4.8	3	7.0	8.4	3.6	-36	0.05	6.1	0.05	6.1	0.79	TANG.
497	24.90	0.90	79	5.3	24.90	0.90	79.0	4.9	3	5.1	10.4	4.5	79	0.05	4.4	0.05	4.4	0.80	NEAR
498	24.95	-0.90	43	5.5	24.95	-0.90	43.0	4.9	3	3.2	12.3	5.8	-49	0.15	8.3	0.05	2.8	0.00	
499	24.95	-0.55	106	5.7	24.95	-0.55	105.9	5.0	3	6.8	8.6	3.7	-65	0.05	6.0	0.05	6.0	0.78	TANG.
500	24.95	-0.05	93	6.1	24.95	-0.06	93.0	4.9	4	5.8	9.6	4.1	-6	0.05	5.1	0.10	10.1	0.69	
501	24.95	0.10	43	6.6	24.95	0.10	43.3	5.5	8	3.2	12.2	5.8	5	0.05	2.8	0.05	2.8	2.16	
502	25.00	0.60	116	7.7	25.00	0.60	115.6	6.0	4	7.7	7.7	3.6	80	0.05	6.7	0.05	6.7	1.03	TANG.
503	25.05	0.10	52	5.6	25.04	0.10	52.0	4.6	4	3.7	11.7	5.4	6	0.10	6.4	0.05	3.2	0.69	
504	25.10	-0.10	91	5.3	25.11	-0.11	92.5	4.5	11	5.8	9.6	4.1	-11	0.15	15.1	0.10	10.1	1.78	
505	25.10	-0.05	100	7.3	25.10	-0.07	99.8	5.6	5	6.2	9.1	3.9	-7	0.05	5.5	0.10	10.9	0.73	
506	25.10	0.75	41	5.4	25.11	0.72	40.3	4.6	9	3.0	12.4	5.9	37	0.15	7.8	0.15	7.8	0.66	NEAR
507	25.15	-0.60	25	7.3	25.15	-0.55	25.0	5.6	9	2.0	13.4	6.8	-18	0.05	1.7	0.15	5.1	0.77	
508	25.15	0.05	45	7.9	25.15	0.06	45.7	5.5	15	3.3	12.1	5.7	3	0.05	2.9	0.15	8.7	1.63	
509	25.15	0.55	111	5.8	25.15	0.55	111.0	4.9	3	7.7	7.7	3.6	73	0.05	6.7	0.05	6.7	0.78	TANG.
510	25.25	-0.25	98	9.8	25.19	-0.25	97.2	5.6	14	6.1	9.3	4.0	-26	0.20	21.1	0.05	5.3	1.46	
511	25.25	0.05	103	5.4	25.25	0.05	103.0	4.9	3	6.5	8.9	3.8	5	0.05	5.7	0.05	5.7	0.79	TANG.
512	25.25	0.25	53	7.6	25.20	0.17	54.0	4.9	23	3.8	11.6	5.3	11	0.15	9.9	0.20	13.2	1.00	
513	25.25	0.30	47	11.2	25.25	0.30	47.0	7.6	5	3.4	12.0	5.6	17	0.05	2.9	0.05	2.9	1.20	
A	25.25	0.30	47	11.2	25.25	0.30	47.0	9.6	3				17	0.05	2.9	0.05	2.9	0.78	
514	25.30	0.35	46	6.6	25.33	0.35	45.6	5.3	8	3.3	12.1	5.7	20	0.10	5.7	0.05	2.9	1.07	
515	25.35	0.00	92	5.4	25.35	-0.01	90.8	4.9	4	5.7	9.7	4.2	-1	0.05	4.9	0.10	9.9	0.84	
516	25.35	0.25	41	14.9	25.37	0.24	40.9	8.7	9	3.0	12.4	5.9	12	0.10	5.2	0.10	5.2	1.04	
517	25.40	0.10	95	9.1	25.40	0.12	94.5	5.7	18	5.9	9.5	4.1	11	0.15	15.4	0.10	10.3	3.12	
518	25.40	0.55	16	7.4	25.40	0.55	16.8	6.4	7	1.4	14.0	7.3	13	0.05	1.2	0.05	1.2	1.92	NEAR
519	25.45	-0.20	120	9.3	25.65	-0.25	116.3	5.9	89	7.7	7.7	3.7	-33	0.50	66.9	0.25	33.4	2.58	TANG.
A	25.45	-0.20	120	9.3	25.45	-0.20	120.0	8.7	3				-26	0.05	6.7	0.05	6.7	0.80	
520	25.45	-0.20	65	12.0	24.66	-0.18	52.8	5.2	2687	3.7	11.7	5.3	-11	2.15	140.5	1.25	81.7	5.76	NEAR
A	24.50	-0.15	44	11.8	24.52	-0.18	44.0	9.3	14				-11	0.10	6.5	0.10	6.5	1.35	
B	24.85	-0.10	48	9.6	24.86	-0.12	47.7	8.7	17				-7	0.20	13.1	0.15	9.8	1.02	
C	24.85	0.15	46	10.7	24.86	0.14	45.5	9.0	4				9	0.10	6.5	0.10	6.5	0.50	
D	25.20	-0.25	64	9.9	25.17	-0.27	63.6	8.9	7				-17	0.10	6.5	0.10	6.5	0.90	
E	25.45	-0.20	65	12.0	25.42	-0.20	64.7	9.9	7				-13	0.10	6.5	0.05	3.3	0.99	
521	25.45	0.10	88	6.0	25.47	0.05	89.0	4.4	19	5.6	9.8	4.2	4	0.10	9.7	0.15	14.6	1.92	
522	25.45	0.45	47	9.1	25.45	0.45	47.0	7.0	3	3.4	12.0	5.6	26	0.05	2.9	0.05	2.9	0.75	
523	25.50	0.05	57	5.4	25.50	0.05	57.0	4.7	3	3.9	11.4	5.2	3	0.05	3.4	0.05	3.4	0.79	
524	25.50	0.20	98	5.2	25.52	0.20	98.0	4.8	4	6.1	9.2	4.0	21	0.10	10.7	0.05	5.3	0.70	
525	25.50	0.25	91	5.3	25.50	0.28	91.3	4.6	5	5.7	9.6	4.2	27	0.05	5.0	0.10	9.9	1.02	
526	25.50	0.40	99	5.8	25.47	0.40	98.4	5.0	7	6.1	9.2	4.0	42	0.15	16.1	0.05	5.4	0.92	
527	25.55	-0.40	116	7.6	25.45	-0.36	117.2	5.4	30	7.7	7.7	3.7	-47	0.25	33.5	0.15	20.1	1.85	TANG.
528	25.60	0.75	48	5.2	25.56	0.76	49.0	4.5	8	3.5	11.9	5.6	46	0.15	9.1	0.10	6.1	0.98	NEAR
529	25.65	-0.10	94	12.8	25.59	-0.17	95.0	5.9	510	5.9	9.4	4.1	-17	0.85	87.8	0.65	67.1	4.23	
A	25.45	-0.15	95	11.8	25.43	-0.14	95.9	9.4	25				-14	0.15	15.5	0.15	15.5	2.22	
B	25.65	-0.10	94	12.8	25.70	-0.16	93.2	9.1	35				-16	0.35	36.1	0.15	15.5	1.74	
C	25.70	-0.05	100	9.0	25.70	-0.05	99.0	8.5	3				-5	0.05	5.2	0.05	5.2	0.82	
530	25.65	-0.05	81	6.7	25.65	-0.05	80.5	5.8	4	5.1	10.2	4.5	-4	0.05	4.5	0.05	4.5	1.06	
531	25.65	0.05	26	6.2	25.63	0.05	25.7	4.9	7	2.0	13.3	6.8	1	0.10	3.5	0.05	1.7	0.98	
532	25.65	0.35	115	5.9	25.65	0.36	114.6	5.1	5	7.7	7.7	3.7	47	0.05	6.7	0.10	13.4	0.99	TANG.
533	25.70	-0.35	12	5.4	25.71	-0.38	12.2	4.5	7	1.1	14.2	7.5	-7	0.20	3.7	0.15	2.8	0.37	
534	25.70	-0.25	27	5.1	25.72	-0.25	26.1	4.7	8	2.0	13.3	6.7	-8	0.10	3.5	0.15	5.3	1.03	
535	25.70	0.05	54	7.4	25.70	0.05	54.8	6.2	5	3.8	11.5	5.3	3	0.05	3.3	0.05	3.3	1.32	
536	25.70	0.15	32	5.4	25.68	0.15	31.4	4.6	5	2.4	13.0	6.5	6	0.10	4.1	0.05	2.1	1.02	
537	25.75	0.10	103	5.7	25.75	0.10	102.5	5.2	4	6.5	8.8	3.9	11	0.05	5.6	0.05	5.6	1.07	TANG.
538	25.75	0.35	103	5.7	25.75	0.35	103.0	4.8	3	6.5	8.8	3.9	39	0.05	5.7	0.05	5.7	0.78	TANG.
539	25.75	0.40	93	5.8	25.73	0.40	92.8	4.8	5	5.8	9.5	4.1	40	0.10	10.1	0.05	5.0	0.73	

© American Astronomical Society • Provided by the NASA Astrophysics Data System

TABLE 1—*Continued*

CLOUD (1)	l_p ° (2)	b_p ° (3)	v_p (4)	T_p K (5)	<l> ° (6)	<b> ° (7)	<v> km s^{-1} (8)	<T> K (9)	N (10)	d_N kpc (11)	d_P kpc (12)	R kpc (13)	<z> pc (14)	Δl ° (15)	ΔL pc (16)	Δb ° (17)	ΔB pc (18)	σ_v km s^{-1} (19)	NOTES (20)
540	25.80	-0.70	106	5.2	25.80	-0.70	106.9	4.7	3	7.0	8.3	3.8	-85	0.05	6.1	0.05	6.1	0.80	TANG.
541	25.80	-0.10	62	5.9	25.78	-0.06	61.0	4.6	16	4.1	11.2	5.1	-4	0.20	14.4	0.15	10.8	1.41	
542	25.80	-0.05	91	5.4	25.80	-0.05	91.0	5.1	3	5.7	9.6	4.2	-4	0.05	5.0	0.05	5.0	0.80	
543	25.80	0.05	109	5.3	25.80	0.05	109.0	4.8	3	7.7	7.7	3.7	6	0.05	6.7	0.05	6.7	0.79	TANG.
544	25.80	0.10	30	5.1	25.83	0.11	30.4	4.7	8	2.3	13.0	6.5	4	0.10	4.0	0.10	4.0	0.97	
545	25.80	0.25	110	15.9	25.30	0.20	106.5	5.4	428	6.9	8.4	3.7	23	1.10	133.0	0.50	60.4	4.34	TANG.
A	25.20	0.15	105	11.2	25.22	0.15	105.7	9.4	7				18	0.10	12.1	0.05	6.0	1.00	
B	25.80	0.25	109	15.9	25.77	0.26	110.0	11.0	19				31	0.15	18.1	0.10	12.1	1.75	
546	25.80	0.45	48	6.3	25.68	0.50	47.5	4.8	76	3.4	11.9	5.6	29	0.50	29.5	0.45	26.6	1.43	
547	25.85	0.15	105	11.6	26.02	-0.01	102.6	5.3	635	6.5	8.8	3.9	0	0.85	96.2	0.95	107.5	4.49	NEAR
A	25.85	0.15	105	11.6	25.85	0.15	105.0	10.3	3				16	0.05	5.7	0.05	5.7	0.79	
B	26.20	0.05	107	9.6	26.20	0.05	106.0	9.4	3				5	0.05	5.7	0.05	5.7	0.81	
548	25.90	-0.45	89	5.8	25.90	-0.45	89.0	5.0	3	5.6	9.7	4.3	-43	0.05	4.9	0.05	4.9	0.78	
549	25.90	-0.25	109	7.5	26.02	-0.24	110.8	4.9	28	7.6	7.6	3.7	-32	0.30	40.0	0.10	13.3	1.80	TANG.
550	25.90	0.15	61	5.1	25.89	0.13	61.0	4.6	5	4.1	11.2	5.1	9	0.10	7.2	0.10	7.2	0.61	
551	25.90	0.20	69	5.4	25.93	0.21	69.4	4.6	24	4.6	10.7	4.8	16	0.20	15.9	0.20	15.9	1.18	
552	25.95	-0.60	63	5.9	25.93	-0.48	62.7	4.5	36	4.2	11.1	5.1	-35	0.25	18.4	0.25	18.4	1.09	
553	25.95	-0.35	101	5.4	26.00	-0.36	102.1	4.5	12	6.4	8.8	3.9	-40	0.15	16.8	0.10	11.2	1.09	TANG.
554	25.95	0.00	62	5.2	25.95	0.00	62.0	4.7	5	4.2	11.1	5.1	0	0.15	10.9	0.05	3.6	0.88	
555	26.00	-0.25	104	5.6	25.98	-0.25	104.2	4.7	7	6.6	8.6	3.9	-29	0.10	11.6	0.05	5.8	1.00	TANG.
556	26.00	-0.05	90	11.3	26.00	-0.05	90.3	8.4	6	5.6	9.6	4.2	-4	0.05	4.9	0.05	4.9	1.52	
A	26.00	-0.05	90	11.3	26.00	-0.05	90.0	10.4	3				-4	0.05	4.9	0.05	4.9	0.80	
557	26.00	-0.05	71	5.7	26.00	-0.04	70.7	5.1	3	4.6	10.7	4.8	-2	0.05	4.0	0.10	8.1	0.47	
558	26.00	0.10	113	6.8	26.00	0.10	113.0	6.1	3	7.6	7.6	3.7	13	0.05	6.7	0.05	6.7	0.80	TANG.
559	26.00	0.20	92	5.7	26.00	0.20	92.0	4.9	3	5.7	9.5	4.2	20	0.05	5.0	0.05	5.0	0.78	
560	26.15	0.00	51	5.1	26.14	0.00	52.0	4.5	5	3.6	11.6	5.5	0	0.15	9.5	0.05	3.2	0.64	
561	26.20	0.10	71	6.0	26.17	0.13	70.3	4.7	36	4.6	10.7	4.8	10	0.20	16.0	0.25	20.1	1.57	
562	26.25	0.25	71	5.7	26.30	0.27	71.2	4.6	17	4.6	10.6	4.8	21	0.15	12.2	0.15	12.2	0.87	
563	26.30	-0.35	101	6.0	26.19	-0.30	103.9	4.6	32	6.6	8.6	3.9	-34	0.25	28.9	0.15	17.3	1.75	TANG.
564	26.30	-0.05	114	8.9	26.34	-0.09	112.7	6.0	19	7.6	7.6	3.8	-11	0.10	13.3	0.25	33.2	1.27	TANG.
565	26.30	0.15	115	9.3	26.26	0.15	113.7	6.4	20	7.6	7.6	3.8	20	0.25	33.3	0.10	13.3	1.86	TANG.
A	26.30	0.15	115	9.3	26.30	0.15	114.0	8.9	5				19	0.05	6.7	0.05	6.7	1.40	
566	26.30	0.30	86	5.6	26.30	0.30	87.0	4.8	15	5.5	9.8	4.3	28	0.15	14.3	0.05	4.8	1.57	
567	26.35	-0.40	102	5.8	26.35	-0.40	102.0	5.3	3	6.4	8.8	4.0	-44	0.05	5.6	0.05	5.6	0.80	TANG.
568	26.35	0.05	54	5.7	26.35	0.07	55.0	4.4	13	3.8	11.4	5.4	4	0.15	9.9	0.10	6.6	1.54	
569	26.35	0.80	47	6.6	26.44	0.74	47.7	4.7	23	3.4	11.9	5.7	43	0.30	17.6	0.20	11.7	0.96	NEAR
570	26.40	0.35	115	7.6	26.40	0.35	115.0	6.5	3	7.6	7.6	3.8	46	0.05	6.6	0.05	6.6	0.78	TANG.
571	26.50	-0.60	67	7.9	26.48	-0.61	65.3	5.1	351	4.3	10.9	5.0	-46	0.70	53.0	0.85	64.3	3.61	NEAR
572	26.50	-0.30	91	6.4	26.50	-0.30	90.9	5.9	3	5.7	9.5	4.3	-29	0.05	5.0	0.05	5.0	0.79	
573	26.55	-0.30	108	10.9	26.53	-0.33	107.6	6.0	67	7.2	8.0	3.8	-41	0.40	50.3	0.20	25.2	1.88	TANG.
A	26.55	-0.30	108	10.9	26.55	-0.30	107.1	9.8	5				-37	0.05	6.3	0.05	6.3	1.38	
B	26.60	-0.35	109	10.7	26.58	-0.35	109.6	9.4	5				-44	0.10	12.6	0.05	6.3	1.00	
574	26.55	-0.15	25	6.0	26.59	-0.15	27.6	4.7	17	2.1	13.1	6.7	-5	0.15	5.4	0.15	5.4	2.19	
575	26.55	0.50	87	5.8	26.53	0.50	87.0	5.1	7	5.5	9.8	4.4	47	0.10	9.5	0.05	4.8	1.22	
576	26.55	0.60	122	6.8	26.55	0.60	122.0	5.8	3	7.6	7.6	3.8	79	0.05	6.6	0.05	6.6	0.78	TANG.
577	26.60	-0.55	62	5.5	26.60	-0.55	61.6	4.9	4	4.1	11.1	5.1	-39	0.05	3.6	0.05	3.6	1.08	
578	26.60	-0.05	68	8.1	26.64	-0.05	68.1	5.6	11	4.5	10.7	4.9	-3	0.15	11.7	0.05	3.9	1.42	
579	26.60	0.00	28	7.3	26.59	0.05	27.9	4.9	70	2.1	13.1	6.7	1	0.15	5.5	0.30	10.9	3.00	
580	26.60	0.25	112	7.9	26.58	0.26	111.5	5.4	22	7.6	7.6	3.8	34	0.25	33.2	0.10	13.3	2.03	TANG.
581	26.60	0.45	119	8.5	26.60	0.46	118.9	5.7	5	7.6	7.6	3.8	61	0.05	6.6	0.10	13.3	0.75	TANG.
582	26.60	0.45	89	6.2	26.60	0.43	87.5	4.9	13	5.5	9.7	4.4	41	0.15	14.3	0.10	9.6	1.11	
583	26.60	0.65	119	6.1	26.60	0.65	119.0	5.4	3	7.6	7.6	3.8	86	0.05	6.6	0.05	6.6	0.79	TANG.
584	26.65	-0.05	63	5.5	26.63	-0.04	63.0	4.6	6	4.2	11.0	5.1	-3	0.10	7.3	0.10	7.3	0.80	
585	26.65	0.00	112	6.5	26.73	0.03	110.8	4.8	27	7.6	7.6	3.8	3	0.25	33.1	0.15	19.9	1.64	TANG.
586	26.65	0.00	100	9.2	26.62	0.08	101.0	5.2	282	6.4	8.8	4.0	9	0.60	66.7	0.70	77.8	3.25	TANG.
587	26.65	0.25	27	5.5	26.66	0.26	28.0	4.5	13	2.1	13.1	6.7	9	0.10	3.7	0.10	3.7	2.16	
588	26.70	-0.85	63	5.4	26.71	-0.83	61.8	4.6	9	4.1	11.0	5.1	-59	0.10	7.2	0.15	10.8	1.30	
589	26.70	0.05	96	7.0	26.70	0.05	96.0	5.7	3	6.0	9.2	4.1	5	0.05	5.2	0.05	5.2	0.77	
590	26.70	0.15	95	6.6	26.70	0.15	95.0	5.8	3	5.9	9.3	4.2	15	0.05	5.2	0.05	5.2	0.79	
591	26.70	0.50	86	7.8	26.70	0.50	86.1	6.5	3	5.4	9.8	4.4	47	0.05	4.7	0.05	4.7	0.76	

© American Astronomical Society • Provided by the NASA Astrophysics Data System

TABLE 1—*Continued*

CLOUD	l_p °	b_p °	v_p	T_p K	<l> °	<b> °	<v> km s^{-1}	<T> K	N	d_N kpc	d_P kpc	R kpc	<z> pc	Δl °	ΔL pc	Δb °	ΔB pc	σ_v km s^{-1}	NOTES
(1)	(2)	(3)	(4)	(5)	(6)	(7)	(8)	(9)	(10)	(11)	(12)	(13)	(14)	(15)	(16)	(17)	(18)	(19)	(20)
592	26.75	0.50	20	6.5	26.75	0.48	20.7	5.1	8	1.6	13.6	7.1	13	0.05	1.4	0.10	2.8	1.28	
593	26.80	0.20	113	6.0	26.80	0.23	113.8	5.0	5	7.6	7.6	3.8	30	0.05	6.6	0.10	13.2	0.71	TANG.
594	26.85	0.00	25	5.0	26.85	0.00	25.9	4.7	3	2.0	13.2	6.8	0	0.05	1.7	0.05	1.7	0.80	
595	26.85	0.20	25	5.5	26.84	0.25	23.0	4.7	13	1.8	13.4	7.0	7	0.10	3.1	0.15	4.6	1.57	
596	26.85	0.40	81	6.1	26.86	0.40	81.0	4.8	4	5.1	10.0	4.6	35	0.10	9.0	0.05	4.5	0.68	
597	26.90	-0.25	86	5.2	26.90	-0.27	86.5	4.7	4	5.4	9.7	4.4	-25	0.05	4.7	0.10	9.5	0.50	
598	26.90	0.10	33	5.1	26.90	0.10	33.0	4.6	5	2.4	12.7	6.4	4	0.05	2.1	0.05	2.1	1.36	
599	26.90	0.10	91	9.7	27.74	0.05	97.6	5.3	1114	6.1	8.9	4.2	5	1.95	209.3	0.70	75.1	4.22	
A	28.20	-0.05	106	9.2	28.21	-0.01	107.0	8.7	7				-1	0.10	10.7	0.15	16.1	1.07	
B	28.20	-0.05	95	9.4	28.20	-0.05	95.0	9.0	3				-5	0.05	5.4	0.05	5.4	0.81	
600	26.95	-0.40	69	12.5	26.94	-0.35	68.0	5.6	47	4.5	10.7	5.0	-26	0.35	27.3	0.15	11.7	1.41	
601	26.95	-0.10	81	7.5	26.82	-0.10	79.6	5.1	50	5.1	10.1	4.6	-9	0.40	35.3	0.20	17.7	1.54	
602	27.00	-0.10	49	5.0	27.00	-0.09	49.0	4.6	4	3.4	11.7	5.7	-5	0.05	3.0	0.10	6.0	0.68	
603	27.05	-0.15	101	7.4	27.04	-0.16	102.2	5.2	28	6.5	8.6	4.0	-18	0.20	22.7	0.15	17.0	1.35	TANG.
604	27.10	-0.55	86	9.5	27.08	-0.58	85.8	5.8	16	5.4	9.7	4.4	-54	0.20	18.8	0.10	9.4	1.01	
605	27.10	-0.10	38	5.2	27.10	-0.08	39.9	4.6	9	2.9	12.3	6.1	-4	0.05	2.5	0.10	5.0	1.65	
606	27.10	-0.10	94	5.9	27.09	-0.12	93.4	4.7	7	5.8	9.3	4.2	-12	0.15	15.3	0.10	10.2	0.90	
607	27.10	0.10	38	5.6	27.11	0.10	36.2	4.7	11	2.6	12.5	6.3	4	0.15	6.8	0.05	2.3	1.52	
608	27.15	-0.30	77	6.0	27.15	-0.30	77.0	5.2	3	4.9	10.2	4.7	-25	0.05	4.3	0.05	4.3	0.79	
609	27.15	0.25	80	5.4	27.15	0.25	80.0	4.7	3	5.1	10.0	4.6	22	0.05	4.4	0.05	4.4	0.78	
610	27.20	-0.15	27	6.9	27.20	-0.13	26.6	5.1	8	2.0	13.1	6.8	-4	0.05	1.7	0.10	3.5	1.07	
611	27.25	0.15	33	8.6	27.26	0.13	32.0	5.5	43	2.3	12.8	6.5	5	0.30	12.2	0.20	8.1	2.76	
612	27.25	0.30	24	6.6	27.25	0.26	24.1	4.8	15	1.8	13.3	6.9	8	0.15	4.8	0.15	4.8	1.10	
613	27.30	-0.30	72	6.5	27.31	-0.25	74.5	5.0	17	4.8	10.3	4.8	-20	0.10	8.4	0.15	12.5	1.94	
614	27.30	-0.30	109	5.9	27.36	-0.31	107.7	4.7	15	7.5	7.6	3.9	-40	0.25	32.9	0.10	13.2	1.05	TANG.
615	27.30	0.40	79	5.4	27.32	0.40	79.3	5.2	3	5.0	10.1	4.6	35	0.10	8.8	0.05	4.4	0.47	
616	27.35	-0.15	50	5.4	27.33	-0.15	50.2	4.8	5	3.5	11.6	5.6	-9	0.10	6.1	0.05	3.0	0.74	
617	27.35	-0.15	93	10.6	27.34	-0.15	92.3	6.1	60	5.8	9.3	4.3	-14	0.25	25.2	0.15	15.1	1.52	
A	27.35	-0.15	93	10.6	27.36	-0.15	92.5	8.8	9				-15	0.15	15.1	0.05	5.0	1.05	
618	27.40	0.05	18	5.7	27.38	0.04	16.9	4.5	12	1.4	13.7	7.3	0	0.15	3.5	0.10	2.4	2.00	
619	27.45	-0.20	76	5.6	27.45	-0.20	76.4	5.0	6	4.9	10.2	4.7	-17	0.05	4.3	0.05	4.3	1.66	
620	27.45	0.25	39	5.4	27.45	0.25	39.0	5.0	3	2.8	12.3	6.2	12	0.05	2.4	0.05	2.4	0.80	
621	27.50	-0.35	95	7.3	27.52	-0.37	95.2	5.4	16	6.0	9.1	4.2	-38	0.10	10.4	0.10	10.4	1.22	
622	27.50	-0.15	47	5.2	27.50	-0.15	47.0	4.6	3	3.3	11.8	5.8	-8	0.05	2.9	0.05	2.9	0.79	
623	27.50	0.00	92	5.5	27.50	0.00	92.1	4.9	3	5.8	9.3	4.3	0	0.05	5.0	0.05	5.0	0.79	
624	27.50	0.20	36	10.2	27.55	0.25	36.5	5.4	30	2.6	12.5	6.3	11	0.15	6.8	0.15	6.8	2.20	
A	27.50	0.20	36	10.2	27.50	0.20	36.0	9.4	3				9	0.05	2.3	0.05	2.3	0.80	
625	27.55	-0.95	86	7.0	27.52	-0.93	85.8	5.6	7	5.4	9.7	4.5	-87	0.10	9.4	0.10	9.4	0.79	
626	27.55	-0.05	94	7.1	27.55	-0.05	94.1	6.1	3	5.9	9.2	4.3	-5	0.05	5.1	0.05	5.1	0.78	
627	27.60	-0.30	95	6.6	27.60	-0.30	95.1	6.0	3	6.0	9.1	4.2	-31	0.05	5.2	0.05	5.2	0.79	
628	27.60	0.00	92	6.5	27.60	0.00	91.9	5.5	3	5.8	9.3	4.3	0	0.05	5.0	0.05	5.0	0.77	
629	27.60	0.05	106	6.3	27.62	0.05	105.7	4.9	7	7.0	8.0	4.0	6	0.10	12.3	0.05	6.1	0.99	TANG.
630	27.65	0.10	83	8.0	27.47	0.14	82.8	5.1	49	5.2	9.9	4.6	12	0.35	31.9	0.15	13.7	1.53	
631	27.70	0.30	95	5.1	27.70	0.30	94.5	4.6	4	5.9	9.1	4.3	31	0.05	5.2	0.05	5.2	1.08	
632	27.75	-0.25	96	5.1	27.75	-0.25	96.0	4.6	3	6.0	9.0	4.2	-26	0.05	5.3	0.05	5.3	0.79	
633	27.75	0.00	104	5.3	27.75	0.00	104.0	4.8	3	6.8	8.3	4.0	0	0.05	5.9	0.05	5.9	0.80	TANG.
634	27.75	0.10	51	5.6	27.75	0.10	51.0	5.1	3	3.5	11.5	5.6	6	0.05	3.1	0.05	3.1	0.80	
635	27.80	-0.30	47	5.0	27.81	-0.26	45.3	4.4	9	3.2	11.9	5.9	-14	0.10	5.5	0.15	8.3	1.35	
636	27.80	0.15	83	6.1	27.80	0.16	82.5	4.8	5	5.2	9.8	4.6	14	0.05	4.5	0.15	13.6	0.50	
637	27.85	-0.25	104	6.9	27.83	-0.24	103.5	5.0	9	6.7	8.3	4.0	-28	0.10	11.7	0.10	11.7	1.03	TANG.
638	27.85	-0.20	82	5.2	27.85	-0.20	82.0	4.8	3	5.2	9.8	4.6	-18	0.05	4.5	0.05	4.5	0.80	
639	27.90	-0.20	103	6.9	27.90	-0.20	103.0	5.8	3	6.7	8.4	4.1	-23	0.05	5.8	0.05	5.8	0.78	TANG.
640	27.90	0.00	48	6.8	27.93	0.01	48.3	5.3	13	3.3	11.7	5.8	0	0.10	5.8	0.15	8.7	1.08	
641	27.90	0.20	94	7.1	27.90	0.20	93.6	5.9	4	5.9	9.2	4.3	20	0.05	5.1	0.05	5.1	1.05	
642	27.95	-0.55	55	9.0	27.95	-0.55	54.5	6.6	4	3.7	11.3	5.5	-35	0.05	3.2	0.05	3.2	0.97	
643	27.95	0.15	90	5.1	27.95	0.15	90.0	4.7	3	5.6	9.4	4.4	14	0.05	4.9	0.05	4.9	0.80	
644	27.95	0.20	41	6.6	27.94	0.20	40.3	5.5	5	2.8	12.2	6.1	9	0.10	5.0	0.05	2.5	1.14	
645	27.95	0.30	98	7.0	27.88	0.28	98.5	5.1	37	6.2	8.8	4.2	30	0.25	27.2	0.20	21.7	1.52	
646	28.00	0.10	58	9.4	28.00	0.00	58.0	5.6	10	3.9	11.1	5.4	5	0.15	10.2	0.10	6.8	0.75	
647	28.05	0.20	105	7.1	28.02	0.18	104.0	5.3	16	6.8	8.2	4.1	21	0.15	17.8	0.10	11.9	1.72	TANG.

© American Astronomical Society • Provided by the NASA Astrophysics Data System

TABLE 1—*Continued*

CLOUD	l_p	b_p	v_p	T_p	$\langle l \rangle$	$\langle b \rangle$	$\langle v \rangle$	$\langle T \rangle$	N	d_N	d_F	R	$\langle z \rangle$	Δl	ΔL	Δb	ΔB	σ_v	NOTES
	°	°		K	°	°	km s^{-1}	K		kpc	kpc	kpc	pc	°	pc	°	pc	km s^{-1}	
(1)	(2)	(3)	(4)	(5)	(6)	(7)	(8)	(9)	(10)	(11)	(12)	(13)	(14)	(15)	(16)	(17)	(18)	(19)	(20)
648	28.10	0.20	51	5.3	28.07	0.19	51.3	4.7	10	3.5	11.5	5.7	11	0.10	6.1	0.15	9.2	1.07	
649	28.15	0.30	37	6.3	28.15	0.29	37.1	4.8	6	2.6	12.4	6.3	13	0.05	2.3	0.10	4.6	1.28	
650	28.20	-0.45	74	5.7	28.19	-0.42	76.1	4.9	9	4.9	10.1	4.8	-35	0.10	8.5	0.10	8.5	1.31	
651	28.20	0.15	109	5.6	28.20	0.15	109.1	5.0	3	7.5	7.5	4.0	19	0.05	6.5	0.05	6.5	0.79	TANG.
652	28.25	0.35	56	7.9	28.24	0.37	56.1	5.8	11	3.8	11.2	5.5	24	0.15	9.9	0.10	6.6	0.75	
653	28.30	-0.35	51	7.7	28.24	-0.38	46.1	5.2	147	3.2	11.8	5.9	-21	0.70	38.9	0.30	16.7	1.95	
654	28.30	0.00	44	5.1	28.30	-0.03	45.4	4.7	7	3.1	11.8	5.9	-1	0.05	2.7	0.15	8.2	1.43	
655	28.30	0.00	33	6.8	28.31	-0.03	33.9	5.0	16	2.4	12.6	6.5	-1	0.15	6.3	0.10	4.2	1.17	
656	28.30	0.25	36	6.4	28.28	0.23	36.1	5.0	14	2.6	12.4	6.4	10	0.20	8.9	0.10	4.5	1.00	
657	28.35	-0.30	71	5.0	28.35	-0.30	71.0	4.7	3	4.6	10.4	5.0	-24	0.05	4.0	0.05	4.0	0.80	
658	28.35	-0.25	100	7.9	28.37	-0.23	101.4	5.2	13	6.6	8.4	4.1	-26	0.10	11.4	0.10	11.4	1.54	TANG.
659	28.35	0.20	98	7.7	28.35	0.20	99.6	5.1	16	6.4	8.6	4.2	22	0.15	16.7	0.05	5.6	2.06	TANG.
660	28.40	-0.60	73	5.8	28.40	-0.62	72.5	4.9	5	4.7	10.3	4.9	-50	0.05	4.1	0.10	8.2	1.01	
661	28.40	-0.05	43	5.8	28.43	-0.01	43.2	4.9	9	3.0	12.0	6.0	0	0.10	5.2	0.15	7.9	0.88	
662	28.40	0.25	101	5.5	28.40	0.25	101.0	4.9	3	6.5	8.4	4.2	28	0.05	5.7	0.05	5.7	0.79	TANG.
663	28.45	0.00	-13	6.9	28.45	0.00	-13.4	5.7	4	15.6	15.6	9.1	0	0.05	13.7	0.05	13.7	1.05	TANG.
664	28.50	0.10	34	6.0	28.50	0.10	34.1	5.3	3	2.4	12.5	6.5	4	0.05	2.1	0.05	2.1	0.78	
665	28.60	-0.25	63	6.2	28.60	-0.26	63.3	5.3	3	4.2	10.8	5.2	-19	0.05	3.6	0.10	7.3	0.47	
666	28.60	0.00	43	7.5	28.59	0.00	42.6	5.6	7	3.0	12.0	6.1	0	0.10	5.2	0.05	2.6	1.32	
667	28.60	0.20	109	5.5	28.60	0.22	108.7	4.8	3	7.5	7.5	4.1	28	0.05	6.5	0.10	13.0	0.46	TANG.
668	28.65	-0.65	89	5.3	28.65	-0.65	88.0	4.5	5	5.5	9.4	4.5	-62	0.05	4.8	0.05	4.8	1.37	
669	28.65	0.45	95	5.9	28.65	0.45	95.0	4.7	3	6.0	8.9	4.3	47	0.05	5.2	0.05	5.2	0.76	
670	28.70	-0.20	102	6.8	28.70	-0.19	102.2	5.4	6	6.7	8.2	4.2	-22	0.05	5.8	0.15	17.5	0.69	TANG.
671	28.70	0.40	92	8.8	28.72	0.43	91.5	6.4	13	5.8	9.1	4.4	43	0.10	10.1	0.10	10.1	1.50	
672	28.80	-1.00	58	7.6	28.80	-1.00	57.9	5.7	3	3.9	11.0	5.4	-67	0.05	3.4	0.05	3.4	0.74	
673	28.80	-0.45	66	5.0	28.81	-0.45	65.4	4.7	3	4.3	10.6	5.2	-33	0.10	7.5	0.05	3.7	0.48	
674	28.85	-0.40	100	5.4	28.85	-0.39	100.6	4.9	3	6.5	8.4	4.2	-43	0.05	5.7	0.10	11.4	0.48	TANG.
675	28.85	0.15	52	8.2	28.84	0.16	51.6	5.5	6	3.5	11.4	5.7	10	0.10	6.1	0.10	6.1	0.90	
676	28.85	0.20	35	6.3	28.83	0.20	35.1	5.0	7	2.5	12.4	6.4	8	0.10	4.3	0.05	2.2	1.17	
677	28.85	0.50	84	6.6	28.82	0.48	83.9	5.1	14	5.3	9.6	4.6	44	0.10	9.3	0.10	9.3	1.30	
678	28.90	0.10	53	7.3	28.90	0.10	53.0	5.9	3	3.6	11.3	5.6	6	0.05	3.1	0.05	3.1	0.77	
679	28.95	-0.65	51	12.1	29.02	-0.72	52.1	7.0	44	3.5	11.3	5.7	-44	0.35	21.5	0.30	18.4	1.14	
A	28.95	-0.65	51	12.1	28.96	-0.66	52.3	9.4	10				-40	0.10	6.1	0.15	9.2	0.91	
B	29.05	-0.75	52	10.3	29.05	-0.75	52.0	9.6	3				-46	0.05	3.1	0.05	3.1	0.80	
680	28.95	-0.50	21	5.2	28.98	-0.48	21.4	4.6	7	1.6	13.3	7.1	-13	0.10	2.8	0.10	2.8	0.49	
681	28.95	-0.40	65	5.2	28.95	-0.42	65.5	4.6	5	4.3	10.6	5.2	-31	0.05	3.7	0.10	7.5	1.00	
682	28.95	0.10	69	7.6	28.95	0.09	69.0	5.8	8	4.5	10.4	5.1	7	0.05	3.9	0.10	7.8	1.61	
683	28.95	0.25	103	8.2	28.94	0.24	105.9	6.0	12	7.4	7.4	4.1	31	0.10	13.0	0.10	13.0	2.20	TANG.
684	28.95	0.30	37	7.0	28.95	0.30	36.9	5.8	3	2.6	12.3	6.4	13	0.05	2.3	0.05	2.3	0.77	
685	28.95	0.40	96	5.5	28.95	0.40	95.5	4.9	4	6.1	8.8	4.3	42	0.05	5.3	0.05	5.3	1.08	
686	29.00	0.00	51	5.1	29.00	-0.02	50.5	4.5	4	3.4	11.4	5.7	-1	0.05	3.0	0.10	6.0	0.50	
687	29.10	-0.65	109	5.2	29.10	-0.65	109.0	4.8	3	7.4	7.4	4.1	-84	0.05	6.5	0.05	6.5	0.80	TANG.
688	29.10	-0.60	47	7.0	29.10	-0.62	47.1	5.8	4	3.2	11.6	5.9	-34	0.05	2.8	0.10	5.6	0.68	
689	29.15	-1.00	57	7.2	29.15	-1.00	56.6	5.8	6	3.8	11.1	5.5	-66	0.05	3.3	0.15	9.9	0.50	
690	29.15	-0.15	48	7.6	29.14	-0.14	48.4	4.9	16	3.3	11.6	5.8	-8	0.15	8.6	0.15	8.6	1.29	
691	29.15	0.05	46	6.3	29.15	0.05	45.9	5.3	3	3.1	11.7	6.0	2	0.05	2.7	0.05	2.7	0.78	
692	29.20	-0.70	98	5.8	29.20	-0.70	97.9	5.2	3	6.3	8.5	4.3	-77	0.05	5.5	0.05	5.5	0.79	TANG.
693	29.20	-0.25	96	5.7	29.20	-0.25	94.7	4.7	6	6.0	8.8	4.4	-26	0.05	5.3	0.05	5.3	1.73	
694	29.25	-0.55	20	5.1	29.23	-0.55	20.5	4.4	6	1.5	13.3	7.2	-14	0.10	2.7	0.05	1.3	0.95	
695	29.25	-0.10	47	5.2	29.25	-0.10	46.5	4.9	4	3.2	11.7	5.9	-5	0.05	2.8	0.05	2.8	1.11	
696	29.25	0.25	57	5.1	29.25	0.25	57.0	4.6	3	3.8	11.0	5.5	16	0.05	3.3	0.05	3.3	0.80	
697	29.25	0.45	80	7.2	29.25	0.42	80.3	5.9	6	5.1	9.7	4.8	37	0.05	4.5	0.15	13.4	0.74	
698	29.30	-0.15	47	5.7	29.30	-0.15	47.9	5.2	3	3.3	11.6	5.9	-8	0.05	2.8	0.05	2.8	0.80	
699	29.35	-0.55	64	6.4	29.30	-0.51	64.1	4.7	116	4.2	10.6	5.3	-37	0.40	29.3	0.35	25.7	1.72	
700	29.35	-0.20	21	5.6	29.35	-0.20	21.4	5.0	4	1.6	13.2	7.2	-5	0.05	1.4	0.05	1.4	1.09	
701	29.35	-0.15	73	5.2	29.35	-0.15	73.0	4.7	3	4.7	10.1	5.0	-12	0.05	4.1	0.05	4.1	0.80	
702	29.35	0.40	90	5.9	29.35	0.40	90.0	5.1	3	5.7	9.1	4.5	39	0.05	5.0	0.05	5.0	0.78	
703	29.40	-1.05	57	6.3	29.41	-1.02	56.8	5.0	5	3.8	11.0	5.5	-67	0.10	6.6	0.15	9.9	0.39	
704	29.40	-0.15	86	5.7	29.38	-0.15	85.0	4.9	4	5.4	9.4	4.6	-14	0.10	9.4	0.05	4.7	0.73	
705	29.45	0.00	29	5.7	29.45	0.00	29.4	4.8	4	2.1	12.7	6.8	0	0.05	1.8	0.05	1.8	1.07	

© American Astronomical Society • Provided by the NASA Astrophysics Data System

TABLE 1—*Continued*

CLOUD (1)	l_p ° (2)	b_p ° (3)	v_p (4)	T_p K (5)	<l> ° (6)	<b> ° (7)	<v> km s^{-1} (8)	<T> K (9)	N (10)	d_N kpc (11)	d_F kpc (12)	R kpc (13)	<z> pc (14)	Δl ° (15)	ΔL pc (16)	Δb ° (17)	ΔB pc (18)	σ_v km s^{-1} (19)	NOTES (20)
706	29.45	0.20	42	6.5	29.45	0.20	42.0	5.6	3	2.9	11.9	6.2	10	0.05	2.5	0.05	2.5	0.78	
707	29.50	-0.45	103	5.0	29.50	-0.45	103.0	4.7	3	7.1	7.7	4.2	-56	0.05	6.2	0.05	6.2	0.80	TANG.
708	29.50	0.10	26	6.1	29.49	0.09	27.7	4.9	8	2.0	12.8	6.8	3	0.10	3.5	0.10	3.5	1.59	
709	29.50	0.40	82	8.0	29.50	0.40	81.6	6.1	4	5.2	9.6	4.7	36	0.05	4.5	0.05	4.5	1.02	
710	29.55	0.35	95	5.3	29.55	0.34	94.3	4.4	6	6.0	8.8	4.4	36	0.05	5.3	0.10	10.5	1.46	
711	29.60	-0.60	75	7.9	29.63	-0.65	75.4	5.0	100	4.8	9.9	4.9	-54	0.40	33.7	0.40	33.7	3.35	
712	29.60	-0.50	71	5.2	29.58	-0.49	72.3	4.8	6	4.7	10.1	5.0	-40	0.10	8.1	0.10	8.1	0.75	
713	29.60	0.15	109	5.9	29.60	0.15	108.1	5.3	3	7.4	7.4	4.2	19	0.05	6.4	0.05	6.4	0.79	TANG.
714	29.75	-0.85	76	6.8	29.73	-0.86	76.0	5.1	7	4.9	9.9	4.9	-72	0.10	8.5	0.10	8.5	0.75	
715	29.75	-0.30	81	6.1	29.73	-0.31	81.1	4.9	7	5.2	9.6	4.8	-28	0.10	9.0	0.10	9.0	0.64	
716	29.75	-0.25	92	8.2	29.78	-0.23	90.0	5.2	39	5.7	9.0	4.5	-23	0.20	20.0	0.25	25.0	2.02	
717	29.75	-0.10	81	6.3	29.71	-0.13	81.4	4.9	14	5.2	9.6	4.8	-11	0.15	13.6	0.10	9.0	1.57	
718	29.75	0.35	108	5.6	29.75	0.35	108.0	5.3	3	7.4	7.4	4.2	45	0.05	6.4	0.05	6.4	0.80	TANG.
719	29.75	0.70	73	6.3	29.75	0.70	72.5	5.5	4	4.7	10.1	5.0	57	0.05	4.1	0.05	4.1	1.06	NEAR
720	29.80	0.15	83	5.6	29.80	0.20	83.1	4.9	15	5.3	9.5	4.7	18	0.15	13.8	0.15	13.8	1.05	
721	29.85	-0.70	71	6.2	29.85	-0.70	70.6	5.6	4	4.6	10.2	5.1	-55	0.05	4.0	0.05	4.0	1.06	
722	29.85	-0.05	100	20.5	30.01	-0.04	91.1	5.7	11063	5.8	8.9	4.5	-3	4.55	462.9	1.35	137.3	10.40	NEAR
A	28.15	0.00	80	9.1	28.17	0.01	80.6	8.5	5				1	0.10	10.2	0.10	10.2	0.49	
B	28.15	0.20	89	10.1	28.15	0.20	89.0	9.5	3				20	0.05	5.1	0.05	5.1	0.80	
C	28.30	-0.10	81	13.1	28.28	-0.08	80.4	9.6	15				-8	0.15	15.3	0.10	10.2	1.32	
D	28.30	0.05	78	9.1	28.26	0.05	78.5	8.5	9				5	0.15	15.3	0.05	5.1	1.25	
E	28.60	-0.20	87	9.0	28.60	-0.20	87.5	8.8	4				-20	0.05	5.1	0.05	5.1	1.11	
F	28.60	0.05	100	10.0	28.60	0.05	100.0	9.1	3				5	0.05	5.1	0.05	5.1	0.79	
G	28.65	0.05	95	9.1	28.65	0.05	95.0	8.5	3				5	0.05	5.1	0.05	5.1	0.80	
H	28.65	0.10	107	9.4	28.65	0.10	106.0	8.8	7				10	0.05	5.1	0.05	5.1	1.96	
I	28.85	-0.25	88	15.8	28.85	-0.24	87.4	10.7	9				-24	0.05	5.1	0.15	15.3	1.42	
J	28.85	-0.20	94	9.7	28.85	-0.21	94.9	8.7	7				-21	0.05	5.1	0.10	10.2	1.23	
K	28.95	-0.55	76	10.5	28.96	-0.52	79.2	9.3	19				-52	0.15	15.3	0.10	10.2	2.59	
L	28.95	-0.20	95	11.2	28.96	-0.20	95.4	9.7	5				-20	0.10	10.2	0.05	5.1	0.99	
M	29.00	0.05	98	10.9	29.00	0.06	97.4	9.6	5				6	0.05	5.1	0.10	10.2	1.00	
N	29.10	-0.30	94	10.7	29.10	-0.30	94.0	9.7	3				-30	0.05	5.1	0.05	5.1	0.80	
O	29.25	-0.45	83	9.8	29.22	-0.45	83.4	8.9	7				-45	0.10	10.2	0.05	5.1	1.56	
P	29.35	-0.45	77	12.3	29.33	-0.45	78.2	10.5	13				-45	0.10	10.2	0.05	5.1	1.98	
Q	29.35	-0.35	91	10.7	29.26	-0.35	92.3	9.2	21				-35	0.30	30.5	0.05	5.1	1.37	
R	29.45	-0.25	94	10.8	29.44	-0.23	95.2	9.1	10				-23	0.10	10.2	0.10	10.2	1.23	
S	29.45	0.15	80	9.9	29.40	0.16	80.7	9.0	10				16	0.15	15.3	0.10	10.2	0.89	
T	29.55	0.20	79	11.1	29.54	0.20	79.6	9.4	11				20	0.10	10.2	0.15	15.3	0.87	
U	29.85	-0.05	100	20.5	29.92	-0.04	98.5	10.9	98				-4	0.25	25.4	0.20	20.3	2.88	
V	30.10	0.05	105	11.0	30.10	0.05	105.1	9.7	3				5	0.05	5.1	0.05	5.1	0.79	
W	30.30	-0.25	105	14.9	30.30	-0.25	104.2	10.0	48				-25	0.25	25.4	0.30	30.5	1.41	
X	30.35	0.00	94	9.7	30.33	0.01	94.1	8.8	10				1	0.15	15.3	0.15	15.3	1.05	
Y	30.35	0.10	95	9.5	30.35	0.10	95.0	8.9	3				10	0.05	5.1	0.05	5.1	0.80	
Z	30.35	0.40	94	9.6	30.35	0.40	94.0	8.9	3				40	0.05	5.1	0.05	5.1	0.80	
a	30.40	-0.30	99	9.7	30.39	-0.30	99.2	8.9	4				-30	0.10	10.2	0.05	5.1	0.83	
b	30.40	-0.10	88	13.0	30.40	-0.10	88.4	11.3	4				-10	0.05	5.1	0.05	5.1	1.07	
c	30.45	-0.25	105	12.9	30.45	-0.23	104.1	10.1	10				-23	0.05	5.1	0.10	10.2	1.49	
d	30.50	-0.40	106	10.9	30.50	-0.41	107.5	9.2	9				-41	0.05	5.1	0.15	15.3	1.42	
e	30.55	-0.20	85	9.1	30.57	-0.23	85.8	8.6	6				-23	0.10	10.2	0.10	10.2	0.68	
f	30.55	-0.20	95	11.6	30.55	-0.12	93.4	9.0	75				-12	0.25	25.4	0.50	50.9	1.89	
g	30.55	-0.10	103	10.4	30.55	-0.10	103.5	9.5	4				-10	0.05	5.1	0.05	5.1	1.08	
h	30.60	-0.45	94	11.3	30.67	-0.46	93.8	9.2	13				-46	0.15	15.3	0.10	10.2	1.14	
i	30.60	0.25	94	10.2	30.60	0.22	93.8	8.9	6				22	0.05	5.1	0.15	15.3	0.67	
j	30.75	-0.05	82	9.7	30.72	-0.02	80.9	8.7	10				-2	0.10	10.2	0.10	10.2	1.44	
k	30.80	-0.05	92	16.2	30.80	-0.02	94.4	10.1	278				-2	0.35	35.6	0.45	45.8	4.53	
l	30.85	0.00	84	9.2	30.85	0.00	84.0	8.8	3				0	0.05	5.1	0.05	5.1	0.81	
m	30.90	-0.05	84	10.3	30.90	-0.05	84.1	9.4	5				-5	0.05	5.1	0.05	5.1	1.37	
n	30.90	0.15	108	15.1	30.89	0.16	105.7	10.8	13				16	0.10	10.2	0.10	10.2	1.77	
o	31.00	-0.25	85	9.8	30.98	-0.25	86.1	8.6	7				-25	0.10	10.2	0.05	5.1	1.24	
p	31.15	0.25	102	10.4	31.12	0.25	99.9	8.9	10				25	0.15	15.3	0.05	5.1	1.86	
q	31.25	0.05	107	9.8	31.27	0.05	107.5	8.7	8				5	0.10	10.2	0.05	5.1	1.11	

© American Astronomical Society • Provided by the NASA Astrophysics Data System

TABLE 1—*Continued*

CLOUD	l_p °	b_p °	v_p	T_p K	<l> °	<b> °	<v> km s^{-1}	<T> K	N	d_N kpc	d_F kpc	R kpc	<z> pc	Δl °	ΔL pc	Δb °	ΔB pc	σ_v km s^{-1}	NOTES
(1)	(2)	(3)	(4)	(5)	(6)	(7)	(8)	(9)	(10)	(11)	(12)	(13)	(14)	(15)	(16)	(17)	(18)	(19)	(20)
r	31.75	0.15	97	9.4	31.75	0.15	96.1	8.9	3				15	0.05	5.1	0.05	5.1	0.80	
s	32.00	0.00	98	10.6	32.04	0.06	96.6	9.2	19				6	0.15	15.3	0.15	15.3	1.58	
723	29.90	0.20	82	5.9	29.90	0.20	81.6	5.2	4	5.2	9.5	4.8	18	0.05	4.5	0.05	4.5	1.07	
724	29.95	-0.85	74	6.8	29.95	-0.84	72.6	4.8	18	4.7	10.1	5.0	-68	0.15	12.2	0.15	12.2	1.25	
725	29.95	-0.80	84	7.7	29.96	-0.75	83.7	5.3	50	5.3	9.4	4.7	-69	0.45	41.9	0.20	18.6	1.33	
726	29.95	0.10	38	7.6	29.93	0.12	38.0	4.8	39	2.6	12.1	6.4	5	0.25	11.4	0.20	9.1	2.13	
727	30.00	0.30	100	6.8	30.02	0.30	100.1	5.3	6	6.7	8.0	4.3	35	0.10	11.7	0.05	5.9	0.77	TANG.
728	30.05	0.60	69	6.1	30.04	0.62	70.3	4.9	8	4.5	10.2	5.1	49	0.15	11.9	0.10	7.9	0.88	
729	30.10	-0.05	89	5.3	30.11	-0.05	87.5	4.9	7	5.6	9.1	4.6	-4	0.10	9.7	0.05	4.9	1.57	
730	30.15	-0.55	103	7.2	30.13	-0.57	103.3	5.3	17	7.3	7.4	4.3	-72	0.20	25.7	0.10	12.8	1.04	TANG.
731	30.15	0.15	76	6.0	30.15	0.15	75.5	5.3	4	4.8	9.9	5.0	12	0.05	4.2	0.05	4.2	1.06	
732	30.15	0.20	87	7.0	30.14	0.14	85.0	4.9	20	5.4	9.3	4.7	13	0.15	14.2	0.15	14.2	1.61	
733	30.20	0.05	100	5.7	30.20	0.05	100.0	5.0	3	6.8	7.9	4.3	5	0.05	5.9	0.05	5.9	0.79	TANG.
734	30.20	0.20	44	6.0	30.18	0.20	43.6	5.4	8	3.0	11.7	6.1	10	0.10	5.2	0.05	2.6	1.26	
735	30.20	0.35	71	7.7	30.21	0.35	70.4	5.7	14	4.6	10.1	5.1	27	0.15	11.9	0.20	15.9	1.09	
736	30.25	0.60	68	5.6	30.25	0.60	68.0	4.9	3	4.4	10.3	5.2	46	0.05	3.9	0.05	3.9	0.79	
737	30.30	0.15	46	6.9	30.29	0.13	44.7	5.2	14	3.0	11.6	6.1	6	0.10	5.3	0.15	7.9	1.59	
738	30.35	-0.70	86	5.4	30.37	-0.70	86.5	4.8	6	5.5	9.1	4.7	-67	0.10	9.7	0.05	4.8	0.95	
739	30.35	-0.35	91	5.5	30.32	-0.32	91.5	4.6	12	5.9	8.8	4.5	-33	0.15	15.4	0.10	10.3	1.48	
740	30.35	0.05	44	6.7	30.35	0.05	43.0	5.1	9	2.9	11.8	6.2	2	0.10	5.1	0.10	5.1	1.83	
741	30.35	0.10	112	6.7	30.32	0.10	112.5	5.5	6	7.3	7.3	4.3	12	0.10	12.8	0.05	6.4	0.93	TANG.
742	30.40	-0.30	13	5.6	30.44	-0.27	13.0	4.8	5	1.1	13.6	7.6	-4	0.15	2.8	0.10	1.8	0.00	
743	30.40	0.35	112	6.1	30.40	0.35	112.4	5.3	4	7.3	7.3	4.3	44	0.05	6.4	0.05	6.4	1.08	TANG.
744	30.40	0.45	45	10.0	30.44	0.46	45.2	5.5	22	3.1	11.6	6.1	24	0.15	8.0	0.30	16.0	0.95	
745	30.40	0.50	15	6.4	30.38	0.50	15.5	5.0	5	1.2	13.5	7.5	10	0.10	2.1	0.05	1.1	1.00	
746	30.45	-0.65	93	9.0	30.45	-0.66	92.5	5.7	9	6.0	8.7	4.5	-69	0.10	10.4	0.10	10.4	1.31	
747	30.45	0.00	106	6.1	30.45	0.00	106.0	5.0	3	7.3	7.3	4.3	0	0.05	6.4	0.05	6.4	0.77	TANG.
748	30.50	-0.65	12	15.3	30.50	-0.53	12.1	6.4	37	1.0	13.6	7.7	-9	0.30	5.2	0.35	6.1	0.68	
A	30.50	-0.65	12	15.3	30.49	-0.58	12.1	10.3	6				-10	0.10	1.7	0.20	3.5	0.34	
749	30.50	-0.55	92	8.2	30.53	-0.63	93.3	5.5	47	6.1	8.6	4.5	-66	0.20	21.1	0.40	42.3	3.18	
750	30.50	0.05	70	6.8	30.50	0.05	70.0	5.6	3	4.5	10.1	5.1	3	0.05	4.0	0.05	4.0	0.77	
751	30.55	0.25	46	5.9	30.53	0.25	46.8	4.7	13	3.1	11.5	6.0	13	0.15	8.2	0.15	8.2	0.95	
752	30.60	-0.35	109	5.7	30.60	-0.35	108.6	5.0	4	7.3	7.3	4.3	-44	0.05	6.4	0.05	6.4	1.08	TANG.
753	30.60	-0.05	43	7.2	30.56	0.04	41.5	5.2	110	2.8	11.8	6.2	2	0.25	12.3	0.35	17.2	3.35	
754	30.60	0.40	62	5.6	30.60	0.40	62.0	5.1	3	4.1	10.6	5.4	28	0.05	3.5	0.05	3.5	0.80	
755	30.65	-0.80	94	5.9	30.65	-0.82	94.0	5.1	4	6.1	8.5	4.5	-88	0.05	5.3	0.10	10.7	0.70	TANG.
756	30.65	0.60	92	6.7	30.65	0.60	92.0	5.8	3	6.0	8.7	4.5	62	0.05	5.2	0.05	5.2	0.79	
757	30.70	-0.35	54	5.9	30.71	-0.37	53.0	5.1	7	3.5	11.1	5.8	-22	0.10	6.2	0.10	6.2	1.18	
758	30.70	-0.35	36	5.1	30.70	-0.37	35.8	4.7	5	2.5	12.2	6.5	-15	0.05	2.1	0.10	4.3	0.74	
759	30.70	-0.05	38	5.8	30.72	-0.05	37.8	5.0	9	2.6	12.0	6.4	-2	0.10	4.5	0.05	2.3	1.28	
760	30.70	0.05	106	6.1	30.70	0.05	106.1	5.4	3	7.3	7.3	4.3	6	0.05	6.4	0.05	6.4	0.78	TANG.
761	30.70	0.10	38	5.5	30.70	0.10	38.0	4.7	3	2.6	12.0	6.4	4	0.05	2.3	0.05	2.3	0.78	
762	30.70	0.70	79	5.4	30.70	0.70	79.5	4.8	4	5.1	9.5	4.9	62	0.05	4.4	0.05	4.4	1.07	
763	30.75	-0.85	79	5.1	30.77	-0.88	79.9	4.4	9	5.1	9.5	4.9	-78	0.10	8.9	0.20	17.9	0.86	
764	30.75	0.65	81	5.2	30.78	0.65	79.3	4.9	9	5.1	9.5	4.9	57	0.10	8.9	0.05	4.4	1.30	
765	30.85	-0.15	53	11.6	30.84	-0.17	51.7	6.6	42	3.4	11.2	5.8	-10	0.20	12.0	0.25	15.0	1.93	
A	30.85	-0.15	53	11.6	30.85	-0.14	52.6	9.9	7				-8	0.05	3.0	0.10	6.0	1.35	
766	30.85	0.60	79	5.1	30.85	0.60	79.5	4.7	4	5.1	9.5	4.9	53	0.05	4.4	0.05	4.4	1.10	
767	30.90	-0.60	102	7.3	30.92	-0.57	97.8	5.4	58	6.6	8.0	4.4	-66	0.35	40.4	0.20	23.1	2.74	TANG.
768	30.90	-0.55	72	5.6	30.86	-0.50	70.5	4.6	16	4.6	10.0	5.1	-39	0.15	11.9	0.15	11.9	1.78	
769	30.90	-0.35	110	9.5	30.90	-0.35	110.0	7.8	3	7.3	7.3	4.4	-44	0.05	6.4	0.05	6.4	0.77	TANG.
770	30.90	-0.15	38	5.2	30.90	-0.15	38.9	4.7	5	2.7	11.9	6.4	-6	0.05	2.3	0.05	2.3	1.40	
771	30.90	0.20	59	5.6	30.85	0.22	59.7	4.7	19	3.9	10.7	5.5	15	0.25	17.1	0.10	6.8	1.29	
772	30.95	-0.10	35	5.1	30.95	-0.10	35.5	4.7	4	2.4	12.1	6.5	-4	0.05	2.1	0.05	2.1	1.08	
773	30.95	0.10	40	7.8	30.92	0.15	39.4	5.3	75	2.7	11.9	6.4	7	0.20	9.4	0.30	14.0	2.59	
774	31.00	-0.75	83	5.4	30.96	-0.73	81.8	4.5	20	5.3	9.3	4.8	-67	0.15	13.7	0.15	13.7	1.68	
775	31.00	-0.15	102	5.1	31.00	-0.15	102.0	4.6	3	7.3	7.3	4.4	-19	0.05	6.4	0.05	6.4	0.80	TANG.
776	31.00	0.25	47	6.7	31.01	0.25	46.3	5.5	5	3.1	11.5	6.1	13	0.10	5.4	0.05	2.7	1.15	
777	31.00	0.30	113	5.6	31.00	0.32	113.1	4.5	14	7.3	7.3	4.4	41	0.15	19.1	0.20	25.4	0.74	TANG.
778	31.05	0.00	39	6.0	31.04	0.00	37.6	5.0	10	2.6	12.0	6.4	0	0.10	4.5	0.10	4.5	1.50	

© American Astronomical Society • Provided by the NASA Astrophysics Data System

TABLE 1—*Continued*

CLOUD (1)	l_p ° (2)	b_p ° (3)	v_p (4)	T_p K (5)	<l> ° (6)	<b> ° (7)	<v> km s^{-1} (8)	<T> K (9)	N (10)	d_N kpc (11)	d_P kpc (12)	R kpc (13)	<z> pc (14)	Δl ° (15)	ΔL pc (16)	Δb ° (17)	ΔB pc (18)	σ_v km s^{-1} (19)	NOTES (20)
779	31.10	-0.20	102	6.7	31.14	-0.20	101.3	5.4	11	7.3	7.3	4.4	-25	0.15	19.0	0.05	6.3	1.56	TANG.
780	31.10	0.45	30	7.2	31.11	0.44	29.5	5.1	14	2.1	12.5	6.8	15	0.15	5.4	0.10	3.6	2.04	
781	31.15	-0.30	90	6.6	31.15	-0.30	89.5	5.3	4	5.8	8.7	4.6	-30	0.05	5.1	0.05	5.1	1.03	
782	31.15	-0.25	107	6.6	31.15	-0.25	107.4	5.6	4	7.3	7.3	4.4	-31	0.05	6.3	0.05	6.3	1.06	TANG.
783	31.25	-0.30	99	5.6	31.31	-0.31	101.0	4.9	12	7.3	7.3	4.4	-38	0.15	19.0	0.10	12.7	1.71	TANG.
784	31.25	-0.05	101	6.0	31.22	-0.06	100.1	4.8	8	7.3	7.3	4.4	-7	0.10	12.7	0.10	12.7	1.14	TANG.
785	31.30	-0.25	107	5.5	31.27	-0.24	105.1	4.9	7	7.3	7.3	4.4	-30	0.10	12.7	0.10	12.7	1.29	TANG.
786	31.30	-0.20	26	5.1	31.30	-0.20	25.5	4.7	4	1.8	12.7	7.0	-6	0.05	1.6	0.05	1.6	1.10	
787	31.30	0.45	89	5.6	31.24	0.46	88.8	4.5	19	5.8	8.8	4.7	46	0.20	20.1	0.10	10.1	2.02	
788	31.40	-0.55	85	5.7	31.40	-0.55	85.7	4.5	22	5.5	9.0	4.7	-52	0.15	14.5	0.25	24.2	1.31	
789	31.40	-0.20	33	6.9	31.40	-0.20	32.6	5.6	4	2.2	12.3	6.7	-7	0.05	2.0	0.05	2.0	1.04	
790	31.40	0.00	39	8.9	31.28	0.00	40.4	5.3	126	2.7	11.8	6.3	0	0.35	16.7	0.40	19.1	3.34	
791	31.40	0.20	18	6.6	31.40	0.20	18.5	5.5	4	1.4	13.1	7.4	4	0.05	1.2	0.05	1.2	1.03	
792	31.45	-0.30	96	8.0	31.45	-0.28	95.5	6.1	10	6.4	8.1	4.5	-31	0.05	5.6	0.10	11.2	1.39	TANG.
793	31.45	-0.10	90	6.1	31.45	-0.10	89.9	5.1	3	5.9	8.6	4.6	-10	0.05	5.1	0.05	5.1	0.77	
794	31.50	-0.05	98	5.3	31.50	-0.05	97.6	4.8	4	6.8	7.7	4.5	-5	0.05	6.0	0.05	6.0	1.10	TANG.
795	31.50	0.35	108	5.3	31.49	0.35	108.2	4.5	4	7.2	7.2	4.4	44	0.10	12.7	0.05	6.3	0.81	TANG.
796	31.55	-0.45	97	8.2	31.67	-0.35	100.3	5.0	156	7.2	7.2	4.5	-43	0.30	37.9	0.65	82.0	3.19	TANG.
797	31.60	-0.30	36	6.0	31.58	-0.30	35.1	5.0	6	2.4	12.1	6.6	-12	0.10	4.2	0.05	2.1	1.26	
798	31.60	-0.15	32	7.2	31.60	-0.14	32.4	5.9	5	2.2	12.3	6.7	-5	0.05	1.9	0.10	3.9	1.00	
799	31.60	0.10	117	6.6	31.60	0.10	117.0	5.8	3	7.2	7.2	4.5	12	0.05	6.3	0.05	6.3	0.79	TANG.
800	31.60	0.25	116	6.7	31.60	0.24	115.6	5.4	10	7.2	7.2	4.5	30	0.05	6.3	0.20	25.3	0.92	TANG.
801	31.65	-0.30	81	5.8	31.65	-0.27	80.9	4.6	6	5.2	9.3	4.9	-24	0.05	4.6	0.15	13.7	0.70	
802	31.65	-0.25	44	8.0	31.55	-0.14	42.5	5.5	59	2.9	11.6	6.2	-6	0.30	14.9	0.25	12.5	3.09	
803	31.65	-0.15	25	6.2	31.65	-0.15	25.0	5.5	3	1.8	12.7	7.1	-4	0.05	1.5	0.05	1.5	0.79	
804	31.70	-0.35	82	5.2	31.69	-0.42	80.9	4.4	9	5.2	9.2	4.9	-38	0.10	9.1	0.20	18.2	0.99	
805	31.75	-0.35	88	5.8	31.73	-0.36	88.7	4.7	4	5.8	8.7	4.7	-36	0.10	10.1	0.10	10.1	0.46	
806	31.75	-0.15	39	5.9	31.76	-0.17	37.4	4.7	17	2.5	11.9	6.5	-7	0.15	6.6	0.10	4.4	1.73	
807	31.75	0.00	104	5.8	31.75	0.00	103.9	5.2	3	7.2	7.2	4.5	0	0.05	6.3	0.05	6.3	0.79	TANG.
808	31.85	-0.10	101	6.7	31.85	-0.10	101.0	5.6	3	7.2	7.2	4.5	-12	0.05	6.3	0.05	6.3	0.78	TANG.
809	31.90	0.35	99	6.6	31.97	0.35	97.2	5.2	17	7.1	7.3	4.5	44	0.20	24.9	0.15	18.6	1.32	TANG.
810	31.95	-0.30	97	6.2	32.02	-0.26	97.2	4.8	71	7.2	7.2	4.5	-32	0.30	37.7	0.25	31.4	1.75	TANG.
811	32.00	-0.65	69	6.9	31.97	-0.53	70.7	5.3	19	4.6	9.8	5.2	-42	0.15	12.0	0.25	20.0	1.07	
812	32.10	-0.35	104	5.4	32.10	-0.37	102.6	4.8	8	7.2	7.2	4.5	-47	0.05	6.3	0.10	12.6	1.48	TANG.
813	32.25	0.05	83	6.2	32.27	0.06	82.8	5.3	6	5.4	9.0	4.9	6	0.10	9.4	0.10	9.4	0.65	
814	32.25	0.25	25	7.2	32.25	0.23	24.4	5.9	17	1.7	12.7	7.1	6	0.05	1.5	0.20	6.0	1.16	
815	32.40	0.05	97	5.5	32.42	0.05	97.5	4.9	4	7.2	7.2	4.6	6	0.10	12.5	0.05	6.3	0.50	TANG.
816	32.40	0.80	27	7.0	32.40	0.80	27.0	5.6	3	1.9	12.5	7.0	26	0.05	1.6	0.05	1.6	0.77	NEAR
817	32.45	0.20	51	6.4	32.48	0.23	51.1	4.9	33	3.4	11.0	5.9	13	0.20	11.8	0.15	8.8	1.62	
818	32.50	-0.05	96	5.8	32.50	-0.04	95.8	4.9	5	7.0	7.3	4.6	-5	0.05	6.1	0.10	12.3	1.11	TANG.
819	32.60	-0.25	90	10.5	32.72	-0.27	90.3	5.8	39	6.1	8.2	4.7	-28	0.35	37.2	0.10	10.6	1.28	TANG.
820	32.65	-0.65	0	5.9	32.65	-0.65	0.0	5.2	3	0.5	14.0	8.3	-5	0.05	0.4	0.05	0.4	0.79	
821	32.65	-0.20	51	5.5	32.65	-0.22	51.0	5.0	4	3.4	10.9	6.0	-13	0.05	2.9	0.10	5.9	0.68	
822	32.65	-0.15	111	6.6	32.65	-0.15	111.0	5.5	3	7.2	7.2	4.6	-18	0.05	6.2	0.05	6.2	0.77	TANG.
823	32.70	-0.05	100	7.9	32.80	-0.01	94.1	4.9	289	6.7	7.6	4.6	-1	0.50	58.4	0.40	46.7	4.43	TANG.
824	32.80	-0.60	88	5.9	32.82	-0.60	87.9	5.0	5	5.9	8.4	4.8	-61	0.10	10.2	0.05	5.1	0.74	
825	32.80	0.20	29	6.1	32.78	0.20	30.5	4.9	11	2.1	12.2	6.8	7	0.10	3.6	0.05	1.8	1.97	
826	32.85	-0.15	104	5.1	32.85	-0.15	104.0	4.7	3	7.1	7.1	4.6	-18	0.05	6.2	0.05	6.2	0.80	TANG.
827	32.95	0.60	91	5.2	32.95	0.58	91.0	5.0	4	6.2	8.0	4.7	62	0.05	5.4	0.10	10.9	0.70	TANG.
828	33.00	-0.55	51	5.4	33.00	-0.55	51.0	4.9	3	3.4	10.9	6.0	-32	0.05	2.9	0.05	2.9	0.79	
829	33.00	-0.35	90	5.5	33.00	-0.34	90.4	4.5	7	6.2	8.1	4.7	-36	0.05	5.4	0.10	10.8	1.35	TANG.
830	33.00	-0.35	51	6.9	33.00	-0.37	50.9	5.6	6	3.4	10.9	6.0	-21	0.05	2.9	0.10	5.9	0.78	
831	33.00	0.05	85	5.3	33.00	0.05	85.4	4.8	4	5.7	8.6	4.9	4	0.05	4.9	0.05	4.9	1.08	
832	33.00	0.15	72	6.6	33.04	0.13	71.4	4.9	16	4.7	9.6	5.3	10	0.15	12.2	0.10	8.1	1.49	
833	33.15	-0.10	74	5.1	33.13	-0.10	75.8	4.6	9	4.9	9.3	5.1	-8	0.10	8.6	0.10	8.6	1.42	
834	33.15	-0.05	24	5.7	33.15	-0.09	24.1	5.0	6	1.7	12.5	7.1	-2	0.05	1.5	0.25	7.4	0.35	
835	33.20	-0.15	95	5.1	33.20	-0.15	95.0	4.9	3	7.1	7.1	4.7	-18	0.05	6.2	0.05	6.2	0.81	TANG.
836	33.25	-0.05	75	5.5	33.27	-0.04	75.9	4.6	7	5.0	9.3	5.1	-3	0.10	8.7	0.10	8.7	1.07	
837	33.30	0.10	69	5.2	33.30	0.12	69.4	4.4	8	4.5	9.7	5.3	9	0.05	3.9	0.10	7.9	1.48	
838	33.30	0.25	24	10.8	33.30	0.20	24.3	8.0	7	1.7	12.5	7.1	6	0.05	1.5	0.15	4.5	0.61	

© American Astronomical Society • Provided by the NASA Astrophysics Data System

TABLE 1—*Continued*

CLOUD	l_p °	b_p °	v_p	T_p K	<l> °	<b> °	<v> km s^{-1}	<T> K		d_N kpc	d_F kpc	R kpc	<z> pc	Δl °	ΔL pc	Δb °	ΔB pc	σ_v km s^{-1}	NOTES
(1)	(2)	(3)	(4)	(5)	(6)	(7)	(8)	(9)		(11)	(12)	(13)	(14)	(15)	(16)	(17)	(18)	(19)	(20)
A	33.30	0.25	24	10.8	33.30	0.21	24.2	9.4	4				6	0.05	1.5	0.15	4.5	0.43	
839	33.30	0.35	24	6.6	33.30	0.37	24.4	5.7	4	1.7	12.5	7.1	11	0.05	1.5	0.10	3.0	0.50	
840	33.35	-0.55	92	6.7	33.42	-0.57	91.4	4.8	38	6.4	7.8	4.7	-63	0.35	39.2	0.30	33.6	1.06	TANG.
841	33.35	0.20	86	7.6	33.39	0.15	83.7	4.9	18	5.6	8.6	4.9	14	0.15	14.5	0.15	14.5	1.49	
842	33.40	-0.40	91	5.4	33.40	-0.37	89.9	4.9	13	6.2	8.0	4.8	-39	0.15	16.2	0.10	10.8	1.17	TANG.
843	33.40	-0.30	49	6.3	33.40	-0.30	48.1	5.4	5	3.2	11.0	6.1	-16	0.05	2.8	0.05	2.8	1.37	
844	33.40	0.00	75	13.3	33.43	0.01	72.7	5.8	36	4.7	9.4	5.2	0	0.30	24.9	0.15	12.4	2.24	
A	33.40	0.00	75	13.3	33.40	0.00	74.5	10.8	6				0	0.05	4.1	0.05	4.1	1.58	
845	33.45	-0.10	51	6.0	33.45	-0.10	50.2	5.0	5	3.3	10.9	6.0	-5	0.05	2.9	0.05	2.9	1.37	
846	33.45	-0.10	87	7.3	33.46	-0.13	86.6	4.9	51	5.8	8.3	4.9	-13	0.25	25.5	0.25	25.5	1.59	
847	33.50	-0.20	55	7.1	33.50	-0.20	52.2	4.8	20	3.4	10.7	5.9	-12	0.15	9.0	0.15	9.0	2.54	
848	33.50	0.15	68	10.7	33.49	0.15	67.8	6.7	8	4.4	9.8	5.4	11	0.10	7.7	0.10	7.7	1.11	
A	33.50	0.15	68	10.7	33.50	0.15	67.9	9.7	3				11	0.05	3.9	0.05	3.9	0.79	
849	33.60	-0.30	53	5.0	33.64	-0.28	52.7	4.3	6	3.5	10.7	5.9	-17	0.15	9.0	0.10	6.0	0.47	
850	33.60	0.00	88	6.2	33.64	0.04	83.3	4.8	31	5.6	8.6	4.9	3	0.25	24.2	0.15	14.5	2.09	
851	33.60	0.15	93	5.0	33.60	0.16	92.7	4.6	4	6.9	7.3	4.7	19	0.05	6.0	0.10	12.0	0.81	TANG.
852	33.65	0.20	42	6.1	33.66	0.21	41.8	4.9	21	2.8	11.4	6.4	10	0.25	12.1	0.15	7.3	1.17	
853	33.70	-0.80	93	5.1	33.70	-0.80	93.0	4.6	3	7.1	7.1	4.7	-98	0.05	6.2	0.05	6.2	0.80	TANG.
854	33.70	0.30	39	5.5	33.71	0.30	38.3	5.0	6	2.6	11.6	6.5	13	0.10	4.5	0.05	2.2	1.46	
855	33.75	-0.25	12	5.0	33.75	-0.27	11.8	4.5	5	1.0	13.2	7.7	-4	0.05	0.8	0.20	3.4	0.39	
856	33.75	0.10	93	5.5	33.74	0.10	93.3	4.8	4	7.1	7.1	4.7	12	0.10	12.3	0.05	6.2	0.80	TANG.
857	33.75	0.20	93	5.2	33.75	0.20	93.0	4.9	3	7.1	7.1	4.7	24	0.05	6.2	0.05	6.2	0.80	TANG.
858	33.75	0.25	55	5.9	33.74	0.24	55.6	4.8	11	3.6	10.5	5.8	14	0.10	6.4	0.15	9.5	0.86	
859	33.80	-0.20	48	7.2	33.79	-0.19	50.9	5.3	21	3.3	10.8	6.0	-10	0.10	5.8	0.15	8.8	2.34	
860	33.85	0.00	61	5.7	33.85	0.00	61.5	5.1	4	4.0	10.1	5.6	0	0.05	3.5	0.05	3.5	1.07	
861	33.85	0.00	89	6.5	33.87	0.02	89.1	4.8	39	6.2	7.9	4.8	1	0.30	32.5	0.20	21.6	1.42	TANG.
862	33.90	0.10	106	9.5	33.61	0.01	105.0	5.4	297	7.1	7.1	4.7	1	0.85	105.0	0.35	43.2	2.78	TANG.
A	33.90	0.10	106	9.5	33.90	0.10	107.0	8.7	5				12	0.05	6.2	0.05	6.2	1.38	
863	33.95	-0.25	89	6.3	33.95	-0.25	89.1	5.4	3	6.2	7.9	4.8	-27	0.05	5.4	0.05	5.4	0.78	TANG.
864	34.05	0.10	34	7.4	34.04	0.10	35.6	5.4	11	2.4	11.7	6.7	4	0.10	4.1	0.15	6.2	1.36	
865	34.10	-0.25	39	5.3	34.14	-0.23	38.6	4.7	11	2.6	11.5	6.5	-10	0.15	6.7	0.10	4.5	0.64	
866	34.10	0.45	34	7.1	34.10	0.45	34.5	5.8	6	2.3	11.8	6.7	18	0.05	2.0	0.05	2.0	1.56	
867	34.15	-0.10	89	6.9	34.18	-0.12	88.6	5.1	25	6.2	7.9	4.8	-13	0.20	21.7	0.20	21.7	1.37	TANG.
868	34.20	0.00	46	5.1	34.20	0.00	45.9	4.6	3	3.0	11.0	6.2	0	0.05	2.6	0.05	2.6	0.79	
869	34.20	0.10	43	5.4	34.20	0.10	43.5	5.0	4	2.9	11.2	6.3	5	0.05	2.5	0.05	2.5	1.00	
870	34.25	-0.25	91	5.7	34.25	-0.27	90.4	5.0	5	6.6	7.4	4.8	-30	0.05	5.8	0.10	11.5	0.99	TANG.
871	34.25	-0.05	47	5.9	34.26	-0.07	44.6	4.7	11	2.9	11.1	6.3	-3	0.10	5.1	0.10	5.1	1.99	
872	34.25	0.05	40	6.0	34.23	0.03	39.2	4.7	15	2.6	11.5	6.5	1	0.10	4.5	0.10	4.5	1.60	
873	34.25	0.10	53	8.3	34.13	0.05	56.7	4.9	100	3.7	10.4	5.8	3	0.45	29.1	0.30	19.4	2.38	
874	34.25	0.20	62	6.3	34.24	0.17	62.6	4.7	13	4.1	10.0	5.6	12	0.15	10.7	0.10	7.1	1.07	
875	34.35	-0.85	13	5.4	34.32	-0.66	13.0	4.4	178	1.0	13.0	7.7	-11	0.55	9.8	0.80	14.3	0.74	NEAR
876	34.40	-0.55	43	5.1	34.40	-0.58	43.5	4.6	4	2.9	11.2	6.3	-28	0.05	2.5	0.10	5.0	0.50	
877	34.40	-0.20	53	6.4	34.36	-0.21	52.5	4.7	34	3.4	10.6	6.0	-12	0.40	24.0	0.20	12.0	1.34	
878	34.40	-0.05	37	5.5	34.39	-0.06	38.1	4.6	15	2.5	11.5	6.6	-2	0.10	4.4	0.15	6.6	2.39	
879	34.40	0.00	45	5.2	34.36	0.00	46.3	4.7	6	3.0	11.0	6.2	0	0.15	8.0	0.05	2.7	0.95	
880	34.45	-0.90	44	7.3	34.45	-0.91	44.5	5.3	15	2.9	11.1	6.3	-46	0.10	5.1	0.30	15.3	0.87	
881	34.45	0.00	90	7.7	34.43	0.03	89.5	5.4	12	6.5	7.6	4.8	3	0.10	11.3	0.15	16.9	1.06	TANG.
882	34.45	0.25	60	6.3	34.45	0.25	59.9	5.7	3	3.9	10.1	5.7	17	0.05	3.4	0.05	3.4	0.79	
883	34.50	0.05	47	6.5	34.50	0.04	48.0	5.2	16	3.2	10.9	6.2	2	0.15	8.3	0.10	5.5	1.25	
884	34.55	-0.10	96	5.1	34.57	-0.07	96.1	4.5	6	7.0	7.0	4.8	-8	0.10	12.2	0.10	12.2	0.67	TANG.
885	34.60	-0.40	55	5.9	34.58	-0.41	55.8	4.8	7	3.7	10.3	5.9	-25	0.10	6.4	0.10	6.4	0.98	
886	34.65	-0.85	37	5.0	34.63	-0.92	36.7	4.6	10	2.4	11.5	6.6	-38	0.10	4.3	0.15	6.4	0.89	
887	34.65	-0.80	55	7.2	34.50	-0.78	56.7	4.7	227	3.7	10.3	5.8	-50	0.75	48.6	0.60	38.9	2.25	
888	34.65	0.10	96	5.0	34.62	0.09	96.2	4.6	6	7.0	7.0	4.8	11	0.10	12.2	0.10	12.2	0.68	TANG.
889	34.70	-0.50	82	10.1	34.68	-0.50	82.5	6.4	7	5.6	8.4	5.0	-48	0.10	9.8	0.05	4.9	0.98	
890	34.70	-0.10	85	6.8	34.70	-0.10	85.0	5.8	3	5.9	8.1	5.0	-10	0.05	5.1	0.05	5.1	0.78	TANG.
891	34.75	0.10	52	6.1	34.74	0.08	52.4	4.7	10	3.4	10.5	6.0	4	0.10	6.0	0.10	6.0	0.99	
892	34.80	-0.15	76	6.8	34.66	-0.15	77.6	4.6	92	5.2	8.8	5.2	-13	0.35	31.6	0.35	31.6	1.99	
893	34.80	0.15	53	5.3	34.80	0.15	53.5	4.8	4	3.5	10.5	6.0	9	0.05	3.1	0.05	3.1	1.10	
894	34.80	0.35	60	7.6	34.80	0.35	60.4	6.2	4	4.0	10.0	5.7	24	0.05	3.5	0.05	3.5	1.03	

© American Astronomical Society • Provided by the NASA Astrophysics Data System

TABLE 1—*Continued*

CLOUD	l_p °	b_p °	v_p	T_p K	<l> °	<b> °	<v> km s^{-1}	<T> K	N	d_N kpc	d_F kpc	R kpc	<z> pc	Δl °	ΔL pc	Δb °	ΔB pc	σ_v km s^{-1}	NOTES
(1)	(2)	(3)	(4)	(5)	(6)	(7)	(8)	(9)	(10)	(11)	(12)	(13)	(14)	(15)	(16)	(17)	(18)	(19)	(20)
895	34.85	-0.05	49	5.8	34.85	-0.05	49.1	5.2	3	3.2	10.7	6.1	-2	0.05	2.8	0.05	2.8	0.79	
896	34.90	0.65	45	6.3	34.81	0.62	45.7	4.5	25	3.0	11.0	6.3	32	0.25	13.1	0.15	7.9	0.87	
897	34.95	0.05	14	5.1	34.95	0.09	13.8	4.4	4	1.1	12.9	7.6	1	0.05	0.9	0.15	2.8	0.42	
898	34.95	0.20	57	5.1	34.96	0.24	57.4	4.4	27	3.8	10.2	5.8	15	0.25	16.4	0.20	13.1	0.88	
899	35.05	0.30	51	13.8	34.93	-0.24	46.0	5.3	1728	3.0	10.9	6.3	-12	1.15	60.6	1.80	94.9	3.91	NEAR
A	34.70	-0.70	46	10.0	34.70	-0.68	46.5	8.8	4				-35	0.05	2.6	0.10	5.3	0.50	
B	35.05	0.30	51	13.8	35.01	0.33	51.6	9.8	16				17	0.15	7.9	0.10	5.3	1.09	
C	35.15	-0.65	47	9.3	35.15	-0.65	48.0	9.1	3				-34	0.05	2.6	0.05	2.6	0.81	
900	35.15	-0.75	35	22.3	35.23	-0.81	34.8	6.2	358	2.3	11.6	6.7	-32	0.80	32.3	0.55	22.2	2.36	
A	35.15	-0.75	35	22.3	35.17	-0.75	34.3	11.6	50				-30	0.30	12.1	0.15	6.0	2.24	
901	35.15	0.80	74	9.6	35.15	0.79	73.9	6.6	7	4.9	9.0	5.3	67	0.05	4.3	0.10	8.6	1.15	NEAR
902	35.20	-0.55	52	5.1	35.22	-0.55	51.4	4.8	3	3.4	10.5	6.1	-32	0.10	5.9	0.05	2.9	0.48	
903	35.20	-0.20	51	8.2	35.18	-0.21	50.6	5.6	6	3.3	10.6	6.1	-11	0.15	8.7	0.10	5.8	0.77	
904	35.20	0.10	14	6.3	35.28	0.00	13.1	4.6	272	1.0	12.8	7.7	0	0.55	9.9	1.25	22.5	0.93	NEAR
905	35.25	-0.10	57	5.4	35.25	-0.10	57.0	5.0	3	3.7	10.1	5.9	-6	0.05	3.3	0.05	3.3	0.80	
906	35.25	-0.10	61	5.7	35.26	-0.13	61.6	5.0	7	4.0	9.8	5.7	-9	0.15	10.6	0.10	7.0	0.50	
907	35.25	0.45	92	5.9	35.27	0.45	92.2	4.8	5	6.9	6.9	4.9	54	0.10	12.1	0.05	6.1	0.72	TANG.
908	35.30	0.80	80	9.7	35.30	0.80	79.9	7.8	3	5.4	8.4	5.1	75	0.05	4.7	0.05	4.7	0.76	
909	35.35	-0.80	44	5.7	35.35	-0.85	44.3	4.6	14	2.9	11.0	6.4	-43	0.15	7.6	0.20	10.1	0.57	
910	35.35	-0.70	13	5.3	35.34	-0.71	13.0	4.3	10	1.0	12.8	7.7	-12	0.10	1.8	0.15	2.7	0.76	
911	35.35	0.35	94	9.6	35.37	0.39	93.7	5.4	13	6.9	6.9	4.9	46	0.10	12.1	0.15	18.1	1.08	TANG.
912	35.40	-0.20	50	5.2	35.40	-0.20	50.0	4.8	3	3.3	10.6	6.1	-11	0.05	2.9	0.05	2.9	0.80	
913	35.40	0.00	94	6.2	35.36	0.00	93.6	4.9	12	6.9	6.9	4.9	0	0.15	18.1	0.15	18.1	1.02	TANG.
914	35.40	0.25	75	5.3	35.40	0.25	75.9	4.8	5	5.1	8.8	5.3	22	0.05	4.4	0.05	4.4	1.38	
915	35.40	1.00	76	5.6	35.37	1.00	77.1	5.0	6	5.2	8.7	5.2	90	0.10	9.1	0.05	4.5	1.04	NEAR
916	35.45	-1.05	41	5.2	35.42	-1.02	41.0	4.4	8	2.7	11.2	6.5	-48	0.10	4.7	0.15	7.1	0.68	
917	35.45	0.25	49	7.3	35.43	0.26	49.7	5.0	18	3.3	10.6	6.1	14	0.20	11.4	0.10	5.7	2.22	
918	35.50	-0.05	52	6.9	35.52	-0.03	52.3	4.9	74	3.4	10.4	6.0	-1	0.30	17.9	0.30	17.9	2.68	
919	35.50	0.00	61	7.1	35.50	0.00	60.5	5.9	4	4.0	9.9	5.7	0	0.05	3.5	0.05	3.5	1.04	
920	35.50	0.15	14	5.0	35.52	0.15	13.9	4.4	8	1.1	12.8	7.7	2	0.15	2.8	0.15	2.8	0.77	
921	35.55	0.65	12	5.3	35.56	0.63	12.2	4.2	8	1.0	12.9	7.7	10	0.10	1.7	0.25	4.3	0.43	NEAR
922	35.65	-0.25	28	6.2	35.61	-0.25	28.4	4.8	13	1.9	11.9	7.0	-8	0.25	8.4	0.15	5.0	0.49	
923	35.65	0.40	101	5.2	35.66	0.40	100.4	4.6	5	6.9	6.9	5.0	48	0.10	12.1	0.05	6.0	0.99	TANG.
924	35.70	-0.90	57	14.1	35.70	-0.93	57.7	7.4	10	3.8	10.0	5.9	-61	0.10	6.6	0.15	9.9	0.96	
A	35.70	-0.90	57	14.1	35.70	-0.90	57.0	11.7	3				-59	0.05	3.3	0.05	3.3	0.77	
925	35.70	-0.20	56	9.8	35.71	-0.20	57.5	4.8	158	3.8	10.0	5.9	-13	0.85	56.0	0.35	23.0	2.44	
926	35.70	-0.05	50	6.7	35.70	-0.04	48.8	5.0	10	3.2	10.6	6.2	-2	0.10	5.6	0.15	8.4	1.43	
927	35.75	-0.85	57	6.7	35.75	-0.85	57.0	5.3	3	3.7	10.1	5.9	-55	0.05	3.3	0.05	3.3	0.76	
928	35.75	0.15	82	8.5	35.40	0.15	79.1	4.7	239	5.4	8.5	5.2	14	0.80	75.1	0.30	28.2	2.99	
929	35.75	0.20	29	6.0	35.75	0.21	29.1	4.9	14	2.0	11.8	7.0	7	0.25	8.6	0.20	6.9	0.49	
930	35.80	-0.90	59	6.0	35.80	-0.87	59.3	5.3	3	3.9	9.9	5.8	-59	0.05	3.4	0.10	6.8	0.47	
931	35.80	-0.20	29	7.8	36.15	-0.09	29.3	5.1	109	2.0	11.8	7.0	-3	0.90	31.0	0.40	13.8	1.14	
932	35.80	0.35	80	5.4	35.79	0.34	80.3	4.6	7	5.5	8.2	5.2	32	0.10	9.7	0.10	9.7	0.71	
933	35.95	-0.50	58	10.5	36.00	-0.41	57.9	5.0	87	3.8	10.0	5.9	-26	0.35	23.2	0.35	23.2	1.91	
A	35.95	-0.50	58	10.5	35.97	-0.50	58.6	9.1	3				-33	0.10	6.6	0.05	3.3	0.49	
934	35.95	0.30	80	6.0	35.95	0.28	80.2	5.1	5	5.6	8.2	5.2	27	0.05	4.9	0.10	9.7	0.74	
935	36.00	0.40	80	5.1	36.01	0.39	80.5	4.6	10	5.6	8.1	5.2	38	0.10	9.8	0.15	14.7	1.01	
936	36.00	0.70	81	5.5	35.99	0.67	80.1	4.6	10	5.6	8.2	5.2	65	0.10	9.7	0.20	19.4	1.48	
937	36.05	-0.15	39	5.1	36.03	-0.15	39.5	4.5	4	2.6	11.2	6.6	-6	0.10	4.5	0.05	2.3	0.50	
938	36.10	-0.80	29	5.3	36.09	-0.78	29.3	4.4	7	2.0	11.8	7.0	-26	0.15	5.2	0.15	5.2	0.45	
939	36.10	0.10	75	5.2	36.10	0.10	74.0	4.6	5	5.0	8.7	5.3	8	0.05	4.4	0.05	4.4	1.37	
940	36.10	0.65	77	11.5	36.13	0.66	75.5	5.1	85	5.1	8.6	5.3	58	0.30	26.9	0.40	35.8	2.04	
941	36.15	-0.35	87	6.4	36.15	-0.35	86.9	5.7	3	6.9	6.9	5.0	-41	0.05	6.0	0.05	6.0	0.79	TANG.
942	36.25	-0.10	81	5.1	36.25	-0.10	81.0	4.6	3	5.7	8.0	5.2	-9	0.05	5.0	0.05	5.0	0.79	
943	36.35	0.65	76	5.9	36.35	0.67	74.4	4.6	8	5.1	8.6	5.3	58	0.05	4.4	0.10	8.8	1.60	
944	36.40	-0.10	69	5.6	36.40	-0.11	69.3	4.8	6	4.6	9.0	5.5	-8	0.05	4.0	0.20	16.2	0.47	
945	36.40	-0.10	52	8.9	36.49	-0.11	54.2	5.0	609	3.6	10.1	6.0	-6	1.15	71.3	0.85	52.7	2.34	NEAR
946	36.40	0.85	71	6.1	36.38	0.88	71.1	4.9	12	4.8	8.9	5.4	72	0.10	8.3	0.20	16.7	0.73	NEAR
947	36.45	0.95	43	5.2	36.42	0.95	42.5	4.5	7	2.8	10.9	6.5	46	0.10	4.9	0.15	7.3	0.71	NEAR
948	36.50	-0.40	11	5.6	36.50	-0.38	11.5	4.9	4	0.9	12.7	7.8	-6	0.05	0.8	0.10	1.6	0.50	

© American Astronomical Society • Provided by the NASA Astrophysics Data System

TABLE 1—*Continued*

CLOUD (1)	l_p ° (2)	b_p ° (3)	v_p (4)	T_p K (5)	<l> ° (6)	<b> ° (7)	<v> km s^{-1} (8)	<T> K (9)	N (10)	d_N kpc (11)	d_P kpc (12)	R kpc (13)	<z> pc (14)	Δl ° (15)	ΔL pc (16)	Δb ° (17)	ΔB pc (18)	σ_v km s^{-1} (19)	NOTES (20)
949	36.50	-0.15	77	9.9	36.74	-0.22	79.3	5.2	410	5.6	8.0	5.2	-21	0.80	78.1	0.65	63.4	2.34	
950	36.50	0.15	71	5.0	36.48	0.15	71.0	4.6	4	4.8	8.9	5.5	12	0.10	8.3	0.05	4.2	0.71	
951	36.55	-0.05	61	5.4	36.56	-0.05	60.3	4.8	5	4.0	9.7	5.8	-3	0.10	6.9	0.05	3.5	1.14	
952	36.65	-0.60	56	5.6	36.65	-0.60	56.0	4.9	3	3.7	10.0	6.0	-38	0.05	3.2	0.05	3.2	0.79	
953	36.70	0.10	60	7.4	36.66	0.09	60.3	5.0	19	4.0	9.7	5.8	6	0.20	13.9	0.15	10.4	1.23	
954	36.75	-0.35	59	5.0	36.75	-0.37	59.5	4.5	4	3.9	9.7	5.8	-25	0.05	3.4	0.10	6.8	0.50	
955	36.85	0.70	44	5.3	36.83	0.70	44.5	4.9	4	2.9	10.7	6.4	35	0.10	5.1	0.05	2.5	0.50	NEAR
956	36.90	-0.50	58	6.3	36.90	-0.54	58.8	5.0	12	3.9	9.7	5.9	-36	0.05	3.4	0.15	10.1	1.31	
957	36.90	0.15	58	7.2	36.90	0.15	58.0	6.1	3	3.8	9.8	5.9	10	0.05	3.3	0.05	3.3	0.78	
958	36.95	0.35	89	6.4	36.92	0.36	88.6	5.0	5	6.8	6.8	5.1	42	0.10	11.9	0.10	11.9	0.48	TANG.
959	37.00	-0.35	81	5.3	37.00	-0.35	81.0	4.7	3	5.9	7.7	5.2	-35	0.05	5.1	0.05	5.1	0.79	TANG.
960	37.05	-0.75	48	6.1	37.05	-0.73	48.2	5.4	5	3.2	10.4	6.3	-40	0.05	2.8	0.10	5.5	0.73	
961	37.05	-0.20	82	5.1	37.05	-0.20	82.5	4.6	4	6.2	7.4	5.2	-21	0.05	5.4	0.05	5.4	1.00	TANG.
962	37.10	-0.25	77	5.3	37.10	-0.25	77.1	4.7	3	5.4	8.2	5.3	-23	0.05	4.7	0.05	4.7	0.79	
963	37.15	-0.35	42	6.8	37.17	-0.35	42.2	5.1	5	2.8	10.8	6.5	-16	0.10	4.8	0.05	2.4	0.74	
964	37.20	0.30	89	6.1	37.20	0.31	88.9	5.0	4	6.8	6.8	5.1	36	0.05	5.9	0.10	11.8	0.69	TANG.
965	37.25	-0.25	42	7.5	37.27	-0.24	38.4	5.5	14	2.5	11.0	6.7	-10	0.10	4.4	0.10	4.4	2.45	
966	37.25	0.10	92	6.0	37.26	0.09	91.7	4.7	13	6.8	6.8	5.1	11	0.15	17.7	0.10	11.8	1.19	TANG.
967	37.30	-0.10	47	7.1	37.30	-0.10	46.5	6.1	4	3.0	10.5	6.4	-5	0.05	2.7	0.05	2.7	1.06	
968	37.35	0.25	88	6.5	37.48	0.16	86.0	4.7	143	6.7	6.7	5.2	18	0.40	47.1	0.55	64.7	2.26	TANG.
969	37.45	-0.05	57	9.8	37.42	-0.04	56.5	6.5	17	3.7	9.8	6.0	-2	0.20	13.0	0.10	6.5	1.34	
970	37.45	0.10	41	9.3	37.51	0.07	41.8	6.3	35	2.7	10.7	6.5	3	0.20	9.6	0.25	11.9	1.34	
971	37.55	-0.10	53	9.9	37.55	-0.10	52.8	7.9	7	3.5	10.0	6.1	-6	0.05	3.0	0.05	3.0	1.78	
A	37.55	-0.10	53	9.9	37.55	-0.10	52.5	9.4	4				-6	0.05	3.0	0.05	3.0	1.10	
972	37.60	0.00	64	5.6	37.55	0.06	63.7	4.5	9	4.3	9.2	5.7	4	0.15	11.1	0.15	11.1	0.47	
973	37.65	-0.65	54	5.1	37.65	-0.65	54.0	4.6	3	3.6	9.9	6.1	-40	0.05	3.1	0.05	3.1	0.79	
974	37.65	-0.40	19	5.3	37.67	-0.40	18.4	4.4	5	1.3	12.1	7.5	-9	0.10	2.3	0.05	1.2	1.01	
975	37.65	-0.05	40	7.2	37.66	-0.05	39.5	5.5	7	2.6	10.9	6.6	-2	0.15	6.8	0.05	2.3	0.84	
976	37.65	0.30	46	5.9	37.65	0.30	45.5	5.4	4	3.0	10.5	6.4	15	0.05	2.6	0.05	2.6	1.09	
977	37.65	0.40	87	5.1	37.65	0.40	87.0	4.5	3	6.7	6.7	5.2	46	0.05	5.9	0.05	5.9	0.79	TANG.
978	37.70	-0.70	57	6.0	37.70	-0.70	56.9	5.1	5	3.8	9.7	6.0	-45	0.05	3.3	0.05	3.3	1.35	
979	37.75	-0.70	45	5.3	37.75	-0.70	45.5	4.7	4	3.0	10.5	6.4	-36	0.05	2.6	0.05	2.6	1.10	
980	37.75	-0.25	48	8.0	37.72	-0.27	48.2	5.1	21	3.2	10.3	6.3	-15	0.10	5.5	0.15	8.3	2.17	
981	37.75	-0.20	60	8.0	37.78	-0.31	62.6	4.8	53	4.2	9.3	5.8	-22	0.15	11.0	0.35	25.6	3.57	
982	37.75	0.10	94	5.3	37.76	0.11	92.8	4.6	9	6.7	6.7	5.2	12	0.15	17.6	0.10	11.7	1.30	TANG.
983	37.75	0.20	45	10.5	37.75	0.22	46.2	7.5	8	3.0	10.4	6.4	11	0.05	2.6	0.10	5.3	1.29	
984	37.80	-0.10	46	7.8	37.76	-0.10	46.2	6.1	10	3.0	10.4	6.4	-5	0.15	7.9	0.05	2.6	1.23	
985	37.80	0.75	37	7.1	37.80	0.75	37.0	5.9	3	2.4	11.0	6.7	31	0.05	2.1	0.05	2.1	0.77	NEAR
986	37.85	-0.65	51	5.4	37.85	-0.64	51.6	4.6	3	3.4	10.0	6.2	-37	0.05	3.0	0.10	5.9	0.49	
987	37.90	-0.60	57	6.3	37.87	-0.60	57.5	5.1	12	3.8	9.6	6.0	-39	0.10	6.6	0.05	3.3	1.78	
988	37.90	-0.40	61	6.0	37.90	-0.40	60.6	5.2	4	4.0	9.4	5.9	-28	0.05	3.5	0.05	3.5	1.06	
989	37.90	0.05	91	5.0	37.91	0.06	89.8	4.5	13	6.7	6.7	5.2	7	0.15	17.6	0.15	17.6	2.00	TANG.
990	37.95	-0.10	54	5.9	37.93	-0.08	54.0	5.0	13	3.6	9.9	6.1	-5	0.10	6.2	0.10	6.2	2.18	
991	38.00	0.05	81	5.1	38.00	0.07	81.5	4.7	6	6.7	6.7	5.2	7	0.05	5.8	0.10	11.7	0.95	TANG.
992	38.05	0.15	43	5.9	38.10	0.17	42.8	4.9	16	2.8	10.6	6.5	8	0.15	7.4	0.15	7.4	0.86	
993	38.15	-0.30	82	6.2	38.15	-0.27	81.8	4.8	7	6.7	6.7	5.3	-31	0.05	5.8	0.15	17.5	1.23	TANG.
994	38.20	0.75	37	5.5	38.20	0.77	37.5	4.8	4	2.5	10.9	6.7	33	0.05	2.2	0.10	4.3	0.50	NEAR
995	38.20	0.75	11	8.1	38.19	0.83	11.0	5.5	5	0.9	12.5	7.8	13	0.10	1.6	0.20	3.2	0.00	NEAR
996	38.25	-0.15	65	7.4	38.25	-0.18	64.4	5.0	36	4.3	9.0	5.8	-13	0.25	19.0	0.15	11.4	2.89	
997	38.25	0.20	36	8.2	38.25	0.18	36.3	5.9	5	2.4	11.0	6.8	7	0.05	2.1	0.10	4.2	0.70	
998	38.30	-0.20	52	9.9	38.30	-0.20	52.1	7.5	5	3.4	9.9	6.2	-11	0.05	3.0	0.05	3.0	1.26	
999	38.30	1.00	44	7.1	38.30	0.99	44.3	6.5	3	2.9	10.4	6.5	50	0.05	2.5	0.10	5.1	0.48	NEAR
1000	38.35	-0.95	18	5.8	38.35	-0.95	18.0	5.3	3	1.3	12.0	7.5	-21	0.05	1.1	0.05	1.1	0.79	
1001	38.40	-0.15	52	5.5	38.40	-0.15	52.9	5.2	5	3.5	9.8	6.2	-9	0.05	3.0	0.05	3.0	1.39	
1002	38.40	0.15	24	6.0	38.44	0.15	23.2	4.7	7	1.6	11.7	7.3	4	0.15	4.2	0.05	1.4	0.95	
1003	38.50	-0.50	77	5.1	38.50	-0.48	76.5	4.8	4	5.6	7.7	5.4	-46	0.05	4.9	0.10	9.8	0.50	TANG.
1004	38.50	0.85	11	12.8	38.50	0.86	10.8	7.7	3	0.9	12.4	7.8	13	0.05	0.8	0.10	1.6	0.39	NEAR
1005	38.60	-0.20	67	6.5	38.60	-0.20	67.0	5.3	5	4.6	8.7	5.7	-16	0.05	4.0	0.05	4.0	1.30	
1006	38.60	0.90	46	5.8	38.60	0.87	45.4	4.9	6	3.0	10.3	6.4	45	0.05	2.6	0.10	5.2	0.95	NEAR
1007	38.65	0.05	36	5.9	38.67	0.05	35.6	4.9	4	2.3	10.9	6.8	2	0.10	4.1	0.05	2.0	0.50	

© American Astronomical Society • Provided by the NASA Astrophysics Data System

TABLE 1—*Continued*

CLOUD	l_p	b_p	v_p	T_p	<l>	<b>	<v>	<T>	N	d_N	d_F	R	<z>	Δl	ΔL	Δb	ΔB	σ_v	NOTES
	°	°		K	°	°	km s^{-1}	K		kpc	kpc	kpc	pc	°	pc	°	pc	km s^{-1}	
(1)	(2)	(3)	(4)	(5)	(6)	(7)	(8)	(9)	(10)	(11)	(12)	(13)	(14)	(15)	(16)	(17)	(18)	(19)	(20)
1008	38.65	0.95	45	5.7	38.66	0.97	43.6	5.0	7	2.9	10.4	6.5	48	0.10	5.0	0.10	5.0	0.93	NEAR
1009	38.70	-0.45	49	7.9	38.70	-0.45	49.4	6.1	6	3.3	10.0	6.3	-25	0.05	2.8	0.05	2.8	1.57	
1010	38.75	-0.50	66	7.3	38.76	-0.49	65.6	5.2	6	4.5	8.8	5.7	-38	0.10	7.8	0.10	7.8	0.92	
1011	38.85	-0.45	61	5.3	38.85	-0.47	60.5	4.5	5	4.1	9.2	5.9	-33	0.05	3.5	0.10	7.1	1.00	
1012	38.85	-0.20	65	5.1	38.88	-0.19	66.6	4.5	14	4.6	8.7	5.7	-14	0.10	8.0	0.10	8.0	1.96	
1013	38.85	0.05	41	5.6	38.88	0.07	40.5	4.6	6	2.7	10.6	6.6	3	0.10	4.6	0.10	4.6	0.50	
1014	38.90	-0.80	82	7.0	38.90	-0.80	82.0	5.5	3	6.6	6.6	5.3	-92	0.05	5.8	0.05	5.8	0.76	TANG.
1015	38.95	-1.05	51	10.1	38.94	-1.03	50.8	6.2	7	3.4	9.9	6.3	-60	0.10	5.9	0.10	5.9	0.69	
1016	38.95	-0.85	72	5.1	38.95	-0.85	72.0	4.5	3	5.1	8.1	5.5	-75	0.05	4.5	0.05	4.5	0.79	
1017	38.95	-0.45	59	5.2	38.96	-0.45	59.1	4.5	7	4.0	9.2	6.0	-31	0.10	6.9	0.05	3.5	1.20	
1018	38.95	-0.45	42	16.3	38.92	-0.43	41.8	6.1	172	2.7	10.5	6.6	-20	0.45	21.6	0.55	26.4	2.09	
A	38.95	-0.45	42	16.3	38.93	-0.40	40.7	11.7	20				-19	0.10	4.8	0.20	9.6	1.36	
1019	39.05	-0.80	84	5.8	39.03	-0.80	83.1	5.3	4	6.6	6.6	5.4	-92	0.10	11.5	0.05	5.8	0.68	TANG.
1020	39.10	-0.25	48	6.1	39.09	-0.25	48.3	5.0	11	3.2	10.0	6.4	-13	0.15	8.3	0.05	2.8	1.29	
1021	39.15	0.50	28	5.1	39.17	0.50	28.6	4.6	3	1.9	11.3	7.1	16	0.10	3.4	0.05	1.7	0.48	
1022	39.25	-0.60	64	5.1	39.27	-0.59	64.1	4.5	8	4.4	8.8	5.8	-45	0.10	7.7	0.10	7.7	0.78	
1023	39.25	-0.05	22	11.2	39.24	-0.07	21.6	6.4	19	1.5	11.7	7.4	-1	0.20	5.3	0.10	2.6	1.91	
A	39.25	-0.05	22	11.2	39.25	-0.05	21.5	10.4	4				-1	0.05	1.3	0.05	1.3	1.09	
1024	39.30	-0.40	69	5.6	39.30	-0.42	69.3	5.0	3	4.9	8.3	5.6	-35	0.05	4.3	0.10	8.5	0.47	
1025	39.40	-0.15	66	5.9	39.40	-0.15	66.0	5.0	3	4.6	8.6	5.8	-11	0.05	4.0	0.05	4.0	0.78	
1026	39.45	-0.55	63	5.3	39.45	-0.52	62.1	4.7	7	4.2	8.9	5.9	-38	0.05	3.7	0.10	7.4	1.22	
1027	39.50	-1.00	53	13.4	39.47	-0.99	53.2	7.8	19	3.5	9.6	6.2	-60	0.15	9.3	0.20	12.4	1.46	
A	39.50	-1.00	53	13.4	39.49	-1.00	53.1	11.5	7				-61	0.10	6.2	0.05	3.1	1.18	
1028	39.60	-0.95	53	9.7	39.60	-0.95	53.0	7.0	3	3.5	9.6	6.2	-58	0.05	3.1	0.05	3.1	0.73	
1029	39.60	-0.20	71	5.7	39.60	-0.20	71.0	4.7	3	5.1	8.0	5.6	-17	0.05	4.5	0.05	4.5	0.77	
1030	39.60	-0.20	65	5.1	39.60	-0.20	64.7	4.5	7	4.5	8.6	5.8	-15	0.05	3.9	0.15	11.7	1.03	
1031	39.65	-0.90	54	6.9	39.67	-0.90	54.0	5.7	4	3.6	9.5	6.2	-56	0.10	6.3	0.05	3.1	0.71	
1032	39.65	-0.05	55	5.2	39.65	-0.05	55.5	4.6	4	3.7	9.4	6.1	-3	0.05	3.2	0.05	3.2	1.08	
1033	39.85	-0.20	57	8.2	39.84	-0.32	59.9	4.8	642	4.1	9.0	6.0	-22	1.40	99.6	0.70	49.8	3.75	
1034	39.90	-0.90	53	9.5	39.90	-0.90	53.2	7.0	3	3.5	9.5	6.2	-55	0.05	3.1	0.05	3.1	0.72	
1035	40.00	-0.45	69	6.2	40.00	-0.48	69.4	5.2	9	5.0	8.0	5.7	-42	0.05	4.3	0.25	21.7	0.49	
1036	40.00	-0.15	83	5.1	40.00	-0.12	83.2	4.7	5	6.5	6.5	5.5	-13	0.05	5.7	0.10	11.4	0.73	TANG.
1037	40.15	-0.95	50	6.3	40.17	-0.95	50.6	5.2	3	3.4	9.6	6.3	-55	0.10	5.9	0.05	2.9	0.49	
1038	40.25	-1.05	50	6.9	40.25	-1.03	50.2	5.5	5	3.3	9.6	6.3	-60	0.05	2.9	0.10	5.8	0.71	
1039	40.25	0.00	73	5.4	40.25	0.00	73.1	4.8	3	5.5	7.4	5.6	0	0.05	4.8	0.05	4.8	0.79	TANG.
1040	40.30	-0.45	74	7.9	40.37	-0.41	73.6	5.2	15	5.7	7.3	5.6	-40	0.20	19.8	0.15	14.8	0.98	TANG.
1041	40.30	-0.25	72	6.1	40.31	-0.26	71.8	5.0	13	5.3	7.6	5.6	-24	0.10	9.3	0.15	14.0	1.02	
1042	40.40	-0.10	58	5.1	40.40	-0.09	57.8	4.4	10	3.9	9.0	6.1	-5	0.05	3.4	0.10	6.9	1.90	
1043	40.40	0.00	71	6.4	40.40	0.00	71.9	5.5	5	5.4	7.6	5.6	0	0.05	4.7	0.05	4.7	1.34	
1044	40.40	0.80	32	5.3	40.42	0.80	32.5	4.8	4	2.2	10.8	7.0	30	0.10	3.8	0.05	1.9	0.50	NEAR
1045	40.45	-0.40	57	5.4	40.45	-0.40	57.0	4.7	3	3.9	9.1	6.1	-26	0.05	3.4	0.05	3.4	0.78	
1046	40.45	-0.05	70	6.6	40.45	-0.05	69.5	5.3	4	5.1	7.9	5.7	-4	0.05	4.4	0.05	4.4	1.02	
1047	40.55	-0.70	67	6.3	40.57	-0.68	67.1	5.1	13	4.8	8.1	5.8	-57	0.10	8.4	0.10	8.4	1.13	
1048	40.60	-0.10	65	5.4	40.60	-0.10	65.0	5.0	3	4.6	8.3	5.8	-8	0.05	4.0	0.05	4.0	0.80	
1049	40.70	-0.60	57	5.7	40.70	-0.60	57.0	5.4	3	3.9	9.0	6.1	-40	0.05	3.4	0.05	3.4	0.80	
1050	40.80	-0.20	23	6.0	40.80	-0.20	23.1	5.4	3	1.6	11.3	7.4	-5	0.05	1.4	0.05	1.4	0.79	
1051	40.85	-0.20	54	5.9	40.85	-0.20	54.0	5.0	3	3.6	9.2	6.2	-12	0.05	3.2	0.05	3.2	0.78	
1052	40.95	-0.55	59	6.2	40.93	-0.54	59.3	5.0	19	4.1	8.8	6.0	-38	0.20	14.3	0.10	7.1	1.62	
1053	41.00	-0.60	76	6.4	40.98	-0.60	76.4	5.1	5	6.4	6.4	5.6	-67	0.10	11.2	0.05	5.6	1.02	TANG.
1054	41.00	-0.20	38	6.0	41.07	-0.20	38.5	4.7	144	2.6	10.3	6.8	-8	0.30	13.4	0.55	24.5	1.30	
1055	41.00	0.75	40	6.1	41.03	0.76	39.2	4.9	18	2.6	10.2	6.8	34	0.20	9.1	0.15	6.8	1.19	NEAR
1056	41.05	-0.65	74	5.6	41.05	-0.66	75.3	4.7	7	6.4	6.4	5.6	-74	0.05	5.6	0.10	11.2	1.37	TANG.
1057	41.10	-0.40	53	5.7	41.10	-0.40	53.0	5.3	3	3.6	9.2	6.3	-25	0.05	3.1	0.05	3.1	0.80	
1058	41.15	-0.20	60	11.1	41.22	-0.22	60.4	5.4	216	4.2	8.6	6.0	-16	0.60	44.1	0.75	55.1	2.69	
A	41.05	-0.25	59	10.3	41.05	-0.25	59.5	9.3	4				-18	0.05	3.7	0.05	3.7	1.07	
B	41.15	-0.20	60	11.1	41.16	-0.22	59.7	9.2	9				-16	0.10	7.3	0.10	7.3	1.21	
1059	41.15	-0.15	50	5.3	41.15	-0.15	50.5	5.0	4	3.4	9.4	6.4	-8	0.05	3.0	0.05	3.0	1.09	
1060	41.15	-0.05	68	6.1	41.19	-0.05	67.5	4.7	13	4.9	7.9	5.8	-4	0.15	12.9	0.05	4.3	2.27	
1061	41.20	-0.55	76	6.2	41.20	-0.56	76.0	[illegible]	4	6.4	6.4	5.6	-62	0.05	5.6	0.10	11.2	0.65	TANG.
1062	41.20	-0.20	54	5.8	41.20	-0.18	54.2	[illegible]	6	3.7	9.1	6.2	-11	0.05	3.2	0.10	6.4	1.01	

© American Astronomical Society • Provided by the NASA Astrophysics Data System

TABLE 1—*Continued*

CLOUD	l_p	b_p	v_p	T_p	<l>	<b>	<v>	<T>	N	d_N	d_F	R	<z>	Δl	ΔL	Δb	ΔB	σ_v	NOTES
	°	°		K	°	°	km s^{-1}	K		kpc	kpc	kpc	pc	°	pc	°	pc	km s^{-1}	
(1)	(2)	(3)	(4)	(5)	(6)	(7)	(8)	(9)	(10)	(11)	(12)	(13)	(14)	(15)	(16)	(17)	(18)	(19)	(20)
1063	41.20	0.35	72	6.0	41.21	0.37	71.7	4.9	5	5.6	7.2	5.7	35	0.10	9.8	0.10	9.8	0.81	TANG.
1064	41.25	0.20	39	5.3	41.27	0.20	39.1	4.5	13	2.6	10.2	6.8	8	0.15	6.8	0.15	6.8	1.06	
1065	41.60	0.30	59	6.1	41.60	0.28	58.9	5.1	4	4.1	8.6	6.1	19	0.05	3.6	0.10	7.2	0.69	
1066	41.65	-0.25	69	5.6	41.68	-0.26	68.2	4.6	7	5.1	7.6	5.8	-23	0.10	8.9	0.10	8.9	0.97	
1067	41.70	-0.50	57	5.2	41.70	-0.49	57.3	4.5	11	4.0	8.7	6.1	-33	0.15	10.4	0.15	10.4	1.04	
1068	41.70	-0.15	58	6.5	41.69	-0.14	58.7	5.0	12	4.1	8.6	6.1	-9	0.10	7.1	0.15	10.7	1.65	
1069	41.70	0.20	14	5.3	41.70	0.20	14.5	4.9	4	1.1	11.6	7.7	3	0.05	1.0	0.05	1.0	1.08	
1070	41.80	0.10	16	6.3	41.78	0.10	14.9	5.2	7	1.1	11.5	7.7	1	0.10	2.0	0.05	1.0	1.21	
1071	41.85	-0.10	19	7.0	41.85	-0.10	19.1	5.6	3	1.4	11.3	7.5	-2	0.05	1.2	0.05	1.2	0.76	
1072	41.90	-0.40	59	6.3	41.88	-0.45	57.2	4.6	29	4.0	8.7	6.1	-31	0.20	13.8	0.25	17.3	2.20	
1073	41.90	-0.20	69	5.0	41.90	-0.20	69.0	4.6	3	5.3	7.3	5.8	-18	0.05	4.6	0.05	4.6	0.80	TANG.
1074	42.00	-0.50	68	5.3	42.01	-0.49	67.2	4.5	13	5.1	7.6	5.8	-42	0.10	8.8	0.20	17.7	1.03	
1075	42.05	0.00	57	5.2	42.04	-0.02	57.6	4.5	5	4.0	8.6	6.1	-1	0.10	7.0	0.10	7.0	0.49	
1076	42.10	-0.45	55	7.5	42.10	-0.45	54.9	6.1	5	3.8	8.8	6.2	-29	0.05	3.3	0.05	3.3	1.29	
1077	42.10	0.35	21	6.3	42.10	0.35	20.9	5.7	3	1.5	11.1	7.5	9	0.05	1.3	0.05	1.3	0.79	
1078	42.15	-0.60	67	10.7	42.13	-0.72	66.9	5.3	95	5.0	7.6	5.8	-63	0.30	26.4	0.40	35.2	1.63	
A	42.15	-0.60	67	10.7	42.15	-0.61	66.6	9.8	3				-53	0.05	4.4	0.10	8.8	0.48	
1079	42.15	-0.15	55	5.8	42.17	-0.12	55.5	4.7	14	3.8	8.8	6.2	-7	0.10	6.7	0.10	6.7	1.36	
1080	42.30	-0.50	75	5.3	42.28	-0.51	75.0	4.7	5	6.3	6.3	5.7	-55	0.10	11.0	0.10	11.0	0.62	TANG.
1081	42.35	-0.05	58	6.7	42.32	-0.09	57.8	4.7	33	4.0	8.5	6.1	-6	0.15	10.6	0.25	17.7	2.43	
1082	42.65	-0.65	60	5.4	42.69	-0.61	60.8	4.5	13	4.4	8.1	6.1	-46	0.20	15.3	0.15	11.5	1.18	
1083	42.70	0.00	60	5.4	42.70	0.00	59.5	4.7	4	4.3	8.2	6.1	0	0.05	3.7	0.05	3.7	1.09	
1084	42.75	-0.35	59	6.1	42.76	-0.34	60.6	4.5	31	4.4	8.1	6.1	-26	0.20	15.3	0.25	19.1	1.48	
1085	42.80	-0.20	62	5.2	42.80	-0.19	60.3	4.7	9	4.3	8.1	6.1	-14	0.05	3.8	0.10	7.6	1.91	
1086	42.90	-0.90	56	5.1	42.88	-0.90	56.9	4.5	4	4.0	8.4	6.2	-63	0.10	7.0	0.05	3.5	0.71	
1087	42.90	-0.10	58	5.2	42.95	-0.14	57.1	4.6	11	4.0	8.4	6.2	-9	0.15	10.6	0.15	10.6	0.88	
1088	43.10	0.05	12	8.8	43.17	-0.03	9.4	5.5	62	0.8	11.6	7.9	0	0.20	2.9	0.20	2.9	3.74	
1089	43.15	-0.75	57	5.2	43.15	-0.75	57.0	4.6	3	4.0	8.4	6.2	-53	0.05	3.5	0.05	3.5	0.79	
1090	43.15	-0.15	61	5.1	43.15	-0.15	61.0	4.6	3	4.5	7.9	6.1	-11	0.05	3.9	0.05	3.9	0.80	
1091	43.20	-0.50	57	8.3	43.09	-0.53	57.5	5.1	40	4.1	8.3	6.2	-37	0.25	17.8	0.20	14.3	1.18	
1092	43.25	-0.20	61	6.0	43.25	-0.20	61.6	4.9	9	4.5	7.8	6.1	-15	0.15	11.9	0.05	4.0	1.23	
1093	43.30	-0.10	64	10.6	43.29	-0.11	65.6	5.7	15	5.1	7.3	5.9	-9	0.15	13.4	0.10	8.9	1.82	
1094	43.35	-0.35	61	6.5	43.33	-0.33	61.6	5.1	16	4.6	7.8	6.1	-26	0.15	11.9	0.15	11.9	1.13	
1095	43.40	0.55	-17	5.1	43.40	0.55	-17.5	4.7	4	13.1	13.1	9.0	125	0.05	11.4	0.05	11.4	1.10	NEAR
1096	43.90	-0.90	55	7.4	43.87	-0.87	54.7	6.2	8	3.9	8.4	6.3	-59	0.10	6.8	0.10	6.8	0.94	
1097	43.90	-0.80	54	6.4	43.90	-0.80	54.4	5.3	4	3.9	8.4	6.3	-54	0.05	3.4	0.05	3.4	1.03	
1098	43.90	-0.20	60	7.6	43.91	-0.21	60.1	5.6	6	4.5	7.8	6.1	-16	0.10	7.8	0.10	7.8	0.69	
1099	44.05	-0.05	67	7.6	44.05	-0.05	66.6	5.9	4	5.7	6.5	5.9	-4	0.05	5.0	0.05	5.0	1.02	TANG.
1100	44.15	0.00	64	6.8	44.15	0.00	63.5	6.2	4	5.0	7.2	6.0	0	0.05	4.4	0.05	4.4	1.08	
1101	44.20	0.05	57	6.0	44.24	0.06	57.6	4.8	32	4.2	8.0	6.2	4	0.20	14.8	0.25	18.4	1.36	
1102	44.30	0.00	65	6.3	44.31	-0.01	65.3	4.8	15	5.4	6.8	6.0	-1	0.15	14.2	0.10	9.4	1.49	TANG.
1103	44.35	-0.80	62	8.1	44.37	-0.81	63.7	5.7	13	5.1	7.1	6.0	-71	0.10	8.9	0.15	13.3	1.36	TANG.
1104	44.35	-0.20	64	7.4	44.50	-0.32	61.1	4.9	157	4.7	7.4	6.1	-26	0.40	32.8	0.45	36.9	3.24	
1105	44.45	-0.85	59	5.2	44.48	-0.83	58.1	4.5	8	4.3	7.8	6.2	-62	0.10	7.5	0.10	7.5	1.17	
1106	44.45	0.05	69	6.6	44.45	0.05	68.0	5.7	5	6.1	6.1	6.0	5	0.05	5.3	0.05	5.3	1.34	TANG.
1107	44.55	-0.95	48	5.9	44.53	-0.95	48.5	4.9	4	3.4	8.7	6.5	-56	0.10	5.9	0.05	3.0	0.50	
1108	44.55	0.00	63	5.2	44.55	0.00	62.1	4.6	5	4.9	7.3	6.1	0	0.05	4.2	0.05	4.2	1.40	
1109	44.60	-0.35	69	5.8	44.60	-0.33	68.8	4.8	7	6.1	6.1	6.0	-34	0.05	5.3	0.10	10.6	0.98	TANG.
1110	44.65	0.35	18	5.2	44.65	0.35	17.5	4.7	4	1.3	10.8	7.6	7	0.05	1.1	0.05	1.1	1.08	
1111	44.70	-0.75	48	5.1	44.70	-0.73	48.6	4.7	3	3.4	8.7	6.5	-43	0.05	3.0	0.10	6.0	0.48	
1112	44.70	-0.55	67	6.0	44.66	-0.55	66.9	5.0	8	6.0	6.0	6.0	-58	0.15	15.8	0.05	5.3	0.76	TANG.
1113	44.75	-0.55	46	8.3	44.75	-0.55	46.8	6.6	5	3.3	8.8	6.6	-31	0.05	2.9	0.05	2.9	1.29	
1114	44.75	-0.50	66	5.1	44.75	-0.50	66.5	4.6	4	6.0	6.0	6.0	-52	0.05	5.3	0.05	5.3	1.10	TANG.
1115	44.85	-0.75	68	6.5	44.87	-0.75	68.2	4.8	5	6.0	6.0	6.0	-78	0.10	10.5	0.05	5.3	0.72	TANG.
1116	44.85	0.10	64	5.1	44.85	0.10	63.6	4.6	4	5.2	6.8	6.0	9	0.05	4.6	0.05	4.6	1.09	TANG.
1117	44.90	0.20	67	7.2	44.90	0.16	67.5	5.1	13	6.0	6.0	6.0	17	0.05	5.3	0.20	21.0	1.55	TANG.
1118	44.95	0.35	69	6.6	44.95	0.35	68.5	5.0	4	6.0	6.0	6.0	36	0.05	5.2	0.05	5.2	1.04	TANG.
1119	45.00	0.20	64	5.0	45.00	0.20	64.9	4.7	3	6.0	6.0	6.0	20	0.05	5.2	0.05	5.2	0.81	TANG.
1120	45.05	-0.50	64	7.2	45.07	-0.49	65.0	5.5	9	6.0	6.0	6.0	-50	0.10	10.5	0.10	10.5	0.74	TANG.
1121	45.15	-0.75	66	6.2	45.15	-0.75	66.1	5.4	3	6.0	6.0	6.0	-78	0.05	5.2	0.05	5.2	0.78	TANG.

© American Astronomical Society • Provided by the NASA Astrophysics Data System

TABLE 1—*Continued*

CLOUD (1)	l_p ° (2)	b_p ° (3)	v_p (4)	T_p K (5)	<l> ° (6)	<b> ° (7)	<v> km s^{-1} (8)	<T> K (9)	N (10)	d_N kpc (11)	d_F kpc (12)	R kpc (13)	<z> pc (14)	Δl ° (15)	ΔL pc (16)	Δb ° (17)	ΔB pc (18)	σ_v km s^{-1} (19)	NOTES (20)
1122	45.20	-0.80	66	6.1	45.20	-0.81	65.8	5.0	4	6.0	6.0	6.0	-84	0.05	5.2	0.10	10.5	0.81	TANG.
1123	45.40	-0.75	59	7.3	45.39	-0.73	59.3	4.8	18	4.6	7.3	6.2	-59	0.15	12.1	0.15	12.1	2.34	
1124	45.45	0.05	58	10.6	45.42	0.07	58.7	5.6	178	4.5	7.4	6.2	5	0.55	43.5	0.35	27.7	2.75	
A	45.45	0.05	58	10.6	45.45	0.03	58.7	9.1	11				2	0.05	4.0	0.10	7.9	1.56	
1125	45.45	0.15	67	5.3	45.45	0.17	66.5	4.6	4	6.0	6.0	6.1	18	0.05	5.2	0.10	10.4	0.50	TANG.
1126	45.50	0.25	56	5.8	45.50	0.24	55.7	4.9	4	4.2	7.7	6.3	17	0.05	3.6	0.10	7.3	0.79	
1127	45.55	-0.70	62	5.6	45.57	-0.69	61.7	4.7	12	5.1	6.8	6.1	-61	0.15	13.3	0.10	8.9	1.00	TANG.
1128	45.55	-0.30	51	6.0	45.55	-0.30	51.0	5.0	3	3.7	8.2	6.5	-19	0.05	3.2	0.05	3.2	0.78	
1129	45.55	-0.05	7	5.0	45.55	-0.06	7.0	4.6	5	0.7	11.2	8.0	0	0.05	0.6	0.15	1.9	0.63	
1130	45.70	0.15	63	5.4	45.70	0.19	63.0	4.7	16	5.6	6.3	6.1	18	0.15	14.7	0.15	14.7	1.00	TANG.
1131	45.75	-0.30	48	7.3	45.76	-0.30	48.3	5.3	11	3.5	8.4	6.6	-18	0.10	6.0	0.10	6.0	1.74	
1132	45.75	0.00	70	5.2	45.75	-0.02	70.0	4.7	4	5.9	5.9	6.1	-2	0.05	5.2	0.10	10.3	0.70	TANG.
1133	45.85	-0.55	50	5.1	45.85	-0.57	50.5	4.7	4	3.7	8.2	6.5	-36	0.05	3.2	0.10	6.4	0.50	
1134	45.85	-0.20	12	5.7	45.87	-0.17	13.1	4.9	7	1.1	10.8	7.8	-3	0.10	1.9	0.10	1.9	0.83	
1135	45.85	0.30	62	6.0	45.87	0.28	62.6	4.7	12	5.6	6.3	6.1	27	0.20	19.4	0.10	9.7	0.84	TANG.
1136	45.90	-0.25	13	6.0	45.90	-0.25	13.0	5.3	3	1.1	10.8	7.8	-4	0.05	0.9	0.05	0.9	0.79	
1137	45.95	-0.40	61	5.5	45.95	-0.40	61.5	4.9	4	5.2	6.6	6.1	-36	0.05	4.5	0.05	4.5	1.07	TANG.
1138	46.00	-0.10	17	6.7	46.00	-0.10	17.4	5.6	4	1.3	10.5	7.6	-2	0.05	1.1	0.05	1.1	1.05	
1139	46.10	-0.10	50	5.3	46.08	-0.10	49.2	4.6	6	3.6	8.2	6.6	-6	0.10	6.2	0.05	3.1	1.04	
1140	46.10	0.40	28	5.4	46.10	0.40	28.0	4.8	3	2.0	9.8	7.3	13	0.05	1.7	0.05	1.7	0.79	
1141	46.20	-0.80	52	5.1	46.20	-0.77	51.7	4.5	3	3.8	7.9	6.5	-51	0.05	3.3	0.10	6.7	0.46	
1142	46.20	-0.55	51	8.9	46.22	-0.55	50.6	5.9	6	3.7	8.0	6.5	-35	0.10	6.5	0.05	3.2	0.92	
1143	46.20	0.25	61	5.2	46.20	0.25	60.9	4.6	3	5.2	6.6	6.2	22	0.05	4.5	0.05	4.5	0.79	TANG.
1144	46.30	-0.20	59	7.7	46.37	-0.21	54.1	4.9	52	4.1	7.6	6.4	-14	0.40	28.6	0.15	10.7	2.72	
1145	46.30	0.05	58	5.9	46.30	0.05	57.1	5.2	5	4.5	7.3	6.3	3	0.05	3.9	0.05	3.9	1.34	
1146	46.40	0.65	24	5.8	46.40	0.65	23.1	5.2	3	1.7	10.1	7.5	18	0.05	1.5	0.05	1.5	0.80	
1147	46.85	0.35	57	5.9	46.85	0.37	57.2	4.9	9	4.6	7.0	6.3	29	0.05	4.0	0.10	8.1	1.27	
1148	47.00	-0.40	48	5.7	47.00	-0.40	48.0	4.8	3	3.5	8.1	6.6	-24	0.05	3.1	0.05	3.1	0.78	
1149	47.05	0.25	55	9.3	47.09	0.28	57.2	5.3	55	4.7	6.9	6.3	23	0.45	36.9	0.15	12.3	1.89	
A	47.05	0.25	55	9.3	47.05	0.25	56.0	8.9	3				20	0.05	4.1	0.05	4.1	0.81	
1150	47.15	-1.05	7	5.3	47.21	-1.01	7.6	4.5	18	0.8	10.8	8.0	-13	0.25	3.3	0.20	2.7	0.67	
1151	47.40	-1.00	7	5.4	47.41	-0.99	6.8	4.6	10	0.7	10.8	8.0	-12	0.15	1.9	0.15	1.9	0.58	
1152	47.55	-0.55	59	5.7	47.55	-0.55	59.1	4.5	19	5.6	5.9	6.3	-53	0.15	14.6	0.15	14.6	1.05	TANG.
1153	47.75	-0.45	58	5.1	47.73	-0.45	58.7	4.5	10	5.5	5.9	6.3	-43	0.20	19.3	0.05	4.8	0.90	TANG.
1154	47.85	-0.85	46	8.9	47.86	-0.85	46.1	6.5	4	3.4	8.0	6.7	-50	0.10	6.0	0.05	3.0	0.80	
1155	48.45	-0.70	57	5.1	48.45	-0.70	57.0	4.7	3	5.4	5.9	6.4	-66	0.05	4.7	0.05	4.7	0.80	TANG.
1156	48.45	0.00	56	5.5	48.45	0.00	55.9	4.9	3	4.9	6.3	6.4	0	0.05	4.3	0.05	4.3	0.79	TANG.
1157	48.50	-0.65	56	6.9	48.52	-0.63	56.7	5.4	11	5.3	5.9	6.4	-58	0.10	9.3	0.10	9.3	1.20	TANG.
1158	48.55	-0.35	34	5.2	48.55	-0.35	34.0	4.6	3	2.5	8.8	7.1	-15	0.05	2.1	0.05	2.1	0.79	
1159	48.55	-0.25	57	5.2	48.50	-0.28	56.7	4.6	10	5.3	6.0	6.4	-26	0.15	13.9	0.10	9.3	0.89	TANG.
1160	48.60	-0.50	32	5.7	48.60	-0.50	32.0	5.2	3	2.3	8.9	7.2	-20	0.05	2.0	0.05	2.0	0.80	
1161	48.60	-0.30	35	5.1	48.62	-0.30	34.5	4.6	6	2.5	8.7	7.1	-13	0.10	4.4	0.05	2.2	0.94	
1162	48.60	0.00	20	13.5	48.61	0.02	18.0	6.6	27	1.4	9.8	7.7	0	0.20	4.9	0.20	4.9	2.00	
A	48.60	0.00	20	13.5	48.60	0.00	19.0	12.2	5				0	0.05	1.2	0.05	1.2	1.36	
1163	48.60	0.25	10	7.0	48.64	0.23	10.7	5.1	29	1.0	10.3	7.9	3	0.20	3.3	0.15	2.5	2.23	
1164	48.60	0.35	36	6.2	48.60	0.35	36.0	5.6	3	2.6	8.6	7.0	16	0.05	2.3	0.05	2.3	0.80	
1165	48.65	-0.75	64	7.6	48.65	-0.75	63.9	6.1	5	5.6	5.6	6.4	-73	0.05	4.9	0.05	4.9	1.29	TANG.
1166	48.65	-0.15	17	5.4	48.64	-0.15	16.4	5.0	3	1.3	9.9	7.7	-3	0.10	2.3	0.05	1.1	0.48	
1167	48.65	0.10	20	7.4	48.68	0.12	18.2	5.0	10	1.4	9.8	7.6	2	0.15	3.7	0.10	2.5	1.57	
1168	48.75	-0.70	58	6.4	48.75	-0.70	57.9	5.4	3	5.6	5.6	6.4	-68	0.05	4.9	0.05	4.9	0.78	TANG.
1169	48.75	-0.50	63	6.0	48.74	-0.50	62.4	4.8	5	5.6	5.6	6.4	-48	0.10	9.8	0.05	4.9	0.96	TANG.
1170	48.75	-0.45	69	6.3	48.75	-0.45	68.9	5.6	3	5.6	5.6	6.4	-44	0.05	4.9	0.05	4.9	0.79	TANG.
1171	48.75	-0.45	59	5.2	48.76	-0.45	59.0	4.6	4	5.6	5.6	6.4	-44	0.10	9.8	0.05	4.9	0.67	TANG.
1172	48.75	-0.15	67	8.5	48.77	-0.15	66.5	5.7	8	5.6	5.6	6.4	-14	0.10	9.8	0.05	4.9	1.03	TANG.
1173	48.75	-0.15	18	5.5	48.75	-0.15	18.0	5.0	3	1.4	9.8	7.7	-3	0.05	1.2	0.05	1.2	0.80	
1174	48.80	-0.65	58	8.5	48.80	-0.65	57.9	6.6	3	5.6	5.6	6.4	-63	0.05	4.9	0.05	4.9	0.75	TANG.
1175	48.85	-0.55	55	6.0	48.81	-0.54	55.7	4.7	16	5.1	6.1	6.4	-48	0.15	13.4	0.15	13.4	1.47	TANG.
1176	48.85	-0.40	67	8.7	48.82	-0.40	66.6	5.5	10	5.6	5.6	6.4	-39	0.10	9.8	0.10	9.8	1.40	TANG.
1177	48.85	0.05	54	6.7	48.83	0.05	54.5	6.0	4	4.8	6.4	6.5	4	0.10	8.3	0.05	4.2	0.50	TANG.
1178	48.85	0.15	51	8.1	48.76	0.14	51.8	4.8	35	4.2	7.0	6.5	10	0.30	22.2	0.35	25.9	1.58	

© American Astronomical Society • Provided by the NASA Astrophysics Data System

TABLE 1—*Continued*

CLOUD	l_p	b_p	v_p	T_p	<l>	<b>	<v>	<T>	N	d_N	d_F	R	<z>	Δl	ΔL	Δb	ΔB	σ_v	NOTES
	°	°		K	°	°	km s^{-1}	K		kpc	kpc	kpc	pc	°	pc	°	pc	km s^{-1}	
(1)	(2)	(3)	(4)	(5)	(6)	(7)	(8)	(9)	(10)	(11)	(12)	(13)	(14)	(15)	(16)	(17)	(18)	(19)	(20)
1179	48.85	Ø.25	16	5.8	48.84	Ø.26	11.3	4.8	19	1.Ø	1Ø.2	7.9	4	Ø.1Ø	1.7	Ø.1Ø	1.7	3.4Ø	
118Ø	48.9Ø	-Ø.4Ø	62	5.3	48.87	-Ø.4Ø	61.7	4.7	7	5.6	5.6	6.4	-39	Ø.1Ø	9.8	Ø.Ø5	4.9	1.Ø2	TANG.
1181	48.9Ø	-Ø.Ø5	62	6.6	48.86	-Ø.Ø5	59.8	5.6	1Ø	5.6	5.6	6.4	-4	Ø.1Ø	9.8	Ø.Ø5	4.9	2.22	TANG.
1182	48.9Ø	Ø.35	52	5.1	48.87	Ø.37	52.4	4.5	9	4.4	6.8	6.5	28	Ø.1Ø	7.6	Ø.1Ø	7.6	Ø.82	
1183	48.95	-Ø.15	51	6.1	48.95	-Ø.15	5Ø.9	5.1	3	4.1	7.Ø	6.6	-1Ø	Ø.Ø5	3.6	Ø.Ø5	3.6	Ø.77	
1184	49.ØØ	-Ø.3Ø	68	2Ø.5	48.99	-Ø.29	66.1	7.7	69	5.6	5.6	6.4	-28	Ø.4Ø	38.9	Ø.15	14.6	3.ØØ	TANG.
A	48.9Ø	-Ø.25	68	1Ø.3	48.88	-Ø.25	67.Ø	9.2	6				-24	Ø.1Ø	9.7	Ø.Ø5	4.9	1.27	
B	49.ØØ	-Ø.3Ø	68	2Ø.5	48.98	-Ø.3Ø	67.7	13.7	13				-29	Ø.1Ø	9.7	Ø.Ø5	4.9	1.87	
C	49.1Ø	-Ø.25	66	11.6	49.1Ø	-Ø.25	65.5	1Ø.4	4				-24	Ø.Ø5	4.9	Ø.Ø5	4.9	1.Ø7	
1185	49.Ø5	-Ø.45	71	5.4	49.Ø5	-Ø.45	7Ø.9	5.1	3	5.6	5.6	6.4	-43	Ø.Ø5	4.9	Ø.Ø5	4.9	Ø.8Ø	TANG.
1186	49.Ø5	-Ø.45	58	6.Ø	49.Ø5	-Ø.45	58.5	5.4	4	5.6	5.6	6.4	-43	Ø.Ø5	4.9	Ø.Ø5	4.9	1.Ø9	TANG.
1187	49.Ø5	-Ø.1Ø	55	6.3	49.Ø5	-Ø.11	55.2	5.3	7	5.1	6.1	6.4	-9	Ø.Ø5	4.4	Ø.1Ø	8.9	1.2Ø	TANG.
1188	49.Ø5	Ø.5Ø	54	5.1	49.Ø5	Ø.49	54.Ø	4.5	4	4.7	6.4	6.5	4Ø	Ø.Ø5	4.1	Ø.1Ø	8.2	Ø.7Ø	TANG.
1189	49.15	Ø.Ø5	62	5.3	49.13	Ø.13	61.9	4.6	14	5.6	5.6	6.4	12	Ø.1Ø	9.7	Ø.2Ø	19.4	Ø.73	TANG.
119Ø	49.4Ø	Ø.Ø5	52	6.4	49.4Ø	Ø.Ø7	52.5	5.3	6	4.5	6.5	6.5	5	Ø.Ø5	4.Ø	Ø.1Ø	7.9	Ø.88	
1191	49.45	Ø.ØØ	53	6.1	49.45	Ø.ØØ	52.9	5.1	3	4.6	6.4	6.5	Ø	Ø.Ø5	4.1	Ø.Ø5	4.1	Ø.77	TANG.
1192	49.5Ø	-Ø.4Ø	57	24.2	49.45	-Ø.27	59.7	6.5	872	5.5	5.5	6.5	-26	Ø.75	72.3	Ø.8Ø	77.2	5.54	TANG.
A	49.2Ø	-Ø.3Ø	66	11.8	49.2Ø	-Ø.3Ø	66.5	1Ø.1	6				-28	Ø.Ø5	4.8	Ø.Ø5	4.8	1.61	
B	49.25	-Ø.35	71	11.6	49.25	-Ø.35	71.Ø	9.9	5				-33	Ø.Ø5	4.8	Ø.Ø5	4.8	1.34	
C	49.35	-Ø.35	68	11.1	49.35	-Ø.35	68.1	9.8	3				-33	Ø.Ø5	4.8	Ø.Ø5	4.8	Ø.79	
D	49.4Ø	Ø.ØØ	61	9.8	49.4Ø	Ø.ØØ	61.5	9.5	4				Ø	Ø.Ø5	4.8	Ø.Ø5	4.8	1.11	
E	49.45	-Ø.55	6Ø	1Ø.9	49.45	-Ø.57	6Ø.Ø	9.1	4				-54	Ø.Ø5	4.8	Ø.1Ø	9.6	Ø.67	
F	49.45	-Ø.5Ø	62	9.9	49.43	-Ø.5Ø	62.5	8.8	5				-48	Ø.1Ø	9.6	Ø.Ø5	4.8	1.Ø2	
G	49.45	-Ø.4Ø	72	1Ø.2	49.45	-Ø.4Ø	71.1	9.5	3				-38	Ø.Ø5	4.8	Ø.Ø5	4.8	Ø.8Ø	
H	49.5Ø	-Ø.4Ø	57	24.1	49.46	-Ø.36	56.2	12.8	1Ø8				-34	Ø.25	24.1	Ø.35	33.8	4.17	
I	49.5Ø	-Ø.35	69	15.7	49.5Ø	-Ø.36	69.2	12.2	5				-34	Ø.Ø5	4.8	Ø.1Ø	9.6	1.1Ø	
J	49.5Ø	-Ø.25	58	11.7	49.5Ø	-Ø.25	58.4	1Ø.4	4				-24	Ø.Ø5	4.8	Ø.Ø5	4.8	1.Ø9	
K	49.55	Ø.ØØ	57	9.6	49.55	-Ø.Ø2	56.5	9.Ø	4				-1	Ø.Ø5	4.8	Ø.1Ø	9.6	Ø.5Ø	
L	49.6Ø	-Ø.25	57	1Ø.2	49.58	-Ø.25	56.4	9.5	7				-24	Ø.1Ø	9.6	Ø.Ø5	4.8	1.57	
M	49.65	-Ø.3Ø	61	11.8	49.65	-Ø.3Ø	61.Ø	1Ø.5	5				-28	Ø.Ø5	4.8	Ø.Ø5	4.8	1.36	
1193	49.5Ø	Ø.15	-16	7.3	49.5Ø	Ø.17	-15.5	5.8	4	11.6	11.6	8.9	34	Ø.Ø5	1Ø.1	Ø.1Ø	2Ø.2	Ø.5Ø	TANG.
1194	49.5Ø	Ø.4Ø	52	8.1	49.52	Ø.4Ø	51.2	5.6	9	4.3	6.7	6.6	3Ø	Ø.2Ø	15.1	Ø.Ø5	3.8	1.3Ø	
1195	49.55	-Ø.9Ø	43	5.2	49.55	-Ø.9Ø	43.Ø	4.8	3	3.3	7.7	6.8	-51	Ø.Ø5	2.9	Ø.Ø5	2.9	Ø.8Ø	
1196	49.55	Ø.Ø5	62	6.3	49.55	Ø.18	62.6	4.6	3Ø	5.5	5.5	6.5	16	Ø.2Ø	19.2	Ø.3Ø	28.9	Ø.91	TANG.
1197	49.55	Ø.1Ø	57	5.2	49.53	Ø.1Ø	57.5	4.7	4	5.5	5.5	6.5	9	Ø.1Ø	9.6	Ø.Ø5	4.8	Ø.5Ø	TANG.
1198	49.7Ø	Ø.15	25	5.2	49.7Ø	Ø.13	25.Ø	4.6	6	1.9	9.1	7.4	4	Ø.Ø5	1.6	Ø.1Ø	3.3	Ø.79	
1199	49.75	-Ø.55	68	1Ø.7	49.74	-Ø.53	68.Ø	5.9	39	5.5	5.5	6.5	-51	Ø.3Ø	28.8	Ø.2Ø	19.2	1.Ø2	TANG.
A	49.75	-Ø.55	68	1Ø.7	49.75	-Ø.53	68.3	1Ø.Ø	3				-5Ø	Ø.Ø5	4.8	Ø.1Ø	9.6	Ø.47	
12ØØ	49.75	-Ø.35	65	5.6	49.75	-Ø.35	65.Ø	4.8	5	5.5	5.5	6.5	-33	Ø.Ø5	4.8	Ø.Ø5	4.8	1.36	TANG.
12Ø1	49.75	Ø.Ø5	48	6.1	49.75	Ø.Ø5	48.1	5.1	3	3.9	7.1	6.7	3	Ø.Ø5	3.4	Ø.Ø5	3.4	Ø.78	
12Ø2	49.8Ø	-Ø.3Ø	59	5.5	49.83	-Ø.3Ø	58.8	4.5	6	5.5	5.5	6.5	-28	Ø.15	14.4	Ø.Ø5	4.8	Ø.69	TANG.
12Ø3	49.95	Ø.15	9	5.Ø	49.95	Ø.2Ø	9.Ø	4.4	5	Ø.9	1Ø.1	8.Ø	3	Ø.Ø5	Ø.8	Ø.15	2.3	Ø.63	
12Ø4	5Ø.ØØ	-Ø.1Ø	47	7.6	5Ø.ØØ	-Ø.1Ø	46.9	6.1	3	3.8	7.1	6.7	-6	Ø.Ø5	3.3	Ø.Ø5	3.3	Ø.75	
12Ø5	5Ø.Ø5	-Ø.65	38	6.3	5Ø.Ø5	-Ø.65	38.9	5.6	3	3.Ø	8.Ø	7.Ø	-33	Ø.Ø5	2.6	Ø.Ø5	2.6	Ø.8Ø	
12Ø6	5Ø.Ø5	-Ø.5Ø	7Ø	5.1	5Ø.Ø5	-Ø.5Ø	71.4	4.5	4	5.5	5.5	6.5	-47	Ø.Ø5	4.8	Ø.Ø5	4.8	1.12	TANG.
12Ø7	5Ø.Ø5	Ø.Ø5	55	12.Ø	5Ø.Ø3	Ø.Ø1	55.Ø	7.4	17	5.5	5.5	6.5	Ø	Ø.15	14.3	Ø.15	14.3	1.17	TANG.
A	5Ø.Ø5	Ø.Ø5	55	12.Ø	5Ø.Ø5	Ø.Ø4	55.2	9.7	4				3	Ø.Ø5	4.8	Ø.1Ø	9.5	Ø.8Ø	
12Ø8	5Ø.Ø5	Ø.25	53	7.1	5Ø.Ø6	Ø.27	53.5	5.7	8	5.5	5.5	6.5	25	Ø.1Ø	9.5	Ø.1Ø	9.5	Ø.8Ø	TANG.
12Ø9	5Ø.Ø5	Ø.6Ø	-2	1Ø.6	5Ø.Ø4	Ø.58	-1.9	5.9	48	Ø.5	1Ø.7	8.3	5	Ø.25	2.2	Ø.3Ø	2.6	1.52	
A	5Ø.Ø5	Ø.6Ø	-2	1Ø.6	5Ø.Ø5	Ø.6Ø	-1.9	9.1	8				5	Ø.15	1.3	Ø.Ø5	Ø.4	Ø.78	
121Ø	5Ø.1Ø	Ø.85	3Ø	7.Ø	5Ø.1Ø	Ø.85	3Ø.Ø	6.Ø	3	2.2	8.7	7.3	33	Ø.Ø5	2.Ø	Ø.Ø5	2.Ø	Ø.78	NEAR
1211	5Ø.25	-Ø.5Ø	38	6.1	5Ø.26	-Ø.5Ø	38.Ø	5.Ø	1Ø	2.9	8.Ø	7.Ø	-25	Ø.1Ø	5.1	Ø.15	7.6	1.1Ø	
1212	5Ø.3Ø	-Ø.4Ø	15	8.5	5Ø.3Ø	-Ø.4Ø	15.Ø	6.9	3	1.2	9.6	7.8	-8	Ø.Ø5	1.1	Ø.Ø5	1.1	Ø.77	
1213	5Ø.3Ø	Ø.7Ø	26	5.1	5Ø.3Ø	Ø.7Ø	26.Ø	4.5	3	2.Ø	8.9	7.4	23	Ø.Ø5	1.7	Ø.Ø5	1.7	Ø.79	
1214	5Ø.5Ø	1.ØØ	55	7.6	5Ø.5Ø	1.ØØ	55.8	6.3	3	5.4	5.4	6.6	94	Ø.Ø5	4.7	Ø.Ø5	4.7	Ø.77	TANG.
1215	5Ø.55	-Ø.1Ø	63	6.Ø	5Ø.55	-Ø.1Ø	62.9	5.5	3	5.4	5.4	6.6	-9	Ø.Ø5	4.7	Ø.Ø5	4.7	Ø.79	TANG.
1216	5Ø.7Ø	-Ø.35	44	5.9	5Ø.7Ø	-Ø.38	44.4	4.7	7	3.6	7.2	6.8	-23	Ø.Ø5	3.1	Ø.2Ø	12.5	Ø.49	
1217	5Ø.8Ø	-Ø.5Ø	63	7.2	5Ø.82	-Ø.5Ø	63.2	5.7	6	5.4	5.4	6.6	-46	Ø.1Ø	9.4	Ø.Ø5	4.7	1.ØØ	TANG.
1218	5Ø.85	-Ø.15	59	6.9	5Ø.85	-Ø.15	58.5	6.Ø	4	5.4	5.4	6.6	-14	Ø.Ø5	4.7	Ø.Ø5	4.7	1.Ø5	TANG.
1219	5Ø.85	Ø.25	43	7.1	5Ø.79	Ø.19	43.3	5.2	28	3.5	7.3	6.9	11	Ø.2Ø	12.1	Ø.25	15.2	Ø.98	

© American Astronomical Society • Provided by the NASA Astrophysics Data System

TABLE 1—*Continued*

CLOUD (1)	l_p ° (2)	b_p ° (3)	v_p (4)	T_p K (5)	<l> ° (6)	<b> ° (7)	<v> km s^{-1} (8)	<T> K (9)	N (10)	d_N kpc (11)	d_F kpc (12)	R kpc (13)	<z> pc (14)	Δl ° (15)	ΔL pc (16)	Δb ° (17)	ΔB pc (18)	σ_v km s^{-1} (19)	NOTES (20)
1220	50.95	-0.10	57	5.3	50.93	-0.09	57.9	4.6	10	5.4	5.4	6.6	-8	0.10	9.3	0.10	9.3	1.43	TANG.
1221	50.95	0.25	43	6.1	50.97	0.25	42.8	4.8	5	3.5	7.3	6.9	15	0.10	6.0	0.05	3.0	0.71	
1222	51.00	-0.30	56	5.1	51.00	-0.31	55.6	4.7	3	5.3	5.4	6.6	-29	0.05	4.7	0.10	9.3	0.48	TANG.
1223	51.00	-0.20	52	5.4	51.00	-0.20	52.1	4.8	3	5.3	5.4	6.6	-18	0.05	4.7	0.05	4.7	0.79	TANG.
1224	51.05	0.10	51	5.0	51.05	0.10	51.0	4.6	3	5.1	5.6	6.6	8	0.05	4.4	0.05	4.4	0.80	TANG.
1225	51.35	-0.05	54	11.6	51.40	-0.05	54.3	5.8	31	5.3	5.3	6.6	-4	0.20	18.5	0.15	13.9	1.51	TANG.
A	51.35	-0.05	54	11.6	51.35	-0.05	54.0	10.1	3				-4	0.05	4.6	0.05	4.6	0.79	
1226	51.65	0.70	2	6.7	51.67	0.73	1.9	5.0	21	0.5	10.1	8.2	6	0.20	1.7	0.10	0.9	1.75	NEAR
1227	51.85	0.20	53	5.2	51.85	0.20	53.0	4.7	3	5.2	5.3	6.7	18	0.05	4.6	0.05	4.6	0.79	TANG.
1228	51.85	0.80	5	5.5	51.86	0.80	4.9	4.6	7	0.7	9.8	8.1	9	0.15	1.7	0.05	0.6	0.82	NEAR
1229	52.00	-0.35	56	5.2	52.00	-0.33	57.2	4.6	9	5.2	5.2	6.7	-30	0.05	4.6	0.10	9.1	1.32	TANG.
1230	52.00	0.30	6	5.1	51.99	0.30	5.8	4.5	4	0.7	9.8	8.1	3	0.10	1.2	0.05	0.6	0.82	
1231	52.05	-0.35	61	5.2	52.06	-0.35	60.4	4.8	3	5.2	5.2	6.7	-31	0.10	9.1	0.05	4.6	0.48	TANG.
1232	52.15	0.00	57	6.3	52.15	0.00	57.5	5.2	4	5.2	5.2	6.7	0	0.05	4.6	0.05	4.6	1.05	TANG.
1233	52.25	-0.85	65	6.3	52.25	-0.83	65.5	5.3	5	5.2	5.2	6.7	-75	0.05	4.5	0.10	9.1	0.98	TANG.
1234	52.25	-0.80	57	5.3	52.22	-0.79	57.0	4.8	5	5.2	5.2	6.7	-71	0.10	9.1	0.10	9.1	0.63	TANG.
1235	52.25	-0.65	35	5.9	52.27	-0.65	35.5	5.0	6	2.8	7.6	7.1	-32	0.10	5.0	0.05	2.5	0.94	
1236	52.25	0.75	4	10.4	52.24	0.74	4.2	6.2	23	0.6	9.8	8.1	7	0.15	1.6	0.15	1.6	1.45	NEAR
A	52.25	0.75	4	10.4	52.25	0.75	4.0	9.8	3				8	0.05	0.5	0.05	0.5	0.80	
1237	52.35	-0.45	52	5.9	52.33	-0.43	52.1	4.5	9	5.2	5.2	6.7	-39	0.10	9.1	0.20	18.1	0.73	TANG.
1238	52.35	-0.15	52	5.8	52.29	-0.07	51.3	4.7	30	5.2	5.2	6.7	-6	0.20	18.1	0.25	22.7	1.18	TANG.
1239	52.45	-0.05	59	5.1	52.45	-0.03	59.5	4.6	4	5.2	5.2	6.7	-2	0.05	4.5	0.10	9.0	0.50	TANG.
1240	52.55	-0.95	64	13.4	52.63	-0.96	60.0	5.5	182	5.2	5.2	6.8	-86	0.85	76.5	0.25	22.5	2.46	TANG.
A	52.55	-0.95	64	13.4	52.57	-0.95	63.5	10.1	5				-85	0.10	9.0	0.05	4.5	1.01	
B	52.90	-0.90	57	10.0	52.90	-0.90	57.0	9.1	3				-81	0.05	4.5	0.05	4.5	0.80	
1241	52.70	0.55	40	6.1	52.70	0.57	40.6	5.3	3	3.5	6.8	7.0	34	0.05	3.0	0.10	6.0	0.49	
1242	52.90	-0.65	47	9.1	52.90	-0.65	47.0	7.5	3	5.1	5.2	6.8	-57	0.05	4.4	0.05	4.4	0.77	TANG.
1243	52.95	-0.55	48	10.1	52.95	-0.55	48.4	7.5	4	5.1	5.1	6.8	-49	0.05	4.5	0.05	4.5	1.00	TANG.
1244	53.00	0.05	5	5.8	53.02	0.07	5.8	4.8	11	0.7	9.5	8.1	0	0.10	1.3	0.10	1.3	1.75	
1245	53.15	-0.25	61	10.7	53.19	-0.25	62.0	5.4	26	5.1	5.1	6.8	-22	0.25	22.2	0.15	13.3	1.70	TANG.
A	53.15	-0.25	61	10.7	53.15	-0.25	61.0	9.6	3				-22	0.05	4.4	0.05	4.4	0.79	
1246	53.15	0.20	5	9.1	53.15	0.20	4.1	7.0	5	0.6	9.6	8.1	2	0.05	0.5	0.05	0.5	1.26	
1247	53.15	0.35	1	5.0	53.15	0.35	1.0	4.6	3	0.5	9.8	8.2	3	0.05	0.4	0.05	0.4	0.80	
1248	53.20	-0.30	43	6.0	53.19	-0.33	42.3	5.1	11	3.8	6.4	6.9	-21	0.10	6.6	0.10	6.6	1.15	
1249	53.20	0.10	7	5.4	53.20	0.11	6.6	4.7	5	0.8	9.4	8.1	1	0.05	0.7	0.10	1.4	0.99	
1250	53.25	-0.25	44	5.0	53.25	-0.25	43.1	4.7	3	3.9	6.2	6.9	-17	0.05	3.4	0.05	3.4	0.80	
1251	53.25	-0.15	44	5.4	53.27	-0.15	44.5	4.8	6	4.3	5.9	6.9	-11	0.10	7.4	0.05	3.7	0.96	TANG.
1252	53.30	0.15	24	6.0	53.32	0.17	23.8	4.8	5	1.9	8.2	7.5	5	0.10	3.4	0.10	3.4	0.42	
1253	53.40	-0.30	57	5.1	53.40	-0.30	57.0	4.4	3	5.1	5.1	6.8	-26	0.05	4.4	0.05	4.4	0.78	TANG.
1254	53.45	0.00	42	8.4	53.45	0.00	42.1	6.5	3	3.8	6.3	6.9	0	0.05	3.3	0.05	3.3	0.75	
1255	53.55	0.05	23	17.8	53.45	0.04	23.4	6.2	190	1.9	8.2	7.5	1	1.05	35.0	0.45	15.0	1.29	
A	53.55	0.05	23	17.8	53.60	0.05	23.7	11.4	27				1	0.25	8.3	0.20	6.7	0.90	
1256	53.60	-0.25	60	13.7	53.60	-0.24	59.7	8.3	5	5.0	5.0	6.8	-21	0.05	4.4	0.10	8.8	0.92	TANG.
A	53.60	-0.25	60	13.7	53.60	-0.25	60.0	10.9	3				-22	0.05	4.4	0.05	4.4	0.76	
1257	53.60	-0.15	61	5.2	53.64	-0.13	60.8	4.5	5	5.0	5.0	6.8	-11	0.15	13.2	0.10	8.8	0.39	TANG.
1258	53.60	0.25	40	5.7	53.60	0.25	39.4	5.2	4	3.5	6.6	7.0	15	0.05	3.0	0.05	3.0	1.07	
1259	53.65	-0.10	47	5.9	53.65	-0.12	46.2	5.2	6	5.0	5.0	6.8	-10	0.05	4.4	0.10	8.8	1.05	TANG.
1260	53.70	0.50	24	5.2	53.70	0.50	24.1	4.7	3	2.0	8.1	7.5	17	0.05	1.7	0.05	1.7	0.79	
1261	53.75	-0.10	47	6.2	53.75	-0.10	45.6	5.8	4	5.0	5.0	6.9	-8	0.05	4.4	0.05	4.4	1.11	TANG.
1262	53.80	-0.15	48	8.0	53.80	-0.15	47.9	6.1	5	5.0	5.0	6.9	-13	0.05	4.4	0.05	4.4	1.25	TANG.
1263	53.85	-0.20	46	8.0	53.85	-0.20	46.0	6.1	3	5.0	5.0	6.9	-17	0.05	4.4	0.05	4.4	0.75	TANG.
1264	53.85	-0.10	45	5.9	53.85	-0.10	43.6	5.2	6	4.3	5.7	6.9	-7	0.05	3.8	0.05	3.8	1.66	TANG.
1265	54.10	-0.05	40	14.2	54.14	-0.08	39.0	7.1	36	3.5	6.4	7.0	-5	0.20	12.3	0.15	9.2	1.77	
A	54.10	-0.05	40	14.2	54.11	-0.07	39.8	11.0	10				-4	0.10	6.1	0.10	6.1	1.22	
1266	54.15	-1.05	44	6.3	54.11	-1.05	44.0	4.9	3	4.7	5.3	6.9	-86	0.15	12.3	0.05	4.1	0.00	TANG.
1267	54.25	0.25	32	6.7	54.25	0.25	32.0	5.1	3	2.7	7.2	7.3	11	0.05	2.4	0.05	2.4	0.75	
1268	54.45	0.40	9	5.1	54.45	0.40	9.1	4.7	3	1.0	8.9	8.0	6	0.05	0.8	0.05	0.8	0.80	
1269	54.45	1.00	36	10.4	54.44	1.00	35.3	6.7	6	3.1	6.8	7.2	53	0.10	5.4	0.05	2.7	1.33	
1270	54.60	0.85	28	5.6	54.61	0.85	28.2	5.1	4	2.4	7.5	7.4	35	0.10	4.2	0.05	2.1	0.82	
1271	54.65	0.55	37	5.7	54.67	0.60	36.7	4.5	18	3.3	6.5	7.1	34	0.20	11.5	0.20	11.5	0.92	

© American Astronomical Society • Provided by the NASA Astrophysics Data System

TABLE 1—*Continued*

CLOUD (1)	l_p ° (2)	b_p ° (3)	v_p (4)	T_p K (5)	<l> ° (6)	<b> ° (7)	<v> km s^{-1} (8)	<T> K (9)	N (10)	d_N kpc (11)	d_P kpc (12)	R kpc (13)	<z> pc (14)	Δl ° (15)	ΔL pc (16)	Δb ° (17)	ΔB pc (18)	σ_v km s^{-1} (19)	NOTES (20)
1272	54.65	0.80	31	6.3	54.65	0.78	33.5	4.9	37	2.9	6.9	7.2	39	0.20	10.1	0.20	10.1	1.83	
1273	54.80	-0.40	40	5.4	54.79	-0.39	39.9	4.4	13	3.8	6.0	7.0	-25	0.15	10.0	0.10	6.7	1.30	
1274	54.95	-0.50	-16	7.3	54.95	-0.49	-15.4	5.8	3	10.3	10.3	8.8	-87	0.05	9.0	0.10	18.0	0.49	TANG.
1275	54.95	-0.25	37	5.1	54.99	-0.25	36.8	4.4	4	3.4	6.4	7.1	-14	0.15	8.8	0.05	2.9	0.42	
1276	55.10	0.00	29	5.4	55.10	0.00	28.9	4.9	3	2.5	7.2	7.4	0	0.05	2.2	0.05	2.2	0.79	
1277	55.30	0.20	30	7.3	55.38	0.19	32.4	4.7	41	2.9	6.8	7.3	9	0.25	12.6	0.30	15.1	1.77	
1278	55.60	-0.10	35	6.4	55.55	-0.10	35.3	4.7	25	3.3	6.3	7.2	-5	0.20	11.4	0.15	8.6	1.18	
1279	55.70	0.10	46	5.2	55.73	0.11	46.2	4.4	24	4.8	4.8	7.0	9	0.20	16.7	0.25	20.9	1.01	TANG.
1280	56.00	-0.10	40	8.2	56.00	-0.10	39.9	5.3	8	4.8	4.8	7.0	-8	0.15	12.4	0.15	12.4	0.63	TANG.
1281	56.30	-0.10	35	7.4	56.27	-0.13	35.2	4.8	20	3.4	6.0	7.2	-7	0.25	14.9	0.20	11.9	0.65	
1282	56.40	0.00	-5	6.8	56.40	0.00	-4.7	4.9	10	0.5	9.3	8.4	0	0.15	1.3	0.15	1.3	0.62	
1283	57.40	0.20	36	5.9	57.42	0.21	36.1	4.6	8	4.2	5.0	7.2	14	0.10	7.2	0.15	10.9	0.61	TANG.
1284	57.90	-0.40	27	5.3	57.91	-0.43	27.5	4.3	6	2.7	6.4	7.4	-20	0.10	4.6	0.15	7.0	0.50	
1285	58.30	0.30	29	5.8	58.31	0.33	28.5	4.5	6	2.9	6.1	7.4	16	0.10	5.0	0.15	7.5	0.50	
1286	58.40	-0.20	28	5.7	58.41	-0.21	27.8	4.8	4	2.8	6.1	7.4	-10	0.10	4.8	0.10	4.8	0.41	
1287	58.60	-0.20	28	6.4	58.59	-0.20	28.4	5.0	5	2.9	6.0	7.4	-10	0.15	7.6	0.05	2.5	0.49	
1288	59.10	-0.10	26	8.6	59.08	-0.10	26.0	5.8	10	2.7	6.1	7.5	-4	0.20	9.3	0.15	6.9	0.90	
1289	59.30	-0.20	28	11.7	59.18	-0.26	27.4	5.4	73	2.9	5.8	7.4	-13	0.50	25.1	0.30	15.0	0.96	
A	59.30	-0.20	28	11.7	59.29	-0.20	28.3	10.5	3				-10	0.10	5.0	0.05	2.5	0.47	
1290	59.40	0.00	31	10.1	59.40	0.00	30.5	5.8	12	3.5	5.1	7.4	0	0.15	9.2	0.15	9.2	0.75	
1291	59.50	-0.10	32	5.4	59.50	-0.12	32.5	4.8	4	4.3	4.3	7.3	-9	0.05	3.8	0.10	7.5	0.50	TANG.
1292	59.60	0.90	38	6.2	59.60	0.91	37.5	5.1	5	4.3	4.3	7.3	68	0.05	3.8	0.10	7.5	0.98	TANG.
1293	59.70	0.20	-1	5.6	59.70	0.20	-0.9	5.0	3	0.5	8.2	8.3	1	0.05	0.4	0.05	0.4	0.79	
1294	60.00	0.10	22	11.9	59.70	-0.00	23.8	5.7	142	2.5	6.1	7.6	-3	0.65	28.2	0.55	23.8	2.68	
A	59.50	-0.30	28	11.8	59.50	-0.30	28.0	10.0	3				-12	0.05	2.2	0.05	2.2	0.78	
B	59.60	-0.20	27	11.4	59.61	-0.20	26.7	10.3	3				-8	0.10	4.3	0.05	2.2	0.47	
C	59.80	0.10	22	10.3	59.80	0.07	22.2	8.9	7				3	0.05	2.2	0.15	6.5	0.82	
1295	60.20	-0.40	30	5.4	60.19	-0.38	28.7	4.7	6	3.4	5.0	7.4	-22	0.10	6.0	0.15	8.9	0.76	
1296	60.90	-0.10	23	19.9	60.90	-0.11	23.1	7.7	39	2.6	5.7	7.6	-5	0.15	6.7	0.20	9.0	1.07	
A	60.90	-0.10	23	19.9	60.90	-0.10	23.1	11.1	16				-4	0.15	6.7	0.15	6.7	0.89	
1297	61.40	-0.50	23	7.3	61.39	-0.47	22.8	5.4	10	2.6	5.5	7.6	-21	0.10	4.6	0.20	9.2	0.60	
1298	61.50	0.10	22	15.6	61.50	0.11	21.7	6.7	70	2.5	5.6	7.6	4	0.35	15.3	0.25	10.9	1.31	
A	61.50	0.10	22	15.6	61.50	0.10	21.9	10.3	18				4	0.20	8.7	0.15	6.5	1.00	
1299	61.60	-0.30	21	7.6	61.60	-0.22	20.2	4.8	13	2.3	5.8	7.7	-8	0.10	4.0	0.30	12.1	0.99	
1300	61.80	0.30	20	5.8	61.80	0.29	20.3	5.0	3	2.4	5.7	7.7	11	0.05	2.1	0.10	4.1	0.47	
1301	62.90	0.10	24	5.6	62.93	0.10	25.3	4.7	8	3.9	3.9	7.6	6	0.15	10.1	0.05	3.4	0.99	TANG.
1302	63.10	0.40	20	11.9	63.16	0.41	19.8	6.0	57	2.5	5.1	7.7	18	0.30	13.3	0.20	8.9	1.24	
A	63.10	0.40	20	11.9	63.13	0.40	19.7	9.7	8				17	0.15	6.6	0.05	2.2	0.92	
1303	64.10	-0.50	21	8.0	64.10	-0.50	20.5	5.1	12	3.0	4.4	7.7	-26	0.15	7.9	0.15	7.9	0.75	
1304	64.10	0.50	19	5.1	64.10	0.50	19.0	4.8	3	2.6	4.8	7.7	22	0.05	2.3	0.05	2.3	0.81	
1305	64.80	0.20	-16	5.6	64.80	0.20	-16.0	4.9	3	7.9	7.9	8.8	27	0.05	6.9	0.05	6.9	0.79	TANG.
1306	66.80	-0.70	15	6.7	66.77	-0.66	15.0	4.7	14	2.6	4.1	7.8	-29	0.20	9.1	0.20	9.1	0.58	
1307	68.90	-0.90	12	7.0	68.89	-0.91	11.6	4.8	7	2.5	3.6	7.9	-40	0.15	6.6	0.10	4.4	0.49	
1308	69.40	-0.80	9	6.1	69.38	-0.81	9.4	4.6	8	2.1	3.9	8.0	-29	0.15	5.4	0.10	3.6	0.68	
1309	69.50	-1.00	11	7.7	69.53	-0.99	11.6	5.2	15	3.0	3.0	8.0	-51	0.20	10.4	0.10	5.2	0.92	TANG.
1310	70.60	-0.60	10	6.5	70.65	-0.52	11.2	4.8	98	2.8	2.8	8.0	-25	0.40	19.6	0.55	27.0	1.57	TANG.
1311	70.80	0.60	10	5.1	70.80	0.61	10.0	4.4	4	2.8	2.8	8.0	29	0.05	2.4	0.10	4.9	0.69	TANG.
1312	70.90	0.70	12	5.8	70.85	0.73	11.5	4.5	32	2.8	2.8	8.0	35	0.25	12.2	0.25	12.2	0.95	TANG.
1313	71.10	-0.40	10	7.1	71.00	-0.22	10.1	4.8	123	2.8	2.8	8.0	-10	0.60	29.0	0.65	31.4	0.90	TANG.
1314	71.20	0.80	9	8.5	71.20	0.81	8.5	5.2	10	2.7	2.7	8.0	38	0.15	7.2	0.10	4.8	0.76	TANG.
1315	71.30	0.40	8	5.0	71.30	0.40	7.5	4.7	4	2.3	3.2	8.1	15	0.05	2.0	0.05	2.0	1.10	
1316	71.50	-0.40	10	6.6	71.51	-0.40	9.7	5.4	3	2.7	2.7	8.1	-18	0.10	4.7	0.05	2.4	0.47	TANG.
1317	73.30	-0.20	2	5.8	73.26	-0.12	2.9	4.5	16	1.5	3.4	8.2	-3	0.25	6.5	0.20	5.2	0.78	
1318	74.10	0.10	-2	6.7	74.10	0.10	-1.6	5.6	4	1.5	1.5	7.7	2	0.05	1.3	0.05	1.3	1.07	CYG
1319	74.60	-1.00	9	11.0	74.61	-1.00	9.2	6.6	10	1.5	1.5	7.7	-26	0.20	5.2	0.10	2.6	0.72	CYG
1320	74.70	0.60	2	10.0	74.70	0.60	1.7	5.6	13	1.5	1.5	7.7	15	0.15	3.9	0.15	3.9	0.81	CYG
1321	75.00	-0.90	10	13.1	75.00	-0.91	10.0	6.3	18	1.5	1.5	7.7	-23	0.15	3.9	0.15	3.9	0.81	CYG
A	75.00	-0.90	10	13.1	75.00	-0.91	10.1	9.8	4				-23	0.05	1.3	0.10	2.6	0.67	
1322	75.40	-0.20	-6	6.3	75.40	-0.21	-5.4	5.1	5	1.5	1.5	7.7	-5	0.05	1.3	0.15	3.9	0.49	CYG
1323	75.60	0.20	-4	8.9	75.61	0.20	-4.2	5.4	12	1.5	1.5	7.7	5	0.15	3.9	0.15	3.9	0.70	CYG

© American Astronomical Society • Provided by the NASA Astrophysics Data System

1987ApJS...63..821S

TABLE 1—*Continued*

CLOUD (1)	l_p ° (2)	b_p ° (3)	v_p (4)	T_p K (5)	<l> ° (6)	<b> ° (7)	<v> km s^{-1} (8)	<T> K (9)	N (10)	d_N kpc (11)	d_P kpc (12)	R kpc (13)	<z> pc (14)	Δl ° (15)	ΔL pc (16)	Δb ° (17)	ΔB pc (18)	σ_v km s^{-1} (19)	NOTES (20)
1324	75.70	0.40	2	7.6	75.72	0.34	0.5	5.2	44	1.5	1.5	7.7	9	0.20	5.2	0.30	7.9	1.03	CYG
1325	76.10	0.70	6	7.6	76.14	0.69	5.6	5.7	7	1.5	1.5	7.7	18	0.15	3.9	0.10	2.6	0.50	CYG
1326	76.20	0.10	-2	16.3	76.14	0.09	-2.2	6.0	55	1.5	1.5	7.7	2	0.50	13.1	0.25	6.5	1.00	CYG
A	76.20	0.10	-2	16.3	76.19	0.10	-2.1	10.3	11				2	0.15	3.9	0.15	3.9	0.86	
1327	76.30	-0.70	-1	16.0	76.33	-0.67	-0.9	6.6	114	1.5	1.5	7.7	-17	0.30	7.9	0.30	7.9	1.62	CYG
A	76.30	-0.70	-1	16.0	76.32	-0.66	-1.0	10.3	27				-17	0.20	5.2	0.20	5.2	1.09	
1328	76.40	-1.00	1	5.3	76.33	-0.99	0.6	4.9	9	1.5	1.5	7.7	-26	0.20	5.2	0.10	2.6	0.50	CYG
1329	76.80	0.80	4	5.2	76.85	0.80	4.0	4.7	3	1.5	1.5	7.7	20	0.15	3.9	0.05	1.3	0.00	CYG
1330	77.10	0.00	10	5.7	77.10	0.09	9.2	4.8	9	1.5	1.5	7.7	2	0.05	1.3	0.25	6.5	0.61	CYG
1331	77.20	0.70	2	5.9	77.11	0.59	2.3	4.5	25	1.5	1.5	7.7	15	0.30	7.9	0.30	7.9	0.45	CYG
1332	77.30	0.60	9	6.7	77.34	0.60	8.5	5.0	5	1.5	1.5	7.7	15	0.15	3.9	0.05	1.3	0.50	CYG
1333	77.90	0.00	-2	6.3	77.91	-0.01	-2.5	5.0	9	1.5	1.5	7.7	0	0.20	5.2	0.10	2.6	0.50	CYG
1334	78.00	-0.30	-4	8.3	77.95	-0.32	-4.7	5.1	30	1.5	1.5	7.7	-8	0.20	5.2	0.20	5.2	1.16	CYG
1335	78.00	0.60	-1	5.6	78.00	0.54	-2.8	4.7	11	1.5	1.5	7.7	14	0.05	1.3	0.15	3.9	1.50	CYG
1336	78.10	-0.80	0	10.7	78.10	-0.86	-0.5	5.9	195	1.5	1.5	7.7	-22	0.50	13.1	0.50	13.1	1.48	CYG
A	78.10	-0.80	0	10.7	78.11	-0.85	-0.4	9.1	20				-22	0.25	6.5	0.25	6.5	0.72	
1337	78.20	-0.30	-1	6.0	78.19	-0.32	-1.6	4.8	6	1.5	1.5	7.7	-8	0.10	2.6	0.10	2.6	0.73	CYG
1338	78.20	-0.30	14	6.4	78.19	-0.31	14.3	4.6	19	1.5	1.5	7.7	-8	0.30	7.9	0.25	6.5	0.46	CYG
1339	78.20	-0.20	1	8.1	78.20	-0.20	0.7	5.0	10	1.5	1.5	7.7	-5	0.15	3.9	0.15	3.9	0.61	CYG
1340	78.20	0.10	11	6.3	78.19	0.14	12.1	5.0	18	1.5	1.5	7.7	3	0.15	3.9	0.30	7.9	1.62	CYG
1341	78.30	-0.70	-5	5.9	78.30	-0.62	-5.1	4.7	18	1.5	1.5	7.7	-16	0.10	2.6	0.25	6.5	1.17	CYG
1342	78.40	-0.50	14	5.4	78.40	-0.49	14.0	4.4	4	1.5	1.5	7.7	-12	0.05	1.3	0.10	2.6	0.67	CYG
1343	78.40	0.70	-4	6.1	78.41	0.75	-3.7	4.7	13	1.5	1.5	7.7	19	0.15	3.9	0.15	3.9	0.59	CYG
1344	78.50	-0.80	-2	9.1	78.50	-0.80	-1.6	5.4	13	1.5	1.5	7.7	-20	0.15	3.9	0.15	3.9	0.79	CYG
1345	78.50	1.00	-4	6.4	78.51	0.96	-5.3	4.7	16	1.5	1.5	7.7	25	0.20	5.2	0.15	3.9	0.77	CYG
1346	78.50	1.00	3	7.9	78.48	1.00	1.9	5.1	16	1.5	1.5	7.7	26	0.35	9.2	0.10	2.6	0.78	CYG
1347	78.60	0.30	-1	5.2	78.60	0.30	-1.0	4.6	3	1.5	1.5	7.7	7	0.05	1.3	0.15	3.9	0.00	CYG
1348	78.60	0.30	7	6.3	78.54	0.06	8.4	4.6	196	1.5	1.5	7.7	1	0.50	13.1	0.80	20.9	1.16	CYG
1349	78.80	-0.50	-1	11.6	78.70	-0.48	-1.8	5.3	53	1.5	1.5	7.7	-12	0.50	13.1	0.20	5.2	1.23	CYG
A	78.80	-0.50	-1	11.6	78.80	-0.50	-1.1	10.3	3				-13	0.05	1.3	0.05	1.3	0.79	
1350	78.80	-0.30	-6	5.3	78.89	-0.29	-5.7	4.4	22	1.5	1.5	7.7	-7	0.35	9.2	0.10	2.6	0.87	CYG
1351	78.90	-0.30	-2	7.4	78.75	-0.22	-2.6	4.5	100	1.5	1.5	7.7	-5	0.55	14.4	0.30	7.9	1.25	CYG
1352	78.90	0.70	-5	6.6	78.89	0.71	-5.5	4.9	8	1.5	1.5	7.7	18	0.10	2.6	0.10	2.6	0.83	CYG
1353	79.00	-0.10	-6	5.5	79.00	-0.11	-5.2	4.4	11	1.5	1.5	7.7	-2	0.15	3.9	0.10	2.6	0.71	CYG
1354	79.00	0.40	5	8.4	79.01	0.39	5.3	5.5	13	1.5	1.5	7.7	10	0.15	3.9	0.20	5.2	0.68	CYG
1355	79.00	0.60	7	7.1	79.01	0.58	7.5	5.4	6	1.5	1.5	7.7	15	0.10	2.6	0.10	2.6	0.50	CYG
1356	79.10	0.50	-1	6.0	79.11	0.51	-1.2	4.7	9	1.5	1.5	7.7	13	0.20	5.2	0.10	2.6	0.62	CYG
1357	79.10	1.00	7	9.7	79.23	0.97	6.7	5.5	36	1.5	1.5	7.7	25	0.40	10.5	0.20	5.2	0.82	CYG
1358	79.20	-0.30	7	5.4	79.18	-0.29	7.4	4.6	5	1.5	1.5	7.7	-7	0.10	2.6	0.10	2.6	0.49	CYG
1359	79.20	0.10	8	10.0	79.07	0.25	9.7	4.8	103	1.5	1.5	7.7	6	0.40	10.5	0.70	18.3	1.32	CYG
1360	79.30	-1.00	11	7.0	79.23	-0.99	9.8	5.0	16	1.5	1.5	7.7	-25	0.20	5.2	0.10	2.6	1.95	CYG
1361	79.30	-0.40	-3	5.4	79.31	-0.38	-2.6	4.6	5	1.5	1.5	7.7	-9	0.10	2.6	0.10	2.6	0.49	CYG
1362	79.30	0.30	0	7.5	79.32	0.35	0.5	4.8	26	1.5	1.5	7.7	9	0.20	5.2	0.30	7.9	0.73	CYG
1363	79.30	0.70	12	5.9	79.28	0.71	11.8	4.5	6	1.5	1.5	7.7	18	0.10	2.6	0.10	2.6	0.67	CYG
1364	79.40	-0.30	-1	5.2	79.40	-0.29	-1.0	4.4	9	1.5	1.5	7.7	-7	0.15	3.9	0.10	2.6	0.93	CYG
1365	79.50	1.00	12	6.5	79.41	0.96	11.8	4.7	27	1.5	1.5	7.7	25	0.25	6.5	0.20	5.2	1.27	CYG
1366	79.60	-0.60	4	6.6	79.53	-0.69	4.7	4.6	114	1.5	1.5	7.7	-18	0.55	14.4	0.50	13.1	1.51	CYG
1367	79.60	-0.30	3	5.6	79.55	-0.30	3.8	4.6	9	1.5	1.5	7.7	-7	0.20	5.2	0.10	2.6	1.36	CYG
1368	80.10	0.60	11	5.5	80.08	0.61	11.0	4.6	3	1.5	1.5	7.7	16	0.10	2.6	0.10	2.6	0.00	CYG
1369	80.30	0.20	0	5.2	80.25	0.20	-0.5	4.3	4	1.5	1.5	7.7	5	0.15	3.9	0.05	1.3	0.50	CYG
1370	80.30	0.30	-2	6.0	80.30	0.28	-2.3	4.7	7	1.5	1.5	7.7	7	0.05	1.3	0.10	2.6	0.98	CYG
1371	80.40	0.00	-3	6.5	80.41	0.00	-1.3	5.7	5	1.5	1.5	7.7	0	0.10	2.6	0.05	1.3	1.16	CYG
1372	80.40	0.40	8	5.9	80.45	0.33	7.6	4.5	13	1.5	1.5	7.7	8	0.25	6.5	0.15	3.9	0.63	CYG
1373	80.50	0.40	3	6.4	80.50	0.40	3.0	5.0	3	1.5	1.5	7.7	10	0.05	1.3	0.05	1.3	0.76	CYG
1374	80.60	-0.20	0	5.5	80.59	-0.09	0.9	4.6	14	1.5	1.5	7.7	-2	0.15	3.9	0.25	6.5	0.87	CYG
1375	80.60	0.50	-2	5.6	80.55	0.50	-2.2	4.8	6	1.5	1.5	7.7	13	0.15	3.9	0.05	1.3	0.67	CYG
1376	80.70	-0.90	6	5.0	80.68	-0.84	5.8	4.4	11	1.5	1.5	7.7	-21	0.15	3.9	0.20	5.2	0.57	CYG
1377	80.70	0.70	-1	9.4	80.66	0.69	-1.8	5.6	44	1.5	1.5	7.7	18	0.35	9.2	0.30	7.9	1.12	CYG
A	80.70	0.70	-1	9.4	80.70	0.70	-1.0	8.9	3				18	0.05	1.3	0.05	1.3	0.80	
1378	80.80	-0.50	-3	9.1	80.76	-0.58	-3.8	5.5	26	1.5	1.5	7.7	-15	0.20	5.2	0.30	7.9	0.92	CYG

© American Astronomical Society • Provided by the NASA Astrophysics Data System

TABLE 1—*Continued*

CLOUD	l_p	b_p	v_p	T_p	<l>	<b>	<v>	<T>	N	d_N	d_F	R	<z>	Δl	ΔL	Δb	ΔB	σ_v	NOTES
	°	°		K	°	°	km s^{-1}	K		kpc	kpc	kpc	pc	°	pc	°	pc	km s^{-1}	
(1)	(2)	(3)	(4)	(5)	(6)	(7)	(8)	(9)	(10)	(11)	(12)	(13)	(14)	(15)	(16)	(17)	(18)	(19)	(20)
1379	80.80	0.30	6	5.6	80.79	0.32	5.6	4.5	8	1.5	1.5	7.7	8	0.15	3.9	0.15	3.9	0.48	CYG
1380	80.90	-0.60	7	5.1	80.85	-0.36	5.9	4.3	89	1.5	1.5	7.7	-9	0.50	13.1	0.70	18.3	0.68	CYG
1381	80.90	0.30	-2	8.0	80.89	0.31	-1.8	5.2	15	1.5	1.5	7.7	8	0.15	3.9	0.15	3.9	1.09	CYG
1382	81.00	-0.30	-2	8.1	80.96	-0.30	-2.3	5.5	17	1.5	1.5	7.7	-7	0.15	3.9	0.15	3.9	0.98	CYG
1383	81.10	0.20	11	6.0	81.10	0.19	11.0	5.0	4	1.5	1.5	7.7	4	0.05	1.3	0.10	2.6	0.68	CYG
1384	81.20	1.00	13	14.1	81.20	0.70	13.0	5.9	300	1.5	1.5	7.7	18	0.65	17.0	0.65	17.0	2.81	CYG
A	81.20	1.00	13	14.1	81.20	0.88	14.1	10.5	25				23	0.10	2.6	0.30	7.9	1.41	
B	81.30	0.70	15	11.3	81.29	0.70	14.8	9.8	4				18	0.10	2.6	0.05	1.3	0.82	
1385	81.30	0.50	-1	8.0	81.33	0.53	-1.1	5.5	24	1.5	1.5	7.7	13	0.25	6.5	0.20	5.2	0.83	CYG
1386	81.40	0.00	-4	14.1	81.38	-0.01	-5.1	6.0	95	1.5	1.5	7.7	0	0.70	18.3	0.40	10.5	1.15	CYG
A	81.30	-0.10	-6	9.0	81.26	-0.10	-5.3	8.9	4				-2	0.15	3.9	0.05	1.3	0.43	
B	81.40	0.00	-4	14.1	81.39	0.00	-4.0	11.5	4				0	0.10	2.6	0.05	1.3	0.72	
C	81.60	0.10	-6	12.6	81.59	0.10	-6.0	9.9	4				2	0.10	2.6	0.05	1.3	0.67	
1387	81.40	0.70	-2	9.3	81.47	0.74	-1.1	5.6	34	1.5	1.5	7.7	19	0.35	9.2	0.20	5.2	0.67	CYG
1388	81.40	0.90	4	6.4	81.29	0.94	4.8	4.6	19	1.5	1.5	7.7	24	0.25	6.5	0.15	3.9	0.87	CYG
1389	81.60	0.40	-4	6.9	81.60	0.39	-4.3	5.0	3	1.5	1.5	7.7	10	0.05	1.3	0.10	2.6	0.45	CYG
1390	81.70	0.40	16	7.9	81.70	0.40	16.4	5.7	8	1.5	1.5	7.7	10	0.15	3.9	0.10	2.6	0.89	CYG
1391	81.70	0.60	-2	14.0	81.89	0.35	7.0	5.5	649	1.5	1.5	7.7	9	1.40	36.7	1.00	26.2	4.47	CYG
A	81.50	0.20	8	10.3	81.52	0.20	8.6	9.4	3				5	0.10	2.6	0.05	1.3	0.48	
B	81.50	0.50	7	11.4	81.51	0.41	8.1	9.1	19				10	0.25	6.5	0.30	7.9	0.78	
C	81.70	0.60	-2	14.0	81.70	0.57	-2.4	10.3	15				14	0.15	3.9	0.15	3.9	0.93	
D	81.80	0.70	-3	12.8	81.80	0.69	-3.0	10.3	4				18	0.05	1.3	0.10	2.6	0.68	
E	81.90	0.80	12	12.9	81.91	0.80	11.9	10.1	6				20	0.10	2.6	0.05	1.3	1.01	
1392	81.80	0.90	-1	12.0	81.82	0.92	-1.3	6.0	55	1.5	1.5	7.7	24	0.25	6.5	0.25	6.5	1.29	CYG
A	81.80	0.90	-1	12.0	81.79	0.91	-1.1	9.5	7				23	0.10	2.6	0.10	2.6	0.95	
1393	81.90	0.10	14	10.5	81.90	0.09	14.1	5.5	16	1.5	1.5	7.7	2	0.25	6.5	0.15	3.9	0.63	CYG
1394	82.00	-0.60	7	5.6	81.75	-0.63	7.5	4.5	91	1.5	1.5	7.7	-16	0.55	14.4	0.35	9.2	1.19	CYG
1395	82.00	-0.40	5	6.3	81.96	-0.37	5.7	4.4	31	1.5	1.5	7.7	-9	0.30	7.9	0.25	6.5	0.95	CYG
1396	82.00	0.80	-1	8.2	81.99	0.80	-1.3	5.4	6	1.5	1.5	7.7	20	0.10	2.6	0.15	3.9	0.47	CYG
1397	82.20	-0.10	8	5.2	82.20	-0.10	7.6	4.3	10	1.5	1.5	7.7	-2	0.15	3.9	0.15	3.9	0.79	CYG
1398	82.30	0.50	11	7.5	82.34	0.47	10.9	5.0	18	1.5	1.5	7.7	12	0.25	6.5	0.20	5.2	0.90	CYG
1399	82.30	0.70	11	6.0	82.30	0.69	11.3	4.8	3	1.5	1.5	7.7	17	0.05	1.3	0.10	2.6	0.46	CYG
1400	82.40	-0.10	6	5.6	82.40	-0.10	6.2	4.4	6	1.5	1.5	7.7	-2	0.15	3.9	0.15	3.9	0.37	CYG
1401	82.80	0.40	-4	6.5	82.81	0.40	-3.7	5.1	3	1.5	1.5	7.7	10	0.10	2.6	0.05	1.3	0.45	CYG
1402	83.30	-0.20	2	7.5	83.24	-0.17	1.0	4.9	26	1.5	1.5	7.7	-4	0.35	9.2	0.20	5.2	0.64	CYG
1403	83.50	-1.00	2	5.5	83.48	-0.87	2.8	4.3	25	1.5	1.5	7.7	-22	0.20	5.2	0.45	11.8	0.80	CYG
1404	83.70	-0.50	1	5.3	83.67	-0.52	1.1	4.4	14	1.5	1.5	7.7	-13	0.30	7.9	0.20	5.2	0.69	CYG
1405	83.70	0.00	1	7.2	83.90	0.05	1.1	4.8	56	1.5	1.5	7.7	1	0.50	13.1	0.25	6.5	0.63	CYG
1406	83.90	0.80	-6	6.4	84.06	0.78	-5.6	4.7	18	1.5	1.5	7.7	20	0.35	9.2	0.20	5.2	0.74	CYG
1407	84.20	-0.40	5	7.9	84.51	-0.78	2.7	4.6	285	1.5	1.5	7.7	-20	0.85	22.3	0.70	18.3	1.22	CYG
1408	84.50	-1.00	-4	7.5	84.51	-0.99	-4.2	5.2	6	1.5	1.5	7.7	-25	0.10	2.6	0.10	2.6	0.67	CYG
1409	84.50	1.00	-4	7.1	84.44	0.97	-5.4	5.0	16	1.5	1.5	7.7	25	0.15	3.9	0.15	3.9	1.23	CYG
1410	84.60	0.20	-1	12.7	84.62	0.19	0.2	5.9	308	1.5	1.5	7.7	4	0.70	18.3	0.90	23.6	2.05	CYG
A	84.60	0.20	-1	12.7	84.62	0.25	-1.2	9.7	43				6	0.25	6.5	0.40	10.5	0.92	
1411	84.70	-0.70	-6	7.7	84.67	-0.83	-3.9	4.9	42	1.5	1.5	7.7	-21	0.35	9.2	0.25	6.5	1.51	CYG
1412	84.80	-0.30	2	5.4	84.78	-0.30	1.8	4.4	8	1.5	1.5	7.7	-7	0.20	5.2	0.15	3.9	0.43	CYG
1413	84.90	-0.20	-3	5.4	84.94	-0.04	-2.9	4.6	19	1.5	1.5	7.7	0	0.15	3.9	0.40	10.5	0.63	CYG
1414	84.90	0.30	-2	5.8	84.93	0.30	-2.7	4.6	10	1.5	1.5	7.7	7	0.15	3.9	0.15	3.9	0.47	CYG
1415	84.90	0.50	-1	5.0	85.01	0.51	-1.1	4.3	20	1.5	1.5	7.7	13	0.25	6.5	0.25	6.5	0.84	CYG
1416	85.00	-0.70	-35	5.5	85.00	-0.70	-34.0	4.8	5	4.6	4.6	9.3	-56	0.05	4.1	0.05	4.1	1.35	TANG.
1417	85.00	-0.50	4	5.0	85.00	-0.53	3.3	4.4	7	1.5	1.5	7.7	-13	0.05	1.3	0.25	6.5	0.45	CYG
1418	85.00	-0.50	-4	8.4	85.00	-0.43	-4.8	5.3	51	1.5	1.5	7.7	-11	0.30	7.9	0.35	9.2	1.09	CYG
1419	85.10	-0.30	0	5.8	85.07	-0.24	0.9	4.7	12	1.5	1.5	7.7	-6	0.15	3.9	0.20	5.2	0.76	CYG
1420	85.10	-0.10	-4	10.7	85.13	-0.02	-2.8	5.2	69	1.5	1.5	7.7	0	0.25	6.5	0.60	15.7	2.40	CYG
A	85.10	-0.10	-4	10.7	85.10	-0.10	-4.0	9.5	3				-2	0.05	1.3	0.05	1.3	0.79	
1421	85.20	-1.00	3	7.1	85.14	-0.97	3.4	5.1	30	1.5	1.5	7.7	-25	0.25	6.5	0.15	3.9	0.86	CYG
1422	85.20	-0.40	7	9.1	85.20	-0.42	7.2	5.5	9	1.5	1.5	7.7	-10	0.15	3.9	0.20	5.2	0.62	CYG
1423	85.20	0.50	-3	7.0	85.18	0.48	-2.6	5.2	7	1.5	1.5	7.7	12	0.10	2.6	0.10	2.6	0.49	CYG
1424	85.30	0.00	-8	5.6	85.30	0.00	-8.0	4.7	3	1.5	1.5	7.7	0	0.05	1.3	0.05	1.3	0.78	CYG
1425	85.40	0.00	-38	8.8	85.40	0.00	-37.4	5.5	16	4.9	4.9	9.5	0	0.15	12.7	0.15	12.7	1.24	TANG.

© American Astronomical Society • Provided by the NASA Astrophysics Data System

© American Astronomical Society • Provided by the NASA Astrophysics Data System

1987ApJS...63..821S

TABLE 1—*Continued*

CLOUD	l_p	b_p	v_p	T_p	<l>	<b>	<v>	<T>	N	d_N	d_F	R	<z>	Δl	ΔL	Δb	ΔB	σ_v	NOTES
	°	°		K	°	°	km s^{-1}	K		kpc	kpc	kpc	pc	°	pc	°	pc	km s^{-1}	
(1)	(2)	(3)	(4)	(5)	(6)	(7)	(8)	(9)	(10)	(11)	(12)	(13)	(14)	(15)	(16)	(17)	(18)	(19)	(20)
1426	86.70	0.40	-10	6.1	86.73	0.35	-10.4	4.8	9	1.7	1.7	8.6	10	0.15	4.3	0.20	5.8	0.65	TANG.
1427	89.30	0.00	-11	5.3	89.33	-0.02	-10.6	4.4	9	1.2	1.2	8.6	0	0.15	3.2	0.15	3.2	0.68	TANG.

Col. (1).—Cloud number and hot core designation (noted by letter).

Cols. (2)–(5).—Longitude, latitude, LSR velocity, and CO temperatures at the position of peak CO emission.

Cols. (6)–(9).—Centroid (l, b, V) and mean temperature for CO emission.

Col. (10).—Total number of (l, b, V) points contained in cloud within the 4 K boundary.

Cols. (11)–(13).—The near kinematic distance, far kinematic distance, and Galactic radius obtained from the (l, b, V) centroid using Clemens's (1985*b*) rotation curve with $R_0 = 8.5$ kpc and $\theta_0 = 220$ km s^{-1}. In cases where the distance ambiguity cannot be resolved from the Z-height or association with the 3 kpc or Cygnus arms (see text), the near distance is adopted for the linear sizes used in cols. (14), (16), and (18).

Col. (14).—The Z distance corresponding to the cloud centroid latitude.

Cols. (15) and (16).—The maximum extent of the cloud in the longitude direction (i.e., the difference of the highest and lowest longitude points within the cloud). The length is expressed in degrees and parsecs. These *maximum* extents are typically a factor of 1.36 larger than the square-root areas ($A^{1/2}$) given in Table 2.

Cols. (17) and (18).—The maximum extent of the cloud in latitude (i.e., the difference between the highest and lowest latitudes).

Col. (19).—The velocity dispersion measured for points above the 4 K or 8 K thresholds.

Col. (20).—Clouds for which the distance can be resolved based on Z-height, proximity to the tangent point (i.e., less than 40% difference between near and far distances), and location in the 3 kpc or Cygnus arms. Any clouds not noted have ambiguous distances.

TABLE 2

H II Region Clouds

HII REGION (1)	L_{HII} Jy kpc^2 (2)	l_p ° (3)	b_p ° (4)	v_p km s^{-1} (5)	T_p K (6)	<l> ° (7)	<b> ° (8)	<v> km s^{-1} (9)	<T> K (10)	N (11)	d_N kpc (12)	d_F kpc (13)	R kpc (14)	Δl ° (15)	ΔL pc (16)	Δb ° (17)	ΔB pc (18)	$A^{\frac{1}{2}}$ pc (19)	L_{CO} (20)	σ_v km s^{-1} (21)	T_c K (22)	NOTES (23)
G 9.62+0.20(V= 4)	0.5	10.10	-0.40	6	5.8	9.29	-0.14	4	3.8	1176	4.7	4.7	3.4	0.76	62	0.33	26	61	75236	4.8	3.2	3 KPC
G 9.98-0.75(V= 34)	84.0	9.80	-0.80	28	8.7	9.94	-0.61	29	5.4	466	3.8	12.9	4.8	0.38	25	0.44	29	38	28551	2.3	4.3	NEAR
G10.07-0.41(V= 12)	110.0	10.20	-0.30	8	10.9	10.20	-0.22	12	5.4	468	4.7	4.7	3.4	0.41	33	0.35	28	42	42249	3.6	4.2	3 KPC
G10.16-0.35(V= 13)	1700.0																					
G10.31-0.26(V= 12)	40.0																					
G10.32-0.15(V= 12)	450.0																					
G10.19-0.43(V= 3)	180.0	10.60	-0.40	-2	16.8	10.51	-0.38	-2	5.3	370	16.8	16.8	8.6	0.44	128	0.23	67	130	420669	2.0	3.4	OUTER
G10.62-0.38(V= -2)	240.0																					
G10.66-0.47(V= -3)	75.0																					
G10.46+0.02(V= 70)	60.0	10.40	0.10	68	5.0	10.28	-0.06	68	2.6	463	6.1	10.6	2.8	0.41	43	0.27	28	50	33500	2.7	1.8	NEAR
G11.90+0.75(V= 25)	30.0	11.90	0.80	26	10.5	11.78	0.74	25	4.8	218	3.3	13.4	5.3	0.31	17	0.31	17	23	8632	1.4	3.6	AMBIG.
G11.94-0.62(V= 36)	31.0	12.00	-0.60	35	7.1	11.93	-0.64	36	5.0	170	4.0	12.7	4.7	0.26	18	0.26	18	28	10222	1.6	4.6	AMBIG.
G11.94-0.04(V= 41)	62.0	12.00	-0.20	50	7.5	11.73	-0.19	45	4.2	221	4.9	11.7	3.8	0.33	28	0.19	16	34	17189	3.8	3.5	AMBIG.
G12.20-0.12(V= 25)	690.0	12.20	-0.10	23	10.0	12.22	-0.10	27	4.7	101	4.8	4.8	3.4	0.23	19	0.16	13	22	8197	3.9	3.1	3 KPC
G12.74-0.15(V= 46)	260.0	12.80	-0.20	44	10.6	13.07	-0.12	51	5.5	757	4.4	12.2	3.4	0.47	36	0.40	30	47	61099	3.8	4.3	AMBIG.
G13.17-0.14(V= 50)	38.0																					
G13.19+0.04(V= 54)	145.0																					
G12.75-0.15(V= 34)	140.0	12.80	-0.20	32	22.5	13.01	-0.24	36	6.9	961	4.8	4.8	4.3	0.80	66	0.36	30	62	118120	2.5	5.2	3 KPC
G12.81-0.20(V= 35)	610.0																					
G12.86-0.23(V= 34)	100.0																					
G12.91-0.28(V= 30)	25.0																					
G13.38+0.07(V= 18)	60.0	14.00	-0.60	18	15.3	13.86	-0.42	19	7.3	1828	2.2	14.3	6.4	0.59	22	0.48	18	36	48195	2.6	5.5	NEAR
G13.83-0.76(V= 24)	113.0																					
G14.06-0.53(V= 20)	6.0																					
G14.44-0.65(V= 11)	6.0																					
G13.87+0.28(V= 53)	129.0	13.90	0.30	49	9.0	13.98	0.24	47	4.9	147	4.5	12.0	4.3	0.22	17	0.22	17	26	11124	1.6	3.7	AMBIG.
G14.00-0.13(V= 31)	50.0	14.20	-0.20	39	15.5	14.24	-0.20	39	7.0	905	4.9	4.9	3.4	0.67	57	0.35	29	60	116347	2.3	5.5	3 KPC
G14.20-0.13(V= 36)	12.0																					
G14.60+0.01(V= 35)	380.0																					
G14.63+0.09(V= 38)	230.0																					
G15.03-0.69(V= 11)	1670.0	15.00	-0.70	20	42.6	15.06	-0.62	18	10.7	273	2.3	14.2	6.3	0.41	16	0.22	8	14	11436	1.7	4.9	NEAR
G15.08-0.68(V= 19)	2420.0																					
G15.14-0.94(V= 19)	20.0																					
G15.18-0.62(V= 11)	26.0																					
G15.20-0.77(V= 20)	29.0																					
G16.43-0.20(V= 44)	20.0	16.70	-0.50	43	9.9	16.44	-0.38	43	5.1	621	5.1	5.1	3.4	0.48	42	0.40	35	53	63182	2.8	4.0	3 KPC
G16.61-0.32(V= 45)	43.0																					
G16.94+0.76(V= 28)	105.0	16.90	0.30	24	18.0	17.04	0.60	22	7.5	955	2.4	13.8	6.2	0.54	22	0.60	25	31	32124	2.1	4.6	NEAR
G16.98+0.93(V= 25)	84.0																					
G16.99+0.87(V= 23)	58.0																					
G17.14+0.77(V= 27)	7.7																					
G18.14-0.29(V= 52)	111.0	18.10	-0.30	51	19.1	18.16	-0.40	47	7.2	306	5.2	5.2	3.4	0.27	24	0.27	24	38	46029	3.0	4.4	3 KPC
G18.18-0.40(V= 45)	59.0																					
G18.23-0.25(V= 47)	178.0																					
G18.26-0.30(V= 47)	103.0																					
G18.30-0.39(V= 32)	30.0	18.30	-0.40	34	11.2	18.33	-0.39	31	3.3	62	3.1	13.1	5.7	0.12	6	0.20	10	9	1451	3.2	1.3	NEAR
G18.88-0.39(V= 67)	534.0	18.85	-0.50	66	17.9	18.81	-0.47	65	6.3	1234	5.3	5.3	3.4	0.51	47	0.45	41	66	169195	3.1	4.5	3 KPC
G18.94-0.44(V= 68)	295.0																					
G19.04-0.43(V= 65)	125.0																					
G19.05-0.59(V= 68)	58.0																					
G19.07-0.28(V= 61)	172.0																					
G18.95-0.02(V= 50)	64.0	18.85	0.05	50	11.7	19.02	-0.02	47	6.4	130	4.0	12.1	4.9	0.21	14	0.19	13	20	10136	2.0	4.4	NEAR
G19.48+0.14(V= 24)	15.6	19.15	0.35	28	9.7	19.47	0.12	25	3.9	785	2.5	13.5	6.2	0.60	26	0.37	16	27	14985	2.9	2.4	AMBIG.
G19.61-0.23(V= 40)	125.0	19.10	0.10	45	11.0	19.34	-0.09	37	3.8	468	3.7	12.4	5.2	0.46	29	0.32	20	32	18594	5.8	2.8	NEAR
G19.61-0.13(V= 61)	73.0	19.60	-0.05	58	8.2	19.63	-0.13	59	3.9	124	4.3	11.7	4.6	0.18	13	0.18	13	20	6993	2.9	2.9	NEAR
G19.67-0.14(V= 55)	49.0																					
G20.07-0.14(V= 46)	30.0	20.20	-0.05	47	7.6	20.14	-0.17	44	3.1	114	3.7	12.2	5.2	0.22	14	0.14	9	16	3725	2.8	2.4	NEAR
G20.68-0.14(V= 57)	94.0	20.75	-0.10	59	15.9	20.77	-0.20	60	4.2	439	4.3	11.6	4.7	0.33	24	0.31	23	36	26384	4.2	2.6	AMBIG.
G20.73-0.09(V= 57)	1618.0																					
G21.00+0.09(V= 18)	350.0	21.00	0.10	21	9.7	21.16	0.19	22	2.8	255	1.9	14.0	6.8	0.24	57	0.24	57	88	106513	3.5	1.4	FAR

© American Astronomical Society • Provided by the NASA Astrophysics Data System

TABLE 2—*Continued*

HII REGION (1)	L_{HII} Jy kpc^2 (2)	l_p ° (3)	b_p ° (4)	v_p km s^{-1} (5)	T_p K (6)	<l> ° (7)	<b> ° (8)	<v> km s^{-1} (9)	<T> K (10)	N (11)	d_N kpc (12)	d_F kpc (13)	R kpc (14)	Δl ° (15)	ΔL pc (16)	Δb ° (17)	ΔB pc (18)	$A^{\frac{1}{2}}$ pc (19)	L_{CO} (20)	σ_v km s^{-1} (21)	T_c K (22)	NOTES (23)
G22.76-0.48(V= 73)	438.0	23.00	-0.40	74	13.5	23.05	-0.27	77	6.9	1131	4.9	10.8	4.4	0.60	112	0.39	72	138	691056	3.6	5.2	FAR
G22.95-0.31(V= 75)	609.0																					
G23.00-0.36(V= 78)	609.0																					
G23.25-0.27(V= 77)	563.0																					
G23.87-0.12(V= 75)	191.0																					
G23.12+0.56(V= 29)	34.0	23.15	0.20	19	5.5	23.22	0.15	21	2.0	729	1.6	14.0	7.0	0.41	11	0.52	14	17	2982	3.2	1.2	NEAR
G23.42-0.21(V=104)	760.0	23.40	-0.25	102	13.4	23.44	-0.05	97	5.7	892	6.5	9.1	3.6	0.46	52	0.39	44	69	164269	5.1	4.0	NEAR
G23.54-0.04(V= 91)	1260.0																					
G23.71-0.17(V=108)	180.0																					
G23.82+0.22(V=107)	78.0	24.45	0.25	120	16.5	24.37	0.24	111	6.8	789	7.7	7.7	3.5	0.41	55	0.32	43	74	246510	4.6	5.1	TANG.
G23.91+0.07(V=103)	60.0																					
G24.14+0.20(V=114)	55.0																					
G24.19+0.20(V=111)	123.0																					
G24.39+0.07(V=112)	200.0																					
G24.47+0.48(V=102)	400.0																					
G24.48+0.21(V=117)	375.0																					
G24.50-0.04(V=109)	97.0																					
G24.74-0.21(V=115)	118.0																					
G23.96+0.15(V= 80)	360.0	23.95	0.15	79	15.3	23.97	0.13	80	6.8	59	5.1	10.4	4.4	0.16	29	0.11	19	33	33143	1.9	4.8	FAR
G24.22-0.05(V= 89)	130.0	24.20	-0.05	88	8.6	24.07	-0.05	87	5.0	211	5.5	10.0	4.1	0.25	43	0.25	43	64	79702	3.0	3.7	FAR
G24.52-0.25(V= 96)	227.0	24.50	-0.25	101	17.8	24.63	-0.21	94	5.4	255	6.4	9.1	3.8	0.30	33	0.27	30	42	42343	3.1	3.4	AMBIG.
G24.68-0.16(V=112)	260.0	24.65	-0.10	114	9.2	24.64	-0.26	112	4.7	90	7.7	7.7	3.5	0.11	15	0.22	30	28	19139	2.0	2.5	TANG.
G24.80+0.01(V=107)	580.0	24.80	0.10	113	12.8	24.76	0.07	108	6.8	94	7.7	7.7	3.6	0.20	26	0.17	22	30	29058	2.5	5.0	TANG.
G24.81+0.10(V=114)	1000.0																					
G25.26-0.32(V= 64)	45.0	25.45	-0.20	65	12.0	25.34	-0.39	60	4.9	457	4.3	11.0	4.9	0.41	31	0.37	27	42	32155	2.7	3.5	AMBIG.
G25.38-0.18(V= 59)	3480.0																					
G25.40-0.25(V= 63)	410.0																					
G25.29+0.31(V= 45)	11.7	25.35	0.25	41	14.9	25.36	0.27	40	4.3	37	3.0	12.4	5.9	0.12	6	0.15	7	9	1086	2.3	2.0	AMBIG.
G25.40+0.03(V=-14)	350.0	25.45	0.05	-12	5.6	25.45	0.03	-12	2.4	31	16.0	16.0	9.1	0.10	27	0.13	37	39	14247	1.6	1.2	OUTER
G25.70+0.03(V= 52)	430.0	25.70	0.05	54	7.4	25.78	0.04	55	2.9	140	3.8	11.6	5.4	0.22	45	0.22	45	60	41592	2.9	2.0	FAR
G25.70+0.03(V=102)	181.0	25.65	-0.10	94	12.8	25.58	-0.17	95	5.6	599	5.8	9.5	4.1	0.45	45	0.31	31	55	86788	4.1	3.6	NEAR
G25.77+0.21(V=111)	656.0	25.80	0.25	110	15.9	25.68	0.25	109	6.7	112	7.7	7.7	3.7	0.18	24	0.12	16	31	33380	3.4	4.3	TANG.
G26.10-0.07(V= 33)	1220.0	25.15	-0.05	28	5.1	26.20	0.05	27	2.1	142	2.2	13.2	6.6	0.17	39	0.26	59	64	40588	4.0	1.4	FAR
G26.10-0.07(V=104)	420.0	25.90	-0.15	107	10.2	26.09	-0.07	103	5.9	214	7.0	8.3	3.8	0.28	40	0.16	22	51	65414	3.2	4.7	FAR
G26.54+0.42(V= 90)	83.0	26.70	0.50	86	7.7	26.69	0.54	86	2.9	311	5.4	9.8	4.4	0.29	27	0.29	27	39	20014	2.7	1.7	AMBIG.
G26.56-0.31(V=104)	169.0	26.55	-0.30	108	10.9	26.53	-0.34	107	5.5	82	7.3	7.9	3.8	0.19	24	0.12	15	27	18632	2.0	3.5	TANG.
G26.98-0.07(V= 79)	100.0	26.95	-0.10	81	7.5	26.77	-0.08	79	3.6	178	5.1	10.0	4.6	0.26	23	0.17	15	29	12804	2.1	2.2	AMBIG.
G27.28+0.15(V= 33)	280.0	27.50	0.20	36	10.2	27.24	0.16	33	3.7	366	2.6	12.5	6.3	0.37	81	0.19	40	89	161304	5.3	2.4	FAR
G27.49+0.19(V= 35)	675.0																					
G27.29-0.16(V= 97)	631.0	27.35	-0.15	93	10.5	27.34	-0.15	92	5.6	72	5.8	9.3	4.3	0.27	43	0.13	21	32	26559	1.5	3.1	FAR
G28.30-0.38(V= 44)	282.0	28.30	-0.35	51	7.6	28.18	-0.37	45	4.1	325	3.5	11.5	5.7	0.51	31	0.23	13	27	12316	2.0	2.6	AMBIG.
G28.60+0.01(V= 93)	620.0	28.60	0.05	100	10.0	28.65	0.05	103	6.6	85	6.4	8.5	4.2	0.19	28	0.16	23	32	30843	3.8	5.3	FAR
G28.66+0.03(V=100)	520.0																					
G28.80+0.17(V=108)	150.0	28.60	0.05	100	10.0	28.74	0.05	103	5.4	295	6.4	8.5	4.2	0.32	46	0.27	40	64	87711	3.7	4.0	FAR
G28.82-0.23(V= 90)	100.0	28.85	-0.25	88	15.8	28.67	-0.28	87	7.0	109	5.6	9.3	4.5	0.22	21	0.14	13	24	17935	2.1	5.2	AMBIG.
G28.98-0.60(V= 52)	15.0	28.95	-0.65	51	12.0	29.04	-0.74	51	3.6	203	3.5	11.4	5.7	0.33	19	0.21	12	23	6679	2.3	1.6	NEAR
G29.14+0.43(V= 21)	8.7	29.15	0.45	23	3.3	29.21	0.44	17	1.6	50	1.7	13.1	7.1	0.13	3	0.16	4	5	176	3.9	1.1	NEAR
G29.94-0.04(V= 98)	1340.0	29.85	-0.05	100	20.5	29.93	-0.07	99	7.2	433	6.7	8.1	4.3	0.26	36	0.35	49	62	154403	3.8	5.0	FAR
G30.23-0.14(V= 99)	210.0	30.30	-0.25	105	14.9	30.34	-0.26	103	8.5	126	7.3	7.3	4.3	0.21	26	0.18	22	32	44027	2.5	6.3	TANG.
G30.39-0.24(V=103)	316.0																					
G30.50-0.29(V=107)	224.0																					
G30.54+0.02(V= 50)	315.0	30.60	-0.05	43	7.2	30.47	0.04	43	4.3	311	2.9	11.7	6.2	0.32	65	0.25	50	81	140138	4.0	2.6	FAR
G30.60-0.11(V=102)	180.0	30.80	-0.05	92	16.1	30.71	-0.03	94	7.9	1180	6.0	8.6	4.6	0.52	78	0.37	55	99	529463	5.0	6.0	FAR
G30.69-0.26(V= 98)	240.0																					
G30.78-0.03(V= 90)	3050.0																					
G30.85+0.13(V= 36)	100.0	30.95	0.10	40	7.7	31.92	0.15	39	5.2	75	2.7	11.9	6.3	0.13	5	0.19	8	9	2213	2.6	4.0	AMBIG.
G31.05+0.48(V= 28)	8.5	31.10	0.45	30	7.1	31.27	0.48	25	2.5	387	2.1	12.5	6.8	0.39	14	0.24	8	14	3167	3.2	1.4	NEAR
G31.05+0.48(V= 99)	174.0	30.90	0.15	108	15.0	30.95	0.06	102	7.1	553	7.3	7.3	4.4	0.39	49	0.29	37	68	159194	3.4	5.6	TANG.
G31.13+0.28(V=104)	82.0																					
G31.28+0.06(V=104)	51.0																					

© American Astronomical Society • Provided by the NASA Astrophysics Data System

TABLE 2—*Continued*

HII REGION (1)	L_{HII} Jy kpc^2 (2)	l_p ° (3)	b_p ° (4)	v_p km s^{-1} (5)	T_p K (6)	<l> ° (7)	<b> ° (8)	<v> km s^{-1} (9)	<T> K (10)	N (11)	d_N kpc (12)	d_P kpc (13)	R kpc (14)	Δl ° (15)	ΔL pc (16)	Δb ° (17)	ΔB pc (18)	$A^{\frac{1}{2}}$ pc (19)	L_{CO} (20)	σ_v km s^{-1} (21)	T_C K (22)	NOTES (23)
G31.41+0.31(V=104)	87.0																					
G31.40-0.26(V= 90)	900.0	31.40	-0.25	88	8.5	31.45	-0.26	87	5.3	56	5.7	8.8	4.7	0.10	9	0.13	13	19	7324	2.9	3.9	NEAR
G32.80+0.19(V= 17)	900.0	32.80	0.20	29	6.0	32.80	0.21	22	2.2	158	2.0	12.3	6.9	0.25	53	0.20	42	67	39460	4.0	1.5	FAR
G33.12-0.08(V= 97)	501.0	32.70	-0.05	100	7.9	32.82	-0.02	95	4.4	382	7.2	7.2	4.6	0.34	42	0.28	35	49	65775	3.7	3.5	TANG.
G33.19-0.01(V=100)	111.0	33.90	0.10	106	9.5	33.61	0.01	104	5.4	286	7.1	7.1	4.7	0.41	50	0.17	21	46	58426	2.6	3.9	TANG.
G33.91+0.11(V= 98)	76.0	33.90	0.10	106	9.5	33.63	0.02	105	5.7	228	7.1	7.1	4.7	0.36	43	0.17	20	43	49209	2.7	4.4	TANG.
G34.25+0.14(V= 53)	180.0	34.25	0.15	55	8.2	34.13	0.05	56	4.3	272	3.6	10.4	5.9	0.23	14	0.20	12	24	11436	2.8	3.5	NEAR
G34.76-0.68(V= 52)	10.3	34.70	-0.70	46	10.0	34.79	-0.52	42	6.7	194	3.0	11.0	6.3	0.19	10	0.29	15	21	8970	2.4	5.8	NEAR
G35.04-0.50(V= 52)	23.0	34.70	-0.70	46	10.0	34.94	-0.41	44	5.8	769	3.0	11.0	6.3	0.42	22	0.50	26	39	31113	2.3	4.8	AMBIG.
G35.60-0.03(V= 50)	39.0	35.50	-0.05	52	6.9	35.50	-0.06	52	5.0	74	3.4	10.4	6.1	0.15	8	0.09	5	13	3266	3.6	4.0	NEAR
G35.66-0.03(V= 53)	77.0																					
G36.29+0.73(V= 76)	52.0	36.10	0.65	77	11.5	36.20	0.66	75	3.9	400	5.3	8.5	5.3	0.30	27	0.32	29	44	33170	3.6	2.9	NEAR
G37.36-0.23(V= 39)	192.0	37.25	-0.25	42	7.4	37.23	-0.28	40	2.8	170	2.8	10.8	6.5	0.15	28	0.26	49	57	42726	3.7	1.5	FAR
G37.37-0.07(V= 57)	59.2	37.45	-0.05	57	9.7	37.45	-0.07	58	4.4	50	3.8	9.7	6.0	0.11	7	0.13	8	11	2379	3.5	2.9	AMBIG.
G37.44-0.04(V= 61)	569.0																					
G37.54-0.11(V= 55)	302.0																					
G37.64-0.11(V= 52)	262.0	37.55	-0.10	53	9.9	37.78	-0.31	52	3.7	285	3.5	10.0	6.1	0.25	15	0.35	21	25	9732	3.7	2.5	AMBIG.
G37.67+0.13(V= 86)	180.0	37.35	0.25	88	6.4	37.47	0.13	86	4.4	242	6.8	6.8	5.2	0.19	22	0.29	34	44	36697	2.3	3.6	TANG.
G37.76-0.22(V= 61)	516.0	37.75	-0.20	60	8.0	37.83	-0.38	59	3.4	505	4.0	9.4	5.9	0.26	43	0.41	66	70	115361	4.7	2.5	FAR
G37.87-0.40(V= 60)	727.0																					
G39.25-0.06(V= 23)	5.9	39.25	-0.05	22	11.2	39.24	-0.08	22	4.5	41	1.5	11.6	7.4	0.13	3	0.10	2	3	331	2.3	2.4	AMBIG.
G41.10-0.21(V= 58)	78.0	41.15	-0.20	60	11.0	41.22	-0.23	60	4.4	488	4.2	8.6	6.0	0.29	21	0.29	21	36	28411	2.8	3.0	AMBIG.
G41.52+0.03(V= 15)	1.9	41.85	-0.10	19	7.0	41.85	0.00	16	2.7	285	1.4	11.3	7.5	0.33	7	0.35	8	11	1095	1.8	1.9	AMBIG.
G42.11-0.62(V= 66)	60.0	42.15	-0.60	67	10.7	42.13	-0.72	66	4.9	128	5.1	7.6	5.8	0.22	19	0.20	17	26	12136	1.9	3.7	AMBIG.
G43.17+0.00(V= 10)	10100.0	43.10	0.05	12	8.7	43.21	-0.06	12	2.7	382	1.0	11.4	7.8	0.43	84	0.21	42	82	102416	4.0	1.4	FAR
G43.18-0.52(V= 56)	15.0	43.20	-0.50	57	8.2	43.06	-0.55	57	4.1	96	4.1	8.3	6.2	0.18	12	0.18	12	17	4885	1.9	3.0	AMBIG.
G43.89-0.79(V= 55)	17.0	43.90	-0.90	55	7.3	43.84	-0.80	55	2.3	151	3.9	8.3	6.3	0.19	13	0.24	16	21	4122	2.2	1.2	NEAR
G45.13+0.14(V= 57)	630.0	45.45	0.05	58	10.5	45.41	0.07	58	5.2	212	4.4	7.5	6.2	0.24	31	0.18	23	40	46771	2.5	3.4	FAR
G45.45+0.06(V= 54)	800.0																					
G45.47+0.13(V= 53)	226.0																					
G46.49-0.25(V= 57)	101.0	46.30	-0.20	59	7.7	46.26	-0.16	55	3.7	243	4.8	6.9	6.2	0.29	24	0.17	14	30	15884	3.5	2.9	NEAR
G48.60+0.04(V= 17)	1140.0	48.60	0.00	20	13.5	48.74	0.13	14	3.0	528	1.5	9.7	7.6	0.30	50	0.46	78	85	114219	3.7	1.6	FAR
G48.64+0.23(V= 13)	2.2																					
G48.93-0.29(V= 66)	550.0	49.50	-0.40	57	24.1	49.43	-0.20	62	4.6	1796	5.5	5.5	6.5	0.62	59	0.53	50	82	189780	3.6	2.5	TANG.
G49.06-0.26(V= 60)	160.0																					
G49.08-0.38(V= 68)	205.0																					
G49.20-0.35(V= 67)	930.0																					
G49.38-0.30(V= 62)	1810.0																					
G49.44-0.46(V= 59)	274.0																					
G49.49-0.38(V= 57)	6390.0																					
G49.58-0.38(V= 62)	283.0																					
G49.59-0.46(V= 68)	85.0																					
G50.12-0.67(V= 70)	93.0																					
G49.41-0.19(V= 46)	597.0	49.50	-0.40	57	24.1	49.44	-0.24	53	5.3	524	5.5	5.5	6.5	0.33	32	0.33	32	49	64139	3.2	2.5	TANG.
G51.06+0.16(V= 42)	100.0	50.85	0.25	43	7.0	50.88	0.19	44	3.5	153	3.5	7.3	6.9	0.24	14	0.17	10	18	4785	3.3	2.2	AMBIG.
G51.36+0.00(V= 58)	95.5	51.35	-0.05	54	11.6	51.29	-0.01	53	3.4	362	5.3	5.3	6.6	0.29	27	0.29	27	43	26577	2.8	2.5	TANG.
G52.23+0.74(V= -3)	1.0	52.25	0.75	4	10.4	52.24	0.77	3	2.7	152	0.6	9.8	8.1	0.23	2	0.18	1	3	117	2.0	1.2	AMBIG.
G52.94-0.59(V= 43)	10.0	52.95	-0.55	48	10.0	52.85	-0.58	47	3.3	50	5.1	5.1	6.8	0.17	15	0.12	10	16	3297	1.9	1.7	TANG.
G53.18+0.15(V= 8)	350.0																					
G54.09-0.07(V= 43)	38.0	54.10	-0.05	40	14.2	53.99	-0.14	41	3.4	274	3.7	6.3	7.0	0.38	23	0.18	11	24	9479	3.8	1.7	AMBIG.
G59.80+0.24(V= -6)	121.0	59.70	0.20	-1	5.5	59.81	0.32	-3	2.0	230	0.5	8.2	8.3	0.28	2	0.23	1	3	89	2.4	1.2	AMBIG.

© American Astronomical Society • Provided by the NASA Astrophysics Data System

© American Astronomical Society • Provided by the NASA Astrophysics Data System

1987ApJS...63..821S

NOTES TO TABLE 2

Col. (1).—H II region specified by l, b, and V_{LSR} of the radio recombination line from Downes *et al.* (1980) and Lockman (1987).

Col. (2).—The $\lambda = 6$ cm radio luminosity of the H II region, $S_{Jy} d^2_{kpc}$, where d is the kinematic distance (cols. [12] and [13]). In cases where the distance ambiguity is not resolved (see col. [23]), the near distance is adopted.

Cols. (3)–(6).—Longitude, latitude, LSR velocity, and CO temperature at the position of peak CO emission.

Cols. (7)–(10).—Centroid (l, b, V) and mean temperature for the CO emission.

Col. (11).—Total number of (l, b, V) points contained within the cloud boundary defined at the threshold temperature T_c (col. [22]).

Cols. (12)–(14).—Near kinematic distance, far kinematic distance, and Galactic radius obtained from the (l, b, V) centroid of the CO emission using Clemens's (1985*b*) rotation curve with $R_0 = 8.5$ kpc and $\theta_0 = 220$ km s^{-1}.

Cols. (15) and (16).—Mean chord length in l for all latitudes included in the cloud. The length is expressed in degrees and parsecs using the kinematic distance.

Cols. (17) and (18).—Mean chord length in b for all longitudes included in the cloud.

Col. (19).—Square root of the area of the cloud projected onto the plane of the sky.

Col. (20).—CO luminosity (K km s^{-1} pc^2) of the cloud, i.e., the sum of the integrated CO intensities along all lines of sight within the cloud boundary times the pixel area for $3' \times 3'$.

Col. (21).—Velocity dispersion for data above the threshold temperature.

Col. (22).—Threshold temperature defining the cloud boundary in (l, b, V)-space.

Col. (23).—Distance assignment based on Z-distance, proximity to the tangential point, or location in the 3 kpc or Cygnus arms.